# Carboranylphosphines meet dendrimers : Electron-deficient scaffolds for ligand design and applications in catalysis

Max Milewski

# THÈSE

## En vue de l'obtention du
## DOCTORAT DE L'UNIVERSITÉ DE TOULOUSE

**Délivré par l'Université Toulouse 3 - Paul Sabatier**

**Cotutelle internationale: Université de Leipzig**

---

**Présentée et soutenue par**

**Max MILEWSKI**

Le 14 décembre 2023

# Les carboranyl phosphines rencontrent les dendrimères: Des molécules électro-déficientes pour la conception de ligands et des applications en catalyse

---

Ecole doctorale : **SDM - SCIENCES DE LA MATIERE - Toulouse**

Spécialité : **Chimie Organométallique et de Coordination**

Unité de recherche :
**LCC - Laboratoire de Chimie de Coordination**

Thèse dirigée par
**Anne-Marie CAMINADE et Evamarie HEY-HAWKINS**

Jury

**Mme Kirsten ZEITLER,** Rapporteure
**M. Christian MüLLER,** Rapporteur
**M. Noël NEBRA MUNIZ,** Examinateur
**Mme Anne-Marie CAMINADE,** Directrice de thèse
**Mme Evamarie HEY-HAWKINS,** Co-directrice de thèse
**Mme Clara VIñAS TEIXIDOR,** Présidente

# Carboranylphosphines meet dendrimers: Electron-deficient scaffolds for ligand design and application in catalysis

Der Fakultät für Chemie und Mineralogie
der Universität Leipzig

vorgelegte

**D I S S E R T A T I O N**

zur Erlangung des akademischen Grades

DOCTOR RERUM NATURALIUM
(Dr. rer. nat.)

von

**M. Sc. Max Milewski**

geboren am 12.08.1995 in Guben, Deutschland

Toulouse, den 26.10.2023

The experimental part of this thesis was carried out from October 2020 to September 2023 at the Laboratoire de Chimie de Coordination UPR CNRS 8241, Toulouse under the supervision of Dr. Anne-Marie Caminade, at the Institute of Inorganic Chemistry, Faculty of Chemistry and Mineralogy, Leipzig University under the supervision of Prof. Dr. Dr. h. c. Evamarie Hey-Hawkins, at the Universitat Autonòma de Barcelona under the supervision of Prof. Dr. Agustí Lledós, and at BASF SE, Department of Synthesis and Homogeneous Catalysis, Ludwigshafen under the supervision of Dr. Rocco Paciello. This thesis is written in the style of a cumulative dissertation and parts of it were already published. The articles have been included into the thesis where possible, and American spelling is applied throughout this thesis.

M. Milewski, A.-M. Caminade, E. Hey-Hawkins, P. Lönnecke, *Acta Crystallogr. Sect. E Crystallogr. Commun.* **2022**, *78*, 1145–1150. DOI: 10.1107/S205698902201043X.

A.-M. Caminade, M. Milewski, E. Hey-Hawkins, *Pharmaceutics* **2023**, *15*, 2117. DOI: 10.3390/pharmaceutics15082117.

Carboranylphosphines: B9-Substituted Derivatives With Enhanced Reactivity For The Anchoring To Dendrimers**,** M. Milewski, A.-M. Caminade, S. Mallet-Ladeira, A. Lledós, P. Lönnecke, E. Hey-Hawkins, to be submitted.

The project has received funding from the European Union's Horizon 2020 research and innovation program under the Marie Skłodowska-Curie grant No 860322 and was supported by the Laboratoire de Chimie de Coordination (CNRS), the Université Toulouse III – Paul Sabatier, the Leipzig University, the Leipzig Graduate School of Natural Sciences – Building with Molecules and Nano-objects (BuildMoNa), the Gesellschaft Deutscher Chemiker (GDCh), the Graduate Academy Leipzig, the Universitat Autonòma de Barcelona, and the BASF SE.

## Declaration of Originality

I hereby declare that this dissertation was completed independently and without the use of any unauthorized assistance. Other than the sources listed in the bibliography, I have not used any other sources. All text passages taken verbatim or in spirit from published or unpublished writings, as well as all information based on oral information, have been marked. Furthermore, all materials or services provided by third parties are identified as such. Dr. Anne-Marie Caminade (LCC Toulouse, CNRS), Prof. Dr. Dr. h. c. Evamarie Hey-Hawkins (Leipzig University), and Prof. Dr. Agustí Lledós (Universitat Autonòma de Barcelona) assisted me in the selection and analysis of the material, as well as in the preparation of the manuscript. I certify that, aside from the individuals named in the acknowledgements, no other individuals were involved in the intellectual production of the current work, particularly no doctoral advisor, and that no monetary benefits were given to third parties, either directly or indirectly. This thesis has been submitted in the same or similar form to Université Toulouse III - Paul Sabatier and the Leipzig University for the purpose of a doctorate (see cotutelle agreement). There have been no previous failed attempts at a doctorate.

Toulouse, 26.10.2023

_____

Max Milewski

## Bibliographische Beschreibung

Milewski, Max

Carboranylphosphines meet dendrimers: Electron-deficient scaffolds for ligand design and application in catalysis

Universität Paul Sabatier Toulouse und Universität Leipzig, kumulative Dissertationsschrift, 2023
230 Seiten, 300 Literaturzitate, 99 Abbildungen (inklusive der Strukturen im Experimentalteil und der französischen Titelseite), 85 Schemata, 11 Tabellen

## Synopsis

The goal of this dissertation research was to prepare, characterize, and use a novel ligand system for challenging catalytic transformations. Two chemical building blocks served as the foundation for the system: carboranylphosphine monomeric units and a polyphosphorhydrazone dendritic framework. In order to integrate the two structures, a synthetic approach was initially devised to appropriately functionalize the B9 position of the carboranylphosphines for an enhanced reactivity. The second step was the investigation of different methods of linking them to the dendritic backbone.

A thiophosphoryl chloride or a hexachlorocyclotriphosphazene core were used as the starting point for the synthesis of several dendritic phosphorus-containing scaffolds, including symmetrical and unsymmetrical polyphosphorhydrazone dendrimers. The goal was to create dendrimers with specific functionalizations for improved catalytic applications. Nevertheless, difficulties arose throughout the synthesis process, particularly when purifying and monofunctionalizing dendrimers.

In addition, the syntheses of various B9-substituted carboranes and carboranyl-phosphines starting from 1,2-dicarba-*closo*-dodecaboranes(12) were carried out. The resulting carborane derivatives were characterized, and frequently these crystalline materials allowed for the elucidation of their solid-state structures by X-ray diffraction. In order to alter the carborane cage and increase its reactivity for further grafting to other dendritic cores, our research helped developing new protection and deprotection techniques. In particular, the carboranylphosphines' steric and electrical characteristics could be tuned, which made it possible to synthesize novel ligands that were required for the complexation of various transition metals. The potentially bidentate carboranylbisphosphines themselves, appear to be suitable ligands for metal complexes employed in homogeneous catalysis.

DFT calculations suggested that these ligands could form stable complexes with different transition metals, and experimental work supported this concept. Complexation experiments were carried out with $Pd^{II}$, $Cu^{I}$, $Au^{I}$, $Rh^{I}$, and $Ru^{0}$ precursors, using different carboranylphosphine derivatives. Research conducted in an industrial setting also explored catalytic applications, such

as hydrogenation and hydroformylation of olefins, using rhodium and ruthenium precursors. In these reactions, 9-(TBDMS)O-$C_6H_4$-1,2-$(PPh_2)_2$-*ortho*-carborane in particular showed potential.

The project further involved the grafting of carboranes onto model molecules and dendritic compounds. Despite the paucity of entirely carboranylphosphine-substituted molecules and the difficult separation of differentially carborane-substituted dendrimers, numerous carborane-substituted dendrimers were produced, opening the way for future investigations to graft additional functionalities.

In conclusion, the study aimed of developing a new dendrimer-based ligand system for catalytic applications was not met. The research does, however, include the replication of dendritic compounds, the synthesis of novel B9-substituted carboranes and carboranyl-phosphines, and detailed theoretical (DFT) and experimental examinations of their complexation behavior with transition metals. The project might have applications in homogeneous catalysis and the pharmaceutical sector. Future study might focus on additional carboranylphosphines and other catalytic applications in this industry.

## Zusammenfassung

Das Ziel dieses Dissertationsprojektes war die Entwicklung, Charakterisierung und die anschließende Nutzung eines neuartigen Ligandensystems für anspruchsvolle katalytische Umwandlungen. Zwei chemisch sehr unterschiedliche Bausteine bilden dabei die Grundpfeiler für das Ligandensystem: Carboranylphosphane als monomere Einheiten sowie ein polyphosphorhydrazon-basiertes dendritisches Gerüst. Um diese beiden Strukturen miteinander zu verbinden, wurde zunächst ein synthetischer Ansatz entwickelt, der die B9-Position der Carboranylphosphane zur Steigerung der Reaktivität entsprechend funktionalisieren sollte. Im zweiten Schritt wurden verschiedene Methoden untersucht, um die Carboranylphosphane mit dem dendritischen Rückgrat zu verbinden.

Als Ausgangspunkt für die Synthese mehrerer phosphorhaltiger dendritischer Gerüste, einschließlich symmetrischer und unsymmetrischer polyphosphorhydrazonbasierter Dendrimere, wurden Thiophosphorylchlorid und Hexachlorocyclotriphosphazen verwendet. Ziel war die Synthese von Dendrimeren mit geeigneten terminalen Funktionen für verbesserte katalytische Anwendungen. Während des Syntheseprozesses traten jedoch Schwierigkeiten auf, insbesondere bei der Aufreinigung und Monofunktionalisierung der Dendrimere.

Darüber hinaus wurden verschiedene B9-substituierte Carborane und Carboranylphosphane ausgehend von 1,2-Dicarba-*closo*-dodecaboran(12) hergestellt. Die resultierenden Carboranderivate wurden charakterisiert, wobei oftmals auch eine Aufklärung der Festkörperstrukturen dieser kristallinen Materialien mittels Röntgenstrukturanalyse möglich war. Die durchgeführte Forschungsarbeit trug durch die Entwicklung neuer Schutz- und Entschützungstechniken zur Modifizierung des Carborangerüsts bei, welches so verändert wurde,

dass dessen Reaktivität für die Fixierung an verschiedenen dendritischen Kernen erhöht werden konnte. Insbesondere die sterischen und elektrischen Eigenschaften der Carboranylphosphane konnten justiert werden, was die Herstellung neuartiger Liganden ermöglichte, die für die Komplexierung verschiedener Übergangsmetalle erforderlich waren. Die potenziell zweizähnigen Carboranylbisphosphane selbst scheinen geeignete Liganden für Metallkomplexe zu sein, die in der homogenen Katalyse eingesetzt werden können.

DFT-Berechnungen legten nahe, dass diese Liganden stabile Komplexe mit verschiedenen Übergangsmetallen bilden könnten, und experimentelle Arbeiten unterstützten dieses Konzept. Die Komplexierungsversuche wurden mit verschiedenen Orgonometallverbindungen basierend auf $Pd^{II}$, $Cu^{I}$, $Au^{I}$, $Rh^{I}$ und $Ru^{0}$ und unter Verwendung verschiedener Carboranylphosphanderivate durchgeführt. Die in einem industriellen Umfeld durchgeführte Forschung beleuchtete auch katalytische Anwendungen wie die Hydrierung und Hydroformylierung von Olefinen unter Verwendung von Rhodium- und Rutheniumpräkursoren näher. Insbesondere das 9-(TBDMS)O-$C_6H_4$-1,2-$(PPh_2)_2$-*ortho*-carboranderivat zeigte hierbei katalytisches Potenzial.

Das Projekt umfasste außerdem die Substitutionsreaktionen von verschiedenen Carboranen mit einem Modellmolekül sowie weiteren dendritischen Verbindungen. Ein vollständig mit Carboranylphosphanderivaten substituiertes Dendrimer konnte nicht synthetisiert werden. Dennoch war es möglich, verschiedene mit Carboranderivaten substituierte Dendrimere zu synthetisieren auch wenn deren Aufreinigung sich als sehr komplex erwies und eine vollständige Isolation oft ausblieb. Die durchgeführten Experimente zeigen deutlich, dass die Synthese von mit Carboran substituierten Dendrimeren möglich ist und ebnet den Weg für zukünftige Untersuchungen zur Verlinkung dieser beiden Funktionalitäten.

Zusammenfassend konnte das Ziel, ein neues dendrimer-basiertes Ligandensystem für katalytische Anwendungen zu entwickeln, nicht erreicht werden. Die durchgeführten Forschungsarbeiten umfassten die Reproduktion dendritischer Verbindungen, die Synthese neuartiger B9-substituierter Carborane und Carboranylphosphane sowie detaillierte theoretische (DFT-) und experimentelle Untersuchungen ihres Komplexierungsverhaltens mit Übergangsmetallen. Die hergestellten Verbindungen könnte Anwendungen in der homogenen Katalyse und im pharmazeutischen Sektor haben. Zukünftige Studien könnten sich auf neue Carboranylphosphane und andere katalytische Anwendungen in dieser Branche konzentrieren.

## Acknowledgements

I gratefully acknowledge the support of all people and institutions who helped me to successfully complete this doctoral project and make this project a success story and not a tragedy. I wish to explicitly thank:

*Dr. Anne-Marie Caminade* for her supervision throughout the entire project, her availability and consistent help, whether academic, organizational, or personal, her great patience, cheerful mood, and understanding always shown even when topics outside of work were concerned, especially for the opportunity and financial support given to me by the extension of my contract, the freedom given in all my work and the choice of conferences to attend, her faith in my work when attempting things that may not have worked out as planned, as well as her assistance with administrative issues in France.

*Prof. Dr. Dr. h. c. Evamarie Hey-Hawkins* for pointing out this possibility and ultimately paving my way into this research project, her assistance in and out of the laboratory, whether academic, organizational, or personal in nature, not only throughout my dissertation but also my master's thesis, her conference support, and her academic and orthographic rigor, hardly ever missing the slightest ambiguity or typo be it my thesis, a report, a presentation, or a paper. I appreciated the numerous opportunities to collaborate with researchers from around the world, as well as her dedication to the Monash-Leipzig exchange program.

*Prof. Dr. Agustí Lledós* for his passionate and purely inspirational approach to teaching computational chemistry, his positive support and time to answer questions about transition states, structure optimizations, and frequency calculations, and his availability and prompt assistance with manuscript corrections. Special thanks go to *Bernat*, without whom I would have been locked out of BORG numerous times and would still be copying and pasting items with mouse clicks, and *Laura*, who took the time to teach me about molecular dynamics and answer questions about these wiggling molecules.

*Dr. Rocco Paciello, Dr. Edward Richmond and the entire team* for providing invaluable assistance during my industrial internship at BASF SE in Ludwigshafen. Special thanks go to *Thomas Gaczensky*, who performed all of the catalytic experiments for me when I could not be there in person and without whom the automated library synthesis would still not work.

*Dr. Kathleen Moineau* who not only dealt with my daily complaints and problems in and out of the laboratory, but proofread parts of my work and helped me maintaining a positive attitude while dealing with all of the administrative issues I encountered during my time in France. I appreciated your consistent encouragement and support a lot. Thank you very much!

I would also like to thank *Ramona Oehme* for her tireless acquisition of countless mass spectra of not always the most agreeable and suitable composition for their spectrometers, as well as dedicating a significant amount of time and patience to manually measuring my much too large

macromolecular samples over and over again, for complying with my special wishes, and for always maintaining a cheerful mood, as well as *Stefanie Märcker-Recklies* and *Jacqueline Lewandowski* for general laboratory assistance, and *Dr. Peter Lönnecke* for crystal structure measurements and his help with the manuscripts, tables, and figures for my publications.

*Antoine Bonnet* who assisted with all of the NMR measurements, recorded many of my spectra himself, always suggested a better way to acquire a clean NMR spectrum, and was always up for a fruitful discussion.

The funding agencies that supported this project: The *European Union's Horizon 2020 research and innovation programme under the Marie Skłodowska-Curie grant agreement No. 860322* and the *Gesellschaft Deutscher Chemiker* (*GDCh*) for financial support. Furthermore, thanks are due to the *Leipzig Graduate School of Natural Sciences – Building with Molecules and Nano-object*s (*BuildMoNa*), and to the *Graduate Academy Leipzig* for financial and intellectual support throughout this project.

All *Sharkies* I have had the pleasure of getting to know and working with since my first day on the third floor four years ago. I would like to thank *Jan*, *David*, *Axel*, *Kyra*, *Til*, *Sonam*, *Jelena*, and *Philipp* in particular for making Lab 312 such a wonderful place to work over the years. Special thanks go to *Jan* who first introduced me to the world of carboranes, welcomed me so warmly during my Master's thesis, and patiently answered all of my questions, *Saral* and *Zeno*, for their consistent assistance with measuring my NMR samples and lending out their precious dried solvents, and *Philipp* who proofread parts of my work and supported me as good friend throughout all this time.

All members of *Team M*, I appreciated working with and who helped me get settled in the jungle of French administration. Special thanks go to *Aurelien* for his meticulous control of my NMR spectra, lending out special glassware in a communistic manner, and our numerous fruitful discussions that led to successful synthetic results as well as *Valérie* for her proof-reading and steady assistance after climbing the staircase onto the first corridor and working in her lab.

The *CCIMC Network* and its participants. Special thanks to *Alida Lefter* for handling my administrative issues also outside of office hours.

This thesis would not have been possible without the ongoing emotional support of my *friends*, *family*, and *loved ones*. You are too numerous to name, but you know who you are – Thanks for bearing with me!

Last but not least, thank you *Celine* and *Anna* for your constant love, patience, and understanding for extra hours, weekend work, and mental occupation for this project at the most inconvenient times. For you, my time abroad and my dedication to work has not always been easy but even in the most difficult times, you did not give up on me and you made my life better in every way. I am deeply indebted to you.

Für meine Großeltern, Anneliese und Georg Teise

# Table of Contents

# Abbreviations

| | |
|---|---|
| Ac | acetyl |
| acac | acetylacetonate |
| Ar | aryl |
| BNCT | boron neutron capture therapy |
| Boc | *tert*-butyloxycarbonyl |
| br | broad |
| CCDC | Cambridge Crystallographic Data Centre |
| Cp | cyclopentadienyl |
| Cp* | pentamethylcyclopentadienyl |
| cod | 1,5-cyclooctadiene |
| d/dd/ddd/dddd | doublet / doublet of doublets / doublet of doublets of doublets / doublet of doublets of doublets of doublets |
| dq | doublet of quartets |
| dt | doublet of triplets |
| DBU | 1,8-diazabicyclo[2.4.0]undec-7-ene |
| DFT | density functional theory |
| depc | 1,2-bis(diethylphosphino)-*ortho*-carborane |
| dipc | 1,2-bis(diisopropylphosphino)-*ortho*-carborane |
| diphos | 1,2-bis(diphenylphosphino)ethane |
| DMSO | dimethyl sulfoxide |
| doepc | 1,2-bis(diethyl phosphite)-*ortho*-carborane |
| dppb | 1,2-bis(diphenylphosphino)-benzene |
| dppc | 1,2-bis(diphenylphosphino)-*ortho*-carborane |
| eq. | equivalent(s) |
| ESI | electrospray ionization |
| Et | ethyl |
| EtOAc | ethyl acetate |
| EtOH | ethanol |
| $Et_2O$ | diethyl ether |
| 1-Gn | generation n (n = 0, 1, 2, 3) of a $N_3P_3Cl_6$-based dendrimer with terminal $P(S)Cl_2$ functions |
| 2-Gn | generation n (n = 0, 1, 2) of a $N_3P_3Cl_6$-based dendrimer with terminal aldehyde functions |

| | |
|---|---|
| Gof | goodness of fit (factor) |
| HRMS | high-resolution mass spectrometry |
| Hz | hertz |
| *i*PrOH | isopropanol |
| m | multiplet |
| M | metal |
| Me | methyl |
| MeCN | acetonitrile |
| MeOH | methanol |
| $MMHSPCl_2$ | monomethylhydrazidedichlorothiophosphate, $H_2NNMeP(S)Cl_2$ |
| MS | mass spectrometry |
| NMR | nuclear magnetic resonance |
| OTf | trifluoromethanesulfonate |
| p | quintet |
| Ph | phenyl |
| PPH | polyphosphorhydrazone |
| ppm | parts per million |
| Pr | propyl |
| q | quartet |
| rt | room temperature |
| s | singlet |
| SMD | solvation model based on density |
| 1-Sn | generation n (n = 0, 1) of a $SPCl_3$-based dendrimer with terminal $P(S)Cl_2$ functions |
| 2-Sn | generation n (n = 0, 1) of a $SPCl_3$-based dendrimer with terminal aldehyde functions |
| t | triplet |
| t.a. | température ambiante (room temperature) |
| *t*Bu | *tert*-butyl |
| TBDMS | *tert*-butyldimethylsilyl ether |
| td | triplet of doublets |
| THF | tetrahydrofuran |
| tht | tetrahydrothiophene |
| TLC | thin-layer chromatography |
| TS | transition state |
| XRD | X-ray diffraction analysis |

# Symbols

| Symbol | Unit | Meaning |
|---|---|---|
| *J* | Hz | coupling constant |
| δ | ppm | chemical shift |
| $\Delta\delta_P$ | ppm | chemical shift difference |
| ΔG | kcal $mol^{-1}$ | GIBBS energy |

# Chapter 1: Introduction and Objectives

# 1 Introduction and Objectives

The first chapter is devoted to a study of the literature and the categorization of the topic within the context of state-of-the-art science. More information is provided on the two project pillars, carboranes or carboranylphosphines, and dendrimers, respectively. The introduction of carboranes and the sudden transition into the field of dendrimers can appear a little strange. To comprehend how these two groups of substances may benefit from one another and might be employed in a "symbiotic" fashion, it is in fact required to present these two incredibly unlike topics.

A brief description of icosahedral *closo*-dicarbadodecaboranes(12) (carboranes), their isomers, and reactivity will be followed by a more in-depth look at the compound class of carboranylphosphines. An overview of the different transition metal complexes formed with carboranylphosphines will be given, reviewing the complexation chemistry that has been developed over the past years and highlighting more state-of-the-art findings. Then, more information is provided on the compound class of dendrimers, including its terminology, general synthesis, and uses. The class of phosphorus-containing dendrimers and its advantages for the use in homogeneous catalysis are addressed in particular. Finally, a project work flow is detailed, along with an explanation of the project's motivation.

## 1.1 Boron-containing clusters and their phosphine derivatives

### 1.1.1 Diving into the chemistry of carboranes

Carboranes, formally known as carbaboranes, are polyhedral boron-carbon molecular clusters that are stabilized by electron-delocalized bonding in the skeletal framework. Each boron and carbon atom in the cluster is bound to a hydrogen atom, and the cluster framework may also include additional metallic and non-metallic elements. The first literature reports of carboranes in 1962 covered *closo*- (deltahedral structure with triangular faces) and *nido*-carboranes (*closo*-carborane minus one boron vertex) with small, sub-icosahedral structures.[1] Only one year later, acetylene and decaborane derivatives were used to synthesize the first example of the now well-known icosahedral *closo*-dicarbadodecaboranes(12).[2] Based on these results, 1,2- (*ortho*), but also 1,7- (*meta*) and 1,12-dicarba-*closo*-dodecaboranes(12) (*para* isomer) have been extensively studied (**Fig. 1.1.1**).

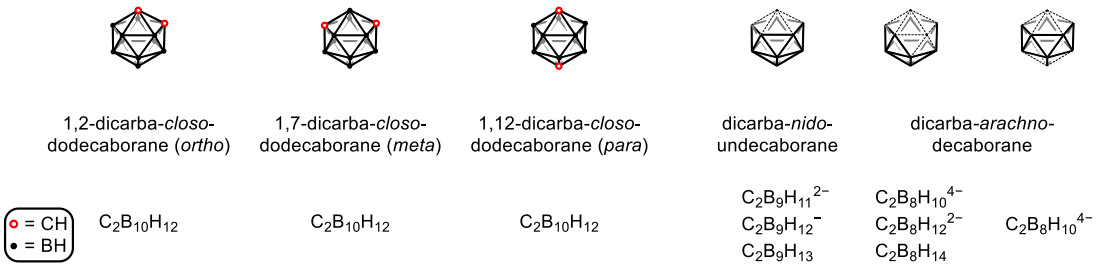


**Fig. 1.1.1.** Examples of the general structure of different carborane species with 13 skeleton electron pairs and their possible molecular formula. The explicit position of the carbon atoms as well as the exact number of hydrogen atoms in the *nido* and *arachno* derivatives is not displayed.[1]

All isomers are very stable and their derivatives often bear exceptional organomimetic features, with a chemical reactivity comparable to traditional organic molecules yet structurally similar to inorganic and organometallic compounds.[1] From herein, the term 'carborane' only refers to icosahedral dicarba-*closo*-dodecaboranes(12).

### 1.1.2 Isomers of dicarba-*closo*-dodecaboranes(12) and their differences

After the preparation of various *ortho*-carboranes, the other isomers could be easily accessed *via* thermal cage-rearrangements at elevated temperatures which was first reported by GRAFSTEIN et al.[1,3] Comparing all isomers, several general differences can be observed due to the lower polarity and the weaker inductive effect in *meta* and *para* isomers. The CH acidity sharply decreases from *ortho* to *meta* isomers, but only shows a small difference between *meta* and *para* isomers which lowers the reactivity towards metalation reactions at carbon. The lower polarity is further reflected in higher volatility and lower melting points of *meta* and *para* isomers than those of their *ortho*-carborane counterparts.[1] All these findings can be generally seen as the result of the more even distribution of electron density compared to the *ortho*-carborane systems. Although there is a lower carborane reactivity, an array of *meta*- and *para*-carboranes were prepared. However, the *ortho* isomer, first discovered and characterized, is the most available of the carborane family and has been studied extensively since the early 1960s. It is most commonly used because of its cage stability towards degradation under a variety of conditions such as exposure to strong acids or oxidants, the loss of only one boron vertex if strong bases are applied forming *nido*-carboranes, and its convenient arrangement of carbon atoms in close proximity, which facilitates the synthesis of chelating ligands.[1]

### 1.1.3 Reactivity of dicarba-*closo*-dodecaboranes(12)

The current state of research shows a large number of methods to generate carboranes with various combinations of metal and non-metal atoms and includes functionalizations of both boron and carbon vertices. These substitutions on the parental carborane cluster are influenced by two fundamental electronic properties: the electron delocalization and the electron-withdrawing character of its skeletal carbon atoms.[1] The electron withdrawal at the skeletal carbons causes

an acidic character at the carbon-bound protons, which facilitates a nucleophilic attack with LEWIS bases. The acidity can be further adjusted by introducing electron-withdrawing or electron-donating substituents at the boron vertices.[4] This led to the synthesis of a wide variety of C-substituted derivatives of *ortho* and *meta* isomers, respectively. Using different synthetic approaches other vertices of these boron-rich clusters could be easily modified utilizing straightforward methods. Depending on the vertex substituted, the carborane moieties possess extremely different electronic influences on their substituents.[1]

In 2011, SPOKOYNY and co-workers[5] carried out experimental investigations with computational support and showed that C-attached substituents experience an electron-withdrawing effect whereas B-attached substituents are exposed to a strong electron-donating influence. This contrasting behavior is a direct consequence of the electronegativity differences between carbon and boron and the electron distribution in such boron clusters.[1,4] That is, the carbon atoms contribute more electrons to the cluster bonding because of their greater electronegativity which makes them more electron-deficient than boron atoms and *vice versa*.[1,5] Similarly, the converse behavior of carboranyl substituents depending on which vertex is functionalized has been discovered. It was found that different attachment points of phosphine-thioether ligands in *ortho*- and *meta*-carboranes influence their electronic properties and coordination strength to platinum(II).[5]

This indicates that carborane derivatives exhibit a remarkable contrast in their coordination chemistry, converse to carbon-based ligands. These unique properties are based on the element boron and its electron deficiency as well as the structural features of the cluster. Because of its $C_2$ symmetry (similar to an ethylene or *ortho*-phenylene moiety), the *ortho*-carborane cluster is of great interest. Having the strongest electron-withdrawing effect of all three isomers, the *ortho*-carborane behaves, depending on the position of the substitution on the cluster, as an electron acceptor (carboran-1-yl) or as an electron donor (carboran-9-yl).[6]

The chemistry of the *ortho* isomer is dominated by five general reaction modes: substitution at carbon, substitution at boron, thermal cage rearrangement into its *meta* and *para* isomer (if the derivatives are not decomposing), base-promoted deboronation using bases such as alkoxides, alkylamines or piperidine that remove a boron vertex to form *nido*-carboranes or *nido*-carborane–base adducts, and reductive cage opening by two-electron reductions without loss of boron to form *nido*-dianions (as shown in **Fig. 1.1.2**). In the following, only the first two reaction modes will be discussed in detail.[1]

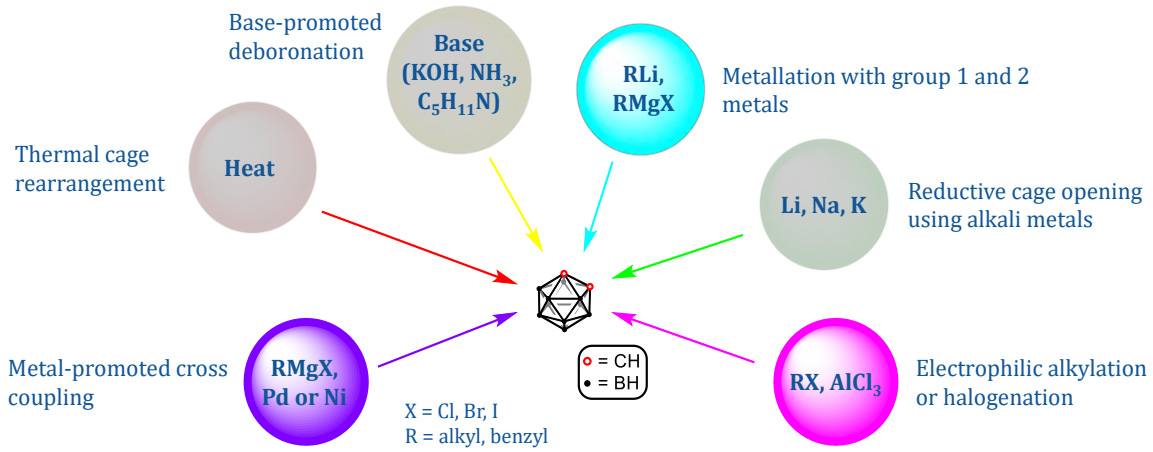


**Fig. 1.1.2.** Different possibilities for the modification of the *ortho*-carborane cluster.[1]

A versatile approach towards the substitution of one or both of the CH protons in the parent *ortho*-carborane involves the replacement with an alkali or alkaline-earth metal to generate 1-M-$C_2B_{10}H_{11}$ or 1,2-$M_2$-$C_2B_{10}H_{10}$ (M = metal) which can be further modified by the reaction with different electrophiles.[1,7] Based on the polarity differences between C-bound and B-bound hydrogen atoms, a selective removal is possible. The more acidic character of the C-bound hydrogen atoms allows a removal by nucleophiles such as organolithium compounds while a replacement of the more hydridic hydrogen atoms from boron is possible *via* electrophilic iodination.[6] A general approach towards homo- and heteronuclear C-substituted carboranes is displayed in **Scheme 1.1.1**. For the symmetrical carboranes, *ortho*-carborane is reacted with two equivalents of *n*-butyllithium forming the 1,2-dilithiocarborane. This lithium salt can be further functionalized by treatment with two equivalents of an electrophile to yield a symmetrical disubstituted carborane (bottom pathway). In the case of the unsymmetrical compounds, a selective mono-lithiation is necessary before the first electrophile can be reacted with the lithium salt. The obtained monosubstituted compound can be used as a monodentate ligand or a second substituent can be introduced. However, it is necessary to introduce a substituent first, which does not react with *n*-butyllithium to avoid the cleavage of already formed bonds, especially the C–P bond.[6]

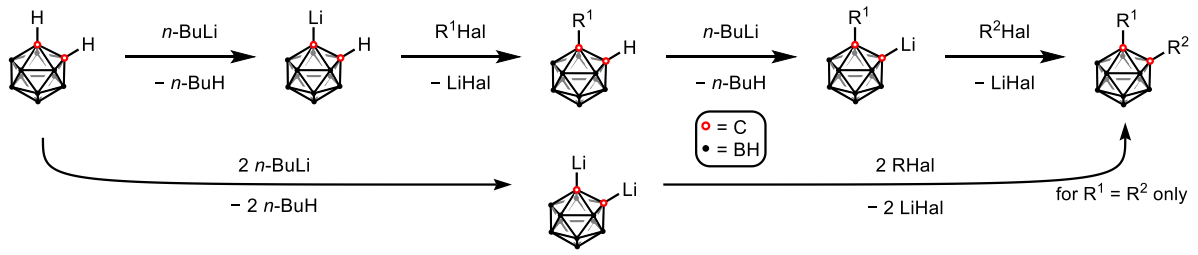


**Scheme 1.1.1.** General reaction pathway for the synthesis of symmetrical (bottom pathway) and unsymmetrical C-substituted *ortho*-carboranes (top pathway) by utilization of *n*-butyllithium.[6]

It is further possible to introduce functional groups at boron atoms, though it is more challenging due to the lowered polarity of BH and lesser reactivity towards nucleophiles. The reaction of B–H to B–X is limited to halogens, mercury, sulfur, thallium and transition metals. Usually, the introduction of substituents is accomplished by reactions on an existing *closo*-carborane cage but a synthesis starting from decaborane derivatives or *nido*-$C_2B_9$- or $C_2B_{10}$-dianions is possible (indirect approach).[1] More often, a direct substitution is performed employing nucleophilic displacement using $PhI^+$, electrophilic alkylation using $AlCl_3$, electrophilic halogenation, thermal iodination, photochemical (radical) halogenation, fluorination, B–Hg bond formation, and metal-promoted cross-coupling of B-halo-*ortho*-carboranes (for a brief overview, see **Scheme 1.1.2**).[1]

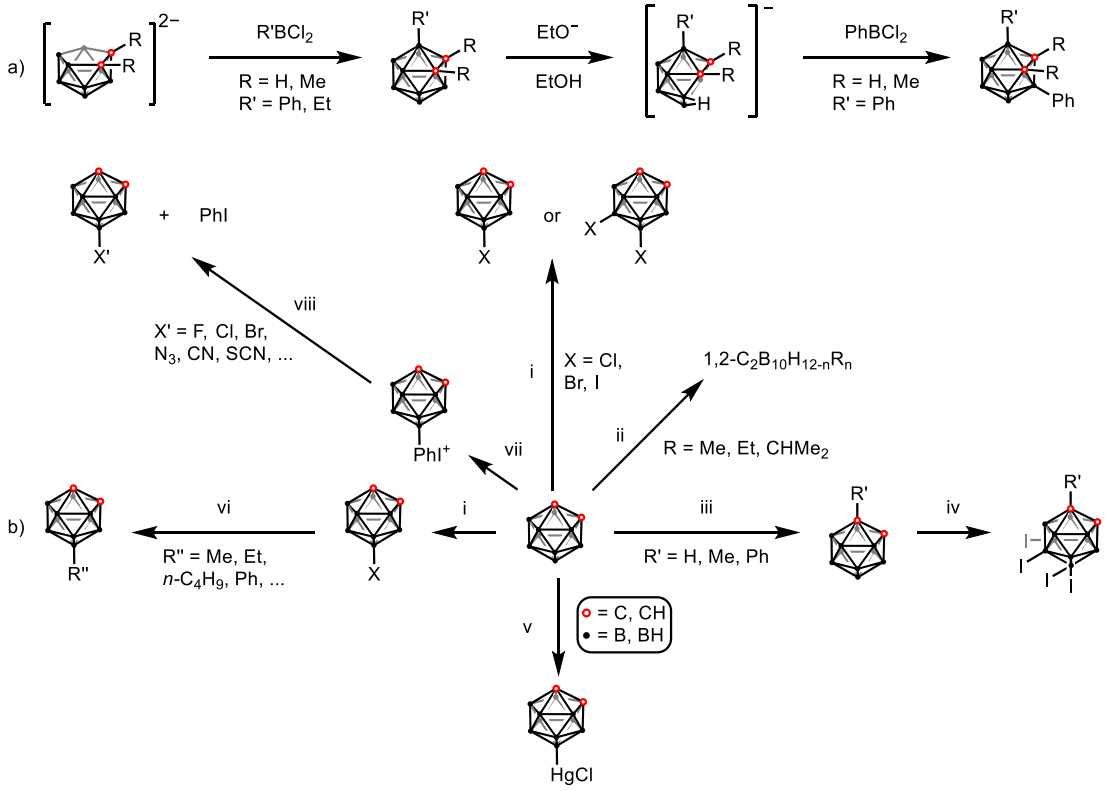


**Scheme 1.1.2.** (a) Indirect approach: Boron insertion into *nido*-$R_2C_2B_9H_{10}$ dianions to generate *closo*-1,2-$C_2B_{10}H_{12}$ derivatives, followed by deboronation and a second boron insertion to form B(3,6)-disubstituted products. (b) Direct approach: (i) $X_2$, $AlCl_3$/$FeCl_3$/strong acid; (ii) RX, $AlCl_3$; (iii) *n*-butyllithium, $CH_2Br_2$, Mg, $H_2O$ (R' = Me) or *n*-butyllithium, CuCl, PhI, pyridine for (R' = Ph); (iv) $I_2$, no solvent, 270 °C; (v) $[(CF_3CO_2)_2Hg]$, $CF_3COOH$, NaCl; (vi) R''MgX, $[Pd(PPh_3)_4]$; (vii) $H^+$, $K_2S_2O_8$, PhH; (viii) $X'^-$.[1]

Their delocalized three-dimensional aromatic bonding, high stability, and potential for a site-selective functionalization make carboranes a multifaceted class of electronically tunable compounds. Therefore, it is not surprising that many research groups found interest in carboranes in recent years as building blocks for medicinal applications, supramolecular assemblies, metal complexes, and macrocyclic compounds.[8–11]

### 1.1.4 Carboranylphosphines

Phosphorus ligands are among the most widely used ligands in coordination chemistry which is associated with their utilization in phosphine transition metal complexes applied in catalysis.[12] Specifically, bidentate phosphines play a major role. Ethylene or *ortho*-phenylene bridged ligands with a $C_2$ symmetry are favored because of the formation of stable five-membered rings with transition metals. Depending on the attached substituents, the phosphorus atom can be electron-donating or electron-withdrawing. On the level of orbitals, a lone electron pair promotes the formation of σ bonds, and empty σ* orbitals are available facilitating a π backbonding with the transition metal. The σ donor strength decreases with more electron-withdrawing substituents while the π backbonding is increased.[6]

Substitution of the hydrogen atoms in carboranes by different heteroatoms such as carbon, nitrogen, oxygen, phosphorus, and sulfur already yielded a big scope of PP,[13–15] PN,[16] PS,[17] PC,[18] as well as other (hemilabile) ligands for transition metal complexes and catalytically active metals (see **Fig. 1.1.3**)

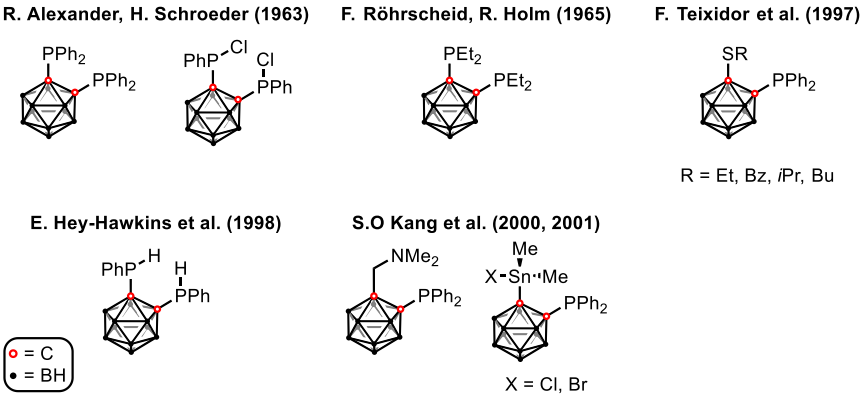


**Fig. 1.1.3.** Different C-substituted *ortho*-carboranes containing at least one C–P bond (homo- and hetero-donor centers) and their year of publication.[13–18]

The combination of carboranes and phosphines often leads to remarkable properties that cannot be seen or are not accessible with their organic counterparts.[6] Generally spoken, a synergy effect between both moieties can be observed: The phosphorus atoms in mono- and bisphosphino-*ortho*-carboranes grant a unique adaptability on the C–C distance and they can be used as mono-, bi- or even tridentate ligands.[19] In particular, the easily accessible carborane-based phosphines where a phosphorus atom is directly linked to the carborane cage are a family of versatile compounds, where the carborane cage attracts with appealing features such as its adaptable C–C bond length, its electron-withdrawing effect, and the ability of hydridic B–H groups to engage in metal bonding.[20] As a result, they have been in focus of research for quite a while after they have been synthesized by ALEXANDER and SCHROEDER for the first time (see **Scheme 1.1.3**).[13]

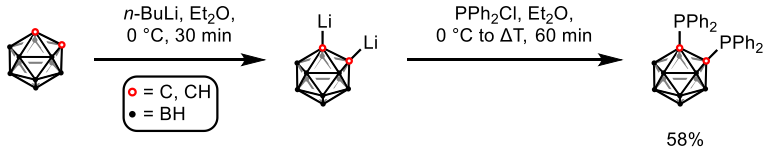


**Scheme 1.1.3.** First synthesis of 1,2-bis(diphenylphosphino)-*ortho*-carborane (dppc) in 1963.[13]

Later, a series of various symmetric and asymmetric 1,2-substituted *ortho*-carboranylphosphines were synthesized. If the synthesis of homodisubstituted phosphine derivatives of *ortho*-carborane is relatively simple by employing one equivalent of carborane, two equivalents of *n*-butyllithium and two equivalents of the appropriate halophosphine, the synthesis of monosubstituted phosphine derivatives or heterodisubstituted phosphine derivatives of *ortho*-carborane is more complex.[19]

The high stability of phosphines attached to carboranes in their solid state and in solution in the presence of oxygen, alcohols or acids is reflected in their $^{31}$P NMR chemical shifts (see **Fig. 1.1.4**).

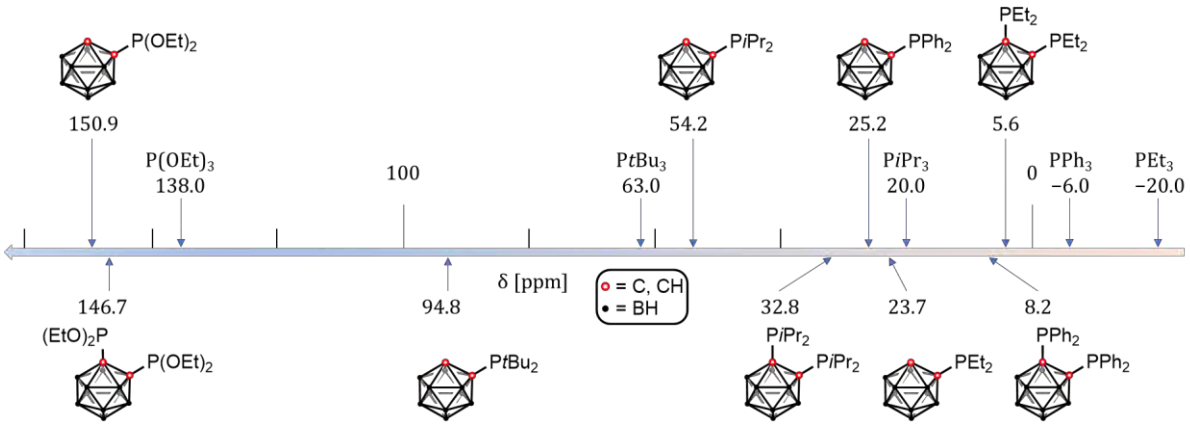


**Fig. 1.1.4.** $^{31}$P NMR chemical shifts (in ppm) of selected alkyl-, aryl- and carboranyl-phosphines.[19,21] The deuterated solvents can vary.

The electron density drawn away from the phosphorus atoms directly attached to the $C_{Cage}$ atoms leads to $^{31}$P NMR signals at higher resonances than compared with trialkyl- or triarylphosphines $PR_3$ (R = Et, *i*Pr, *t*Bu, Ph). This means that the carboranyl moiety has a strong electron-acceptor character (bigger than a phenyl group).[19]

As mentioned before, not only C–P bonds can be formed. To form B–P bonds, two steps are necessary (see **Scheme 1.1.4**). After synthesizing the 9-iodo derivative in a FRIEDEL-CRAFTS-like reaction using $AlCl_3$ as LEWIS acid, subsequent Pd-catalyzed cross-coupling reactions can be used to introduce a phosphorus atom at the B9 atom.[22]

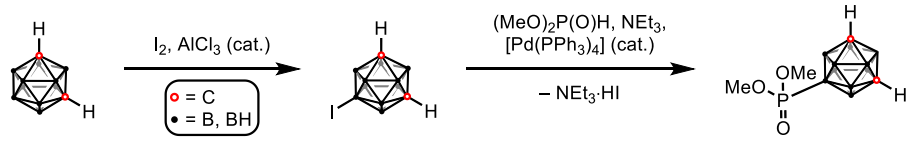


**Scheme 1.1.4.** Synthesis of boron-substituted *meta*-carboranyl phosphonates.[22]

A similar pathway is possible for the *para* isomer but cannot be applied for the *ortho*-carborane because the 9-iodo-*ortho*-carborane, as well as other *ortho*-carborane derivatives, were cleaved at elevated temperatures at 85 °C to 90 °C with triethylamine in toluene.[22] To obtain *ortho*-carboranes with phosphorus in the B9 position, it is necessary to introduce a chalcogen spacer *via* a FRIEDEL-CRAFTS reaction. In this reaction, elemental sulfur or another chalcogen chloride is used with $AlCl_3$ and subsequently reacted with a chlorophosphine in the presence of a base to obtain the carboranyl phosphite (see **Scheme 1.1.5**).[6]

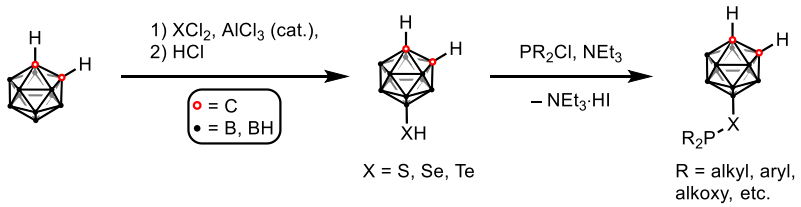


**Scheme 1.1.5.** Synthesis of boron-substituted *ortho*-carboranylchalcogenophosphines.[6]

In conclusion, the easily accessible 1,2-diphosphorylated carboranes are a class of versatile compounds with appealing properties based on the carborane scaffold such as their adaptable C–C bond, their electron-withdrawing effect, and the ability of hydridic B–H groups to engage in metal bonding.[6] Carboranylphosphines are hence intriguing ligands for metal complexes utilized in homogeneous catalysis.[12]

## 1.2 Carboranylphosphines as ligands for the complexation of transition metals

An accurate selection of the ligand is often as decisive as the choice of the metal for metal-catalyzed homogeneous catalysis. As already demonstrated, the carborane cage used as a backbone produces a variety of new phosphines with remarkable properties. These in turn can be further tailored on demand and transformed into suitable ligands.[19] So far, twelve different catalytic processes with carboranylphosphines have been described ranging from hydrogenation, hydroformylation, hydrosilylation, carbonylation, amination, alkylation and sulfonylation, KHARASCH reaction, polymerization, ring-opening metathesis polymerization, and cyclopropanation to cross-coupling with GRIGNARD reagents, and finally, a SONOGASHIRA coupling with hydride transfer.[6]

The *ortho*-carborane, but also the *nido*-carborane derivatives have obtained the most attention due to the convenient arrangement of the carbon atoms, facilitating the synthesis of

chelating ligands and their availability.[12] The following examples will only deal with carboranylphosphine-based metal complexes where the phosphorus atom is directly attached to the carborane cage.

### 1.2.1 First complexes formed

After the first synthesis of 1,2-bis(diphenylphosphino)-*ortho*-carborane (dppc),[13] almost immediately researchers directed their interest towards its application to form transition metal complexes starting with nickel (see **Scheme 1.2.1**). If properly substituted, this new basic molecular framework provided by the carborane can be used as a bifunctional ligand. The carbon atoms in the cluster can be implicated in five-membered exocyclic rings.[14] The first square-planar $Ni^{II}$ complexes with a stoichiometry of 1:1 or 1:2 ($Ni^{II}$/ligand) were formed from different $Ni^{II}$ salts.[14,23,24] ALLENDER and SMITH prepared the first five-coordinated $Ni^{II}$ complexes $(Et_4N)[NiX_3(dppc)]$ (X = Cl, Br, I) in a $PPX_3$ environment which was not possible with other known phosphines before such as 1,2-bis(diphenylphosphino)ethane (diphos) or triphenylphosphine yielding only tetrahedral complexes.[25]

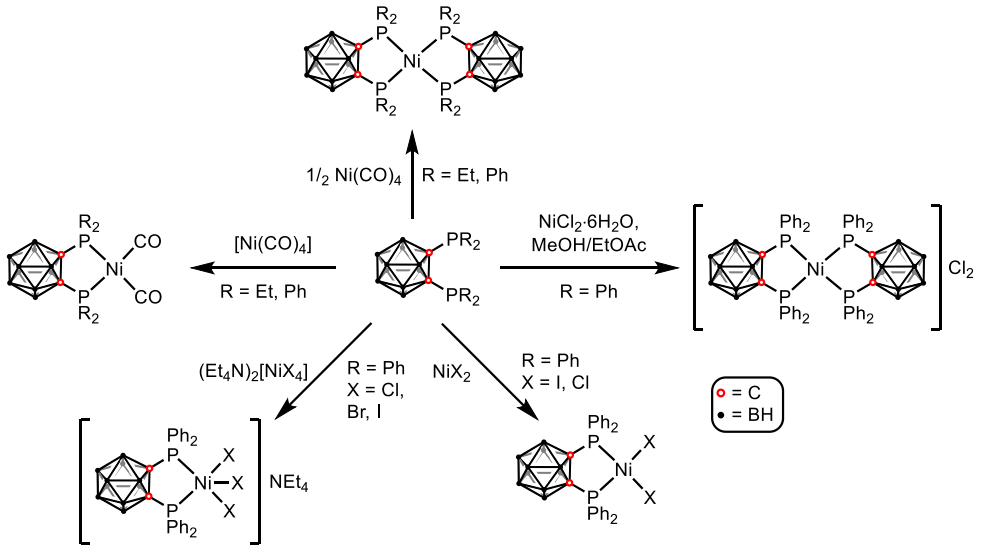


**Scheme 1.2.1.** First complexes formed with the dppc as ligand from different $Ni^{II}$ salts[14,23,24] as well as the first five-coordinate $PPNiX_3$ species.[25]

Most structural investigations and methods of characterization at this time focused on the electronic spectra of these complexes. Interestingly, the nickel dicarbonyl complex (R = Ph) showed two strong carbonyl vibrations at 2021 and 1966 $cm^{-1}$. These frequencies are 30–40 $cm^{-1}$ higher than those found for other similar tetrahedral complexes indicating the greater tendency of the bisphosphino-*ortho*-carboranyl moiety to back-accept electron density.[14] When comparing the complex geometries formed from monophosphino- and bisphosphino-*ortho*-carborane derivatives, it can be seen that with $Ni^{II}$, but also with $Pd^{II}$ and $Pt^{II}$, *trans*-square planar complexes are favored for the monophosphines and *cis*-square planar complexes for the bisphosphines.

By now, transition metal complexes with transition metals from group six to twelve have been synthesized (Cr, Mo, W, Mn, Re, Fe, Ru, Os, Co, Rh, Ir, Ni, Pd, Pt, Cu, Ag, Au, Zn, Hg).[12]

### 1.2.2 Palladium complexes

Palladium complexes of carboranylphosphines are well studied, similar to the nickel complexes.[12] Mixing dppc with [$PdCl_2$(cod)] (cod = 1,5-cyclooctadiene) or [$PdCl_2(PhCN)_2$] in non-nucleophilic solvents yielded *cis*-[$PdCl_2$(dppc)] which crystallizes with a slightly distorted square-planar geometry.[26] Other complexes were obtained by replacement of cod in [PdClMe(cod)] by dppc, 1,2-(P*i*$Pr_2$)$_2$-1,2-$C_2B_{10}H_{10}$ (dipc), or by the reaction of [$PdCl_2$L] (L = dipc, dppc) with $SnMe_4$. The carboranylphosphine acts as a bidentate ligand and binds *via* its two phosphorus atoms to the $Pd^{II}$ atom, while the remaining substituents in *cis* positions have a distorted square-planar geometry.[27] Over time, different other metal complex precursors were used to synthesize a variety of $Pd^{II}$ complexes (shown in **Scheme 1.2.2**).[24,26,28,29] Some of these carboranylphosphine palladium complexes have been further used for an in-depth $^{31}$P NMR spectroscopic analysis and comparison of the electronic properties with their organic analogs 1,2-bis(diphenyl-phosphino)benzene (dppb), 1,2-bis(diisopropylphosphino)benzene, diphos and 1,2-bis(diiso-propylphosphino)ethane.[27]

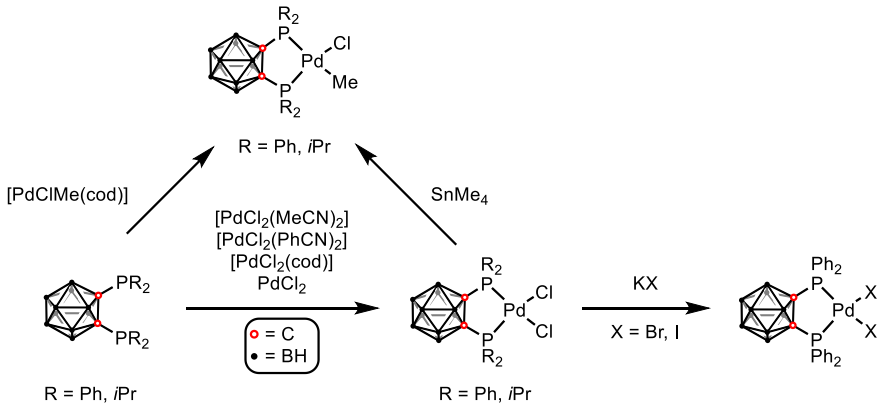


**Scheme 1.2.2.** Different palladium complexes formed with dppc or dipc.[24,26,28,29]

For most of the dichlorido complexes, a deboronation seems favored if nucleophiles are around forming *nido*-carboranylphosphine complexes. For this reason any nucleophilic solvent should be avoided during the preparation of these compounds if a deboronation should be suppressed.[26] Another interesting aspect of the palladium coordination chemistry could only be achieved using carboranylphosphines. Octa- and nonanuclear palladium complexes were obtained by decomposition of [$PdCl_2${1,2-(P*t*BuCl)$_2$-1,2-*closo*-$C_2B_{10}H_{10}$}] in $CH_2Cl_2$ or toluene after several months in the dark without stirring (see **Scheme 1.2.3**).[30]

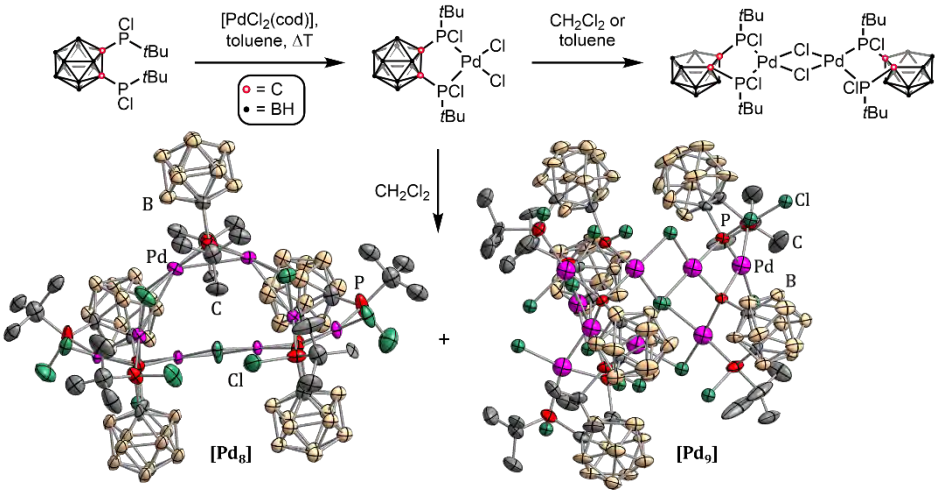


**Scheme 1.2.3.** Synthesis of $[PdCl_2\{1,2\text{-}(PtBuCl)_2\text{-}1,2\text{-}closo\text{-}C_2B_{10}H_{10}\}]$[31] and display of the molecular structures of its decomposition products, a new octanuclear complex $[Pd_8Cl_8\{1,2\text{-}(PtBu)_2C_2B_{10}H_{10}\}(1\text{-}P\text{-}2\text{-}PtBuCl\text{-}C_2B_{10}H_{10})_2(1\text{-}PCl\text{-}2\text{-}PtBuCl\text{-}C_2B_{10}H_{10})_2]$ as $CH_2Cl_2$ solvate (left) and a nonanuclear palladium complex $[Pd_9Cl_9(1\text{-}PCl\text{-}2\text{-}PtBuCl\text{-}C_2B_{10}H_{10})_3(1\text{-}P\text{-}2\text{-}PtBuCl\text{-}C_2B_{10}H_{10})_3]$ as $CH_2Cl_2$ solvate (right)[30] with thermal ellipsoids drawn at the 50% probability level. Hydrogen atoms have been omitted for clarity. P atoms red, Pd atoms violet, Cl atoms green, B atoms beige, C atoms black.

Both structures have similar core features. Some of the $Pd^{II}$ atoms are either coordinated by four carboranyl phosphorus ligands or bridged by two chlorido ligands. The resemblance of both structures seems to indicate a self-assembly process during the decomposition of $[PdCl_2\{1,2\text{-}(PtBuCl)_2\text{-}1,2\text{-}closo\text{-}C_2B_{10}H_{10}\}]$.[30]

Until recently, no data on the synthesis of B-substituted carboranylphosphines has been reported, even though substituents at the carborane cage should impact the characteristics of the phosphine groups linked to carbon atoms and hence the catalytic activity of complexes generated by them. The first series of B9-substituted carboranylphosphines was synthesized by KALININ and co-workers to look for novel carboranylphosphines for catalytic systems and investigate their behavior. Starting with 9-R-*ortho*-carborane derivatives (R = I, *i*Pr, $SCH_3$),[7] various palladium, chromium, and molybdenum complexes were prepared. Furthermore, heating of a mixture of the dppc ligand with metal carbonyls (M = Cr, Mo) resulted in the formation of several new complexes. In the presence of $[PdCl_2(PhCN)_2]$ another $Pd^{II}$ complex could be formed (see **Scheme 1.2.4**).[7]

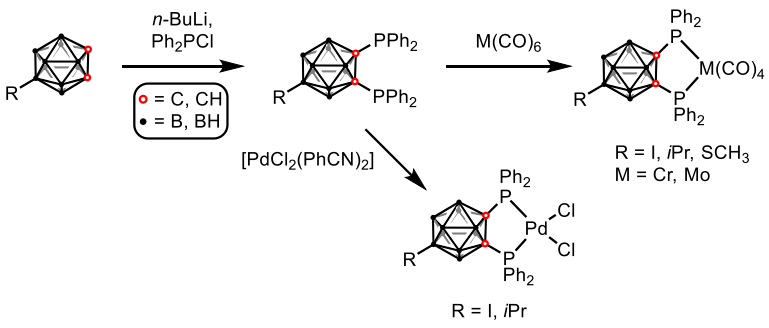


**Scheme 1.2.4.** First synthesis of B9-substituted carboranylphosphines and complexation reactions.[7]

$^{31}P\{^{1}H\}$ NMR spectroscopy was used to explore the impact of the substituents in the B9 position and the ligand environment on the complexing ability of the produced ligands.[7] In the $^{31}P\{^{1}H\}$ NMR spectra of the synthesized complexes, as well as in the spectra of the free ligands, the two phosphorus signals appeared as an AB spin system. Nonequivalence of the phosphine substituents is determined by the presence of the substituent in B9 position, which reduces the symmetry of the carborane cage.

In general, the affinity of a bisphosphine ligand for a metal can be estimated by the difference between the phosphorus chemical shifts in the $^{31}P\{^{1}H\}$ NMR spectra of the metal and the corresponding free ligand and often is expressed as the chemical shift difference ($\Delta\delta_P = \delta_P\text{complex} - \delta_P\text{ligand}$).[32] The reason is the deshielding of the phosphorus atoms upon complexation as a result of the reduction of electron density at the phosphorus atoms due to the coordination to the metal. Therefore, within a series of structurally related bisphosphine ligands, the larger chemical shift difference indicates higher chelating power of the ligand.[27] Different substituents in the 1,2-bisphosphanyl-substituted carborane ligands should affect the chemical shift difference. Analysis by $^{31}P\{^{1}H\}$ NMR spectroscopy showed that the substituent at B9 affects the complexing power of carboranyl ligands; however, the nature of the metal and its ligand environment are the most important factors determining the chemical shift difference (see **Tab. 1.2.1**).[7]

**Tab. 1.2.1.** $^{31}P\{^{1}H\}$ NMR data (in $CDCl_3$) for the B9-substituted dppc ligands and their complexes with transition metals.[7]

| B9-substituent | Free ligand $\delta_P$ / ppm | $J_{AB}$ / Hz | Metal | $\delta_P$ / ppm | $J_{AB}$ / Hz | Chemical shift difference $\Delta\delta_P$ / ppm |
|---|---|---|---|---|---|---|
| **R = I** | 5.9, 7.8 | 121.5 | **Pd** | 78.5, 79.6 | 12.1 | 72.7, 71.8 |
| | | | **Mo** | 91.1, 91.1 | 27.7 | 85.2, 83.3 |
| | | | **Cr** | 113.5, 113.6 | 41.1 | 107.7, 105.8 |
| **R = *i*Pr** | 5.0, 6.9 | 123.0 | **Pd** | 76.5, 77.1 | 10.4 | 71.6, 70.2 |
| | | | **Mo** | 87.2, 88.2 | 26.7 | 82.2, 81.3 |
| | | | **Cr** | 109.6, 110.4 | 39.9 | 104.6, 103.5 |
| **R = $SCH_3$** | 5.3, 7.4 | 121.5 | **Mo** | 88.4, 89.4 | 27.4 | 83.1, 82.0 |
| | | | **Cr** | 110.8, 111.6 | 40.1 | 105.5, 104.3 |

### 1.2.3 Cobalt complexes

After the preparation of the nickel complexes, other divalent salts of the 3d series of transition metals moved into the focus of research. In 1974,[33] different $Co^{II}$ complexes were synthesized

and characterized (see **Scheme 1.2.5**). There are only a few examples where cobalt salts were used for the complexation because these complexes are easily decomposed by solvents like EtOH or water.[19]

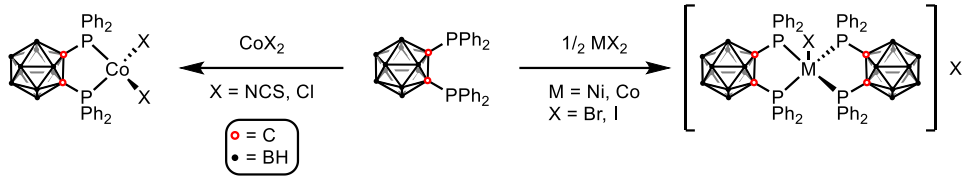


**Scheme 1.2.5.** Different complexes formed from divalent $Ni^{II}$ and $Co^{II}$ salts.[33]

$[CoX_2(dppc)]$ (X = Cl, NCS) appeared to be typical tetrahedral species based on their electronic spectra and nonconductive behavior in nitromethane, while $[CoX(dppc)_2]^+$ is similar to the pentacoordinate square-pyramidal structure of $[CoX(diphos)_2]^+$.[33,34]

### 1.2.4 Rhodium complexes

The first rhodium complexes with carboranylphosphines were described by HART and OWEN in 1985 (see **Scheme 1.2.6**).[35]

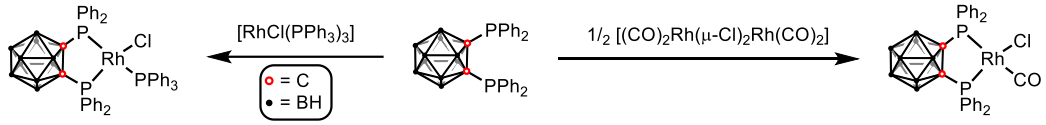


**Scheme 1.2.6.** Different rhodium complexes formed with the dppc ligand.[35]

Both complexes were further tested for their application in the catalytic hydrogenation and hydroformylation reaction of different olefins as shown in **Scheme 1.2.7**. It was indicated that [RhCl(dppc)(CO)] effectively catalyzed the hydroformylation under fairly mild conditions for this reaction. However, it is somewhat unselective regarding the products. The lack of selectivity in the carbonylation reaction is surprising, although $[RhH(diphos)(CO)PPh_3]$, which also incorporates a chelate bisphosphine, shows a similar lack of specificity.[36] At higher temperatures $[RhCl(dppc)PPh_3]$ is an effective hydrogenation catalyst.[35]

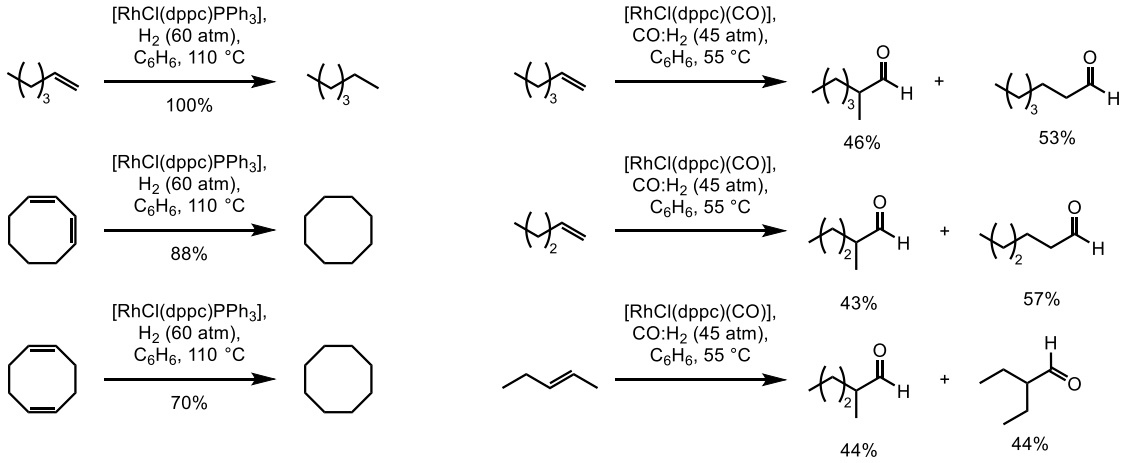


**Scheme 1.2.7.** Hydrogenation and hydroformylation experiments using the aforementioned rhodium(I) carboranylphosphine complexes.[35]

Only a few neutral *ortho*-carborane-based complexes were prepared. The majority of rhodium complexes were prepared with *nido*-carboranes.[12] TEIXIDOR and co-workers[37] described two strategies in 1996 to obtain a family of new $Rh^{I}$ complexes formally analogous to the WILKINSON catalyst, chloridotris(triphenylphosphine)rhodium(I),[38] by substitution of the chlorido ligand and $PPh_3$ group with the anionic bisphosphino ligand. The complexes could be prepared by either partial deboronation if a suitable nucleophile was around (such as EtOH) during the complexation reaction or by reaction with the previously prepared *nido*-carboranylbisphosphine. The synthesized complexes only marked the starting point for many other $Rh^{I}$ complexes formed with the new anionic ligand by the exchange of the carbonyl ligands with N- or P-donor ligands (see **Scheme 1.2.8**).

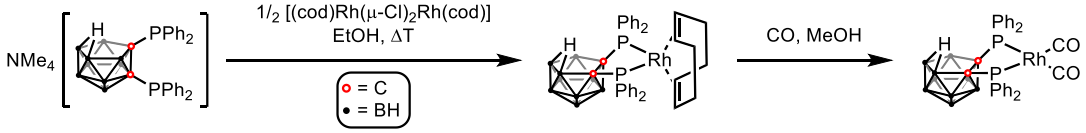


**Scheme 1.2.8.** Starting point for several different *nido*-carboranylbisphosphine rhodium(I) complexes.[37]

### 1.2.5 Ruthenium complexes

Neutral ruthenium complexes were prepared, however, a catalytic application could be only found for anionic ruthenium complexes in cyclopropanation and KHARASCH addition reactions.[39,40] The complexes were prepared from either dppc, 1,2-bis(diethylphosphino)-*ortho*-carborane (depc), or 1,2-bis(diethyl phosphite)-*ortho*-carborane (doepc) in refluxing EtOH (see **Scheme 1.2.9**).[41]

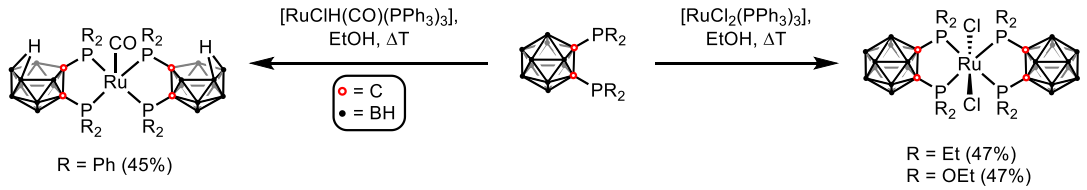


**Scheme 1.2.9.** Different ruthenium complexes formed with the carboranylbisphosphine ligands.[39,40]

Even though mostly dirhodium carboxylates or carboxamidates, as well as copper complexes modified with nitrogen-containing ligands, were found superior for cyclopropanation reactions of alkenes with diazo compounds, TEIXIDOR and co-workers could show that their $Ru^{II}$ complexes are excellent for the cyclopropanation of activated olefins such as styrene and its derivatives with ethyl diazoacetate but not with cyclic olefins or terminal alkenes (see **Scheme 1.2.10**).[39] In all cases, the *trans* (exo) isomer was favored. After increasing the steric bulk of the diazoacetate from methyl to ethyl and *tert*-butyl, more *trans* product could be obtained.

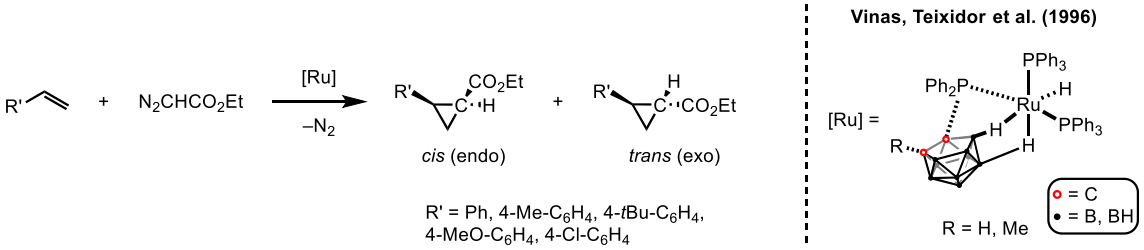


**Scheme 1.2.10.** Catalytic cyclopropanation using a ruthenium complex.[39,41]

They further demonstrated that different carboranylphosphine $Ru^{II}$ complexes could be used for the mediation of a KHARASCH addition of $CCl_4$ across different olefins (styrene, *n*-butyl acrylate, methyl methacrylate) and an atom transfer radical polymerization of methyl methacrylate in a highly controlled manner (see **Scheme 1.2.11**).[40] The complexes prepared by TEIXIDOR and co-workers can be described as unsaturated 14-electron-$Ru^{II}$ complexes with two B–H→Ru agostic interactions which makes them highly efficient catalysts for the promotion of radical reactions.[40]

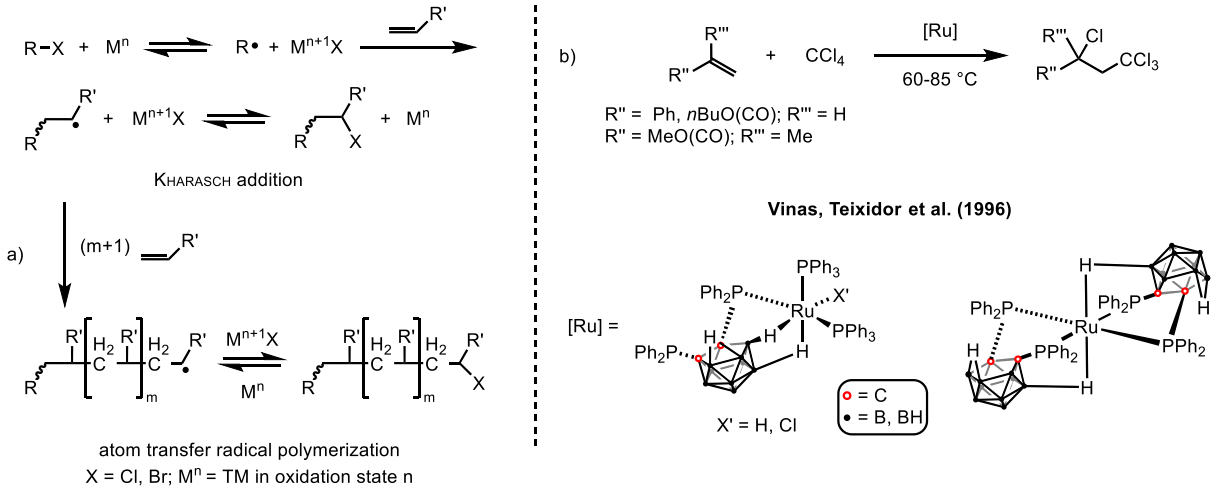


**Scheme 1.2.11.** (a) General mechanism for the KHARASCH and atom transfer radical polymerization reaction. TM = transition metal. (b) KHARASCH addition of carbon tetrachloride to representative olefins catalyzed by ruthenium complexes.[40,41]

### 1.2.6 Coinage metal complexes

Another well-studied group of metal complexes formed with carboranylphosphines are the coinage metals, especially copper and gold.

To establish the coordination ability of carboranylbisphosphine derivatives, the reaction between $Cu^{I}$ and different bisphosphine derivatives was investigated by TEIXIDOR and co-workers.[41,42] In a reaction between $[CuCl(PPh_3)_3]$ and depc, dipc, dppc, or doepc in refluxing EtOH, different mononuclear $Cu^{I}$ complexes could be prepared and no deboronation was observed (see **Scheme 1.2.12** and **Fig. 1.2.1**). $Cu^{I}$ complexes synthesized from CuX (X = Cl, Br, I) and dppc were reported in 2006 for the first time.[43] They are all di-μ-X-bridged structures with the formula $[(dppc)Cu(\mu\text{-}X)_2Cu(dppc)]$ and were synthesized by the reaction of $Cu^{I}$ salts and dppc in boiling EtOH. Surprisingly, no decapitation took place and the carborane cluster stayed intact. Switching the substituents at phosphorus to *i*Pr groups yielded similar copper(I) complexes with a distorted tetrahedral geometry.[44]

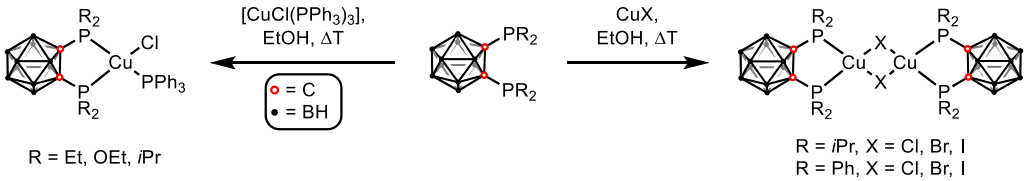


**Scheme 1.2.12.** Different $Cu^{I}$ complexes formed with various carboranylbisphosphines.[41–44]

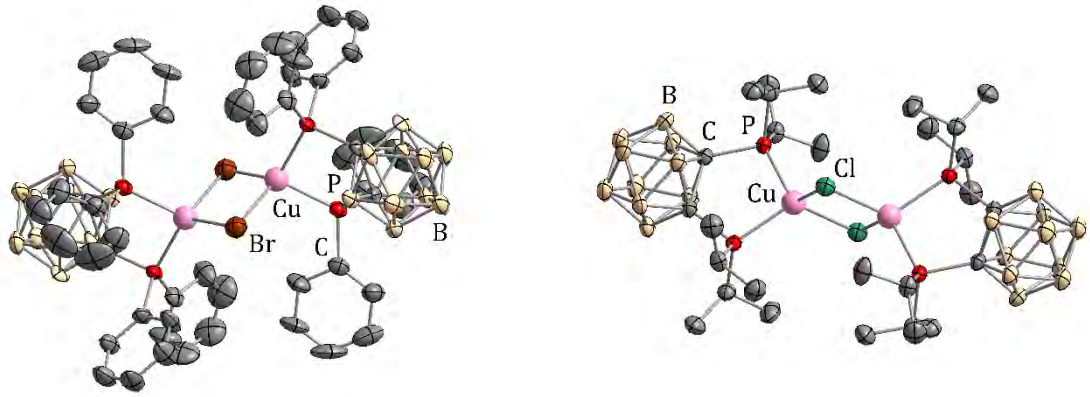


**Fig. 1.2.1.** Molecular structures of two halogen-bridged complexes in the solid state with thermal ellipsoids drawn at the 50% probability level.[43,44] Hydrogen atoms and solvent molecules have been omitted for clarity. P atoms red, Cu atoms pink, Cl atoms green, Br atoms brown, B atoms beige, C atoms black.

[(dppc)$Cu_2$(μ-I)$_2$Cu(dppc)] has been further tested as precatalyst for the catalytic amination of iodobenzene with aniline. In an ULLMANN-type-like reaction, 58% of the amine could be converted. Comparable results have been obtained with other established systems (as shown in **Scheme 1.2.13**).

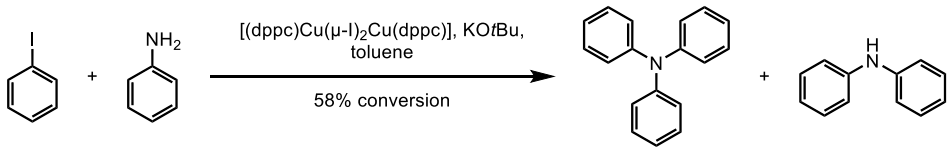


**Scheme 1.2.13.** Stoichiometric amination of iodobenzene with aniline in the presence of [(dppc)$Cu_2$(μ-I)$_2$Cu(dppc)][43]

The coordination chemistry of gold offers a variety of different complexes tunable by the stoichiometry of the reaction. Ditertiary phosphines, 1,2-$(PR_2)_2$-*ortho*-$C_2B_{10}H_{10}$ (R = $NMe_2$, Ph), have been reacted with tetraethylammonium dibromoaurate(I) to form two-, three-, and four-coordinated complexes.[45] Further, gold(I) complexes have been synthesized starting from [AuX(tht)] (X = Cl, $C_6F_5$, tht = tetrahydrothiophene) or [Au(tht)L]$ClO_4$ (L = tht, $PR_3$ or ylide) (as shown in **Scheme 1.2.14**).[46]

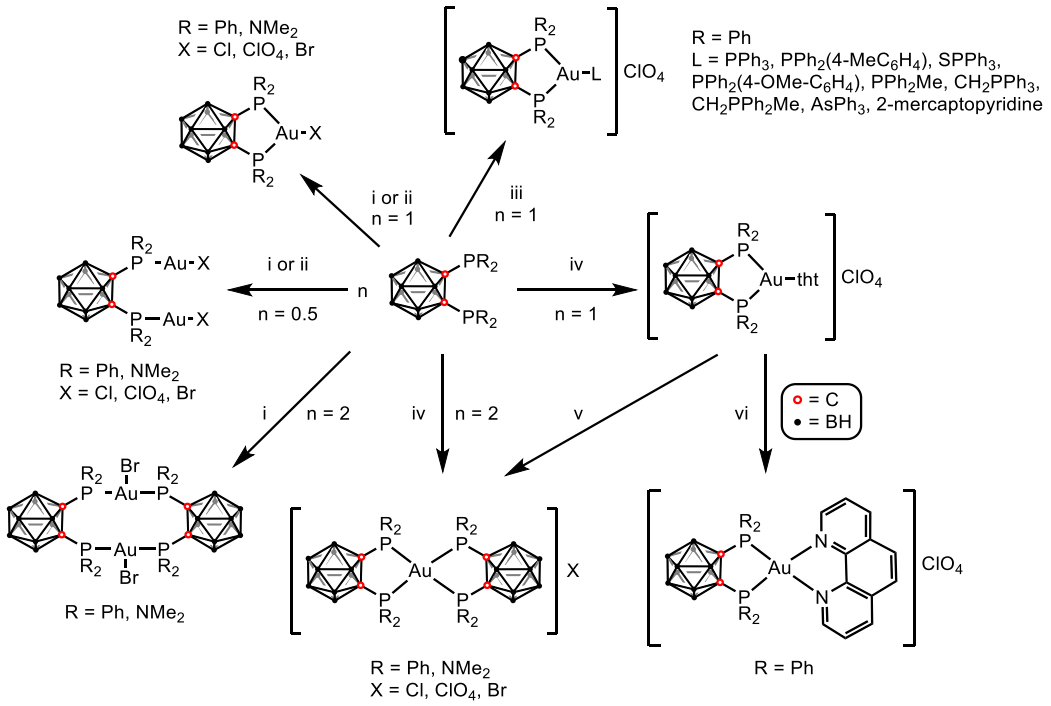


**Scheme 1.2.14.** Synthesis of different gold complexes using n equivalents of carboranylbisphosphine derivatives. (i) $[NEt_4][AuBr_2]$, $EtOH/CH_2Cl_2$; (ii) $[AuX(tht)]$, $CH_2Cl_2$; (iii) $[Au(tht)L]ClO_4$, $CH_2Cl_2$; (iv) $[Au(tht)_2]ClO_4$, $CH_2Cl_2$; (v) dppc, $CH_2Cl_2$; (vi) phenanthroline, $CH_2Cl_2$.[45,46]

Though the first carboranylphosphine was synthesized in 1963, it took more than 30 years to obtain the first *nido*-carboranylphosphine, which had significantly different properties than its parent *closo*-carboranylphosphine due to its anionic nature. Unlike *closo*-carboranylphosphines, *nido*-carboranylphosphines easily coordinate to metals due to their negative charge. The one-pot synthesis of *nido*-carboranylphosphine metal complexes starting from *closo*-carboranyl-phosphine was a watershed moment in the carboranylphosphine complexation chemistry. This breakthrough paved the way for the synthesis of a variety of organometallic complexes. Despite significant advances in the chemistry of transition metal complexes with carboranylphosphine ligands in recent years, much more study is required to better understand how these phosphines might be adjusted to achieve the desired aims. Even areas that appear to be well investigated continue to excite the interest of researchers due to the potential for using carboranylphosphine complexes of transition metals in catalysis and the design of innovative materials. Furthermore, the importance of the carborane backbone is yet unknown, necessitating future computational study on these phosphines.[12,19]

## 1.3 Entering the world of dendrimers

The development of well-defined homogeneous catalysts, enabling selective and rapid transformations and being easily and quantitively separated from the reaction products, is still a paramount challenge. Most separations in an industrial context apply methods including distillation, liquid-liquid separation or extraction, catalyst destruction, and crystallization but

generally do not overcome the separation problem of the homogeneous catalyst from the reaction products.[47,48] One commonly investigated method is the attachment of homogeneous catalysts to insoluble organic, inorganic, or hybrid supports such as silica. Problems with this approach are nonuniformity and partly unknown structures of the heterogenized catalysts, mass transport limitations, generally lower activity compared to their homogeneous analogues and metal leaching.[48] Another approach is their attachment to soluble supports. Macromolecules such as dendrimers with their well-defined architecture allow precise control of the catalyst structure,[48] and are both soluble and recoverable by nanofiltration or precipitation.[49] Furthermore, increased local concentrations of catalytic units located on the surface of dendrimers could lead to dendrimer effects showing different activities, depending on the monomer or dendrimer generation used.[49] The dendrimer effect in catalysis can induce different properties. Because dendritic catalysts are often easier to recover and metal leaching is reduced, they may frequently be reused. The influence on the rate of catalysis by a dendrimer has been already shown in a few examples such as the ester hydrolysis catalyzed by peptide-dendrimers composed of histidine–serine,[50] or [2+2+2] cycloadditions catalyzed by phosphoramidite ligands complexing rhodium(I).[51] In the following part, dendrimers and their possible use for catalytic applications will be discussed in more detail.

### 1.3.1 Dendros (δένδρος) and meros (μέρος) – Structure, synthesis and applications

The term "dendrimer" was coined by D. A. TOMALIA[52] for the first time by combining the two Greek words "dendros" and "meros" to describe its tree-like shape and its chemical structure which is constituted of several associated parts (monomers). Indeed, dendrimers are a part of the polymeric world since they are based on the association of hundreds or thousands of repetitive units. However, they differ fundamentally bearing several striking features and properties due to their arborescent construction, and cannot be synthesized by polymerization reactions. Their synthesis is carried out step-wise starting from a multifunctional core from which branches are progressively grown (see **Scheme 1.3.1**).

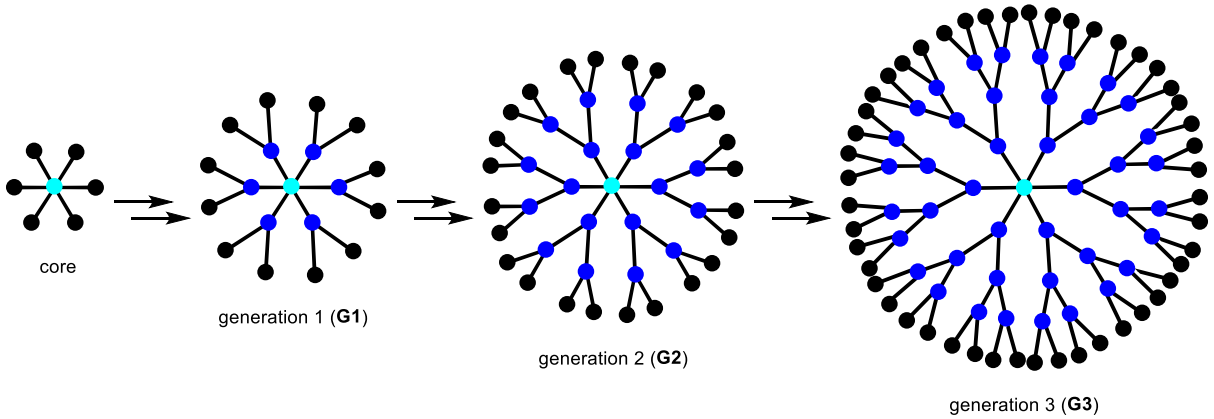


**Scheme 1.3.1.** Principle of the synthesis of dendrimers starting from a central core up to generation 3 (**G3**).

Mostly, a divergent procedure, first described by VÖGTLE and co-workers,[53] is applied for their synthesis. In the first step, an activation or modification of the core takes place. The activated core then reacts with n equivalents (n = number of modifiable groups at the level of the core) of branched monomers affording the first generation (**G1**) of a dendrimer. Consecutively, the **G1** dendrimer can be deprotected or activated again to react with 2n equivalents of a branched monomer yielding the second generation (**G2**). A new generation is obtained every time a new layer of branching units is attached (see **Scheme 1.3.2**). So far, dendrimers up to their 12$^{th}$ generation (**G12**),[54,55] and more recently up to their 13$^{th}$ generation (**G13**) have been prepared.[56] Their terminal surface functions can be easily modified at any time. However, one major drawback of this divergent process is the possible presence of defects in higher generations due to the great number of reactions taking place on a single molecule.[53,54]

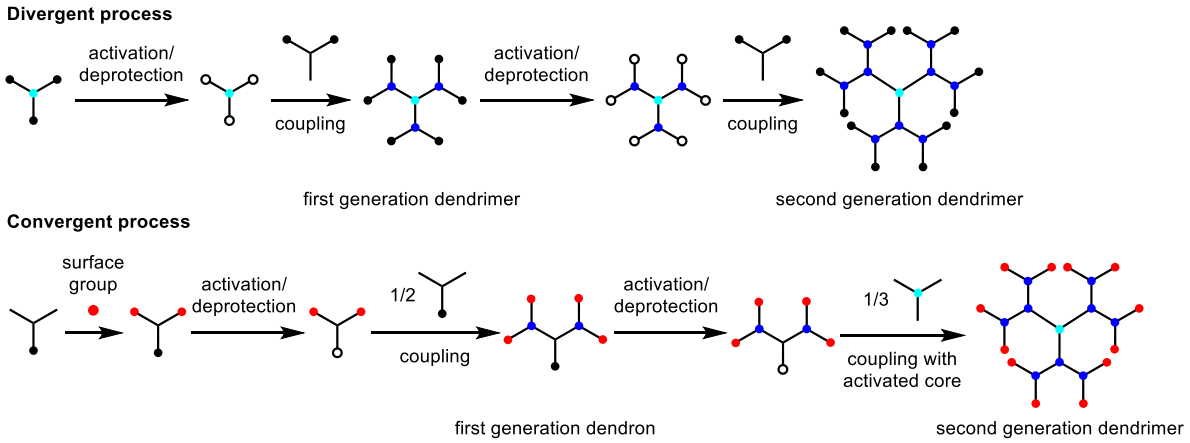


**Scheme 1.3.2.** Divergent and convergent synthetic strategies to obtain dendrimers or dendrons.[54]

A convergent route was first proposed by the group of FRÉCHET.[57] Surface functions are coupled first to an $AB_2$ monomer with one protected and therefore unreactive position. The surface groups will not be modified until the end of the synthesis of the dendritic structure. After deprotection/activation of the unreactive position, this compound is coupled through its core with another $AB_2$ monomer, to afford the first-generation dendron, which is a dendrimeric wedge. This process can be repeated to grow bigger generations of dendrons. It is further possible to attach it to a multifunctional core affording a real dendrimer. Since only a small number of reactions occur in every step, the purity of the products can be easily controlled. However, high generations cannot be synthesized and a modification of the terminal functions is more challenging.[54,58]

Dendrimers have found application in various areas. Catalysis is one of the very first published use of dendrimers.[59] Most of their catalytic properties are studied using organometallic derivatives. The electronic and optoelectronic properties of dendrimers have been

applied in different domains (photovoltaic cells, optical amplifiers, lasers, nonlinear optics). Especially, fluorescent dendrimers have been used for the elaboration of light-emitting diodes but also imaging of biological media or organisms. The modification of the surface of materials at the nanometric scale by a monolayer (or multi monolayers) of dendrimers led to the development of advanced chemical and biological sensors (pH measurement, fluorescence detection of metal cations, desoxyribonucleic acid microarrays). A further application has been found in the medicinal sector for gene transfection or drug delivery using dendrimer conjugates or encapsulation of drugs into dendrimers.[54]

### 1.3.2 Phosphorus-containing dendrimers

Over time, a variety of different dendrimers has been synthesized.[54] Most of them consist of organic fragments with a nitrogen or carbon atom as branching point such as poly(propylenimine), poly(amidoamine), poly(lysine), poly(ether), or poly(ester) dendrimers.[54,60] However, besides organic dendrimers, also main group element-containing dendrimers have been prepared such as silicon- or phosphorus-containing dendrimers.[54] Among them, the phosphorus-containing dendrimers appear to be a very versatile class of compounds with a large palette of properties and applications.[61] They were first described by ENGEL and co-workers[62] in 1990, who prepared different polyphosphonium dendrimers starting from a phosphorus trichloride core (see **Scheme 1.3.3**).

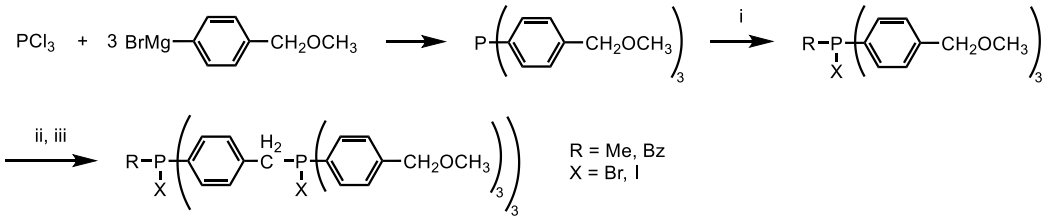


**Scheme 1.3.3.** First described synthesis of phosphorus-containing dendrimers. (i) MeI or $C_6H_5CH_2Br$; (ii) iodotrimethylsilane; (iii) tris(*p*-methoxymethylphenyl)phosphine.[62]

The most important work in the area of phosphorus-containing dendrimers was performed by CAMINADE, MAJORAL and co-workers[63] dating back to 1994. Starting from a central thiophosphoryl chloride core (**1-S0**) dendrimers up to generation 12 (**2-S12**) with 12288 terminal functions,[55] and later from a hexachlorocyclotriphosphazene core (**1-G0**), were built in a two-step reiterative procedure (see **Scheme 1.3.4**).[60]

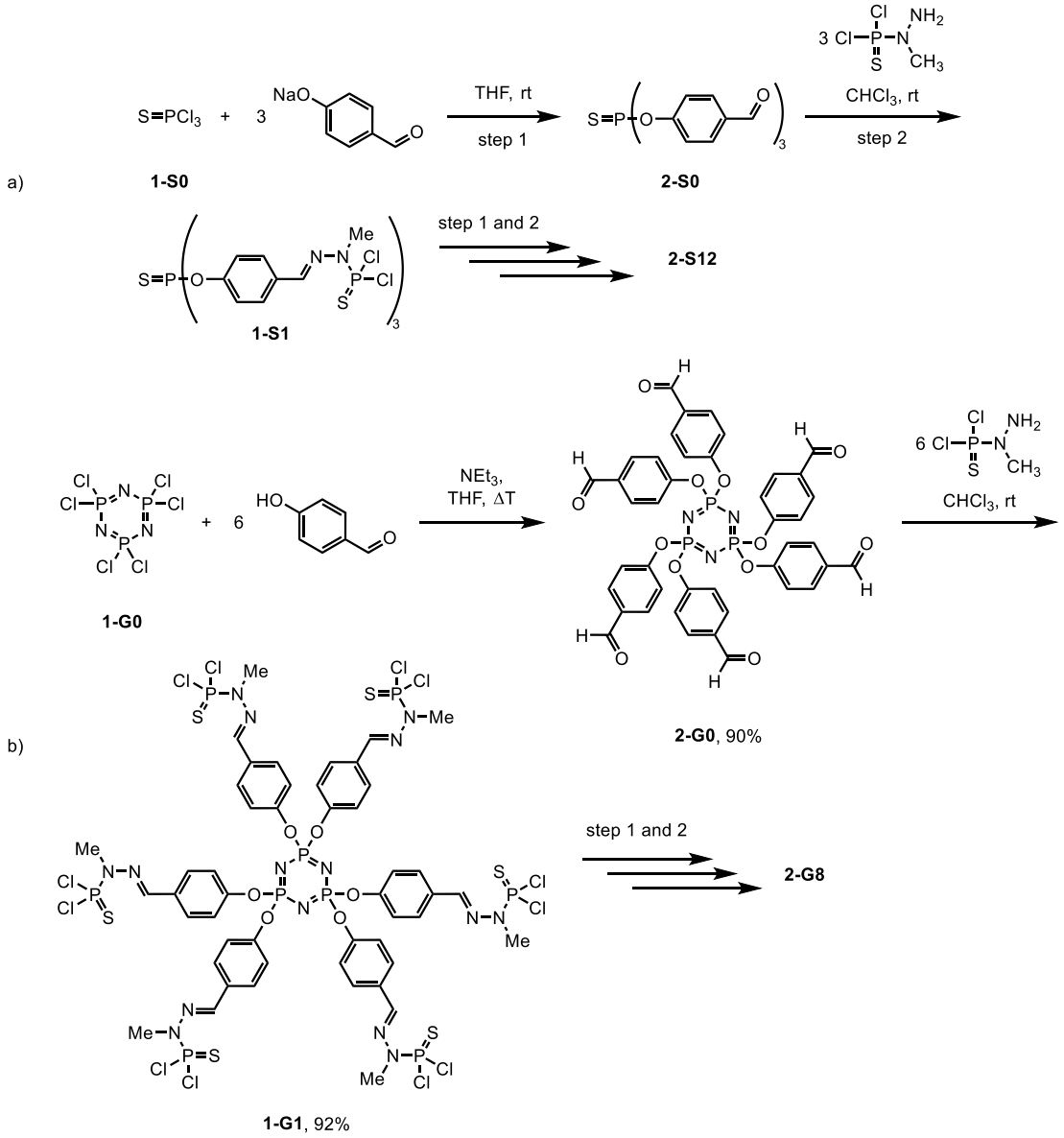


**Scheme 1.3.4.** (a) Synthetic procedure for thiophosphoryl-based dendrimers up to their 12th generation.[55,63] (b) Synthetic procedure for hexachlorocyclotriphosphazene-based dendrimers up to their 8th generation.[64] The notation **1** is indicating terminal $P(S)Cl_2$ groups, **2** is indicating terminal CHO functions.

Using 4-hydroxybenzaldehyde under basic conditions, all chlorides could be replaced by nucleophilic substitution yielding **2-S0** or **2-G0**, and the terminal aldehyde function could be consecutively reacted with the phosphorhydrazide $H_2NNMeP(S)Cl_2$ ($MMHSPCl_2$) in a condensation reaction creating a new branching point (**1-S1**, **1-G1**). Each new level of branching points generated a new generation. This synthetic procedure especially appeals with its ease, the only slight excess of reagents used and its quantitative yields forming solely the two by-products NaCl and $H_2O$.[54,60,63] This method could be later applied to a variety of cores bearing either P–Cl or CHO functions. Particularly the hexachlorocyclotriphosphazene core encountered frequently in inorganic, organic, and high-polymer chemistry has found a lot of interest,[65,66] and could be

synthesized up to generation 8 (**2-G8**) with up to 1536 terminal functions.[64] It can accommodate a greater number of dendrons (more terminal functions) for a given generation compared to the thiophosphoryl chloride core.[66]

Using $^{31}$P NMR spectroscopy, a perfect tool for the characterization of these phosphorus-containing dendrimers could be found. It does not only allow an easy and precise determination of the purity of the products but also the control of the advancement of the reaction progress.[60] The slight difference in the density at each layer, and the slight modification of the angles around the phosphorus atoms necessary to optimize the space occupation induces a slightly different chemical shift for the phosphorus atoms of each layer. In the case of terminal $P(S)Cl_2$ functions reacting with 4-hydroxybenzaldehyde, deshielding upon monosubstitution can be observed followed by shielding of the phosphorus atoms once disubstitution occurs. In the condensation reaction, deshielding can be observed for the phosphorus atoms in the phosphorhydrazide after attachment to the dendrimer.[60]

It is obvious that not only the two reiterative reaction steps can be carried out with these structures. The above-shown terminal aldehyde or phosphorhydrazide functions can be used for different functionalizations to modify the dendrimer as needed. The terminal aldehydes have been further modified with phosphonates,[67] amines,[68] or hydrazides[69] which then reacted with different phosphine species to generate terminal phosphines shown as suitable candidates for catalytic applications. Substitution reactions with phenols or amines are mostly used for dendrimers with terminal $P(S)Cl_2$ groups. The reactivity of each Cl of $P(S)Cl_2$ is different, thus two different substituents can be grafted. In the case that both substituents also possess different functional groups, the dendrimers obtained can have up to four different terminal functions.[70]

This paragraph has illustrated several structural properties of dendrimers and dendrons, as well as their synthesis. It should be emphasized that this is not a comprehensive review, but rather an introduction to this class of compounds. Although much work has already been done on their synthesis, there is still room for improvement, particularly in terms of reducing the time required at the bench. However, given the repeated nature of dendrimers, it is clear that their characterization will never be trivial, especially when their size increases.[54]

## 1.4 Combining the best of two worlds – Anchoring of homogeneous catalysts to dendrimers

### 1.4.1 Advantage of dendrimers in homogeneous catalysis

The catalytic usage of dendrimers was one of the first documented applications,[59] and it is currently one of its most important applications, as evidenced by the number of published reviews. The focus of interest for their application in homogeneous catalysis is based on a well-defined molecular architecture that permits exact control of the position of the catalyst at the perimeter or within the dendrimer (at the core or, less frequently, in the branches). As a result of

this immobilization, novel features emerge that alter reaction speeds, substrate activation, and selectivity,[71] which cannot be observed with the original monomeric catalysts.[54] This phenomenon is known as the "dendrimer effect", and it occurs when a functional group performs differently whether it is alone or when it is attached to a dendrimer. Its properties can even vary depending on the generation of the dendrimers. The dendrimer effect may be observed with every type of dendrimer and for any sort of characteristic, even though that it has been most widely studied in catalysis, biology, and, to a lesser extent, in materials.[72] For peripheral modifications when the catalyst is connected as a terminal function to the surface of the dendrimer, better catalytic performance frequently comes from high local concentrations of the catalyst and the proximal contact of the catalytic sites (positive dendrimer effect). Furthermore, unanticipated selectivities might be caused by the steric crowding of catalytic groups near the surface. However, this proximal connection might result in both cooperative and deactivation effects (negative dendrimer effect).

If the catalyst is enclosed within the dendrimer, steric shielding of the active site can improve the catalyst stability and shape selectivity. If the catalyst is directly attached at the core, these dendrimers can act as biomimetics, forming a particular habitat for substrates (much like enzymes). The isolation further prevents the interaction between different catalytic sites and the formation of inactive dimeric complexes (see **Fig. 1.4.1**).[54]

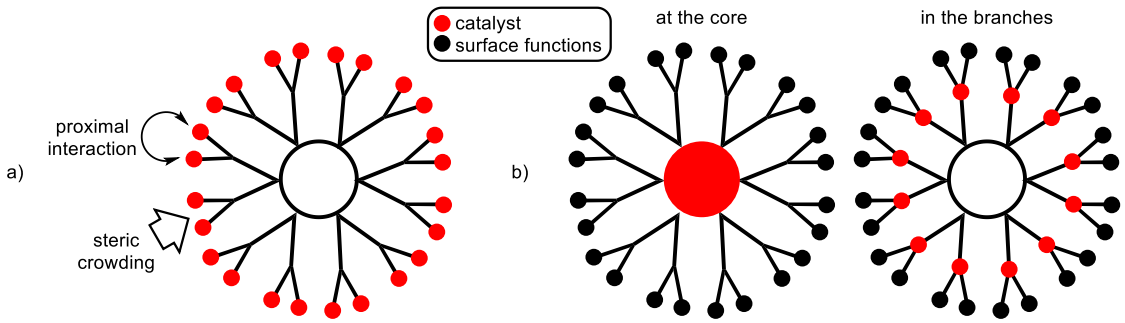


**Fig. 1.4.1.** Different dendrimer architectures: (a) Catalyst located at the periphery. (b) Catalysts located within the dendrimer.[54]

Despite their size, dendrimers are generally soluble in the reaction media. However, they are significantly greater in size than the reagents and products. As a result, by using nanofiltration, precipitation, or column chromatography, these compounds may be readily separated and recovered. The recovery and reuse (recycling) is a significant advantage over traditional monomeric catalysts.[54,73]

### 1.4.2 Peripherical functionalized dendrimers for catalysis

It should be noted that the majority of catalytic dendrimers have organometallic entities as catalytic sites. They were utilized as catalysts in a variety of processes that include the formation of C–X bonds (X = C, N, O; cross-couplings, metathesis, polymerizations) or addition to C=X double

bonds (X = C, N, O; hydrogenations, hydroformylations, KHARASCH reaction), as well as oxidation reactions. [54] Only instances with phosphorus-containing dendrimers with phosphines serving as terminal functions for transition metal complexation will be described here.

Different C–C coupling reactions (STILLE, HECK, SUZUKI, SONOGASHIRA as well as allylic alkylation) were described with complexes formed from palladium and suitable bidentate dendritic ligands (see **Scheme 1.4.1** and **Scheme 1.4.2**).[73–77]

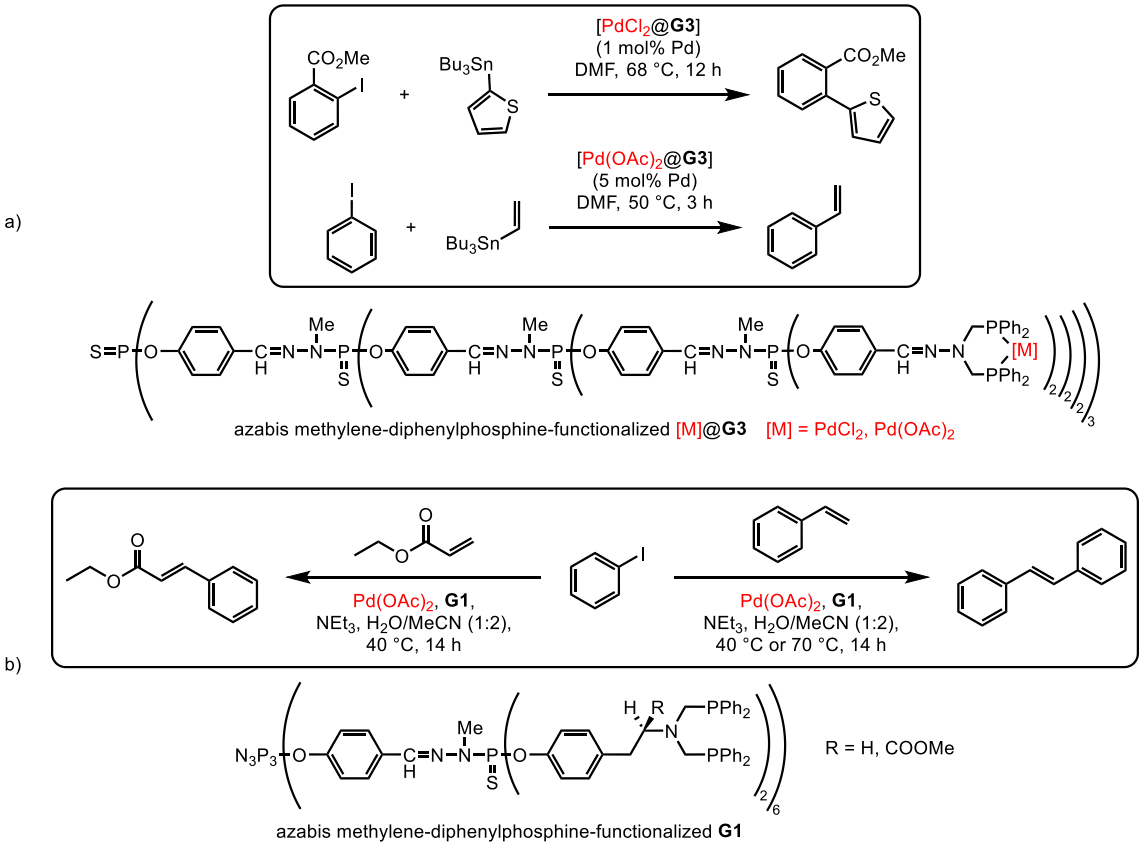


**Scheme 1.4.1.** Examples of different C–C coupling reactions using palladium complexes of phosphorhydrazone dendrimers as catalysts. (a) STILLE coupling using a palladium complex of a dendrimer as catalyst.[74] (b) HECK reaction.[75]

Dendrimers with azabis methylenediphenylphosphine terminal functions (**Scheme 1.4.1**, generations 1–4, a) were utilized in STILLE couplings to catalyze the reaction of methyl-2-iodobenzoate with 2-(tributylstannyl)-thiophene and iodobenzene with tributylvinyltin. The conversion was quantitative in both cases, and the dendritic catalysts could be retrieved and reused again.[74] HECK reactions between styrene and iodobenzene affording *trans*-stilbene, as well as ethyl acetate and iodobenzene, to afford ethyl cinnamate (**Scheme 1.4.1**, b) were carried out. The conversion of styrene is rather modest. On the contrary, the efficiency of generations 0 and 1 for ethyl acetate is more than double that of the monomer.[75]

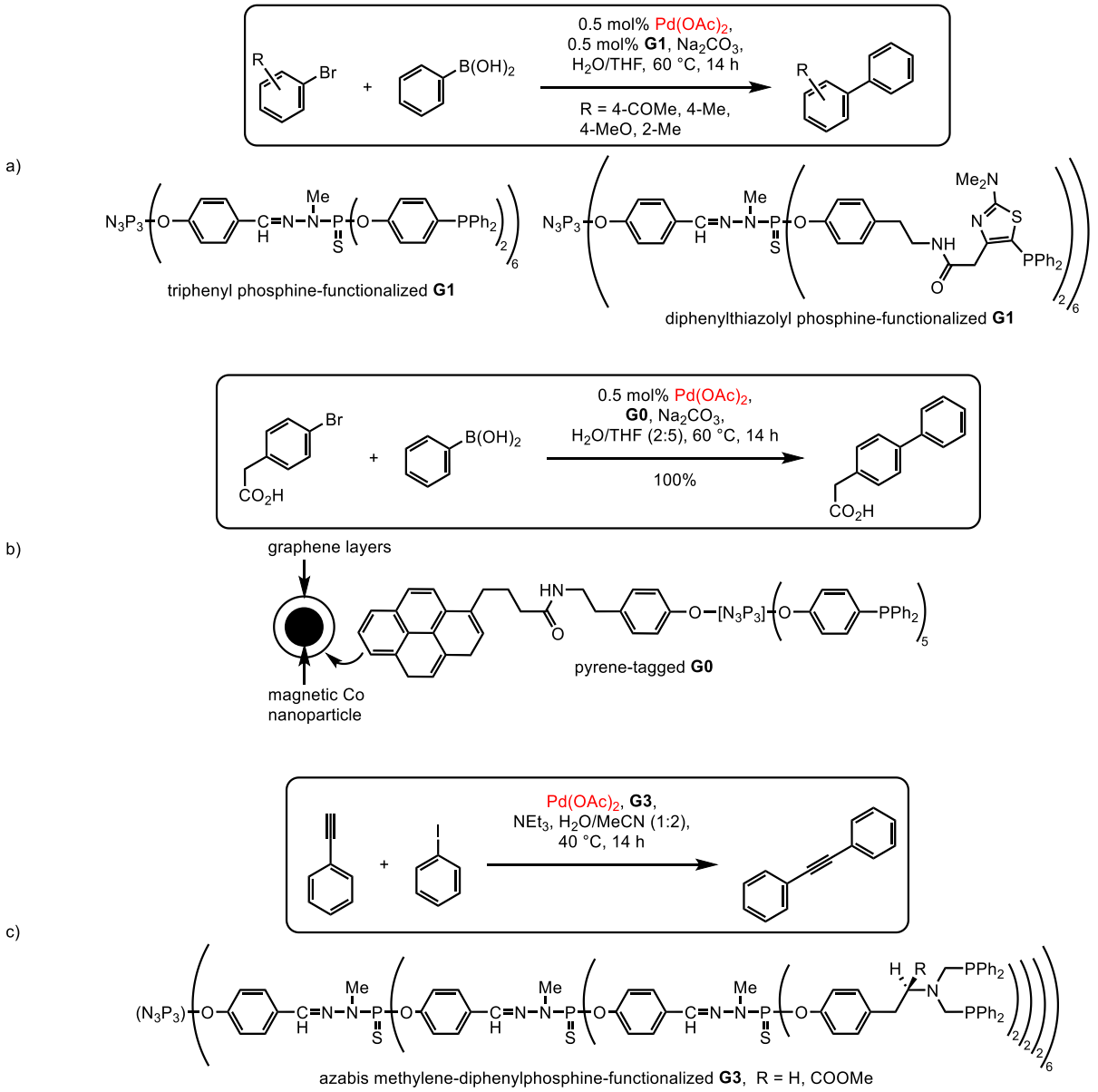


**Scheme 1.4.2.** Examples of different C–C coupling reactions using palladium complexes of phosphorhydrazone dendrimers as catalysts. (a), (b) Examples of different SUZUKI couplings.[76,77] (c) SONOGASHIRA reaction.[75]

The SUZUKI coupling of bromobenzene derivatives with phenylboronic acid (**Scheme 1.4.2**, a) was explored utilizing phosphorhydrazone dendrimers functionalized with triphenylphosphine or diphenylthiazolyl phosphine as ligands. The process was somewhat less effective than the monomeric catalyst coupling, but unlike the monomers, the dendrimers could be recovered and reused several times.[76] In another example, the activity and recyclability of a pyrene-tagged dendritic Pd-phosphine catalyst immobilized by π-stacking onto cobalt magnetic nanoparticles covered with graphene layers towards the SUZUKI coupling of aryl boronic acids and different aryl bromides (**Scheme 1.4.2**, b) were examined.[77] Monomers and dendrimers showed comparable activity. The catalytic system was further applied for the manufacture of Felbinac, an anti-inflammatory drug sold commercially. The compound could be generated quantitatively under

conditions competitive to those described in literature, usually including significantly higher Pd loadings. The catalytic system could be recycled using a magnet and reused without loss up to 11 runs. The SONOGASHIRA reaction between phenylacetylene and iodobenzene (**Scheme 1.4.2**, c) was carried out and it could be shown that the **G3** catalyst was slightly more efficient than the **G1** catalyst (as shown for the HECK reaction in **Scheme 1.4.1**) and the monomer, displaying a slightly positive dendrimer effect.[75]

The employment of simple and stable $Ru^{II}$ catalysts has greatly aided in the development of less expensive and more efficient catalytic systems, softer reaction conditions, and novel reactions in diverse media, particularly for the activation of C–H bonds. In the case of phosphorus dendrimers, ruthenium complexes of phosphines have been used as catalysts in a variety of reactions, including KNOEVENAGEL condensations,[74] MICHAEL additions,[74] hydrogenation,[78] hydration of terminal alkynes,[79] and allylic alcohol isomerization (see **Scheme 1.4.3**).[80]

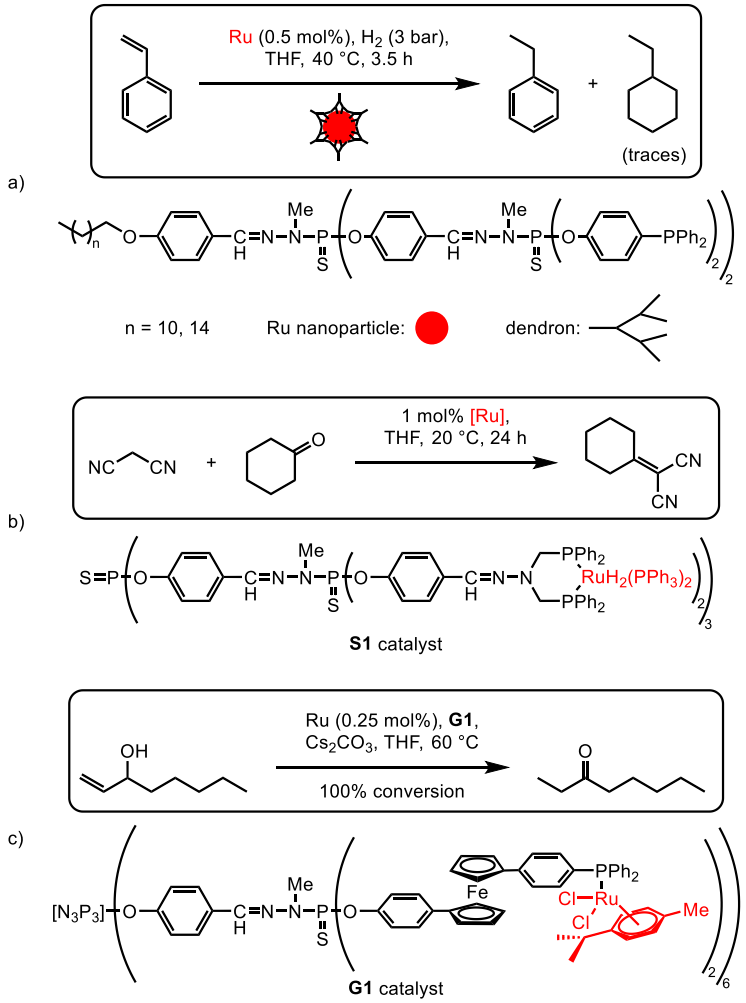


**Scheme 1.4.3.** (a) Ruthenium nanoparticles used as catalysts for the hydrogenation of styrene.[78] (b) KNOEVENAGEL condensation with dendritic ruthenium complexes.[74] (c) Redox-switchable isomerization of 1-octen-3-ol.[80]

A series of dendrons with long alkyl chains were used to generate and stabilize ruthenium nanoparticles generated from $RuCl_3$ suitable for the hydrogenation of styrene yielding almost

exclusively ethylbenzene (ethylcyclohexane being observed only in trace amounts).[78] The complexation of phosphorus dendrimers of generations 1 and 3 (not shown) with $[RuH_2(PPh_3)_2]$ yielded catalysts effective for the KNOEVENAGEL condensation involving malonitrile and cyclohexanone. Both generations were more efficient than the equivalent monomer and could be precipitated and reused twice without losing their catalytic activity.[74] Using monomeric and dendritic ferrocenylphosphines, 1-octen-3-ol was isomerized to 3-octanone in a redox-switchable catalytic allylic alcohol isomerization. The catalytic activity of the complexes may be switched reversibly by introducing a chemical oxidant ($[Fe\{\eta^5\text{-}C_5H_4C(O)Me\}Cp]BF_4$, Cp = $C_5H_5$) or reductant ($[Fe(Cp^*)_2]$, Cp* = $C_5Me_5$). This is the first time a dendritic transition-metal complex has been used for redox-switchable catalysis.[80]

Rhodium catalysts have similar reactivity to other catalyst systems in the production of C–C bonds. Therefore, different rhodium complexes of phosphorus-containing dendrimers have been prepared and used for hydrogenations,[81] isomerization of allylic alcohols,[82] and [2+2+2] cycloadditions.[51] Interestingly, the hydrogenation reaction of dec-1-ene was catalyzed by the very first example of dendrimers with rhodium catalysts at each branching point (shown in **Scheme 1.4.4**). The dendrimers could be recovered and reused three times without a decrease in yield.[80]

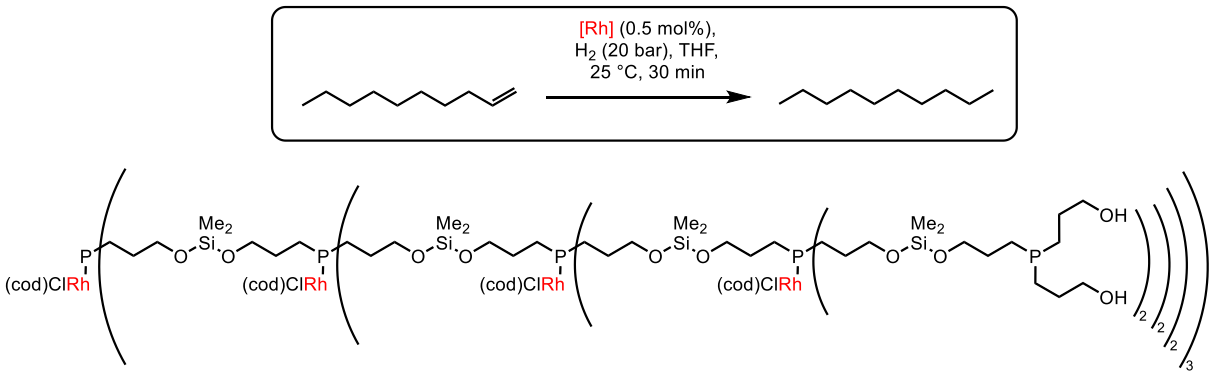


**Scheme 1.4.4.** Hydrogenation using a phosphorus-containing dendrimer bearing rhodium complexes at each branching point as catalysts.[81]

To catalyze [2+2+2] cycloadditions of alkynes, a combination of rhodium(I) and phosphoramidite capped phosphorus dendrimers (generations 1 to 3) were utilized.[51] When dendrimers were utilized as ligands in the reaction between N-tosyl-1,6-diyne and phenylacetylene, the catalytic activity was significantly improved, and yields were nearly quantitative contrarily to the model monomer (**Scheme 1.4.5**).

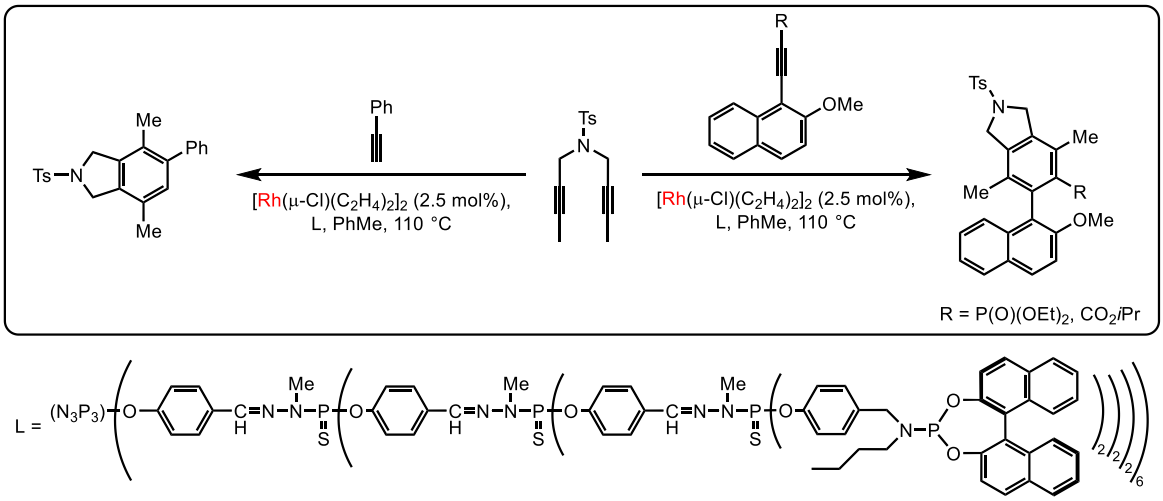


**Scheme 1.4.5.** Dendritic phosphoramidite used as ligand for [2+2+2] cycloaddition reactions.[51]

After the complexation of $Cu^{I}$ by different phosphorhydrazone dendrimers, they were used for C(aryl)–O-and C(aryl)–N-coupling reactions (see **Scheme 1.4.6** and **Scheme 1.4.7**).[83–85] Dendrimers with terminal pyridine imine functions were suitable for the complexation of CuI and could be used for the arylation of 3,5-dimethylphenol with iodobenzene as well as pyrazole with PhX (X = Br, I). The use of the dendritic catalysts increased the yields significantly and was more efficient than the monomeric catalyst. Further, the vinylation of 3,5-dimethylphenol and pyrazole with *E*-bromostyrene was investigated and always showed poorer yields when using the monomeric catalyst. The reaction was further conducted under the mildest conditions ever reported for performing the coupling between vinyl bromides and nucleophiles (azoles or phenols) using catalytic amounts of copper.[83]

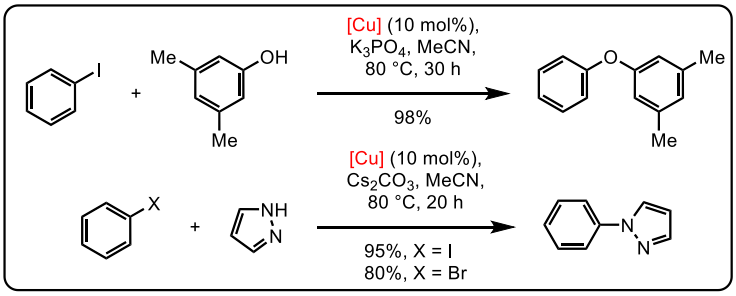


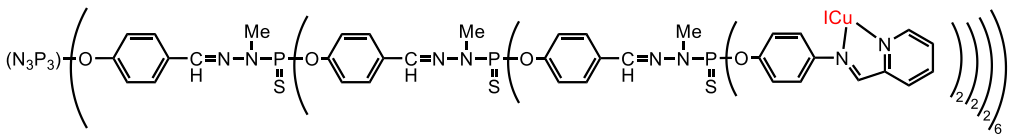


**Scheme 1.4.6.** Example of a dendritic copper complex used for C–O arylation of 3,5-dimethylphenol. and C–N arylation of pyrazole.[83]

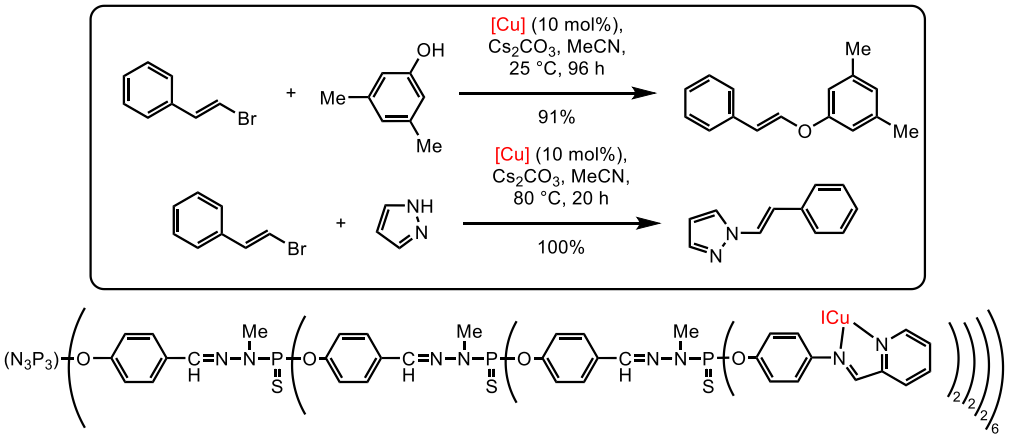


**Scheme 1.4.7.** Examples of a dendritic copper complexes used for C–O vinylation of 3,5-dimethylphenol or C–N vinylation of pyrazole.[83]

Although phosphorus-containing dendrimers were utilized as organocatalysts in the absence of a transition metal, only a few cases were emphasized in the literature.[50,86]

Several instances of peripherally modified dendritic catalysts were shown in this paragraph. They primarily provide two advantages over standard monomeric catalysts: better efficiency and effective recycling, assuming that the number of catalytic sites remains constant over a series of catalytic tests. A dendrimer effect has been observed on a regular basis using phosphorhydrazone dendrimers. For example, in the copper-catalyzed arylation of pyrazole with bromobenzene, where the monomer has practically no activity, but a drastic increase in yield has been seen when the generation of the dendrimer grew.[83] Another noteworthy feature demonstrated is the capacity to recover and reuse dendrimers following the catalytic cycle. Dendritic catalysts are often utilized in solution in organic solvents or water; however, due to their enormous size, they may be separated using methods such as nanofiltration, precipitation, or column chromatography.[54] Another advantage of using dendrimers is that waste is decreased, resulting in more environmentally friendly chemistry. In comparison to monomers, better efficiency implies less metal is required for catalysis. The ability to quickly recover dendritic catalysts means that product purification will be simplified because the catalyst will be more easily removed without polluting the reaction products. Furthermore, as indicated by the undetectable leaching of palladium during the coupling of bromobenzene derivatives with phenylboronic acid (**Scheme 1.4.2**), the metal can be more closely coupled to a dendritic catalyst than to a monomeric catalyst.[76] The majority of the research on dendrimer catalysis shows that the outcome of the catalytic process is generation-dependent but not linearly, and that the optimal generation is not always the same.

## 1.5 Motivation / Aims

Dendrimers functionalized with carboranes exist and have been extensively reviewed, in particular for their biological properties.[86] However, to date, there is no example of a dendrimer

functionalized with carboranylphosphines (or *nido*-carboranylphosphines) and relatively few examples of catalysis with monomeric carboranylphosphines (or *nido*-carboranylphosphines) even though dendrimer-based carboranyl pnictogen and chalcogen compounds seem to be promising ligands for metal complexes applied in homogeneous catalysis.[6]

Therefore, the goal of this dissertation project was to obtain the first dendrimer-based electron-poor carboranyl mono- or bisphosphines or mixed (hemilabile) carboranylphosphine-amines, -alkoxides, -thiols or -thioethers as ligands for challenging catalytic transformations, e.g. C–C coupling or C–H activation. The effect of different dendrimer structures and metals employed on the reactivity, activity and selectivity of the catalysts should be studied, rationalized and applied for an advanced design of improved catalysts. A decrease in metal leaching should be particularly targeted, the objective being to reduce leaching below 1 ppm.

The first part of the project was dedicated to the synthesis of a classical dendrimer up to its second generation with terminal chlorine functions. This compound is well-known in the group of CAMINADE and was prepared starting from a hexachlorocyclotriphosphazene or thiophosphoryl chloride core following known procedures.[64,65] Furthermore, it was aimed to obtain an $AB_5$ dendrimer with a non-growing terminal function with a different reactivity to the other terminal functions to modify the molecule further and assist properties such as water solubility and catalyst recovery.

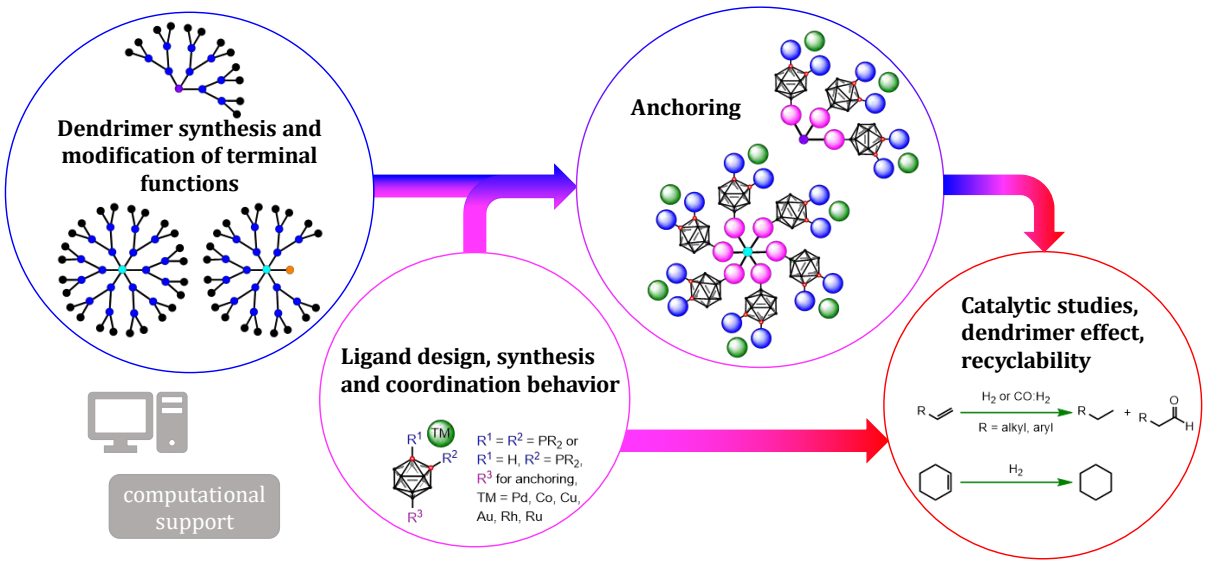


**Scheme 1.5.1.** Planned project workflow. TM = transition metal.

Having the dendrimers in hands, carboranylphosphines and phosphites, for which the HEY-HAWKINS group is the expert, should be synthesized. Based in particular on 1,2-dicarba-*closo*-dodecaborane(12) which is of interest as electron-poor backbone for phosphines, a general synthetic method should be developed. Different new B9-substituted *ortho*-carboranes, carboranylphosphines, and phosphites should be synthesized starting from 1,2-dicarba-*closo*-

dodecaborane(12). Complexation abilities and catalytic behavior of these new monomers should be investigated, even in an industrial context.

Bearing suitable functionalities in the B9 position, these ligands could then be anchored to dendrimers. Especially, the tunability of the steric and electronic properties of the carboranylphosphines assists in the synthesis of new dendritic ligands for the complexation of different transition metals (Co, Pd, Cu, Au, Rh, Ru).

Finally, a selection of the dendrimer-based carboranylphosphines or phosphites should be tested for C–C coupling or C–H activation reactions following successful reactions with the corresponding monomers. Additional studies should be conducted to quantify dendrimer effects and the potential reusability of these compounds.

The synthetic work will be supported by density functional theory (DFT) calculations to allow an in-depth understanding of the chemical processes taking place and an advanced design of improved catalysts.

## 1.6 References

[1] R. N. Grimes, *Carboranes: Third Edition*, Elsevier Inc., **2016** and references therein.

[2] R. L. Hughes, I. C. Smith, E. W. Lawless in *Production of the Boranes and Related Research* (Ed.: R. T. Holzmann), Academic Press, New York, **1967**.

[3] D. Grafstein, J. Dvorak, *Inorg. Chem.* **1963**, *2*, 1128–1133.

[4] A. V. Puga, F. Teixidor, R. Sillanpää, R. Kivekäs, M. Arca, G. Barberà, C. Viñas, *Chem. Eur. J.* **2009**, *15*, 9755–9763.

[5] A. M. Spokoyny, C. W. Machan, D. J. Clingerman, M. S. Rosen, M. J. Wiester, R. D. Kennedy, C. L. Stern, A. A. Sarjeant, C. A. Mirkin, *Nat. Chem.* **2011**, *3*, 590–596.

[6] S. Bauer, E. Hey-Hawkins in *Boron Science* (Ed.: N. S. Hosmane), CRC Press, **2011**, pp. 529–578.

[7] E. V. Oleshkevich, E. G. Rys, V. V. Bashilov, P. V. Petrovskii, V. A. Ol'shevskaya, S. K. Moiseev, A. B. Ponomaryov, V. N. Kalinin, *Russ. J. Gen. Chem.* **2017**, *87*, 2589–2595.

[8] P. Stockmann, M. Gozzi, R. Kuhnert, M. B. Sárosi, E. Hey-Hawkins, *Chem. Soc. Rev.* **2019**, *48*, 3497–3512.

[9] K. Ohta, H. Yamazaki, Y. Endo, *J. Organomet. Chem.* **2009**, *694*, 1646–1651.

[10] P. C. Andrews, M. J. Hardie, C. L. Raston, *Coord. Chem. Rev.* **1999**, *189*, 169–198.

[11] A. F. Armstrong, J. F. Valliant, *Dalton Trans.* **2007**, 4240–4251.

[12] I. B. Sivaev, M. Y. Stogniy, V. I. Bregadze, *Coord. Chem. Rev.* **2021**, *436*, 213795.

[13] R. P. Alexander, H. Schroeder, *Inorg. Chem.* **1963**, *2*, 1107–1110.

[14] F. Röhrscheid, R. H. Holm, *J. Organomet. Chem.* **1965**, *4*, 335–338.

[15] V. P. Balema, M. Pink, J. Sieler, E. Hey-Hawkins, L. Hennig, *Polyhedron* **1998**, *17*, 2087–2093.

[16] H.-S. Lee, J.-Y. Bae, J. Ko, Y. S. Kang, H. S. Kim, S.-J. Kim, J.-H. Chung, S. O. Kang, *J. Organomet.*

*Chem.* **2000**, *614–615*, 83–91.

[17] F. Teixidor, C. Viñas, R. Benakki, R. Kivekäs, R. Sillanpää, *Inorg. Chem.* **1997**, *36*, 1719–1723.

[18] T. Lee, S. W. Lee, H. G. Jang, S. O. Kang, J. Ko, *Organometallics* **2001**, *20*, 741–748.

[19] A. R. Popescu, F. Teixidor, C. Viñas, *Coord. Chem. Rev.* **2014**, *269*, 54–84.

[20] P. Coburger, G. Kahraman, A. Straube, E. Hey-Hawkins, *Dalton Trans.* **2019**, *48*, 9625–9630.

[21] J. B. Stothers, J. R. Robinson, *Can. J. Chem.* **1964**, *42*, 967–970.

[22] V. A. Zakharkin, L.I., Guseva, V.V, Ol'shevskaya, *Russ. J. Gen. Chem.* **2001**, *71*, 903–904.

[23] H. D. Smith, *J. Am. Chem. Soc.* **1965**, *87*, 1817–1818.

[24] L. I. Zakharkin, G. G. Zhigareva, *Bull. Acad. Sci. USSR Div. Chem. Sci.* **1965**, *14*, 905–905.

[25] G. Allender, H. D. Smith, *Inorg. Chim. Acta* **1978**, *26*, L38.

[26] S. Paavola, R. Kivekäs*, F. Teixidor, C. Viñas, *J. Organomet. Chem.* **2000**, *606*, 183–187.

[27] S. Paavola, F. Teixidor, C. Viñas, R. Kivekäs, *J. Organomet. Chem.* **2002**, *645*, 39–46.

[28] M. R. Sundberg, S. Paavola, C. Viñas, F. Teixidor, R. Uggla, R. Kivekäs, *Inorg. Chim. Acta* **2005**, *358*, 2107–2111.

[29] J. Guillermo Contreras, L. Moises Silva-Triviño, M. E. Solis, *Inorg. Chim. Acta* **1986**, *114*, 51–54.

[30] I. Maulana, P. Lönnecke, E. Hey-Hawkins, *Chem. Commun.* **2012**, *48*, 10231.

[31] A. Sterzik, E. Rys, S. Blaurock, E. Hey-Hawkins, *Polyhedron* **2001**, *20*, 3007–3014.

[32] O. Kühl, *Phosphorus-31 NMR Spectroscopy*, Springer, Berlin, **2009**.

[33] W. E. Hill, W. Levason, C. A. McAuliffe, *Inorg. Chem.* **1974**, *13*, 244–245.

[34] W. D. Horrocks, G. R. Van Hecke, D. D. Hall, *Inorg. Chem.* **1967**, *6*, 694–699.

[35] F. A. Hart, D. W. Owen, *Inorg. Chim. Acta* **1985**, *103*, L1–L2.

[36] C. U. Pittman, A. Hirao, *J. Org. Chem.* **1978**, *43*, 640–646.

[37] F. Teixidor, C. Viñas, M. M. Abad, C. Whitaker, J. Rius, *Organometallics* **1996**, *15*, 3154–3160.

[38] J. A. Osborn, F. H. Jardine, J. F. Young, G. Wilkinson, *J. Chem. Soc. A Inorganic, Phys. Theor.* **1966**, 1711–1732.

[39] A. Demonceau, F. Simal, A. F. Noels, C. Viñas, R. Nuñez, F. Teixidor, *Tetrahedron Lett.* **1997**, *38*, 4079–4082.

[40] F. Simal, S. Sebille, A. Demonceau, A. F. Noels, R. Nuñez, M. Abad, F. Teixidor, C. Viñas, *Tetrahedron Lett.* **2000**, *41*, 5347–5351.

[41] F. Teixidor, C. Viñas, M. M. Abad, R. Kivekäs, R. Sillanpää, *J. Organomet. Chem.* **1996**, *509*, 139–150.

[42] R. Kivekäs, R. Sillanpää, F. Teixidor, C. Viñas, M. M. Abad, *Acta Chem. Scand.* **1996**, *50*, 499–504.

[43] D. Zhang, J. Dou, S. Gong, D. Li, D. Wang, *Appl. Organomet. Chem.* **2006**, *20*, 632–637.

[44] J. Dou, D. Zhang, D. Li, D. Wang, *Eur. J. Inorg. Chem.* **2007**, *2007*, 53–59.

[45] S. Al-Baker, W. E. Hill, C. A. McAuliffe, *J. Chem. Soc. Dalton Trans.* **1985**, 1387–1390.

[46] O. Crespo, M. C. Gimeno, A. Laguna, P. G. Jones, *J. Chem. Soc. Dalton Trans.* **1992**, 1601–1605.

[47] R. T. Baker, W. Tumas, *Science* **1999**, *284*, 1477–1479.

[48] R. Van Heerbeek, P. C. J. Kamer, P. W. N. M. Van Leeuwen, J. N. H. Reek, *Chem. Rev.* **2002**, *102*, 3717–3756.

[49] J. Popp, A.-M. Caminade, E. Hey-Hawkins, *Eur. J. Inorg. Chem.* **2020**, *2020*, 1654–1669.

[50] E. Delort, T. Darbre, J.-L. Reymond, *J. Am. Chem. Soc.* **2004**, *126*, 15642–15643.

[51] L. Garcia, A. Roglans, R. Laurent, J. P. Majoral, A. Pla-Quintana, A.-M. Caminade, *Chem. Commun.* **2012**, *48*, 9248–9250.

[52] D. A. Tomalia, H. Baker, J. Dewald, M. Hall, G. Kallos, S. Martin, J. Roeck, J. Ryder, P. Smith, *Polym. J.* **1985**, *17*, 117–132.

[53] E. Buhleier, W. Winfried, F. Vögtle, *Synthesis* **1978**, *1978*, 155–158.

[54] A. Caminade, C. Turrin, R. Laurent, A. Ouali, B. Delavaux-Nicot (Eds.), *Dendrimers: Towards Catalytic, Material and Biomedical Uses*, Wiley, **2011**.

[55] M.-L. Lartigue, B. Donnadieu, C. Galliot, A.-M. Caminade, J.-P. Majoral, J.-P. Fayet, *Macromolecules* **1997**, *30*, 7335–7337.

[56] J. Lim, M. Kostiainen, J. Maly, V. C. P. da Costa, O. Annunziata, G. M. Pavan, E. E. Simanek, *J. Am. Chem. Soc.* **2013**, *135*, 4660–4663.

[57] C. J. Hawker, J. M. J. Frechet, *J. Am. Chem. Soc.* **1990**, *112*, 7638–7647.

[58] S. M. Grayson, J. M. J. Fréchet, *Chem. Rev.* **2001**, *101*, 3819–3867.

[59] J. W. J. Knapen, A. W. van der Made, J. C. de Wilde, P. W. N. M. van Leeuwen, P. Wijkens, D. M. Grove, G. van Koten, *Nature* **1994**, *372*, 659–663.

[60] A.-M. Caminade, R. Laurent, C.-O. Turrin, C. Rebout, B. Delavaux-Nicot, A. Ouali, M. Zablocka, J.-P. Majoral, *Comptes Rendus Chim.* **2010**, *13*, 1006–1027.

[61] E. Cavero, M. Zablocka, A.-M. Caminade, J. P. Majoral, *Eur. J. Org. Chem.* **2010**, 2759–2767.

[62] K. Rengan, R. Engel, *J. Chem. Soc. Chem. Commun.* **1990**, 1084–1085.

[63] N. Launay, A.-M. Caminade, R. Lahana, J.-P. Majoral, *Angew. Chem. Int. Ed. Engl.* **1994**, *33*, 1589–1592.

[64] N. Launay, A.-M. Caminade, J. P. Majoral, *J. Organomet. Chem.* **1997**, *529*, 51–58.

[65] N. Launay, M. Slany, A.-M. Caminade, J. P. Majoral, *J. Org. Chem.* **1996**, *61*, 3799–3805.

[66] M. Touaibia, R. Roy, *J. Org. Chem.* **2008**, *73*, 9292–9302.

[67] D. Prévôté, A.-M. Caminade, J. P. Majoral, *J. Org. Chem.* **1997**, *62*, 4834–4841.

[68] M. Slany, M. Bardaji, M.-J. Casanove, A.-M. Caminade, J.-P. Majoral, B. Chaudret, *J. Am. Chem. Soc.* **1995**, *117*, 9764–9765.

[69] M. Bardají, A.-M. Caminade, J.-P. Majoral, B. Chaudret, *Organometallics* **1997**, *15*, 3489–3497.

[70] M. L. Lartigue, M. Slany, A.-M. Caminade, J. P. Majoral, *Chem. Eur. J.* **1996**, *2*, 1417–1426.

[71] B. Helms, J. M. J. Fréchet, *Adv. Synth. Catal.* **2006**, *348*, 1125–1148.

[72] A.-M. Caminade, A. Ouali, R. Laurent, C. O. Turrin, J. P. Majoral, *Chem. Soc. Rev.* **2015**, *44*, 3890–3899.

[73] A.-M. Caminade, R. Laurent, *Coord. Chem. Rev.* **2019**, *389*, 59–72.

[74] V. Maraval, R. Laurent, A.-M. Caminade, J.-P. Majoral, *Organometallics* **2000**, *19*, 4025–4029.

[75] P. Servin, R. Laurent, A. Romerosa, M. Peruzzini, J.-P. Majoral, A.-M. Caminade, *Organometallics* **2008**, *27*, 2066–2073.

[76] M. Keller, A. Hameau, G. Spataro, S. Ladeira, A.-M. Caminade, J.-P. Majoral, A. Ouali, *Green Chem.* **2012**, *14*, 2807–2815.

[77] M. Keller, V. Collière, O. Reiser, A.-M. Caminade, J.-P. Majoral, A. Ouali, *Angew. Chem. Int. Ed.* **2013**, *52*, 3626–3629; *Angew. Chem*. **2013**, *125*, 3714–3717.

[78] N. G. García-Peña, A.-M. Caminade, A. Ouali, R. Redón, C.-O. Turrin, *RSC Adv.* **2016**, *6*, 64557–64567.

[79] P. Servin, R. Laurent, L. Gonsalvi, M. Tristany, M. Peruzzini, J. P. Majoral, A.-M. Caminade, *Dalton Trans.* **2009**, 4432–4434.

[80] P. Neumann, H. Dib, A.-M. Caminade, E. Hey-Hawkins, *Angew. Chem. Int. Ed.* **2015**, *54*, 311–314; *Angew. Chem.* **2015**, *127*, 316-319.

[81] M. Petrucci-Samija, V. Guillemette, M. Dasgupta, A. K. Kakkar, *J. Am. Chem. Soc.* **1999**, *121*, 1968–1969.

[82] P. Servin, R. Laurent, H. Dib, L. Gonsalvi, M. Peruzzini, J. P. Majoral, A.-M. Caminade, *Tetrahedron Lett.* **2012**, *53*, 3876–3879.

[83] A. Ouali, R. Laurent, A.-M. Caminade, J. P. Majoral, M. Taillefer, *J. Am. Chem. Soc.* **2006**, *128*, 15990–15991.

[84] A. Gissibl, C. Padié, M. Hager, F. Jaroschik, R. Rasappan, E. Cuevas-Yañez, C. O. Turrin, A.-M. Caminade, J. P. Majorai, O. Reiser, *Org. Lett.* **2007**, *9*, 2895–2898.

[85] M. Keller, M. Ianchuk, S. Ladeira, M. Taillefer, A.-M. Caminade, J. P. Majoral, A. Ouali, *Eur. J. Org. Chem.* **2012**, *2012*, 1056–1062.

[86] M. Keller, A. Perrier, R. Linhardt, L. Travers, S. Wittmann, A.-M. Caminade, J. P. Majoral, O. Reiser, A. Ouali, *Adv. Synth. Catal.* **2013**, *355*, 1748–1754.

[87] A.-M. Caminade, M. Milewski, E. Hey-Hawkins, *Pharmaceutics* **2023**, *15*, 2117.

# Chapter 2: Old core, new look – Synthesis of dendrimers and dendrons

# 2 Old core, new look – Synthesis of dendrimers and dendrons

As illustrated in the first chapter, dendrimers and dendrons are created step by step in a reiterative process with, in most cases, identical terminal functions. However, in order to fulfil specified demands, it is occasionally advantageous to have two types of surface functions.[1] Hexachlorocyclotriphosphazene offers the possibility to distinguish the reactivity of one chloride (or more) from the others, allowing the creation of precisely tailored dendritic tools. These precise reactions can generate intriguing dendrimers, which can subsequently be employed as tools for functionalizing materials, as catalysts, as chemical sensors, for $CO_2$ trapping, for cell culture, or in imaging biological processes.[2] This chapter will stress various phosphorus-containing dendritic structures of the phosphorhydrazone type, as well as diverse approaches for the synthesis of distinct generations of symmetrical and non-symmetrical dendrimers and dendrons based on these phosphorus derivatives.

## 2.1 Hexachlorocyclotriphosphazene-based and thiophosphoryl chloride-based dendrimers

### 2.1.1 General aspects towards the synthesis of dendrimers

Starting from either a $N_3P_3Cl_6$ or $P(S)Cl_3$ core, different symmetrical dendrimers were synthesized following known procedures.[3,4] First described in 1994 by CAMINADE and co-workers,[5] the most extensively utilized two-step procedure for the production of phosphorus-containing dendrimers was applied. It entails repeating a substitution reaction with 4-hydroxybenzaldehyde in basic conditions and a condensation reaction with the phosphorhydrazide $H_2NNMeP(S)Cl_2$ ($MMHSPCl_2$). Both procedures are reported to be almost quantitative and produce solely alkali metal chlorides and $H_2O$ as by-products.

In the duration of the project, the synthesis of different classical dendrimers, up to generation one (**2-S1**) or two (**1-G2**), respectively, and $AB_5$ dendrimers, up to generation one (**$AB_5$-2-G1**), was targeted. For clarification: **1-Gn** and **1-Sn** bear terminal $P(S)Cl_2$ functions, **2-Gn** and **2-Sn** carry terminal aldehyde functions. If possible, all structures are represented completely, if not possible, a linear notation of the dendrimers and dendrons is used.

### 2.1.2 Synthesis of polyphosphorhydrazone dendrimer scaffolds bearing the same terminal function

The first part of the project was dedicated to the synthesis of a classical dendrimer with terminal chlorine functions, which is well-known in the group of CAMINADE.[4] In the first step, the $N_3P_3Cl_6$ core (**1-G0**) is reacted with 4-hydroxybenzaldehyde (**1**) using potassium carbonate as the base for the *in situ* generation of the phenoxide. All chlorine functions reacted to yield dendrimer **2-G0** during this nucleophilic substitution. Consecutively, $MMHPSCl_2$ (**3**) was used to react with the terminal aldehyde functions. This condensation led to dendrimer **1-G1** with 12 P–Cl terminal

functions as new branching points. Repeating this sequence of reactions, in replacing potassium carbonate by cesium carbonate, symmetrical polyphosphorhydrazone (PPH) dendrimers in higher generations could be obtained. It was further important to exclude water completely to avoid any side reactions by hydrolysis (**Scheme 2.1.1**).

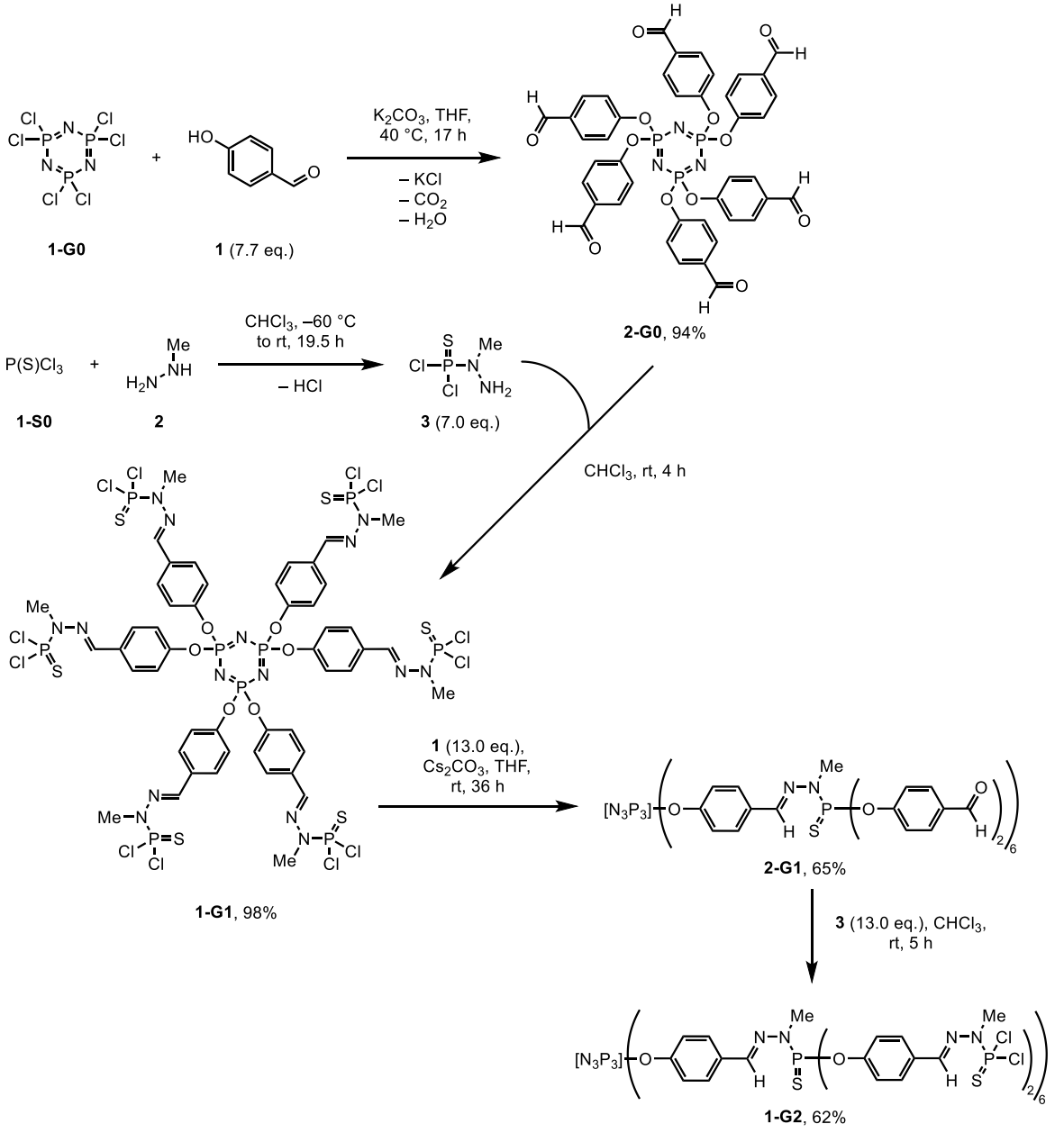


**Scheme 2.1.1.** Synthesis of a symmetrical dendrimer up to generation **1-G2**.

As described in chapter **1.3.2**, $^{31}$P NMR spectroscopy displays a valuable tool to follow the reaction progress and control the purity of the products.[6] The nucleophilic substitution can be easily monitored by $^{31}$P{$^{1}$H} NMR spectroscopy. All spectra were measured in $CDCl_3$. After full substitution, the $^{31}$P signal of the core **1-G0** ($P_0$, $\delta$ = 20.0 ppm) is upfield-shifted to 7.1 ppm (**2-G0**). The core $^{31}$P signal of the fully functionalized **1-G1** dendrimer is only slightly upfield-shifted (from 8.2 ppm for **1-G1** to 8.0 ppm for **2-G1**). Upon disubstitution, the phosphorus signal of the $P(S)Cl_2$

groups experiences an upfield-shift from 62.3 ppm for **1-G1** to 60.4 ppm for **2-G1**. In the case of a monosubstitution, a characteristic signal at approximately 69 ppm can be observed. The formation of the monosubstituted product should be avoided because it significantly complicates the purification process and leads to the formation of undesired by-products. As a result of the condensation with **1**, the phosphorus signals are subject to a downfield shift (**Fig. 2.1.1**).

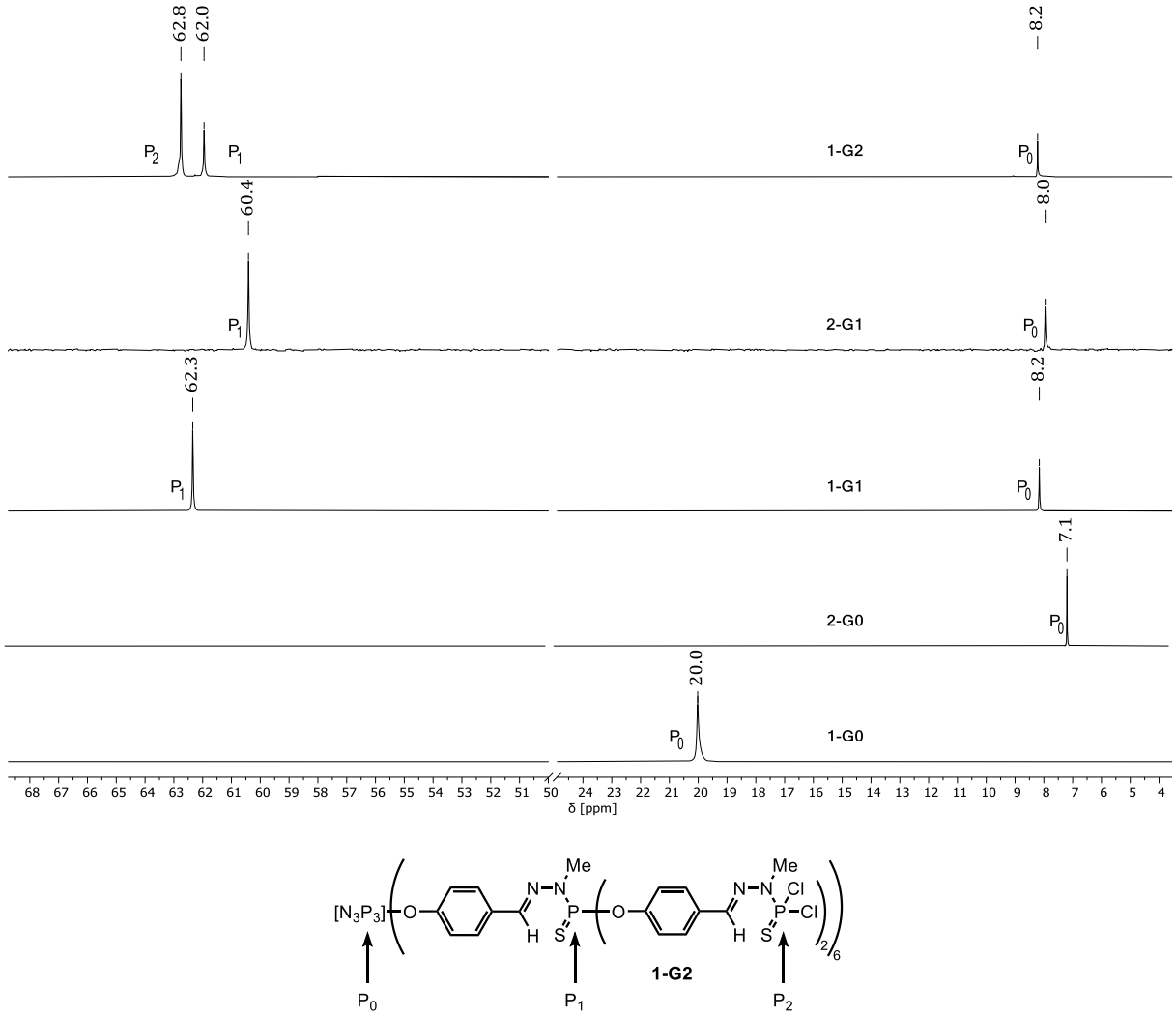


**Fig. 2.1.1.** Evolution of the $^{31}P\{^{1}H\}$ NMR signals in $CDCl_3$ from **1-G0** to **1-G2.**

Another method for monitoring the progress of the condensation reaction is to use $^{1}H$ NMR spectroscopy. The disappearance of the signal of the aldehyde proton at around 10 ppm can be observed. All dendrimers could be synthesized in good yields (62–98%) and acceptable purities according to literature up to generation **1-G2** (as shown in **Scheme 2.1.1**).[4]

In another attempt, dendrimers based on a thiophosphoryl chloride core (**1-S0**) were synthesized with the above-mentioned methods up to generation **2-S1** (see **Scheme 2.1.2**).

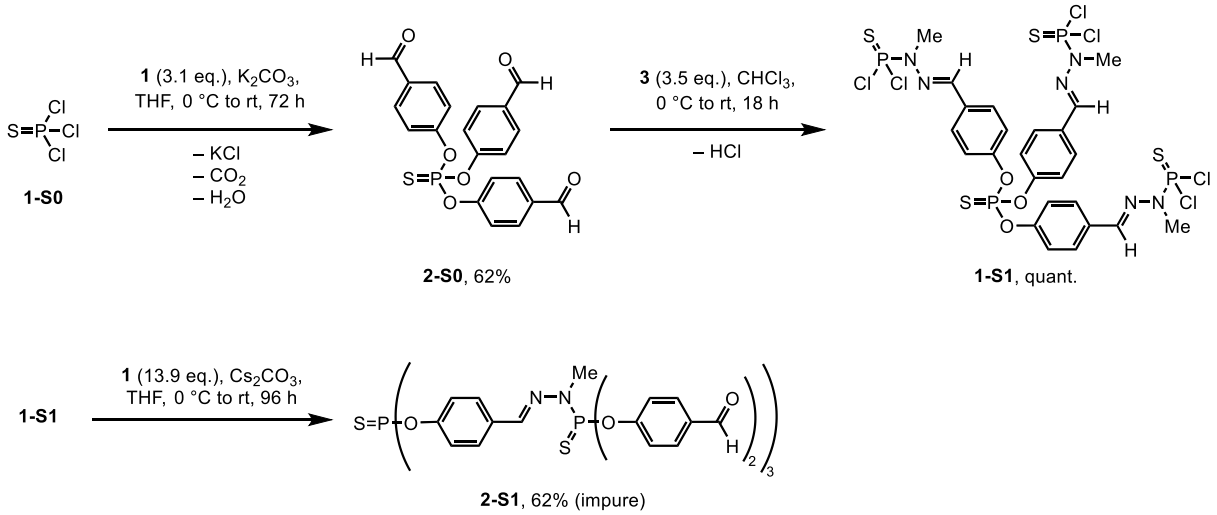


**Scheme 2.1.2.** Synthesis of a symmetrical dendrimer starting from **1-S0** up to generation **2-S1**.

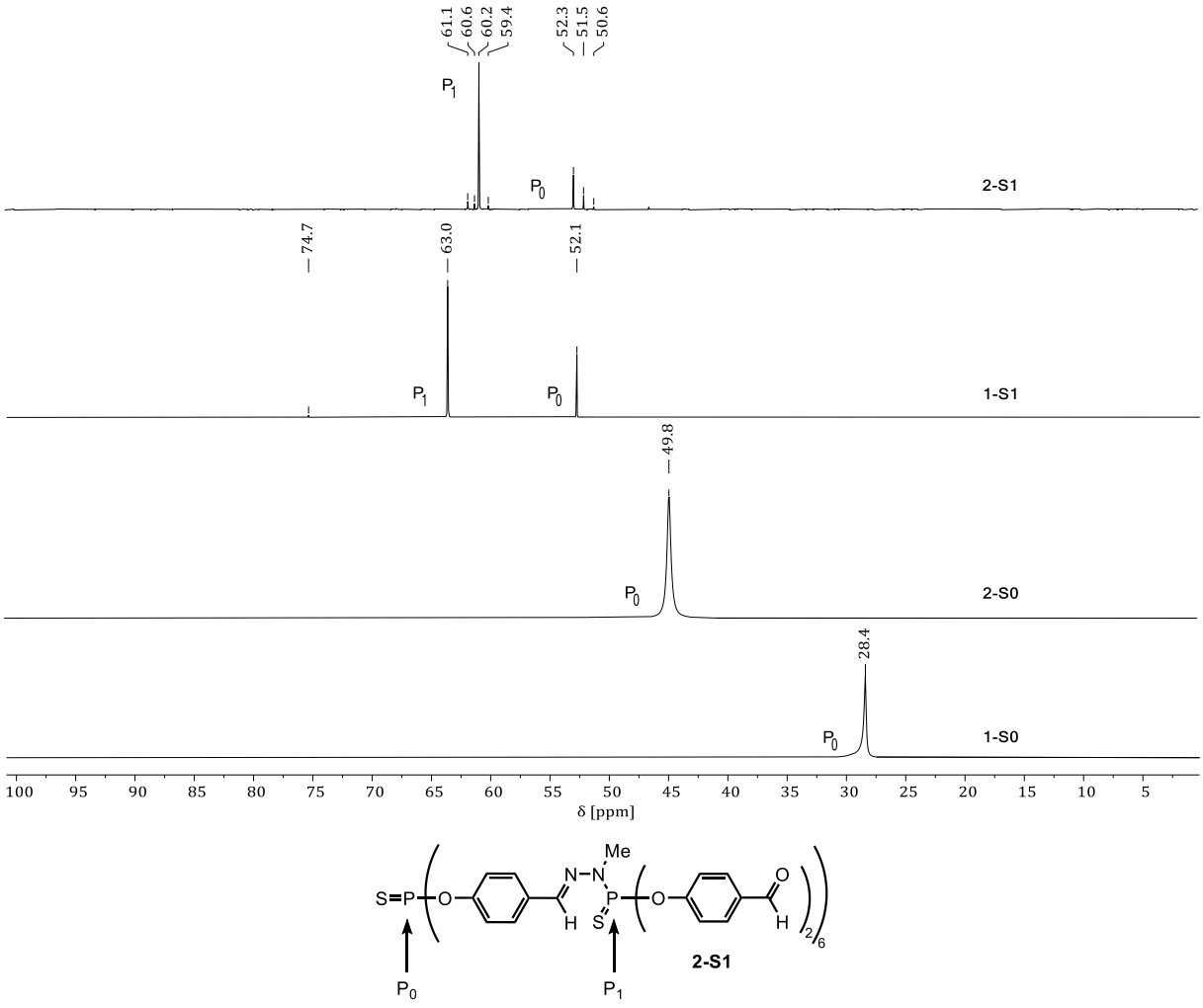


**Fig. 2.1.2.** Evolution of the $^{31}P\{^{1}H\}$ NMR signals in $CDCl_3$ from **1-S0** to **2-S1.**

The reaction progress was monitored by $^{31}P\{^{1}H\}$ and $^{1}H$ NMR spectroscopy. The phosphorus signals experienced the same shifts as previously described and are completely consistent with data reported in the literature.[5] Minor impurities, seen in the $^{31}P\{^{1}H\}$ NMR of **1-S1** could be one

of the reasons for the contaminations found in the $^{31}P\{^{1}H\}$ NMR spectrum of **2-S1**. The growth was stopped at this point because the project's limited time frame did not permit the synthesis of dendrimers larger than **2-S1**.

The following generally applies to the synthesis of dendrimers: Minor impurities (less than 1%) observed by $^{31}P\{^{1}H\}$ NMR spectroscopy were generated due to hydrolysis and impure starting materials and had to be removed to obtain a clean dendrimer. Problems with the reagent $MMHPSCl_2$ (**3**), which was used for the growth of the dendrimer, could not be solved completely. This reagent is synthesized by the reaction of monomethylhydrazide (**2**) and thiophosphoryl chloride (**1-S0**). The latter is commercially available but usually arrives with contaminations of $PCl_3$ and $POCl_3$ which could not be removed completely by distillation, evaporation or any other known method (attempted). To solve these problems the synthetic steps were repeated several times using different purification methods. In general, the purification process of the classical dendrimers is challenging. Precipitation of dissolved products in dichloromethane with *n*-pentane, $Et_2O$, or mixtures of both solvents is the preferred approach, but it has limitations. In most circumstances, column chromatography was not employed since dendrimers bigger than **2-G0** seemed to be sensitive to hydrolysis on silica gel because of their terminal $P(S)Cl_2$ functions. Obtaining **2-S1** and **1-G2**, the synthesis of higher generations such as **2-G2** or **2-S2** was halted and the suitability for grafting to various new phenol- or aniline-linked carborane and carboranylphosphine derivatives was tested first.

### 2.1.3 Synthesis of polyphosphorhydrazone dendrimer scaffolds with one non-growing function

One intriguing aspect of $N_3P_3Cl_6$ is undoubtedly the ability to regio- and stereochemically regulate the nucleophilic substitutions, allowing one (or more) functions to be distinct from the others.[7] It is possible to have one function that is unique from the other five by grafting first the single function, then the five others, or by grafting first the five functions, and then the single function. Purification is simpler in one way or the other depending on the kind of both functions.[2] In this work, the latter method has been used for the synthesis of several $AB_5$ dendrimers (A: 4-(prop-2-yn-1-yloxy)phenol, B: 4-hydroxybenzaldehyde). An alkyne group was chosen because of its nonreactivity towards $MMHPSCl_2$. This function is non-growing and can be used later for the grafting to functional materials or to compounds increasing properties such as water solubility and catalyst recovery.[1]

It was necessary to first synthesize dendron **4** with one chloride function by varying the equivalents of **1** and base, and then separate it chromatographically from the by-products **5** and **2-G0** (**Scheme 2.1.3**).

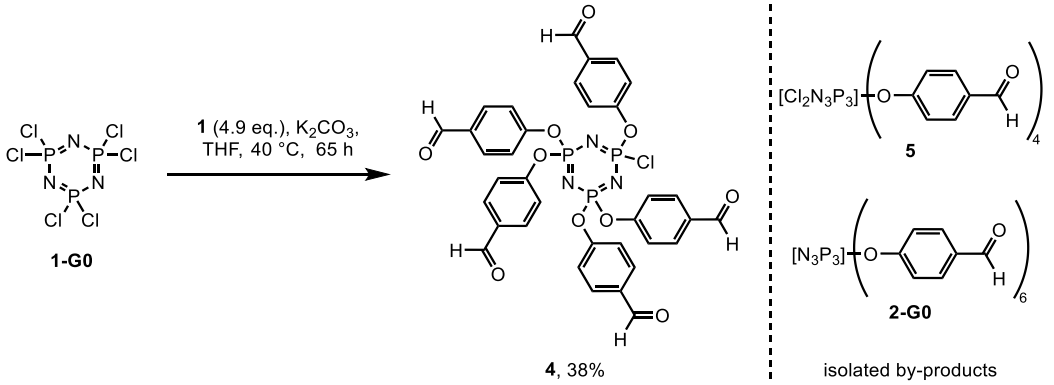


**Scheme 2.1.3.** Synthesis of dendron **4**.

The formation of **4** is accompanied by the formation of **2-G0** and different isomers of **5**. This is due to the sub-stoichiometry of **1**, local concentrations during the reaction (the ratio of equivalents is no longer correct due to variation of the speed of addition), or varying reaction conditions (stirring efficiency, temperature). Furthermore, dendron **4** is partly hydrolyzed (even if all compounds are carefully dried and purified beforehand) which further reduces the yield.

In the next step, hydroquinone (**6**) and propargyl bromide (**7**) were reacted to form 4-(prop-2-yn-1-yloxy)phenol (**8**). The addition of the alkyne **7** to a solution of **6** is the critical step towards the formation of **8**. By-products were formed as a result of either slow or too fast addition. The reaction therefore yielded a mixture of unreacted benzenediol (**6**), propargyloxyphenol (**8**), and bispropargyloxybenzene (**9**). The three chemicals had to be separated twice by column chromatography on silica gel, which further lowered the yield (see **Scheme 2.1.4**).

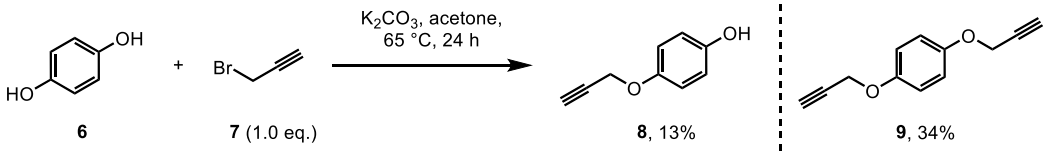


**Scheme 2.1.4.** Synthesis of 4-(prop-2-yn-1-yloxy)phenol (**8**).

Purified propargyloxyphenol was then grafted to **4** yielding **$AB_5$-2-G0**. The formed dendrimer **$AB_5$-2-G0** was then reacted with $MMHPSCl_2$ (condensation reaction) to afford compound **$AB_5$-2-G1** which was then reacted with aldehyde **1** (nucleophilic substitution) in a similar fashion to that used for the symmetrical dendrimers to finally obtain pure dendrimer **$AB_5$-1-G1** as well as its first $^{31}P\{^1H\}$ NMR spectroscopic data (see **Scheme 2.1.5** and **Fig. 2.1.3**).

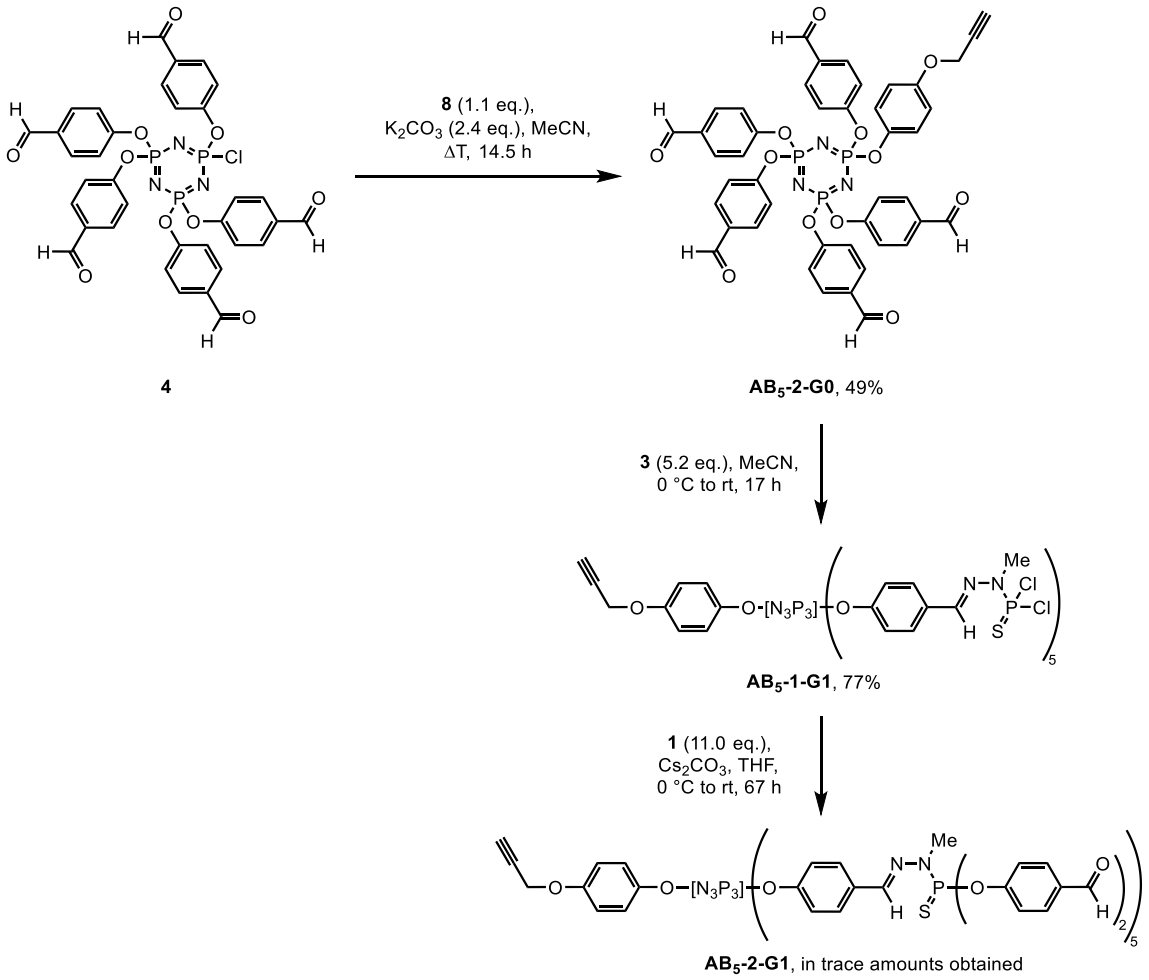


**Scheme 2.1.5.** Synthesis of an $AB_5$ dendrimer with one non-growing terminal function.

Dendrimer **$AB_5$-2-G1** could not be obtained as a pure product and therefore was not fully characterized. However, its formation can be seen in its $^{31}P\{^1H\}$ NMR spectrum. The reaction progress of the other reactions was monitored by $^{31}P\{^1H\}$ NMR and $^1H$ NMR spectroscopy (see **Fig. 2.1.3**).

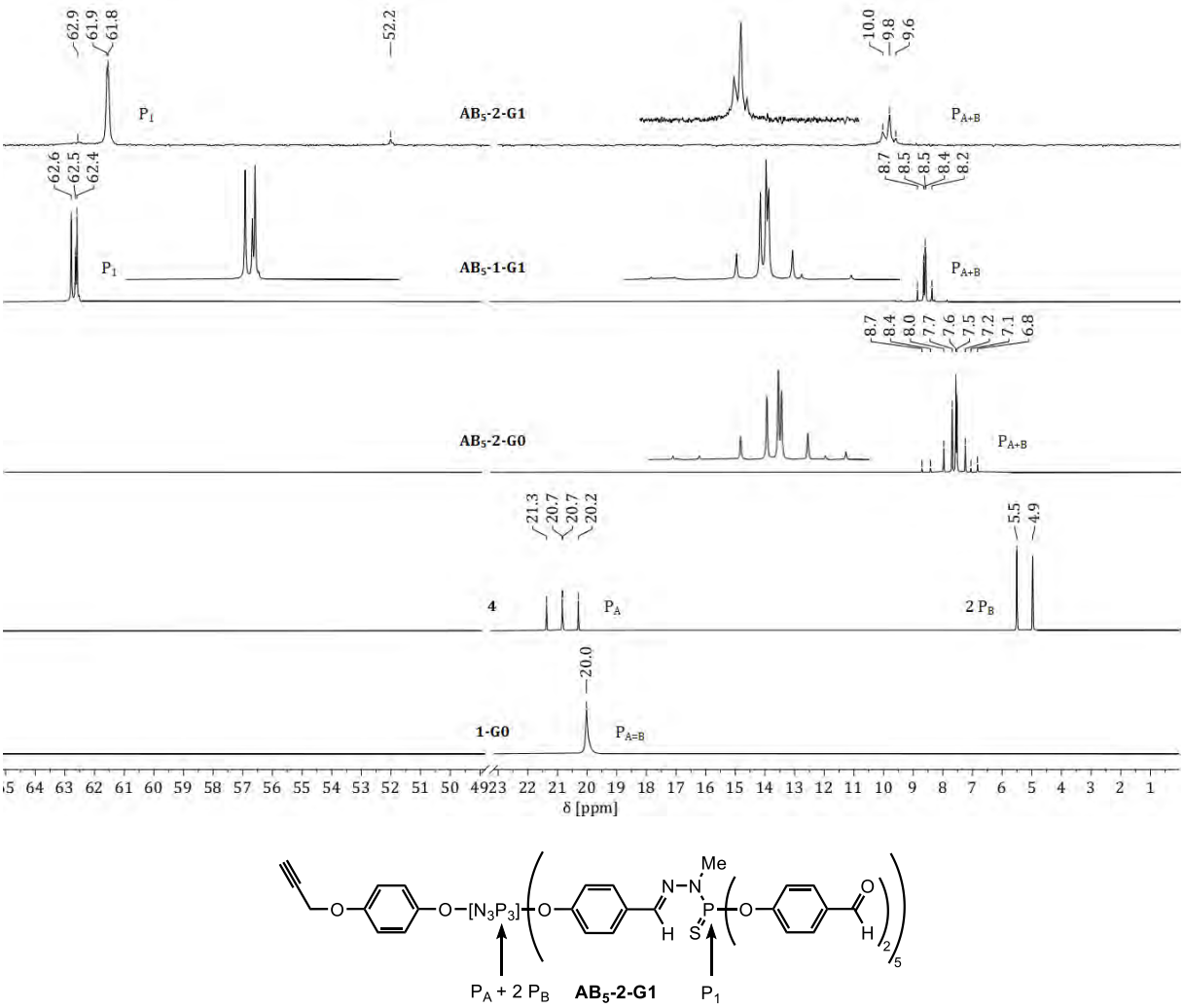


**Fig. 2.1.3.** Evolution of the $^{31}P\{^{1}H\}$ NMR signals from **1-G0** to **$AB_5$-1-G1** in $CDCl_3$ and **$AB_5$-2-G1** in acetonitrile with a $C_6D_6$ capillary. The different substituted phosphorus atoms ($P_A$, $P_B$) can be only distinguished for dendron **4**. In all other cases, they are abbreviated as $P_0$.

Interestingly, by grafting a single function different to the five others, a more complex $^{31}P\{^{1}H\}$ NMR spectrum was obtained for **$AB_5$-2-G0** as well as **$AB_5$-1-G1** due to second order effects. The obtained ABX spin system was extensively analyzed and further compared to a simulation[8] that allowed the determination of the chemical shifts of the three phosphorus atoms as well as their coupling constants (see **Fig. 2.1.4**). In the compounds **$AB_5$-1-G1** and **$AB_5$-2-G1**, the unsymmetrical structure of the $N_3P_3$ core causes further unique characteristics in the $^{31}P\{^{1}H\}$ NMR spectra. Five of the substituents bear a phosphorus atom. Chemically, these five phosphorus atoms are comparable, but the interactions with one another in space (especially with the alkyne substituent) may not be similar, leading to a variety of signals in the $^{31}P\{^{1}H\}$ NMR spectra. Three signals in a 2:1:2 ratio can be observed, clearly implying that the core is composed of a triphosphazene ring with one arm up and one arm down on each phosphorus atom. These

findings are in good alignment with the report of CAMINADE and co-workers observed for similar compounds.[9]

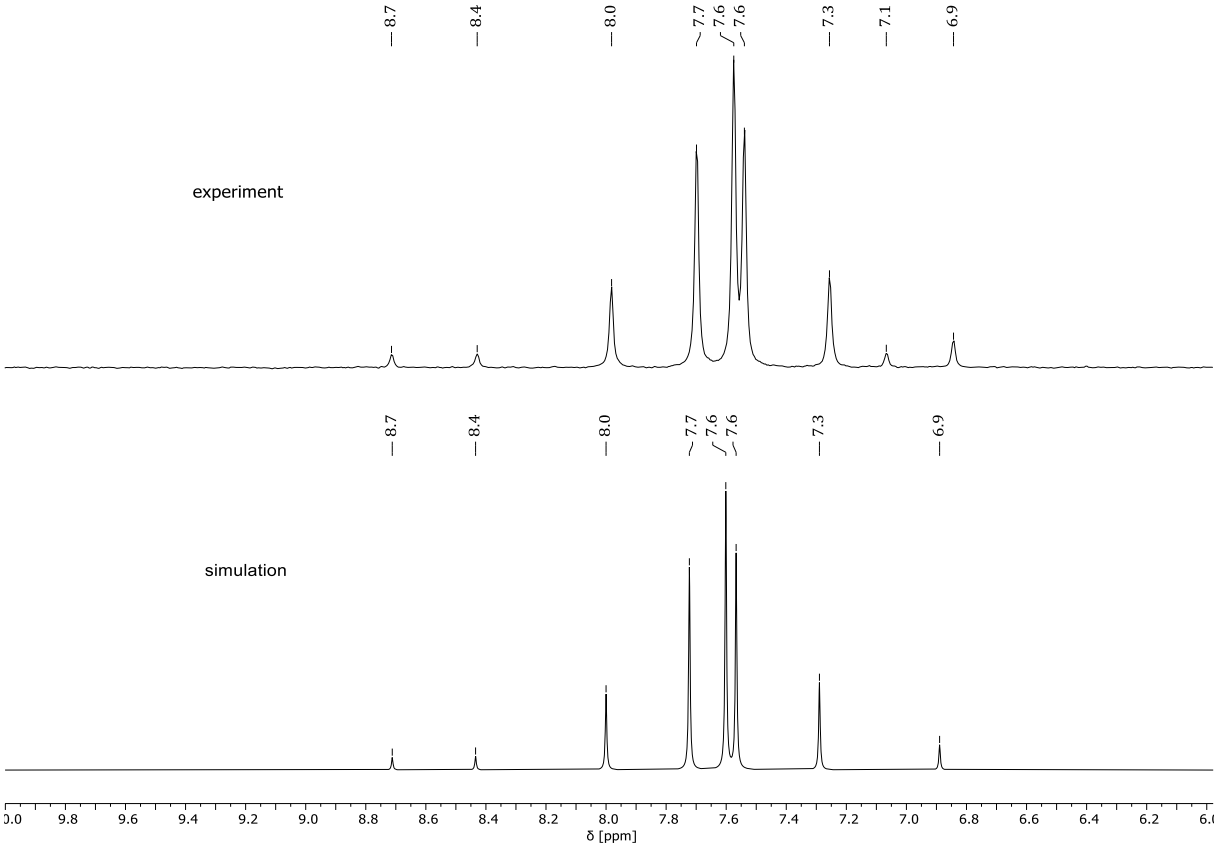


**Fig. 2.1.4.** $^{31}P\{^{1}H\}$ NMR experimental spectrum of compound **$AB_5$-2-G0** in $CDCl_3$ (top) and its simulation (bottom). The phosphorus chemical shifts and coupling constants obtained: $P_1$: 7.4 ppm, $P_2$: 7.5 ppm, $P_3$: 8.0 ppm and $J_{1-2}$: 17 Hz, $J_{2-3}$: 90 Hz, $J_{1-3}$: 90 Hz, respectively.

### 2.1.4 Specific bifunctionalization on the surface of polyphosphorhydrazone dendrimer scaffolds

Mostly, PPH dendrimers have similar terminal functions. However, having two types of surface functions is sometimes helpful in order to fulfil demanded specifications. Although the stochastic functionalization is often used for this purpose, a presence of an uncontrolled number of each type of terminal function can occur.[1] In the following, various efforts to graft different terminal functions stochastically to the **1-G0** core will be addressed. However, some of the resulting molecules have only been modified with one function and will be used to attach carboranes or carboranylphosphines as explained in the following chapter.

In a first attempt, $N_3P_3Cl_6$ was reacted with 4-methoxyphenol (**10**) to obtain different diastereomers of the three-fold substituted product **11** following a similar protocol as reported by WU and co-workers.[10] The same reaction was also carried out with the larger generation **1-G1** to obtain dendrimer **12** which then was intended to be functionalized with **1** (see **Scheme 2.1.6**).

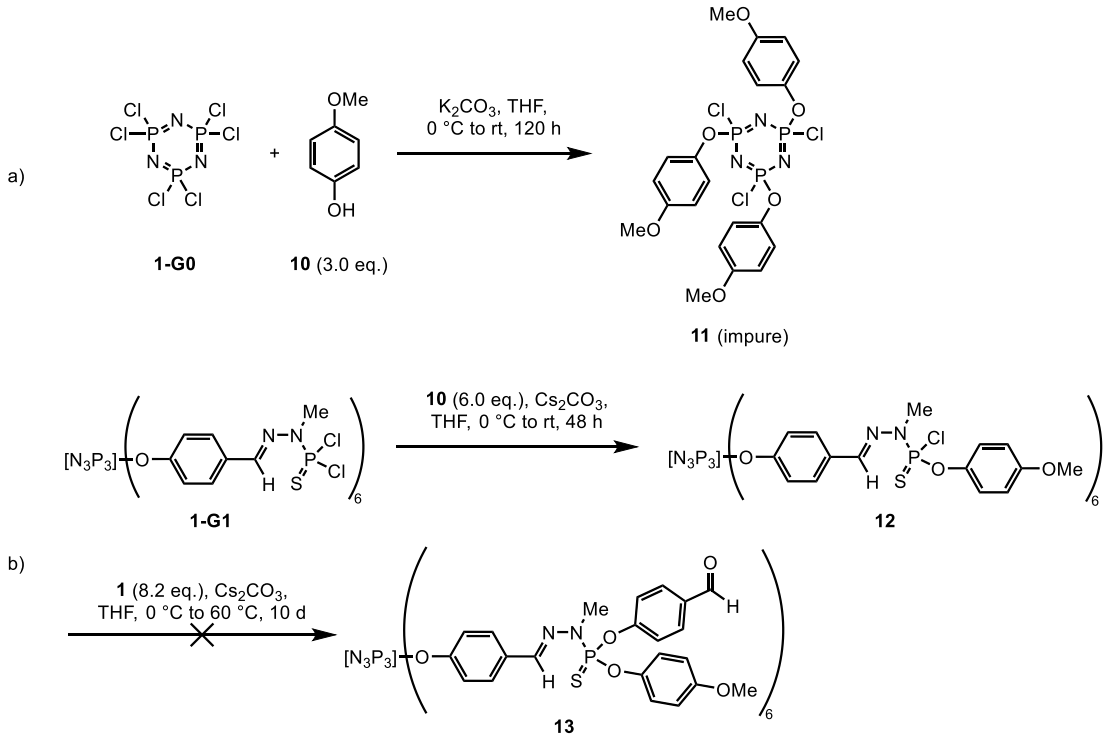


**Scheme 2.1.6.** (a) Attempted synthesis of a three-fold substituted $N_3P_3Cl_6$ core **11.** (b) Synthesis of a monosubstituted dendrimer **12** and attempted synthesis of a bifunctional dendrimer **13**.

The reaction progress was monitored by $^{31}P\{^1H\}$ and $^1H$ NMR spectroscopy. Unfortunately, the $^{31}P\{^1H\}$ NMR spectrum revealed not only the three-fold substituted product **11**, but also two- and four-fold substitution could be observed. The $^1H$ NMR spectrum further showed remaining phenol **10**, and it was not possible to separate **11** from the reaction mixture.

In a parallel attempt, the same reaction was performed with a larger generation to sequentially graft a 4-methoxyphenol function yielding different isomers of dendrimer **12**. Dendrimers that are fully monosubstituted with **10** can occur using the stochastic approach, as can dendrimers in which all the terminal groups but one are monosubstituted. Furthermore, certain dendrimers can be formed where all terminal groups except for two are monosubstituted, but the two disubstitutions can be dispersed all over the surface. It is further possible to obtain dendrimers with three disubstitutions. The obtained mixture of isomers, including compound **12**, has 0.3% disubstituted functionalities that are inert towards the reaction with other phenols (see **Fig. 2.1.5**). The $^{31}P\{^1H\}$ NMR spectrum further indicated that a lot of unreacted starting material remained (43%, signals at –62.5 ppm).

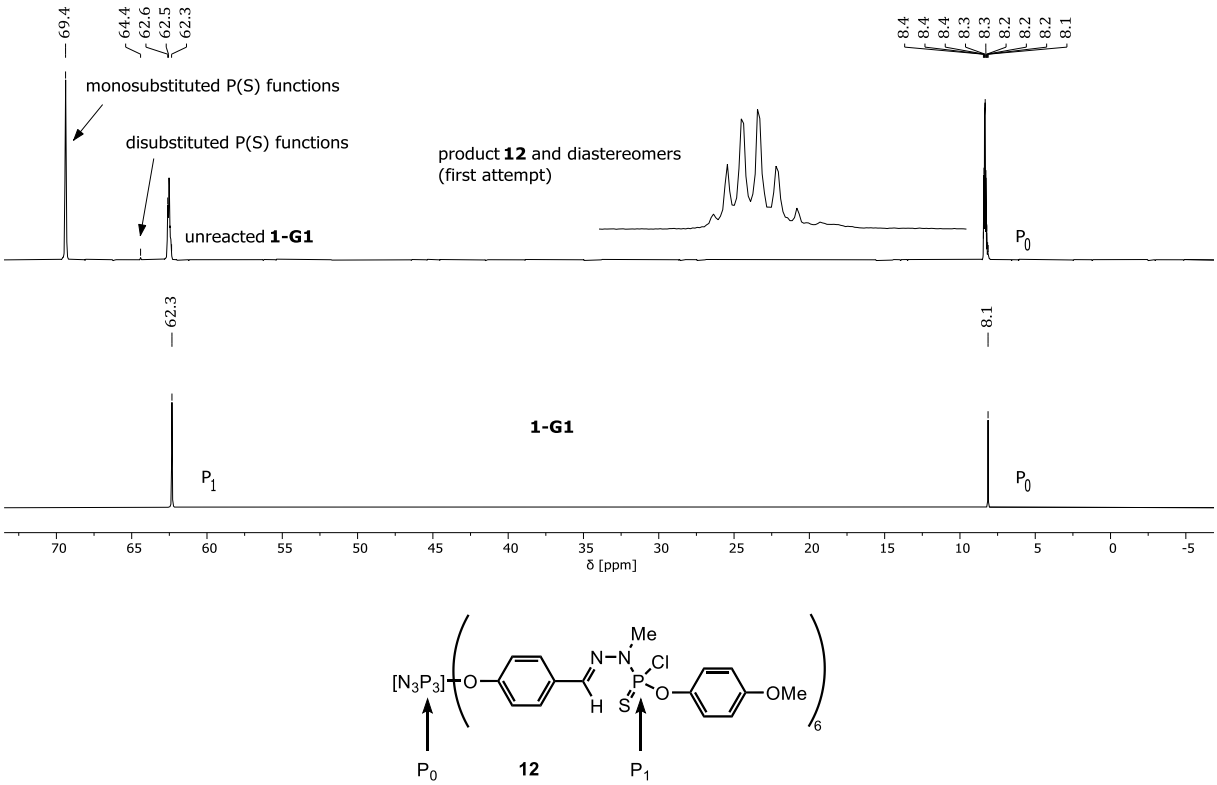


**Fig. 2.1.5.** $^{31}P\{^{1}H\}$ NMR spectra in $CDCl_3$ of monosubstituted dendrimer **12** and the symmetrically disubstituted dendrimer **1-G1**.

In a second attempt, compound **12** was prepared altering the reaction conditions. Leaving the reaction mixture for 12 days at 0 °C led to the complete disappearance of signals for the starting material **1-G1** (see **Scheme 2.1.7**). However, more disubstituted $P(S)(OC_6H_4OMe)_2$ functions (4%) could be observed. The $^{31}P\{^{1}H\}$ spectrum further indicated that hydrolysis took place during the formation of **12** (signal at –2.9 ppm, see **Fig. 2.1.6**).

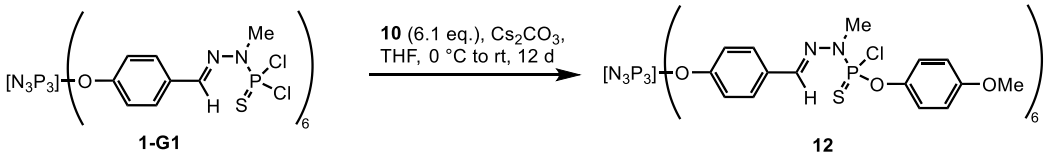


**Scheme 2.1.7.** Synthesis of **12** using an altered approach.

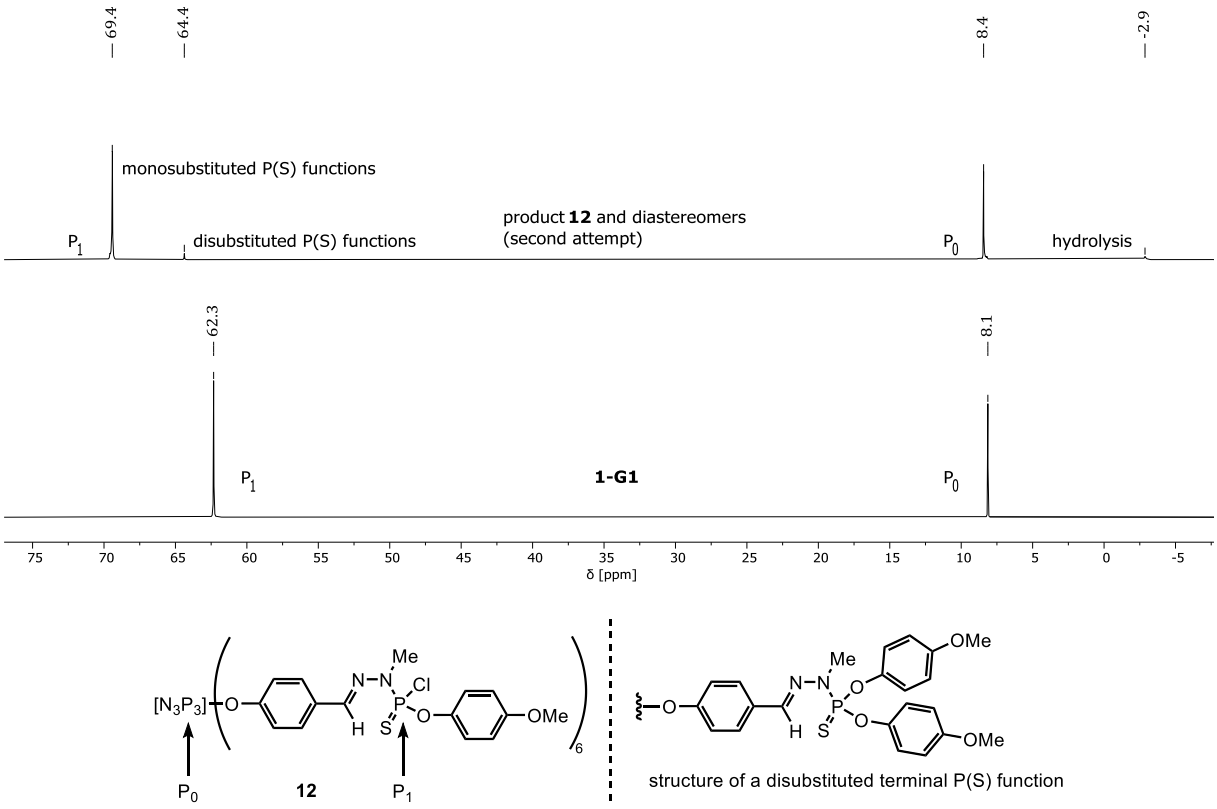


**Fig. 2.1.6.** $^{31}P\{^{1}H\}$ NMR spectra in $CDCl_3$ of monosubstituted dendrimer **12** and the symmetrically disubstituted dendrimer **1-G1**.

A further reaction of **12** with 4-hydroxybenzaldehyde (**1**) was not conducted, because all of the compound was needed for attempts to graft various new phenol- or aniline-linked carborane and carboranylphosphine derivatives. The stochastic grafting, as previously mentioned, results in an uncontrolled number and location of each type of function, resulting in various disubstituted by-products that are functionalized with the same terminal function on one phosphorus atom rather than bifunctionalization with two different terminal functions on one phosphorus atom. This is obviously in conflict with the goal of giving dendrimers a completely predictable and repeatable structure in contrast to traditional polymers.[1]

As previously stated, the synthesis of dendrimers consists of only two reiterative steps and has produced dendrimers with hundreds to thousands of surface functions in good yields in multigram scale. However, it could be shown again, that their synthesis is not trivial, especially if the generation has reached a certain size or bifunctionalization is targeted. The set goal of the synthesis of various dendrimers (classical, unsymmetrical, monofunctionalized) is to evaluate their suitability for grafting to various new phenol- or aniline-linked carboranes and carboranylphosphines. Experimental approaches will be discussed in the following chapter in detail.

## 2.2 Experimental Section

### 2.2.1 General Procedures

*Materials*: Unless otherwise stated, all reactions requiring anhydrous conditions were conducted with oven-dried glassware under an atmosphere of argon using SCHLENK techniques. All glassware was dried at 120 °C for approximately 24 h before use. Anhydrous dichloromethane, diethyl ether, methanol, *n*-pentane, and tetrahydrofuran were obtained using the MBRAUN solvent purification system MB SPS-800. Acetonitrile was distilled prior to use. Potassium and cesium carbonate were dried at 120 °C for more than 24 h before use. 4-Hydroxybenzaldehyde (**1**) was recrystallized from chloroform prior to use. $SPCl_3$ (**1-S0**) was distilled prior to use. Dendrimers **2-G0** to **1-G2**,[4] **2-S0** to **2-S1**,[5] $MMHSPCl_2$,[11] **4**,[12] and **8**[13] were prepared according to literature. All other chemicals were purchased and used as received.

*Methods:* Thin-layer chromatography (TLC) with silica gel 60 $F_{254}$ on glass or aluminium available from Merck KGaA was used for monitoring the reactions. Eluted plates were visualized using a 254 nm UV lamp. For column chromatography, silica gel (60 Å) with a particle diameter in the range of 0.035 to 0.070 mm, 0.052 to 0.073 mm or 0.063 to 0.200 mm from Sigma-Aldrich was used.

*NMR spectroscopy*: Proton ($^1$H), carbon ($^{13}$C), and phosphorus ($^{31}$P) NMR spectra were recorded on a Bruker Avance 300 MHz, a Bruker Avance III HD 400 MHz, Bruker Avance 400 MHz or Bruker Avance NEO 400 MHz NMR spectrometer at room temperature. NMR spectra were recorded at the following frequencies: $^1$H: 300.13 MHz, $^{13}$C: 75.48 MHz, $^{31}$P: 121.49 MHz (Avance 300 MHz) $^1$H: 400.18 MHz, $^{13}$C: 100.64 MHz, $^{31}$P: 162.01 MHz (Avance III HD); $^1$H: 400.16 MHz, $^{13}$C: 100.63 MHz, $^{31}$P: 161.99 MHz (Avance 400 MHz) and $^1$H: 400.13 MHz, $^{13}$C: 100.62 MHz, $^{31}$P: 161.99 MHz (Avance NEO). All chemical shifts are reported in parts per million (ppm). Tetramethylsilane was used as internal reference for $^1$H and $^{13}$C NMR spectra. $H_3PO_4$ was used as internal reference for $^{31}$P NMR spectra. NMR data were listed as follows: Chemical shift (δ) ppm (multiplicity, coupling constants, relative integral, assignment). NMR data were interpreted with MestReNova.[87]

*Electrospray ionization mass spectrometry* was performed with an UPLC Xevo G2 QTOF spectrometer from Waters in negative or positive mode. Acetonitrile, dichloromethane, methanol or mixtures of these solvents were used.

### 2.2.2 Synthetic Procedures and Characterization

#### 2.2.2.1 Synthesis of $AB_5$-2-G0

**4** (867 mg, 1.12 mmol, 1.00 eq.) and $K_2CO_3$ (376 mg, 2.72 mmol, 2.43 eq.) were suspended in MeCN (100 ml). A solution of **8** (198 mg, 1.34 mmol, 1.20 eq.) was then added and the reaction mixture was refluxed for 14.5 h. After cooling to room temperature, the reaction mixture was

filtered and the solvent evaporated. $CH_2Cl_2$ was added for extraction of the product. The product was then precipitated with a mixture of *n*-pentane/$Et_2O$ (4:1, 500 ml). After evaporation of all solvents, a white solid was obtained and further purified by column chromatography (99% $CH_2Cl_2$, 1% THF, silica gel) yielding 439 mg (5.45 mmol, 49%) of an off-white solid.

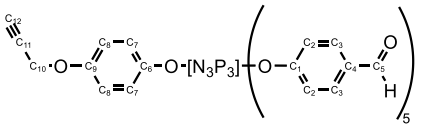

**$R_F$** (96% $CH_2Cl_2$, 4% THF 96:4) 0.53; **$^1$H NMR** (400 MHz, $CDCl_3$): δ=9.93 (d, $^3J_{H,H}$=5 Hz, 5H, $C_5$-*H*), 7.73 (ddd, $^3J_{H,H}$=8, 5, 2 Hz, 10H, $C_3$-*H*), 7.16 (d, $^3J_{H,H}$=7 Hz, 6H, $C_2$-*H*), 7.06 (d, $^3J_{H,H}$=9 Hz, 4H, $C_2$-*H*), 6.89 (d, $^3J_{H,H}$=8 Hz, 2H, $C_7$-*H*), 6.77 (d, $^3J_{H,H}$=7 Hz, 2H, $C_8$-*H*), 4.65 (d, $^3J_{H,H}$=2 Hz, 2H, $C_{10}$-$H_2$), 2.55 ppm (t, $^3J_{H,H}$=2 Hz, 1H, $C_{12}$-*H*); **$^{13}$C{$^1$H} NMR** (101 MHz, $CDCl_3$): δ=190.5–190.4 ($C_5$), 155.1 ($C_6$), 154.9–154.6 ($C_1$), 144.0 ($C_9$), 133.7–133.6 ($C_4$), 131.4–131.3 ($C_3$), 121.7 ($C_7$), 121.2 ($C_2$), 115.7 ($C_8$), 78.2 ($C_{11}$), 76.0 ($C_{12}$), 56.1 ppm ($C_{10}$); **$^{31}$P{$^1$H} NMR** (162 MHz, $CDCl_3$)*: δ=7.4 ($^2J_{1-2}$=17 Hz, $^2J_{1-3}$=90 Hz, $P_1$), 7.5 ($^2J_{1-2}$=17 Hz, $^2J_{2-3}$=90 Hz, $P_2$), 8.0 ppm ($^2J_{1-3}$=90 Hz, $^2J_{2-3}$=90 Hz); **HRMS (ESI+):** [$C_{44}H_{32}N_3O_{12}P_3$], m/z calculated: 888.1277 ([M+H]$^+$); found: 888.1856. *Values taken from a simulation in MestReNova.[87]

### 2.2.2.2 Synthesis of $AB_5$-1-G1

**$AB_5$-2-G0** (780 mg, 0.880 mmol, 1.00 eq.) was dissolved in MeCN (50 ml) and cooled to 0 °C. $MMHSPCl_2$ (20.0 ml, 0.236 mmol ml$^{-1}$, 4.72 mmol, 5.36 eq.) was added dropwise and the reaction mixture was warmed to room temperature over 17 h. After evaporation of all solvents, the crude product was extracted with $CH_2Cl_2$ (10 ml) and then precipitated with *n*-pentane (250 ml). The precipitate was isolated and dissolved in $CH_2Cl_2$ (10 ml) and then again precipitated with a mixture of *n*-pentane/$Et_2O$ (5:1, 250 ml). The product was isolated and dried and then purified by column chromatography (70% *n*-hexane, 30% $CH_2Cl_2$, silica gel) yielding 1099 mg (0.649 mmol, 74%) of an off-white solid.

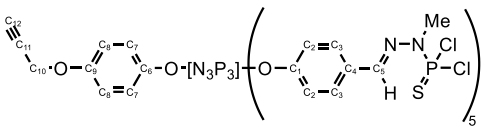

**$^1$H NMR** (400 MHz, $CDCl_3$): δ=7.64 (dd, $^3J_{H,H}$=10, 3 Hz, 10H, $C_5$-*H*), 7.58 (dd, $^3J_{H,H}$=9, 3 Hz, 10H, $C_3$-*H*), 7.09–7.02 (m, 6H, $C_2$-*H*), 7.02–6.94 (m, 4H, $C_2$-*H*), 6.92–6.83 (m, 2H, $C_7$-*H*), 6.79–6.71 (m, 2H, $C_8$-*H*), 4.61 (d, $^3J_{H,H}$=2 Hz, 2H, $C_{10}$-$H_2$), 3.49 (dd, $^3J_{H,H}$=14, 9 Hz, 15H, C$H_3$), 2.50 ppm (t, $^3J_{H,H}$=2 Hz, 1H, $C_{12}$-*H*); **$^{13}$C{$^1$H} NMR** (101 MHz, $CDCl_3$): 154.8 ($C_6$), 151.9–151.7 ($C_1$), 144.4 ($C_9$), 140.8–140.6 ($C_5$), 131.2–131.1 ($C_4$), 128.6 ($C_3$), 121.8 ($C_7$), 121.4–121.3 ($C_2$), 115.6 ($C_8$), 78.4 ($C_{11}$), 75.9 ($C_{12}$), 56.2 ($C_{10}$), 32.0–31.9 ppm ($CH_3$); **$^{31}$P{$^1$H} NMR** (162 MHz, $CDCl_3$): δ=62.6, 62.5, 62.4 (all $P(S)Cl_2$), 8.730* ($^2J_{1-3}$=95 Hz, $^2J_{2-3}$=85 Hz, $P_3$), 8.341* ($^2J_{1-2}$=47 Hz, $^2J_{2-3}$=85 Hz, $P_2$), 8.335* ppm ($^2J_{1-2}$=47 Hz, $^2J_{1-3}$=95 Hz, $P_1$); **HRMS (ESI+):** [$C_{49}H_{47}Cl_{10}N_{13}O_7P_8S_5$], m/z calculated 1693.7113 ([M+H]$^+$); found: 1693.7098. *Values taken from a simulation in MestReNova.[87]

### 2.2.2.3 Attempted synthesis of $AB_5$-2-G1

**1** (87.3 mg, 0.715 mmol, 11.31 eq.) and $Cs_2CO_3$ (277 mg, 0.851 mmol, 13.47 eq.) were suspended in MeCN (15 ml) and cooled to 0 °C. **$AB_5$-1-G1** (107 mg, 0.063 mmol, 1.00 eq.) was added to the suspension. The reaction mixture was warmed to room temperature and stirred for further 67 h, then it was heated to 40 °C and stirred for 21 h. The filtrate of the reaction mixture was centrifuged (2x, 8000 u $min^{-1}$) at 5 °C for 20 min. After evaporation of all solvents, the crude product was dissolved in $CH_2Cl_2$ and EtOAc (1:1, 20 ml) and precipitated with *n*-pentane (150 ml). The crude product was isolated and was obtained as an off-white solid. A full characterization could not be performed.

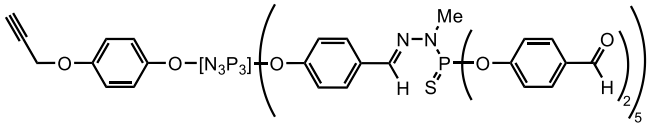


**$^1$H NMR** (400 MHz, $C_6D_6$): δ=9.90, 9.32, 9.22, 7.88, 7.34, 6.28, 6.16, 5.34, 2.79, 2.74, 1.94–1.91 (acetonitrile), 1.77 ppm; **$^{31}$P{$^1$H} NMR** (162 MHz, $C_6D_6$): δ=61.9, 61.8 (all P(S)O) 10.1–9.6 ppm (m, $N_3P_3$).

### 2.2.2.4 Attempted synthesis of 11

**1-G0** (219 mg, 0.630 mmol, 1.00 eq.) was dissolved in THF (8 ml) and cooled to 0 °C. A cooled suspension of **10** (230 mg, 1.85 mmol, 2.94 eq.) and $K_2CO_3$ (530 mg, 3.84 mmol, 6.10 eq.) in THF (10 ml) was added dropwise over 20 min at 0 °C. The reaction mixture was warmed to room temperature and stirred for 120 h, then it was filtered and the filtrate precipitated with *n*-pentane. After evaporation of all solvents, the remaining solid was characterized. A mixture of **1-G0, 10**, **11**, as well as two- and four-fold substituted **1-G0** was obtained and not further purified. **$^1$H NMR** (400 MHz, $CDCl_3$): δ=7.17–7.08 (m, 2H, $C_3$-*H*), 7.89–6.81 (m, 2H, $C_2$-*H*), 3.75 ppm (s, 3H, $OCH_3$); **$^{13}$C{$^1$H} NMR** (101 MHz, $CDCl_3$) δ=150.3 ($C_1$/$C_4$), 121.3–121.2 ($C_2$), 114.4 ($C_3$) 55.5 ppm ($OCH_3$); **$^{31}$P{$^1$H} NMR** (162 MHz, $CDCl_3$): δ=24.8–24.2 (different enantiomers and diastereomers of **11**), 22.5–22.2 (**$A_2B_4$**), 20.0 (**1-G0**), 16.3–15.7 (different enantiomers and diastereomers of **11**), 13.3–12.5 (**$A_2B_4$**), 1.2, 0.0, –3.4 ppm; **HRMS (ESI–):** [$C_{21}H_{21}Cl_3N_3O_6P_3$] m/z calculated 501.9212 ([M–$MeC_6H_4$]$^-$); found: 501.9212.

### 2.2.2.5 Synthesis of 12

**1-G1** (176 mg, 0.095 mmol, 1.00 eq.) was dissolved in THF (5 ml) and cooled to 0 °C. A cooled suspension of **10** (72.0 mg, 0.580 mmol, 6.11 eq.) and $Cs_2CO_3$ (382 mg, 12.32 mmol, 6.10 eq.) in THF (5 ml) was added dropwise over 30 min at 0 °C. The reaction mixture was kept at 10 °C and stirred for 12 d until the reaction control by $^{31}$P{$^1$H} NMR spectroscopy showed a completed reaction. The reaction mixture was filtered, then the filtrate was precipitated with *n*-pentane (150 ml). The crude product was obtained by filtration and dried yielding 591 mg of **12** mixed with different by-products (refer to the explanations in **2.1.4**, as seen by $^{31}$P{$^1$H} NMR spectroscopy).

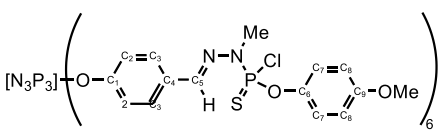

**$^{1}$H NMR** (400 MHz, $CDCl_3$): δ=7.68–7.55 (m, 18H, $C_5$-*H*, $C_3$-*H*), 7.22–7.14 (m, 12H, $C_2$-*H*), 6.99 (d, $^{3}J_{H,H}$=9 Hz, 12H, $C_8$-*H*), 6.82 (dd, $^{3}J_{H,H}$=9, 2 Hz, 12H, $C_7$–*H*), 3.75 (s, 18H, OC*H*$_3$), 3.37 ppm (d, $^{3}J_{H,H}$=13 Hz, 18H, NC*H*$_3$); **$^{13}$C{$^{1}$H} NMR** (101 MHz, $CDCl_3$): δ=157.5 ($C_9$), 151.5 ($C_1$), 145.1 ($C_6$), 139.2 ($C_5$), 131.9 ($C_4$), 128.5 ($C_3$), 122.4 ($C_2$), 121.3 ($C_8$), 114.6 ($C_7$), 55.6 ($OCH_3$), 32.4 ($NCH_3$) ppm; **$^{31}$P{$^{1}$H} NMR** (162 MHz, $CDCl_3$): δ=69.4 (P(S)($OC_6H_4OMe$)Cl), 8.4 ppm ($N_3P_3$).

## 2.3 Conclusion

This chapter focused on the synthesis of symmetrical dendrimers starting from a $P(S)Cl_3$ or an $N_3P_3Cl_6$ core using a two-step procedure. The procedure involved repeating a substitution reaction with 4-hydroxybenzaldehyde and a condensation reaction with the phosphorhydrazide $MMHSPCl_2$. Four classical dendrimers were synthesized in good yields (62–98%) and acceptable purities up to generation **1-G2** or **2-S1**, respectively. The purification process was challenging, with minor impurities observed due to hydrolysis and impure starting materials.

PPH dendrimers typically have similar terminal functions, but having two types of functions can be useful. Five unsymmetrical dendrimers could be obtained by bifunctionalization of $N_3P_3Cl_6$, allowing several functions to be distinct from the others. This method has been used for the synthesis of several $AB_5$ dendrimers, with A being 4-(prop-2-yn-1-yloxy)phenol (**8**) and B being 4-hydroxybenzaldehyde (**1**). Dendron **4** was synthesized with one terminal chloride function first, and then $AB_5$ dendrimers up to generation **$AB_5$-2-G1** were synthesized. Also, other attempts have been made to obtain monosubstituted $P(S)Cl_2$ groups in **1-G0** and **1-G1**. The latter was more successful and yielded two other dendritic compounds which were used for the anchoring attempts of carboranes and carboranylphosphines (see Chapter **3.2.3**).

The reaction progress in all reactions was monitored by $^{31}$P{$^{1}$H} and $^{1}$H NMR spectroscopy. More complex $^{31}$P{$^{1}$H} NMR spectra were obtained for the $AB_5$ dendrimers due to second order effects. This ABX spin system was analyzed and compared to a simulation.

## 2.4 References

[1] M. Petriccone, R. Laurent, C.-O. Turrin, R. M. Sebastián, A.-M. Caminade, *Organics* **2022**, *3*, 240–261.

[2] A.-M. Caminade, A. Ouali, A. Hameau, R. Laurent, C. Rebout, B. Delavaux-Nicot, C. O. Turrin, K. Moineau Chane-Ching, J. P. Majoral, *Pure Appl. Chem.* **2016**, *88*, 919–929.

[3] N. Launay, A.-M. Caminade, J. P. Majoral, *J. Organomet. Chem.* **1997**, *529*, 51–58.

[4] N. Launay, M. Slany, A.-M. Caminade, J. P. Majoral, *J. Org. Chem.* **1996**, *61*, 3799–3805.

[5] N. Launay, A.-M. Caminade, R. Lahana, J.-P. Majoral, *Angew. Chem. Int. Ed. Engl.* **1994**, *33*, 1589–1592.

[6] A.-M. Caminade, R. Laurent, C.-O. Turrin, C. Rebout, B. Delavaux-Nicot, A. Ouali, M. Zablocka, J.-P. Majoral, *Comptes Rendus Chim.* **2010**, *13*, 1006–1027.

[7] C. W. Allen, *Chem. Rev.* **1991**, *91*, 119–135.

[8] MestReNova (v. 14.1.0), Mestrelab Research S.L., **2019**.

[9] D. Riegert, A. Pla-Quintana, S. Fuchs, R. Laurent, C. Turrin, C. Duhayon, J. Majoral, A. Chaumonnot, A.-M. Caminade, *Eur. J. Org. Chem.* **2013**, *2013*, 5414–5422.

[10] X. Zhang, Y. Eichen, Z. Miao, S. Zhang, Q. Cai, W. Liu, J. Zhao, Z. Wu, *Chem. Eng. J.* **2022**, *440*, 135806.

[11] J. P. Majoral, R. Kraemer, J. Navech, F. Mathis, *J. Chem. Soc. Perkin Trans. 1* **1976**, 2093.

[12] G. Franc, S. Mazères, C.-O. Turrin, L. Vendier, C. Duhayon, A.-M. Caminade, J.-P. Majoral, *J. Org. Chem.* **2007**, *72*, 8707–8715.

[13] M. Srinivasan, S. Sankararaman, H. Hopf, I. Dix, P. G. Jones, *J. Org. Chem.* **2001**, *66*, 4299–4303.

# Chapter 3: Carboranylphosphines: B9-substituted derivatives with enhanced reactivity for the anchoring to dendrimers

# 3 Carboranylphosphines: B9-substituted derivatives with enhanced reactivity for the anchoring to dendrimers

As laid out in the introduction, although carborane or carboranyl pnictogen and chalcogen ligands based on a dendritic backbone hold great promise for the construction of transition metal complexes applied in homogeneous catalysis or the pharmaceutical sector, there are no examples of PPH dendrimers functionalized with carboranes or carboranylphosphines and relatively few examples of catalysis with monomeric carboranylphosphines. In the following chapter, the synthesis of new *ortho*-carboranes and carboranylphosphines, which serve as anchors for the complexation of catalytically active metal species is discussed. After a rather simple preparation, computational tests of their stability when tethered to dendrimers were performed. After it was established that these molecules are very stable, synthetic methods were used to produce these compounds. The synthesis proved to be trickier than expected. Even though reactions with carboranylphosphines did not result in a full substitution, unique carborane-substituted dendrimers were synthesized and described, which provided insight into why full substitutions did not occur in contrast to the computational results. The findings presented in this chapter concern a manuscript that will be submitted soon.

## 3.1 Introduction

Icosahedral *closo*-dicarbadodecaboranes (carboranes) have been a focus of interest of many research groups in the past years as building blocks for applications in medicinal chemistry,[1–4] metal complexes,[5–7] supramolecular assemblies, macrocyclic molecules,[8] and luminescent materials.[9,10] Important modifications of carboranes include functionalization of both, boron and carbon vertices, which are influenced by two fundamental electronic properties: the electron delocalization and the electron-withdrawing character of the skeletal carbon atoms.[11] The latter causes an acidic character at the carbon-bound protons, thus facilitating their removal by bases. The acidity can be further adjusted by introducing electron-withdrawing or electron-donating substituents at the boron vertices.[12] Substitution of the carbon-bound hydrogen atoms in carboranes by different heteroatoms such as carbon, nitrogen, oxygen, phosphorus, and sulfur already yielded a wide scope of PP,[13–15] PN,[16] PS,[17] PC,[18] and other ligands for transition metal complexes and catalytically active metals.[19] Especially, the easily accessible 1,2-bisphosphanyl-substituted carboranes (*ortho* isomers) are a family of versatile compounds with appealing features based on the carborane scaffold such as their adaptable C–C bond length, their electron-withdrawing effect, and the ability of hydridic B–H groups to engage in metal bonding.[20] The carborane scaffold further enhances the stability of phosphines towards oxygen in contrast to alkyl- and aryl-substituted phosphines. Certain compounds such as 1,2-bis(chlorophosphino)-

*ortho*-carborane, first reported in 1963,[13] are even inert against the reaction with sulfur up to 200 °C.[19] The aforementioned properties make carboranylphosphines promising ligands for metal complexes applied in homogeneous catalysis. However, the synthesis of homogeneous catalysts capable of selective and fast transformations, while being readily and quantitatively separated from reaction products, remains difficult.[21,22] One commonly investigated method is the attachment of homogeneous catalysts to insoluble supports such as silica. Problems with this strategy include nonuniformity and partially unknown structures of heterogenized catalysts, mass transport limitations, usually reduced activity compared to their homogeneous counterparts, and metal complex leaching.[22] Another approach is the attachment to soluble supports. Because of their well-defined design, macromolecules such as dendrimers offer precise management of a catalyst structure,[22] and are soluble yet recoverable through nanofiltration or precipitation, depending on the organic solvent used.[23] Furthermore, increasing local concentrations of catalytic sites positioned on the surface of dendrimers might result in dendritic effects with varying activity depending on the generation of dendrimer employed.[24] Dendritic effects in catalysis can result in a variety of features, including easier recovery and reuse of dendritic catalysts. This might reduce metal complex leaching. To date, no carboranylphosphine-functionalized dendrimer has been reported, and only a few examples of monomeric carboranylphosphine catalysts are known.[25–27]

However, not only catalytic applications should be considered. Bearing a large number of boron atoms, carboranes have been investigated as suitable building blocks in reagents for boron neutron capture therapy (BNCT).[4,28] To date, the only cluster compound used in clinical trials is sodium mercaptoundecahydro-*closo*-dodecaborate.[29] Thus, using hyperbranched macro-molecules like dendrimers as scaffolds is an intriguing approach to boron-rich molecules. To the best of our knowledge, no dendrimers derived from $N_3P_3Cl_6$ or $SPCl_3$ with carboranes as terminal functions have been reported.

In this chapter, the synthesis of novel B9-functionalized *ortho*-carboranes as well as 1- or 1,2-phosphanyl-substituted *ortho*-carboranes is presented. Furthermore, the grafting of these monomers to dendritic compounds was investigated experimentally and by DFT simulations.

## 3.2 Results and Discussion

### 3.2.1 Synthesis

Starting from commercially available *ortho*-carborane (**14**), 9-iodo-*ortho*-carborane (**15**) was prepared according to the literature.[30] In the next step, different organomagnesium halides were reacted with **15** to yield the B9-substituted carboranes **16**–**19** as well as **20**[31] and **21**[32] according to published protocols (see **Scheme 3.2.1**).[33] The TBDMS (TBDMS = *tert*-butyl-dimethylsilyl) and the dibenzyl protecting groups were introduced prior to the formation of the

GRIGNARD reagents to avoid unwanted side reactions of the hydroxy or amine function.[34–36] Excluding elemental iodine during the synthesis of the GRIGNARD reagents increased the yields of the B9-substituted carboranes significantly.

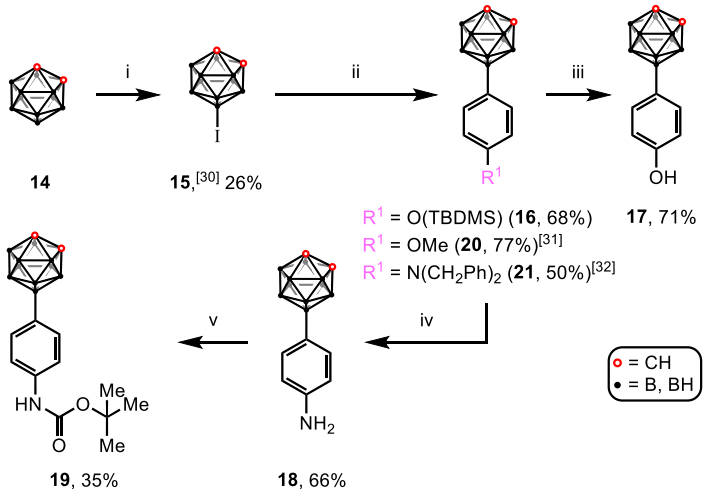


**Scheme 3.2.1.** Synthesis of B9-substituted *ortho*-carboranes. (i) $I_2$, $HNO_3/H_2SO_4$, AcOH, 80 °C, 18 h; (ii) *p*-$R^1C_6H_4$-MgBr, $[PdCl_2(PPh_3)_2]$, for **16**: THF/$Et_2O$, 0 °C, 66 h, for **20**: THF, rt, 120 h,[31] for **21**: THF, rt, 2 d,[32]; (iii) **17** is formed as by-product during the synthesis of **16** (LiCl, THF, rt, 2 d) or was prepared from **20** and HBr (33%), AcOH, ΔT, 24 h; (iv) Pd/C (5%), $H_2$ (20 bar), THF, rt, 96 h; (v) $Boc_2O$, THF, rt, 14 h.

After the Pd-catalyzed coupling (ii in **Scheme 3.2.1**), compounds **16** and **21** were deprotected using different strategies to make them suitable candidates for further modifications ($R^1$ = OH (**17**) or $NH_2$ (**18**)). A phenoxy or a phenylamino group is necessary for grafting to different macromolecules as demonstrated by CAMINADE and co-workers.[37] The methoxyphenyl substituent in **20** mimics the phenoxy linker needed in immobilization reactions. It can be considered as the monomeric equivalent of the carboranyl-substituted dendrimers.

In the following step, carboranylmono- **22**–**24** and bisphosphines **25**–**32** were prepared according to the synthetic pathway described by ALEXANDER and SCHROEDER,[13] employing the lithiation of the carborane derivatives **16**, **17**, and **19**–**21**, followed by treatment with the corresponding chlorophosphines or -phosphite (**Scheme 3.2.2**). Carboranylmonophosphines **22**–**24** were formed as by-products in the synthesis of the carboranylbisphosphines **25**–**32** and isolated in low to moderate yields.

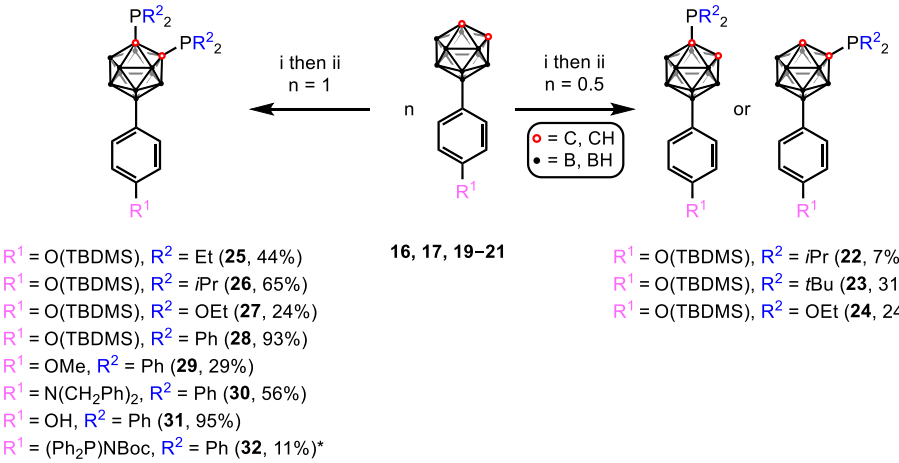


**Scheme 3.2.2.** Synthesis of B9-substituted carboranylphosphines. (i) *n*-butyllithium, $Et_2O$ or THF, −78 °C to rt; (ii) $PR^2{}_2Cl$, $Et_2O$ or THF, −78 °C / 0 °C to rt. *The NH group in **19** was also substituted by $PPh_2$.

Deprotection of the hydroxyl and amino groups was then attempted. Deprotection of **30** to obtain the free phenylamino carboranylphosphine failed despite several attempts applying known hydrogenation methods (Pd/C, $NH_4(HCOO)$; Pd/C, $H_2$).[38,39] Unfortunately, the substitution reaction with *tert*-butyloxycarbonyl (Boc)-protected carborane **19** always resulted in the triphosphanylated product **32**, even when only two equivalents of *n*-butyllithium and chlorodiphenylphosphine were employed. The monophosphines **22** and **24** were hydrolyzed or oxidized over time forming **33** and **34**, respectively (**Scheme 3.2.3**).

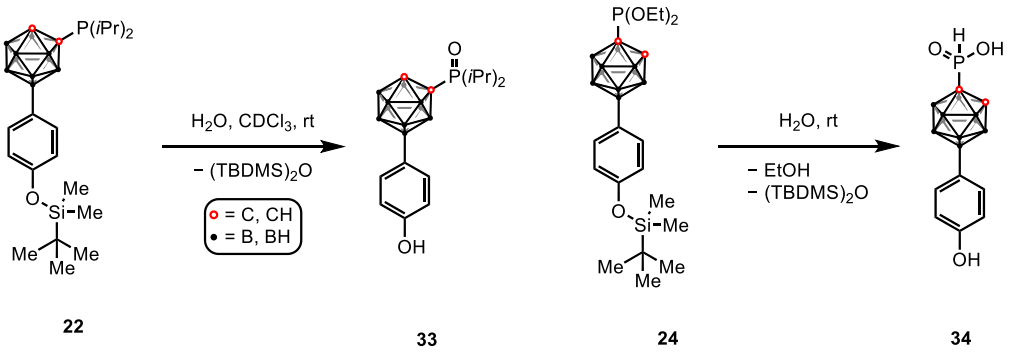


**Scheme 3.2.3.** Decomposition of monophosphines **22** and **24** after exposure to air for several months.

### 3.2.2 Characterization

Compared to the respective chlorophosphines,[40] the $^{31}P\{^1H\}$ NMR signals of the carboranylmono- and bisphosphines **22**–**32** are shifted to higher field (**Table 3.2.1**).

**Table 3.2.1.** Influence of the choice of the phosphorus substituents on the pattern and the $^{31}P\{^{1}H\}$ NMR chemical shifts [ppm] of carboranylmono- and carnoranylbisphosphines as well as of the respective chlorophosphines ($J_{PP}$ coupling constant in Hz).

| Compound | $^{31}P\{^{1}H\}$[a] | | $^{31}P\{^{1}H\}$[a] | | $^{31}P\{^{1}H\}$[a] |
|---|---|---|---|---|---|
| **$Ph_2PCl$**[b] | 81.8 | **28** | 7.3, 5.9 (d, 123) | **$Ph_3P$**[41] | −6 |
| **29** | 7.1, 5.4 (d, 122) | **30** | 7.2, 5.4 (d, 123) | **31** | 7.2, 5.5 (d, 123) |
| **32** | 58.5 (P–N), 7.0, 5.5 (d, 122) | | | | |
| **$Et_2PCl$**[40] | 117.7 | **25** | 4.9, 3.1 (d, 120) | **$Et_3P$**[42] | −20 |
| ***i*$Pr_2PCl$**[b] | 133.8 | **26** | 32.3, 30.2 (d, 107) | ***i*$Pr_3P$**[42] | 19 |
| ***t*$Bu_2PCl$**[b] | 146.6 | **23** | 94.3 ,92.1 (5:4) | ***t*$Bu_3P$**[41] | 63 |
| **$P(OEt)_2Cl$**[b] | 166.4 | **27** | 151.6, 149.9 (d, 136) | **$P(OEt)_3$**[43] | 138 |
| **22** | 58.6, 58.1 (1:1) | **24** | 152.8, 151.7 (1:1) | | |

[a] In $CDCl_3$ at 25 °C. [b] Experimentally measured.

However, compared to the $^{31}P$ resonances of the trialkyl- and triarylphosphines,[41,42] the signals of the carboranylmono- and bisphosphines are shifted downfield. This indicates that the *closo*-carboranyl group displays a strong electron-acceptor character, stronger than hydrocarbons. Interestingly, the $^{31}P\{^{1}H\}$ NMR spectra of the carboranyl bis(diphenyl)phosphines **28**–**32** differ only slightly which indicates that there is almost no influence of the substituents in the B9 position on the electron density around the phosphorus atoms.

Most of the compounds were obtained as single crystals and analyzed by single crystal X-ray diffraction (XRD) analysis (**Fig. 3.2.1**, **Fig. 3.2.2**, and **Fig. 3.2.3**).

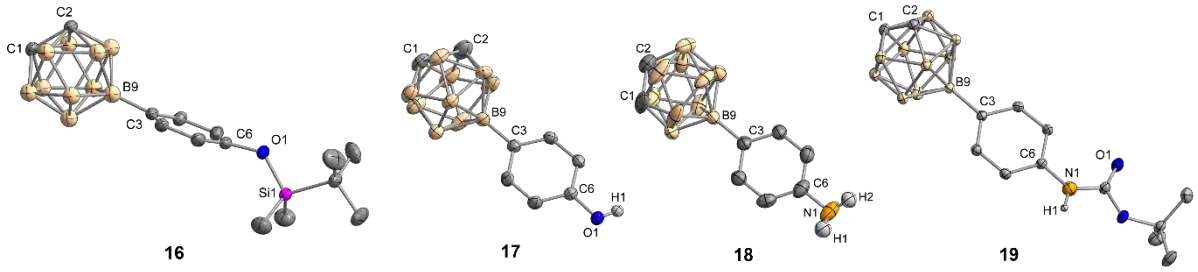


**Fig. 3.2.1.** Molecular structures of carboranes **16**–**19** in the solid state with thermal ellipsoids drawn at the 50% probability level. Hydrogen atoms other than OH and NH are omitted for clarity. Selected bond lengths [Å] of **16**: C1–C2 1.620(3); **17**: C1–C2 1.623(3); **18**: C1–C2 1.596(4); **19**: C1–C2 1.625(1).

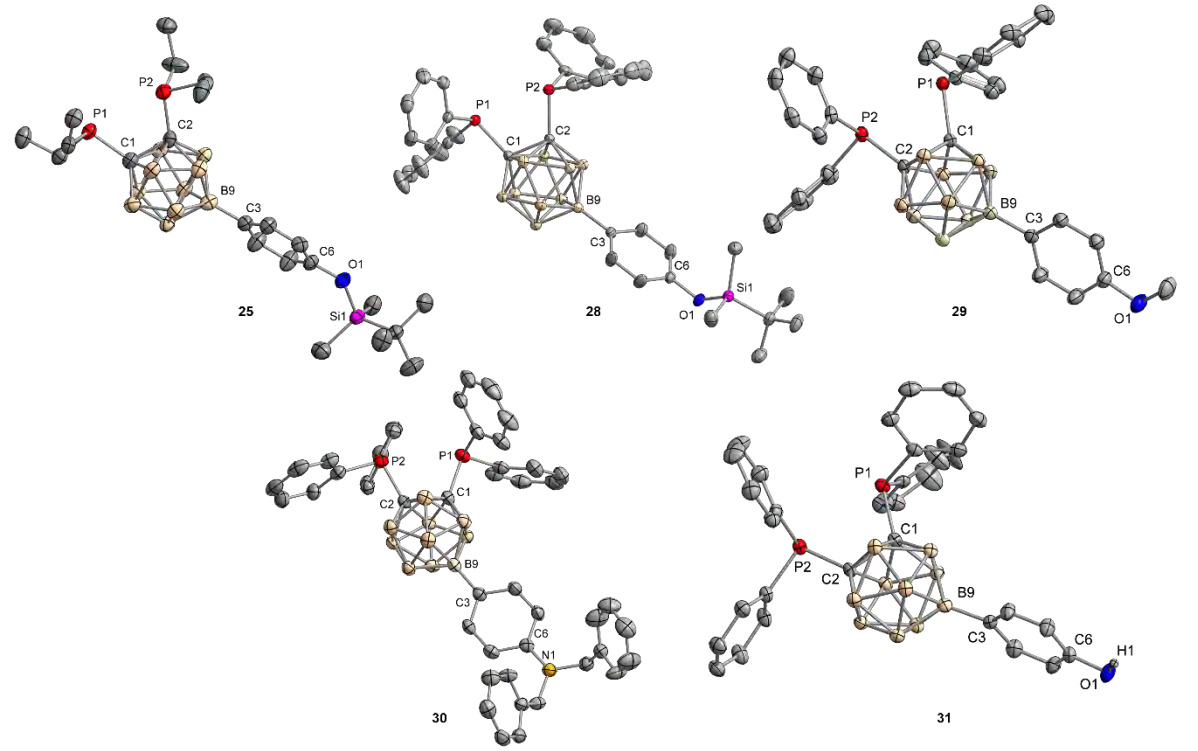


**Fig. 3.2.2.** Molecular structures of carboranylphosphines **25** and **28**–**31** in the solid state with thermal ellipsoids drawn at the 50% probability level. Hydrogen atoms other than OH in **31** are omitted for clarity. Selected bond lengths [Å] of **25**: C1–C2 1.717(10), mean P–C 1.879(1), P1···P2 3.280(2); **28**: C1–C2 1.717(3), mean P–C 1.882(7), P1···P2 3.195(8); **29**: C1–C2 1.717(3), mean P–C 1.881(7), P1···P2 3.224(7); **30**: C1–C2 1.716(2), mean P–C 1.883(7), P1···P2 3.130(1); **31**: C1–C2 1.706(3), mean P–C 1.883(2), P1···P2 3.1827(9).

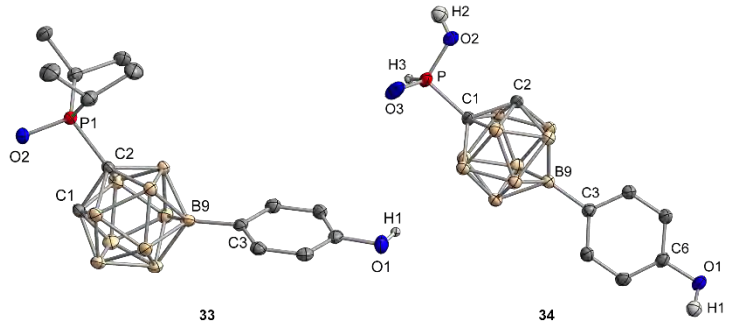


**Fig. 3.2.3.** Molecular structures of carboranylphosphines **33** and **34** in the solid state with thermal ellipsoids drawn at the 50% probability level. Hydrogen atoms other than OH and PH are omitted for clarity. Selected bond lengths [Å] of **33**: C1–C2 1.657(3), C2–P 1.867(3); **34**: C1–C2 1.641(2), C1–P 1.825(2).

A survey of the CSD (Cambridge Structural Database, version 5.43, November 2021) was performed with ConQuest® (version 2022.2.0) and bond lengths of selected carboranyl-phosphines and substituted *ortho*-carboranes were obtained.[44,45] The C1–C2 ($C_{Cage}$–$C_{Cage}$) bond lengths of the carboranylphosphines compare well with other known compounds (1.727(46) Å).[44,45] Compared to the C-unsubstituted and C-monosubstituted carboranes, which also show C1–C2 distances in the same range as already reported (1.630(35) Å for C-unsubstituted,[44,45] and 1.659(20) Å for 1-$PR_2$-*ortho*-carboranes).[44,45] A significant increase of the bond length can be observed in the disubstituted compounds (**16**: 1.620(3) Å vs. **25**: 1.716(2) Å) due to the electronic and steric influence of the substituents on the P atoms. As reported in literature, phosphorus atoms convey a unique tunability to the $C_{Cage}$–$C_{Cage}$ distance.[19]

The mean C–P bond lengths of the carboranylphosphines (C–P between 1.879(1) Å for **25** and 1.883(7) Å for **30**) compare well with other carboranylphosphines (1.898(17) Å).[44,45] The same is true for the P···P distances (literature: 3.295(15) Å).[44,45] The obtained results show that there is only a marginal influence of different substituents in the B9 position on the C1–C2 and C–P bond lengths, but, as expected, a big influence of the substituents at the phosphorus atom. It should therefore be possible to employ these compounds in metal complexation reactions as was already shown for 1,2-diphenylphosphino-*ortho*-carborane.[6]

### 3.2.3 Grafting to Monomers and Dendrimers

The grafting of compounds **17** and **31**, bearing appropriate functionalities for an attachment to different macromolecules, was investigated theoretically and experimentally with various dendritic phosphorus-containing compounds (**35**, **1-G0**, and **1-S0**, see **Fig. 3.2.4**).[46,47] The dendrimer **1-G1** was synthesized applying well-known procedures.[47]

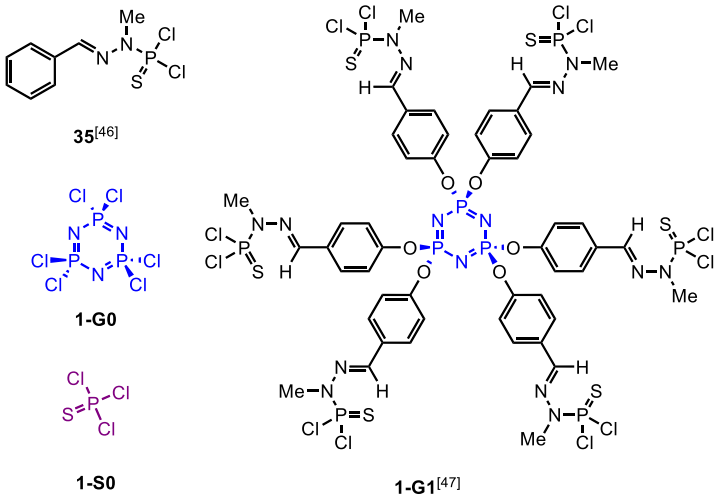


**Fig. 3.2.4.** Different scaffolds tested for grafting reactions with carborane derivative **17** and carboranylphosphine derivative **31**.

Before starting the synthetic work, DFT calculations were carried out to establish the mechanism of the substitution process of one equivalent of **17** on the hexachlorocyclotri-phosphazene core **1-G0**. The investigation started with the optimization of the deprotonated starting material **17*** and product **G01**, showing greater stability of **G01** by 31.1 kcal mol$^{-1}$ relative to the starting material **1-G0**. The reaction proceeds similar to an $S_N2$, with the nucleophilic phenoxide **17*** approaching the electrophilic phosphorus center opposite to the leaving group $Cl^-$, as is also supported by an O–P–Cl angle of 178.3° and a change in geometry from tetrahedral to trigonal-bipyramidal in the transition state (TS) (see **Scheme 3.2.4**).[48,49]

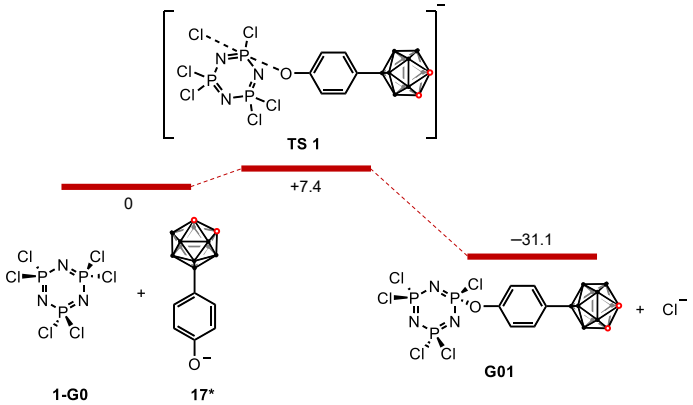


**Scheme 3.2.4.** GIBBS energy profile in THF as solvent (in kcal mol$^{-1}$) for the substitution of **1-G0** with one equivalent of **17***.

Furthermore, also the products of multiple substitution reactions of **1-G0** with **17*** were optimized to computationally check the stability of such products. Even the six-fold substitution of **1-G0** results in a product with greater stability (by 194.5 kcal mol$^{-1}$) than the starting material **1-G0** (see **Scheme 3.2.5**). The energy difference of various substitution patterns was found to be

relatively small. With differences between the diastereomers of 1.1 kcal mol$^{-1}$ (range of van der Waals interactions,[50] less than the rotation barrier in ethane)[51] up to 7.8 kcal mol$^{-1}$ (range of hydrogen bonding)[52] it is evident, that no diastereomer is preferentially formed during the reaction.

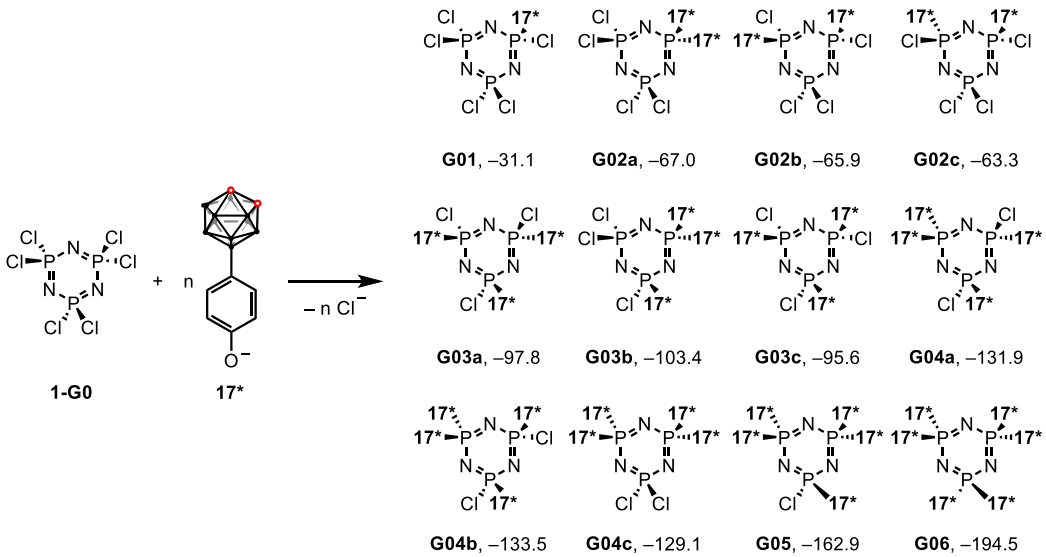


**Scheme 3.2.5.** Computed GIBBS energy values in THF as solvent (in kcal mol$^{-1}$) for the substitution of **1-G0** with n equivalents of **17*** relative to the starting material **1-G0**.

As calculations support the possibility of multiple substitution of chlorides in **1-G0** by phenoxide **17***, this hypothesis was experimentally checked (see **Scheme 3.2.6**).

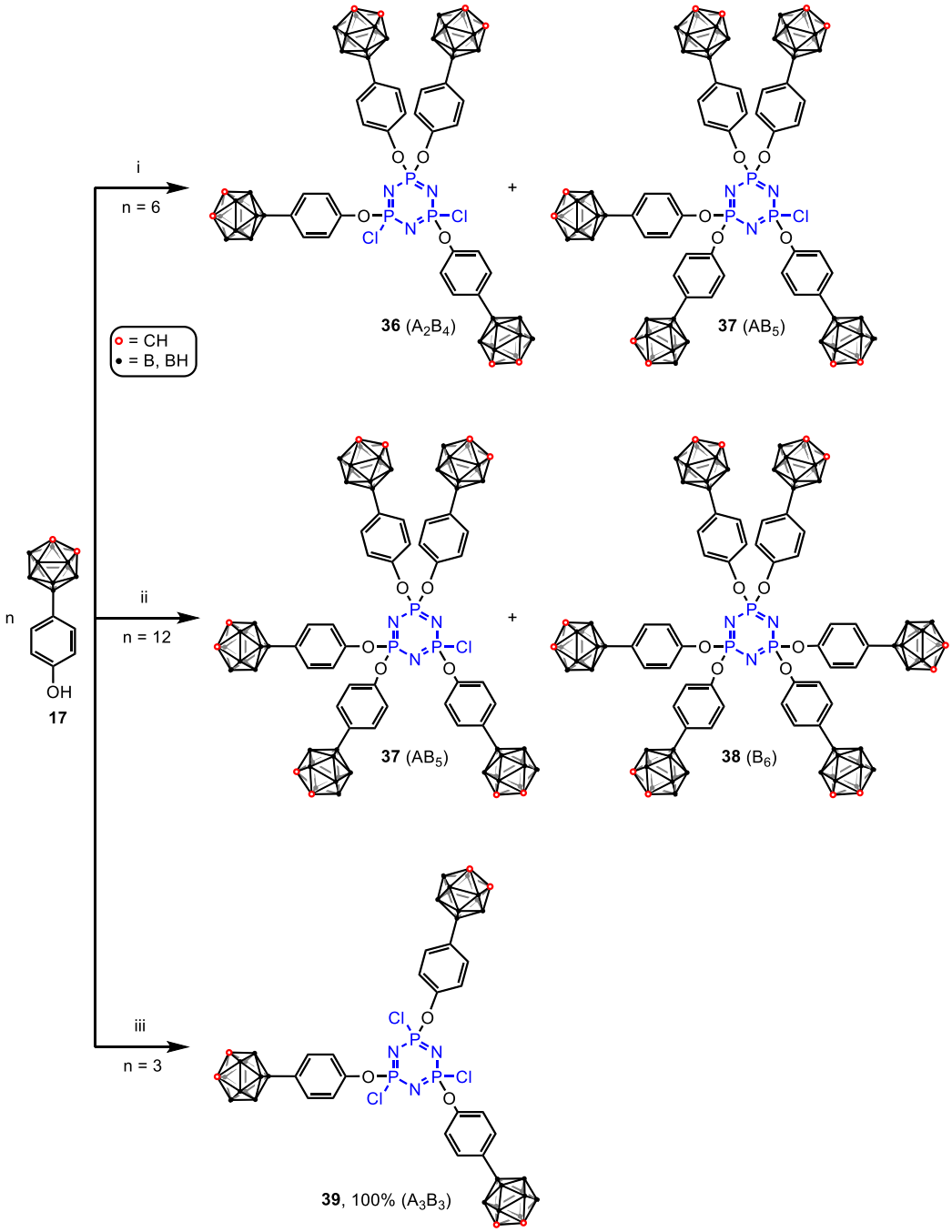


**Scheme 3.2.6.** Reaction of different equivalents of **17** with $N_3P_3Cl_6$. (i) **1-G0**, $K_2CO_3$, acetone, 40 °C for 120 h then rt for 72 h; (ii) **1-G0**, $Cs_2CO_3$, THF, rt, 25 d; (iii) **1-G0**, $K_2CO_3$, acetone, rt, 72 h. All compounds were analyzed by NMR spectroscopy and ESI-MS. Only one isomer of the incompletely substituted dendrimers ($A_3B_3$, $A_2B_4$) is displayed.

Depending on the amount of **17** used, different dendrimers varying from a three-fold (**39**, $A_3B_3$) to a six-fold substitution (**38**, $B_6$) could be obtained. However, neither **36** nor **37** and **38** could be purified successfully. On the contrary, the substitution of only one Cl per phosphorus atom yielded **39** almost quantitatively, albeit as a mixture of isomers.

With thiophosphoryl chloride (**1-S0**), a three-fold substitution was possible, but the product **40** was isolated only in very low yield (**Scheme 3.2.7**), as deboronation occurred with base yielding various *nido*-carborane species (observed by $^{11}B\{^1H\}$ NMR spectroscopy). The subsequent chromatographic purification decreased the yield further. The $^{31}P\{^1H\}$ NMR spectrum only showed one signal at 52.3 ppm which is downfield shifted compared to $P(S)Cl_3$ (28.6 ppm), corresponding to a trisubstitution. The experimental result agrees with the theoretically (DFT) predicted increased stability (90.4 kcal mol$^{-1}$) of the trisubstituted product **40** over the mono- (33.5 kcal mol$^{-1}$) and disubstituted (64.6 kcal mol$^{-1}$) derivatives compared to the starting material **1-S0**.

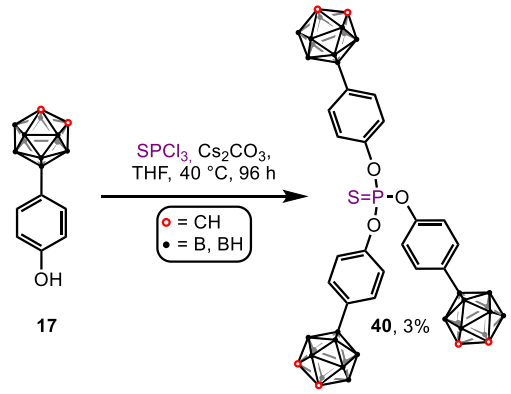


**Scheme 3.2.7.** Synthesis of the triply substituted derivate **40** of **1-S0** using four equivalents of **17**.

Compound **35** with a $P(S)Cl_2$ function was tested as a model for complex dendrimer **1-G1** to obtain further information about the possible substitution on the phosphorus atom. Under the conditions used, a complete conversion into the two-fold substituted compound **41** was not observed (yield only 14%, **Scheme 3.2.8**). This could be due to the only slight excess of **17** used in this reaction.

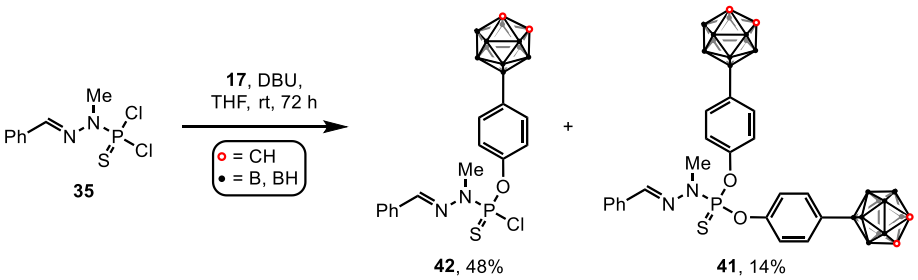


**Scheme 3.2.8.** Reaction of model compound **35** with 2.1 equivalents of **17**. DBU = 1,8-diazabicyclo[2.4.0]undec-7-ene.

Similar experiments were performed with the generation 1 of the phosphorus-containing dendrimer **1-G1** leading to the formation of dendrimer-based carborane **43** (**Scheme 3.2.9**). Its whole structure is further presented because this is the sole carborane derivative based on dendrimers synthesized in this project (see **Fig. 3.2.5**).

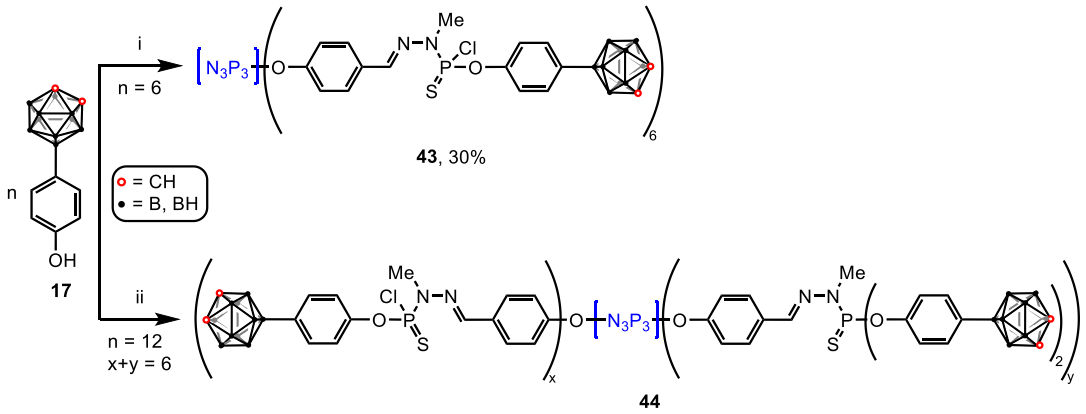


**Scheme 3.2.9.** Reaction of different equivalents of **17** (n = 6 or 12) with generation 1 dendrimer **1-G1**. (i) **1-G1**, $Cs_2CO_3$, THF, rt for 72 h then 40 °C for 23 h; (ii) **1-G1**, $Cs_2CO_3$, THF, rt for 72 h then 40 °C for 23 h.

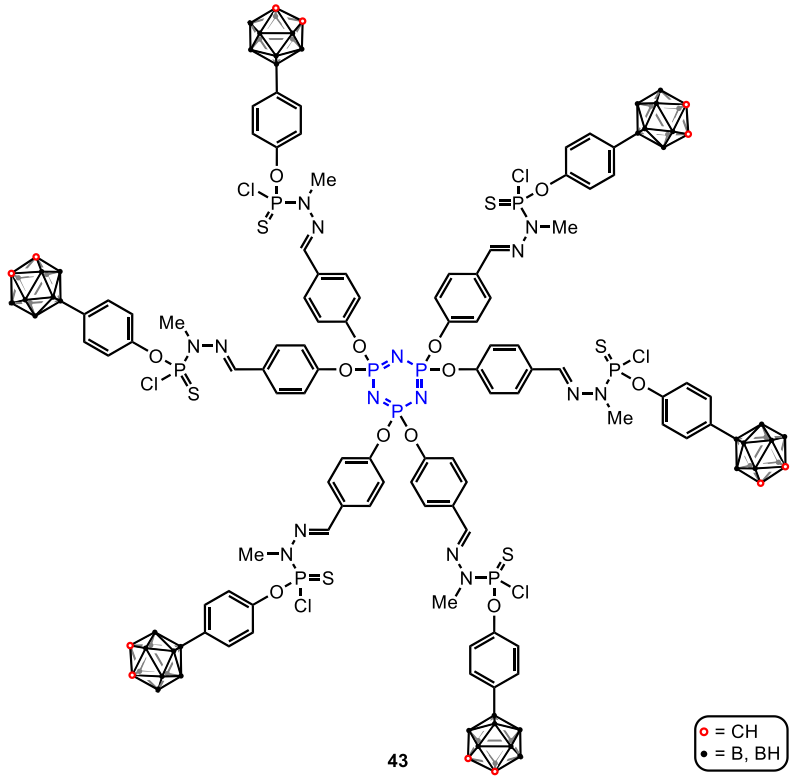


**Fig. 3.2.5.** Full structure of dendrimer **43**.

For reaction (i), only half of the $PCl_2$ functions were substituted to avoid possible steric problems. The $^{31}P\{^1H\}$ NMR spectrum showed only two signals at 67.7 and 8.4 ppm; the number of protons found in the $^1H$ NMR spectrum also hints on the successful formation of **43**.

In the second reaction (ii), the $^{31}P\{^1H\}$ NMR spectrum showed three broad signals at 68.8, 61.9, and 8.1 ppm indicating three different phosphorus atoms in the formed compound. The typical pattern for carborane species could be further observed in the HRMS (ESI+) in the range of m/z 1000 to 5000. The $^1H$ NMR signals are also broad due to the mixture of isomers; thus, no conclusive information about the distribution of **17** at the different branches could be obtained.

With the knowledge obtained for the non-phosphanylated compounds, the more precious carboranylphosphine **31** was employed next in the coupling reaction. Preliminary experiments already indicated an instability of the labile C–P bonds towards the alkali metal carbonates used as base for the deprotonation of the phenolic moiety. Various inorganic and organic bases were tested and DBU was identified as suitable candidate yielding the desired phenoxide of carboranylphosphine **31** without decomposition (reaction followed by $^{31}P\{^{1}H\}$ NMR spectroscopy). Following reactions with **35**, **1-G0**, **1-S0** and **1-G1** were, however, not successful. In the reaction with **1-G0**, the steric bulk and electronic properties of the phosphanyl groups hindered the formation of a six-fold substituted dendrimer. Instead, the literature known dimer $(PhPCl)_2$[53] as well as various by-products which could not be fully characterized were observed. However, when only three equivalents of **31** were used, the $^{31}P\{^{1}H\}$ NMR spectrum obtained hinted on the formation of different diastereomers of **45** (see **Scheme 3.2.10** and **3.3.2.24**).

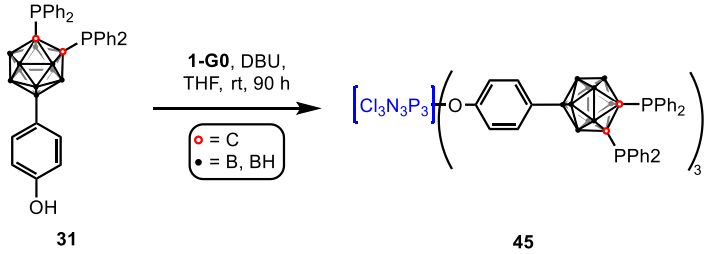


**31** **45**

**Scheme 3.2.10.** Attempted synthesis of the three times substituted derivate **45** of **1-G0** using three equivalents of **31**.

## 3.3 Experimental Section

### 3.3.1 General Procedures

*Materials*: Unless otherwise stated, all reactions requiring anhydrous conditions were conducted with oven-dried glassware under an atmosphere of nitrogen or argon using SCHLENK techniques. All glassware was dried at 120 °C for approximately 24 h before use. Anhydrous dichloromethane, diethyl ether, hexanes (mixture of isomers), methanol, *n*-pentane, tetrahydrofuran and toluene were obtained using the MBRAUN solvent purification system MB SPS-800. Prior to the hydrogenation experiments, dichloromethane and toluene have been subjected to several freeze-pump-thaw cycles. Benzene was dried over $CaH_2$ and distilled. Tetrahydrofuran was further dried over K and distilled. If needed, deuterated solvents ($C_6D_6$, $CDCl_3$) were subjected to several freeze-pump-thaw cycles. All solvents were stored over 3 Å, 4 Å molecular sieves or K (for all non-chlorinated solvents), respectively, under an atmosphere of nitrogen or argon. 9-I-*ortho*-carborane (**15**),[88] (4-bromophenoxy)(*tert*-butyl)dimethylsilane,[89] *N*,*N*-di-benzyl-4-bromo-aniline,[90] carborane derivatives **20** and **21**,[91,92] as well as dendrimer **1-G1**,[64] were prepared according to the literature. Chlorodiphenylphosphine was distilled prior to use. Diethyl chlorophosphite, chlorodiethyl-, chlorodiisopropyl-, and chloro(di-*tert*-butyl)phosphine were

stored in a glovebox under argon after purchase. All other chemicals were purchased and used as received.

*Methods:* Thin-layer chromatography (TLC) with silica gel 60 $F_{254}$ on glass or aluminium available from Merck KGaA was used for monitoring the reactions. Eluted plates were visualized using a 254 nm UV lamp and/or by developing with a suitable stain following heating. This stain included an acidic 5–10% solution of $PdCl_2$ in methanol. For column chromatography, silica gel (60 Å) with a particle diameter in the range of 0.035 to 0.070 mm, 0.052 to 0.073 mm or 0.063 to 0.200 mm from Sigma-Aldrich, the Biotage® Isolera 1, the Biotage® Isolera 4 or the SPOT™ II Ultimate flash chromatography system with SNAP KP-SIL (irregular silica, diameter: 0.050 mm), SNAP Ultra (spherical particle, diameter: 0.025 mm), or puriFlash® SIHP-JP (spherical particle, diameter: 0.030 mm) cartridges were used. The species were detected by an integrated UV/Vis detector.

*NMR spectroscopy*: Proton ($^{1}$H), boron ($^{11}$B), carbon ($^{13}$C), and phosphorus ($^{31}$P) NMR spectra were recorded on a Bruker Avance III HD 400 MHz, a Bruker Avance 300 MHz, Bruker Avance 400 MHz or Bruker Avance NEO 400 MHz NMR spectrometer at room temperature. NMR spectra at the 400 MHz devices were recorded at the following frequencies: $^{1}$H: 400.16 MHz, $^{13}$C: 100.63 MHz, $^{11}$B: 128.38 MHz, $^{31}$P: 161.99 MHz. NMR spectra at the 300 MHz device were recorded at the following frequencies: $^{1}$H: 300.13 MHz, $^{13}$C: 75.48 MHz, $^{11}$B: 96.29 MHz, $^{31}$P: 121.49 MHz, respectively. All chemical shifts are reported in parts per million (ppm). NMR data were listed as follows: Chemical shift (δ) ppm (multiplicity, coupling constants, relative integral, assignment). NMR data were interpreted with MestReNova.[87]

*Electrospray ionization mass spectrometry* was performed with an ESI ESQUIRE 3000 PLUS spectrometer with an IonTrap-analyzer from Bruker Daltonics and an UPLC Xevo G2 QTOF spectrometer from Waters in negative or positive mode. Acetonitrile, dichloromethane, methanol or mixtures of these solvents were used.

*X-ray diffraction* data were collected on a Gemini diffractometer (Rigaku Oxford Diffraction) using Mo-$K_\alpha$ radiation (λ=71.073 pm) and ω-scan rotation (**16**–**19** and **28**–**31**), on a Bruker Kappa Apex II diffractometer equipped with a 30 W air-cooled microfocus source, using Mo-$K_\alpha$ radiation (λ=71.073 pm), or on a Rigaku XtaLAB Synergy Dualflex diffractometer using a PhotonJet X-ray source (Cu, λ=1.54184 Å) with an Oxford Cryosystem Cryostream cooling device to collect the data at low temperature (100(2) K) (**25**, **33** and **34**). Data reduction was performed with CrysAlis Pro[[93] and APEX3[94] including the program SCALE3 ABSPACK[57] and SADABS[94] for empirical absorption correction. The structures were solved by SHELXT (dual space method)[95] and all non-hydrogen atoms were refined anisotropically by means of least-squares procedures on $F^2$ with SHELXL.[59]

### 3.3.2 Synthetic Procedures and Characterization

#### 3.3.2.1 Synthesis and Characterization of 16

Activated Mg turnings (697 mg, 12.5 mmol) were suspended in THF (15 ml) and the suspension was heated to 60 °C. (4-Bromophenoxy)(*tert*-butyl)dimethylsilane (4.70 ml, 19.1 mmol) was slowly added to the suspension at 60 °C over 15 min. Upon discoloration, the mixture was cooled to room temperature and stirred overnight until the Mg was almost consumed. In a second Schlenk, 9-iodo-*ortho*-carborane (**15**) (0.993 g, 3.70 mmol) and $[PdCl_2(PPh_3)_2]$ (9.3 mg, 0.133 mmol) were suspended in THF (25 ml) and degassed thoroughly. The GRIGNARD reagent was dropwise added over 2 h. The black reaction mixture was stirred for further 120 h until no starting material could be observed by TLC or in the $^{11}B\{^1H\}$ NMR spectrum. The content of the flask was slowly quenched with distilled $H_2O$. The aqueous layer was extracted with $Et_2O$ (5x80 ml). The united organic layers were washed with a saturated solution of $Na_2S_2O_3$, dried over $MgSO_4$ and filtered. After evaporation of all solvents, a brown oil was obtained and further purified by column chromatography (85% hexanes, 15% ethyl acetate, silica gel) yielding 1.51 g (1.87 mmol, 68%) of a light brown solid. Single crystals suitable for XRD analysis were obtained by slow evaporation of a solution of 80% hexanes and 20% ethyl acetate at room temperature.

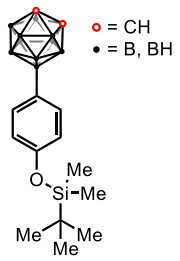


**$R_F$** (85% hexanes, 15% ethyl acetate) 0.36; **$^1$H NMR** (400 MHz, $CDCl_3$): δ=7.21 (d, $^3J_{H,H}$=8 Hz, 2H, Ar-*H*), 6.69 (d, $^3J_{H,H}$=8 Hz, 2H, Ar-*H*), 3.59 (s, 1H, $C_{Cage}$-*H*), 3.48 (s, 1H, $C_{Cage}$-*H*), 3.13–1.49 (m, 9H, B*H*), 0.96 (s, 9H, *t*Bu-*H*), 0.18 ppm (s, 6H, C$H_3$); **$^{11}$B NMR** (128 MHz, $CDCl_3$): δ=8.0 (s, 1B), −2.1 (d, $^1J_{BH}$=150 Hz, 1B), −8.6 (d, $^1J_{BH}$=151 Hz, 2B), −13.8 to −15.5 ppm (m, 6B); **$^{13}$C{$^1$H} NMR** (101 MHz, $CDCl_3$): δ=155.4, 133.6, 133.24, 119.1, 53.1 ($C_{Cage}$), 48.4 ($C_{Cage}$), 25.8, 18.8, −4.2 ppm; **HRMS (ESI+)** $[C_{14}H_{30}B_{10}OSi]$, m/z calculated: 351.3150 ($[M+H]^+$), found: 351.3154.

#### 3.3.2.2 Synthesis and Characterization of 17

Compound **17** was formed as by-product during the synthesis of **16** as well as prepared from **20**. 9-Methoxyphenyl-*ortho*-carborane (**20**) (590.2 mg, 2.36 mmol) was dissolved in glacial acetic acid (25 ml). Bromic acid (33% in AcOH, 2.1 ml, 12.2 mmol) was added dropwise and the reaction mixture was heated to reflux for 24 h. The reaction mixture was cooled to room temperature and the content of the flask was slowly quenched with distilled $H_2O$. The aqueous layer was extracted with ethyl acetate (3x60 ml). The united organic layers were washed with a saturated solution of $NaHCO_3$, dried over $MgSO_4$ and filtered. After evaporation of all solvents, the remaining product was further purified by column chromatography (Biotage SNAP ULTRA 10 g, 80% hexanes, 20% ethyl acetate, silica gel) yielding 393 mg (1.66 mmol, 71%) of a white crystalline solid. Single crystals suitable for XRD analysis were obtained by slow evaporation of a $CDCl_3$ solution at room temperature.

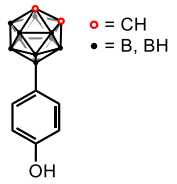


**$R_F$** (85% hexanes, 15% ethyl acetate) 0.10; **$^1$H NMR** (400 MHz, $CDCl_3$): δ=7.25 (d, $^3J_{H,H}$=8 Hz, 2H, Ar-*H*), 6.71 (d, $^3J_{H,H}$=8 Hz, 2H, Ar-*H*), 4.69 (s, 1H, O*H*) 3.59 (s, 1H, $C_{Cage}$-*H*), 3.48 (s, 1H, $C_{Cage}$-*H*), 3.15–1.47 ppm (m, 9H, B*H*); **$^{11}$B NMR** (128 MHz, $CDCl_3$): δ=7.8 (s, 1B), −2.2 (d, $^1J_{BH}$=150 Hz, 1B), −8.7 (d, $^1J_{BH}$=151 Hz, 2B), −13.1 to −16.1 ppm (m, 6B); **$^{13}$C{$^1$H} NMR** (101 MHz, $CDCl_3$): δ=155.4, 134.0, 114.7, 53.3 ($C_{Cage}$), 48.7 ppm ($C_{Cage}$); **HRMS (ESI−)** [$C_8H_{16}B_{10}O$], m/z calculated: 235.2136 ([M−H]$^-$), found: 235.2144.

### 3.3.2.3 Synthesis and Characterization of 18

9-[4-(Dibenzylamino)phenyl]-*ortho*-carborane (**21**) (717 mg, 1.73 mmol) and Pd/C (345 mg, 5%) were suspended in THF (15 ml). The suspension was transferred into a pressurized reactor which was then charged with 20 bar of $H_2$. The reaction was stopped after 14 h. The content of the reactor was filtered through a Celite pad using ethyl acetate (350 ml) and the remaining solution was concentrated under reduced pressure. The remaining oil was purified by column chromatography (Biotage SNAP 100 g, 80% hexanes, 20% ethyl acetate, silica gel) yielding 0.144 g (0.610 mmol, 35%) of a colorless solid. Single crystals suitable for XRD were obtained by layering *n*-pentane over a $C_6D_6$ solution of **18**.

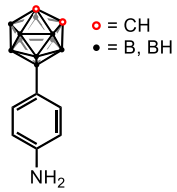


**$R_F$** (80% hexanes, 20% ethyl acetate) 0.18; **$^1$H NMR** (400 MHz, $CDCl_3$): δ=7.09 (d, $^3J_{H,H}$=8 Hz, 2H, Ar-*H*), 6.50 (d, $^3J_{H,H}$=8 Hz, 2H, Ar-*H*), 3.47 (s, 1H, $C_{Cage}$-*H*), 3.36 (s, 1H, $C_{Cage}$-*H*), 3.06–1.33 ppm (m, 9H, B*H*); No signal was observed for N$H_2$; **$^{11}$B NMR** (128 MHz, $CDCl_3$): δ=8.1 (s, 1B), −2.2 (d, $^1J_{BH}$=149 Hz, 1B), −8.7 (d, $^1J_{BH}$=151 Hz, 2B), −13.1 to −16.1 ppm (m, 6B); **$^{13}$C{$^1$H} NMR** (101 MHz, $CDCl_3$): δ=145.8, 133.4, 114.6, 52.9 ($C_{Cage}$), 48.0 ppm ($C_{Cage}$); **HRMS (ESI+)** [$C_8H_{17}B_{10}N$], m/z calculated: 234.2441 ([M+H]$^+$), found: 236.2440.

### 3.3.2.4 Synthesis and Characterization of 19

9-(Aminophenyl)-*ortho*-carborane (**18**) (126 mg, 0.536 mmol, 1.00 eq.) was dissolved in THF (5 ml). Di-*tert*-butyl dicarbonate (158 mg, 0.724 mmol, 1.35 eq.) was added and the reaction stirred at room temperature for 72 h. The reaction mixture was dried and the residue purified by column chromatography (Biotage SNAP ULTRA 10 g, 70% hexanes, 30% ethyl acetate) yielding 150 mg (0.447 mmol, 83%) of a colorless powder. Single crystals suitable for XRD were obtained by layering *n*-pentane over a $CDCl_3$ solution of **19**.

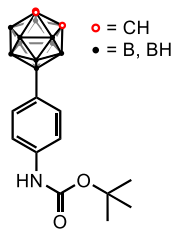


**$R_F$** (70% hexanes, 30% ethyl acetate) 0.34; **$^1$H NMR** (400 MHz, $CDCl_3$): δ=7.28 (m, 2H, Ar-*H*), 6.50 (d, $^3J_{H,H}$=8 Hz, 2H, Ar-*H*), 6.37 (s, 1H, N*H*), 3.60 (s, 1H, $C_{Cage}$-*H*), 3.49 (s, 1H, $C_{Cage}$-*H*), 3.15–1.60 (m, 9H, B*H*), 1.50 ppm (s, 9H, C$H_3$); **$^{11}$B NMR** (128 MHz, $CDCl_3$): δ=7.7 (s, 1B), −2.2 (d, $^1J_{BH}$=149 Hz, 1B), −8.7 (d, $^1J_{BH}$=151 Hz, 2B), −13.1 to −16.1 (m, 6B) ppm; **$^{13}$C{$^1$H} NMR** (101 MHz, $CDCl_3$): δ=152.8, 137.6, 133.0, 117.8,

80.3, 53.0 ($C_{Cage}$), 48.5 ($C_{Cage}$), 28.3 ppm; **HRMS (ESI+):** [$C_{13}H_{25}B_{10}NO_2$], m/z calculated: 336.2968 ([M+H]$^+$); found: 336.2967.

### 3.3.2.5 Synthesis and Characterization of 22

9-Phenoxy-(*tert*-butyl)dimethylsilyl-*ortho*-carborane (**16**) (54.4 mg, 0.155 mmol, 1.00 eq.) was dissolved in $Et_2O$ (5 ml) and the solution was cooled to −78 °C before *n*-butyllithium in *n*-hexane (0.18 ml, 0.315 mmol, 2.03 eq.) was added dropwise. The reaction was slowly warmed to room temperature. The yellow solution was cooled to −25 °C, and a solution of *i*$Pr_2PCl$ (54.6 mg, 0.358 mmol, 2.31 eq.) in $Et_2O$ (3 ml) was added dropwise. The mixture was warmed to room temperature and stirred for further 42 h. The white suspension was filtered, and the filtrate dried *in vacuo*. After quenching with degassed $H_2O$ (20 ml), brine (20 ml) was added, and the aqueous layer extracted with $Et_2O$ (3x50 ml). The combined organic layers were dried over $Na_2SO_4$. After filtration and drying *in vacuo*, the remaining oil was purified by preparative thin-layer chromatography (80% hexanes, 20% ethyl acetate, 250 µm, silica gel) yielding 5.2 mg (0.011 mmol, 7%) of **22** as a white oil.

This monophosphanyl carborane derivative **22** was also formed as a by-product in the preparation of **26**.

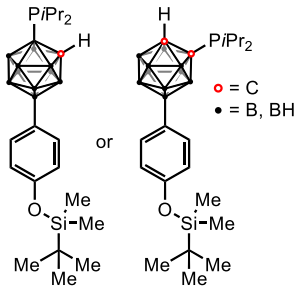


**$^1$H NMR** (400 MHz, $CDCl_3$): δ=7.23 (m, 4H, Ar-*H*), 6.69 (m, 4H, Ar-*H*), 3.60 (s, 1H, $C_{Cage}$-*H*), 3.49 (s, 1H, $C_{Cage}$-*H*), 3.16–1.56 (m, 18H, B*H*), 2.19 (dddd, $^3J_{H,H}$=12, 7, 4, 2 Hz, 2H, C*H*($CH_3$)$_2$), 1.27 (m, 24H, CH(C*H*$_3$)$_2$), 0.96 (s, 18H, *t*Bu-*H*), 0.18 ppm (s, 12H, SiC*H*$_3$); **$^{11}$B{$^1$H} NMR** (128 MHz, $CDCl_3$): δ=8.3 (s, 2B), −1.5 (s, 1B), −2.2 (s, 1B), −7.4 (s, 2B), −8.7 (s, 2B), −11.6 to −15.5 ppm (m, 12B); **$^{31}$P{$^1$H} NMR** (162 MHz, $CDCl_3$): δ=53.8, 51.8 ppm; **HRMS (ESI+):** [$C_{20}H_{43}B_{10}OPSi$], m/z calculated: 468.3884 ([M+H]$^+$); found: 468.3879.

### 3.3.2.6 Synthesis and Characterization of 23

9-Phenoxy-(*tert*-butyl)dimethylsilyl-*ortho*-carborane (**16**) (46.8 mg, 0.133 mmol, 1.00 eq.) was dissolved in THF (4 ml) and the solution was cooled to −78 °C before *n*-butyllithium in *n*-hexane (0.09 ml, 0.158 mmol, 1.18 eq.) was added dropwise. The reaction was slowly warmed to room temperature. After stirring for 1 h at room temperature, the orange suspension was cooled to −25 °C, and a solution of *t*$Bu_2PCl$ (26.2 mg, 0.145 mmol, 1.09 eq.) in THF (3 ml) was added dropwise. The mixture was warmed to room temperature and stirred for further 69 h. After reaction control by $^{31}$P{$^1$H} NMR spectroscopy, the solution was cooled to −78 °C before *n*-butyllithium in *n*-hexane (0.10 ml, 0.175 mmol, 1.32 eq.) was added dropwise. The reaction mixture was slowly warmed to room temperature. The red solution was again cooled to −20 °C, and a solution of *i*$Pr_2PCl$ (22.6 mg, 0.148 mmol, 1.11 eq.) in THF (3 ml) was added dropwise. The mixture was warmed to room temperature and stirred for further 8 d. The content of the flask was

quenched with degassed $H_2O$ (25 ml), then brine (25 ml) was added and the mixture was extracted with $Et_2O$ (3x33 ml). The combined organic layers were dried over $Na_2SO_4$. After filtration and drying *in vacuo*, the remaining oil was purified by preparative thin-layer chromatography (80% hexanes, 20% ethyl acetate, 250 µm, silica gel), yielding 20.6 mg of a white oil (0.042 mmol, 31%).

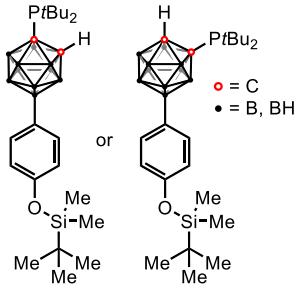


**$R_F$** (80% hexanes, 20% ethyl acetate) 0.82; **$^1$H NMR** (400 MHz, $CDCl_3$): δ=7.22 (m, $^3J_{H,H}$=8 Hz, 4H, Ar-*H*), 6.70 (m, $^3J_{H,H}$=9 Hz, 4H, Ar-*H*), 3.82 (s, 1H, $C_{Cage}$-*H*), 3.70 (s, 1H, $C_{Cage}$-*H*), 1.41 (d, $^3J_{H,H}$=12 Hz, 36H, C(C*H*$_3$)$_4$), 3.40–1.68 (m, 18H, B*H*), 0.97 (s, 18H, *t*Bu-*H*), 0.18 ppm (s, 12H, Si-C*H*$_3$); **$^{11}$B{$^1$H} NMR** (128 MHz, $CDCl_3$): δ=10.4 (1B), 8.2 (1B) 0.3 (1B), −1.8 (1B,), −7.6 (4B), −9.0 to −9.6 (6B), −11.7 to −12.9 (6B) ppm; **$^{13}$C{$^1$H} NMR** (101 MHz, $CDCl_3$): δ=155.4, 155.3, 133.5, 119.1, 119.1, 63.0–62.9 (*C*$_{Cage}$), 58.4–58.3 (*C*$_{Cage}$), 38.2, 37.9, 37.8, 31.6, 31.4, 29.8, 25.9, 17.6, −4.2 ppm; **$^{31}$P{$^1$H} NMR** (162 MHz, $CDCl_3$): δ=94.3, 92.1 ppm; **HRMS (ESI+)** [$C_{22}H_{47}B_{10}OP_2Si$], m/z calculated: 496.4193 ([M+H]$^+$), found: 496.4194.

### 3.3.2.7 Synthesis and Characterization of 24

This monophosphanyl carborane derivative **24** was formed as a by-product in the synthesis of **27** as a white oil (163 mg, 0.347 mmol, 24%).

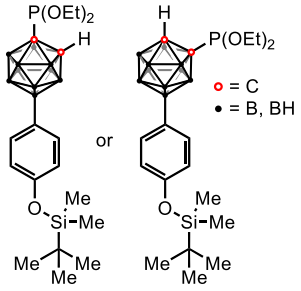


**$^1$H NMR** (400 MHz, $CDCl_3$): δ=7.22 (dq, $^3J_{H,H}$=9, 3 Hz, 4H, Ar-*H*), 6.69 (m, 4H, Ar-*H*), 4.0 (m, 8H, C*H*$_2$CH$_3$), 3.87 (s, 1H, $C_{Cage}$-*H*), 3.76 (s, 1H, $C_{Cage}$-*H*), 3.21–1.48 (m, 18H, B*H*), 1.31 (td, $^3J_{H,H}$=7, 2 Hz, 12H, CH$_2$C*H*$_3$), 0.97 (s, 18H, *t*Bu-*H*), 0.18 ppm (s, 12H, SiC*H*$_3$); **$^{11}$B{$^1$H} NMR** (128 MHz, $CDCl_3$): δ=8.7 (s, 1B), 8.0 (s, 2B), −1.4 (s, 4B), −2.4 (s, 4B), −7.3 (s, 4B), −13.0 to −14.7 ppm (m, 10B); **$^{13}$C{$^1$H} NMR** (101 MHz, $CDCl_3$): δ=155.1, 133.4, 133.4, 118.9, 65.1–64.9, 57.5 (*C*$_{Cage}$), 52.7 (*C*$_{Cage}$), 25.7, 18.14, 16.9–16.8, −4.4 ppm; **$^{31}$P{$^1$H} NMR** (162 MHz, $CDCl_3$): δ=152.8, 151.7 ppm; **HRMS (ESI+):** [$C_{18}H_{39}B_{10}O_3PSi$], m/z calculated: 472.3468 ([M+H]$^+$); found: 472.3461.

### 3.3.2.8 Synthesis and Characterization of 25

9-Phenoxy-(*tert*-butyl)dimethylsilyl-*ortho*-carborane (**16**) (515 mg, 1.47 mmol, 1.00 eq.) was dissolved in THF (10 ml) and the solution was cooled to −78 °C before *n*-butyllithium in *n*-hexane (1.76 ml, 3.09 mmol, 2.10 eq.) was added dropwise. The reaction mixture was slowly warmed to room temperature. After stirring for 1 h at room temperature, the orange suspension was cooled to 0 °C, and a solution of $Et_2PCl$ (458 mg, 3.67 mmol, 2.50 eq.) in THF (3 ml) was added dropwise. The reaction mixture was warmed to room temperature and stirred for further 20.5 h. The content of the flask was quenched with degassed $H_2O$ (75 ml) and stirred for 1.5 h, then brine

(20 ml) was added and the crude product was extracted with $Et_2O$ (3x50 ml). The combined organic layers were dried over $Na_2SO_4$. After filtration and drying *in vacuo*, the remaining white oil was purified by column chromatography (puriFlash SIHP-JP 80 g, 97% petroleum ether, 3% ethyl acetate, silica gel), yielding 339 mg of a white oil (0.644 mmol, 44%). Single crystals suitable for XRD were obtained by cooling a *n*-pentane to solution −20 °C.

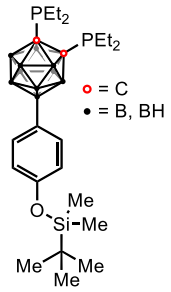


**$R_F$** (97% petroleum ether, 3% ethyl acetate) 0.36; **$^1$H NMR** (400 MHz, $CDCl_3$): δ=7.21 (d, $^3J_{H,H}$=8 Hz, 2H, Ar-*H*), 6.69 (d, $^3J_{H,H}$=9 Hz, 2H, Ar-*H*), 1.79 (dqd, $^3J_{H,H}$=15, 8, 3 Hz, 4H, C*H*$_2$CH$_3$), 1.66 (dqdd, $^3J_{H,H}$=15. 8, 4, 2 Hz, 4H, C*H*$_2$CH$_3$), 3.36–1.46 (m, 9H, B*H*), 1.16 (dtdd, $^3J_{H,H}$=16, 8, 4, 1 Hz, 6H, CH$_2$C*H*$_3$), 0.96 (s, 9H, *t*Bu-*H*), 0.17 ppm (s, 6H, C*H*$_3$); **$^{11}$B NMR** (128 MHz, $CDCl_3$): δ=9.3 (s, 1B), −0.6 (d, $^1J_{BH}$=146 Hz, 1B), −6.8 (d, $^1J_{BH}$=149 Hz, 2B), −11.1 ppm (br s, 6B); **$^{13}$C{$^1$H} NMR** (101 MHz, $CDCl_3$): δ=118.9, 60.4, 25.7, 20.9–20.6 ($C_{Cage}$), 18.2, 14.2, 10.4, 10.2, −4.4 ppm; **$^{31}$P{$^1$H} NMR** (162 MHz, $CDCl_3$, AB spin system): δ=4.9 (d, $^3J_{P,P}$=120 Hz), 3.1 ppm (d, $^3J_{P,P}$=120 Hz); **HRMS (ESI+):** [$C_{22}H_{49}B_{10}OP_2Si$], m/z calculated: 528.4014 ([M+H]$^+$); found: 528.4017.

### 3.3.2.9 Synthesis and Characterization of 26

9-Phenoxy-(*tert*-butyl)dimethylsilyl-*ortho*-carborane (**16**) (457 mg, 1.30 mmol, 1.00 eq.) was dissolved in $Et_2O$ (10 ml) and the solution was cooled to −78 °C before *n*-butyllithium in *n*-hexane (1.70 ml, 3.20 mmol, 2.46 eq.) was added dropwise. The reaction mixture was slowly warmed to room temperature overnight. The light brown orange suspension was cooled to 0 °C, and a solution of *i*Pr$_2$PCl (501 mg, 3.28 mmol, 2.52 eq.) in $Et_2O$ (6 ml) was added dropwise. The reaction mixture was warmed to room temperature and stirred for further 27 h. The content of the flask was cooled to 0 °C and quenched with degassed $H_2O$ (50 ml). Then brine (20 ml) was added and the crude product was extracted with $Et_2O$ (2x50 ml). The combined organic layers were dried over $Na_2SO_4$. After filtration and drying *in vacuo*, the remaining brown oil was purified by column chromatography (puriFlash SIHP-JP 80 g, 95% petroleum ether, 5% ethyl acetate, silica gel), yielding 492 mg (0.850 mmol, 65%) of **26** as a yellow oil.

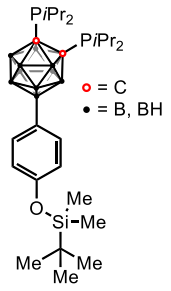


**$^1$H NMR** (400 MHz, $CDCl_3$): δ=7.23 (d, $^3J_{H,H}$=8 Hz, 2H, Ar-*H*), 6.70 (d, $^3J_{H,H}$=8 Hz, 2H, Ar-*H*), 2.25 (dtp, $^3J_{H,H}$=11, 7, 4 Hz, 4H, C*H*(CH$_3$)$_2$), 3.25–1.77 (m, 9H, B*H*), 1.26 (tt, $^3J_{H,H}$=10, 4 Hz, 24H, CH(C*H*$_3$)$_2$), 0.97 (s, 9H, *t*Bu-*H*), 0.18 ppm (s, 6H, SiC*H*$_3$); **$^{11}$B NMR** (128 MHz, $CDCl_3$): δ=9.9 (s, 1B), −0.05 (d, $^1J_{BH}$=149 Hz, 1B), −6.6 (d, $^1J_{BH}$=146 Hz, 2B), −9.3 ppm (br s, 6B); **$^{13}$C{$^1$H} NMR** (101 MHz, $CDCl_3$): δ=155.1, 133.3, 118.9.4, 27.0–26.5 (ddd, $J_{C,P}$=24, 14, 4 Hz, $C_{Cage}$), 25.7, 22.9 (dd, $J_{C,P}$=27, 2 Hz), 18.2, −4.4 ppm; **$^{31}$P{$^1$H} NMR** (162 MHz, $CDCl_3$, AB spin system): δ=32.3 (d, $^3J_{P,P}$=107 Hz), 30.2 ppm (d, $^3J_{P,P}$=107 Hz); **HRMS (ESI+):** [$C_{26}H_{57}B_{10}OP_2Si$], m/z calculated: 584.4643 ([M+H]$^+$); found: 584.4645.

### 3.3.2.10 Synthesis and Characterization of 27

9-Phenoxy-(*tert*-butyl)dimethylsilyl-*ortho*-carborane (**16**) (497 mg, 1.47 mmol, 1.00 eq.) was dissolved in $Et_2O$ (10 ml) and the solution was cooled to −78 °C before *n*-butyllithium in *n*-hexane (1.80 ml, 3.38 mmol, 2.39 eq.) was added dropwise. The reaction mixture was slowly warmed to room temperature. After stirring for 2 h at room temperature, the reaction mixture was cooled to 0 °C, and a solution of $P(OEt)_2Cl$ (515 mg, 3.20 mmol, 2.32 eq.) in $Et_2O$ (5 ml) was added dropwise. The reaction mixture was warmed to room temperature and stirred for further 48 h. The red suspension was quenched with degassed $H_2O$ (75 ml), then brine (20 ml) was added and the crude product was extracted with $Et_2O$ (3x50 ml). The combined organic layers were dried over $Na_2SO_4$. After filtration and drying *in vacuo*, the remaining oil was purified by column chromatography (puriFlash SIHP-JP 80 g, 95% petroleum ether, 5% ethyl acetate, silica gel), yielding 82 mg (0.139 mmol, 10%) of **27** as a colorless solid as well as 163 mg of **24** (0.347 mmol, 24%) as a white oil.

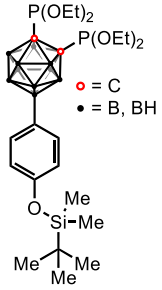


**$^1$H NMR** (400 MHz, $CDCl_3$): δ=7.23 (d, $^3J_{H,H}$=8 Hz, 2H, Ar-*H*), 6.68 (d, 2H, $^3J_{H,H}$=8 Hz, Ar-*H*), 4.01 (dqd, $^3J_{H,H}$=9, 7, 2 Hz, 8H, C*H*$_2$CH$_3$), 3.20–1.49 (m, 9H, B*H*), 1.32 (td, $^3J_{H,H}$=7, 4 Hz, 24H, CH(C*H*$_3$)$_2$), 0.96 (s, 9H, *t*Bu-*H*), 0.17 ppm (s, 6H, SiC*H*$_3$); **$^{11}$B NMR** (128 MHz, $CDCl_3$): δ=9.5 (s, 1B), −0.4 (d, $^1J_{BH}$=149 Hz, 1B), −7.3 (d, $^1J_{BH}$=148 Hz, 2B), −11.7 ppm (br s, 6B); **$^{13}$C{$^1$H} NMR** (101 MHz, $CDCl_3$): δ=155.1, 133.5, 119.0, 64.5, 29.8, 25.9, 18.3, 16.8 (d, $J_{C,P}$=6 Hz), −4.2 ppm; **$^{31}$P{$^1$H} NMR** (162 MHz, $CDCl_3$, AB spin system): δ=151.6 (d, $^3J_{P,P}$=136 Hz), 149.9 ppm (d, $^3J_{P,P}$=136 Hz); **HRMS (ESI+):** [$C_{22}H_{48}B_{10}O_5P_2Si$], m/z calculated: 592.3806 ([M+H]$^+$); found: 592.3807.

### 3.3.2.11 Synthesis and Characterization of 28

9-Phenoxy-(*tert*-butyl)dimethylsilyl-*ortho*-carborane (**16**) (555 mg, 1.58 mmol, 1.00 eq.) was dissolved in $Et_2O$ (25 ml) and the solution was cooled to −78 °C before *n*-butyllithium in *n*-hexane (2.2 ml, 3.32 mmol, 2.10 eq.) was added dropwise. The reaction mixture was slowly warmed to room temperature. After stirring for 30 min at room temperature, the reaction mixture was cooled to 0 °C, and $Ph_2PCl$ (1.10 ml, 4.99 mmol, 3.20 eq.) was added dropwise. The reaction mixture was warmed to room temperature and stirred for 18 h. The beige suspension was cooled to 0°C and quenched with degassed $H_2O$ (25 ml). After stirring for 30 min at 0 °C the organic solvents were removed *in vacuo*. The aqueous layer was removed and the remaining solution was washed again with $H_2O$ (2x3ml). After drying for 1 h at 100 °C *in vacuo*, the product extracted with $Et_2O$ (3x6 ml). After filtration and drying *in vacuo*, the remaining white solid was purified by column chromatography (Biotage SNAP KP-Sil 100 g, 90% hexanes, 10% ethyl acetate, silica gel), yielding 1.06 g (1.47 mmol, 93%) of **28** as a white solid. Single crystals suitable for XRD were obtained by layering a solution of **28** in $Et_2O$ with hexanes.

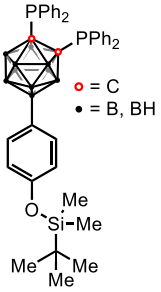


**$R_F$** (95% hexanes, 5% ethyl acetate) 0.34; **$^1$H NMR** (400 MHz, $C_6D_6$): δ=7.89 (dddt, $^3J_{H,H}$=13, 9, 7, 3 Hz, 8H, PPh-*H*), 7.48 (d, $^3J_{H,H}$=8 Hz, 2H, Ar-*H),* 7.06 (tq, $^3J_{H,H}$=13, 9, 7, 3 Hz, 12H, PPh-*H*), 6.80 (d, $^3J_{H,H}$=8 Hz, 2H, Ar-*H*), 3.67–1.94 (m, 9H, B*H*), 0.95 (s, 9H, *t*Bu-*H*), 0.05 ppm (s, 6H, SiC$H_3$); **$^{11}$B NMR** (128 MHz, $C_6D_6$): δ=9.5 (s, 1B), −0.5 (d, $^1J_{BH}$=149 Hz, 1B), −2.8 to −16.8 ppm (m, 8B); **$^{13}$C{$^1$H} NMR** (101 MHz, $C_6D_6$) δ=155.4, 135.8, 135.6, 134.5, 133.7, 130.6, 128.5, 128.4, 119.3, 82.2, 76.9, 25.6, 18.0, −4.7 ppm; **$^{31}$P{$^1$H} NMR** (162 MHz, $C_6D_6$, AB spin system): δ=7.3 (d, $^3J_{P,P}$=123 Hz), 5.9 ppm (d, $^3J_{P,P}$=123 Hz); **HRMS (ESI+):** [$C_{38}H_{48}B_{10}OP_2Si$], m/z calculated: 720.4018 ([M+H]$^+$); found: 720.4102.

### 3.3.2.12 Synthesis and Characterization of 29

9-Methoxyphenyl-*ortho*-carborane (**20**) (141 mg, 0.563 mmol, 1.00 eq.) was dissolved in $Et_2O$ (8 ml) and the solution was cooled to −78 °C before *n*-butyllithium in *n*-hexane (0.78 ml, 1.18 mmol, 2.10 eq.) was added dropwise. The reaction mixture was slowly warmed to room temperature. After stirring for 2 h at room temperature, the white suspension was cooled to 0 °C, and $Ph_2PCl$ (0.33 ml, 1.18 mmol, 2.10 eq.) was added dropwise. The reaction mixture was kept for 2 h at 0 °C and was then allowed to warm to room temperature overnight. The reaction mixture was cooled to 0 °C and quenched with degassed $H_2O$ (10 ml). After stirring for 1 h at 0 °C a white solid was obtained by filtration and washed with degassed $H_2O$ (2x4 ml). $Et_2O$ (10 ml) was added to redissolve the product. The solid residue was further extracted with $Et_2O$ (2x2.5 ml). After filtration and drying *in vacuo*, 102 mg (0.165 mmol, 29%) of **29** were obtained as a white solid. Single crystals suitable for XRD were obtained by layering a solution of **29** in THF with hexanes.

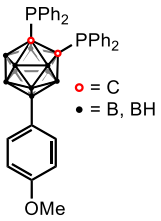


**$R_F$** (95% hexanes, 5% ethyl acetate) 0.43; **$^1$H NMR** (400 MHz, $CDCl_3$): δ=7.78 (dtd, $^3J_{H,H}$=10, 8, 2 Hz, 8H, PPh-*H*), 7.36 (m, 12H, PPh-*H),* 7.07 (d, $^3J_{H,H}$=9 Hz, 2H, Ar-*H*), 6.63 (d, $^3J_{H,H}$=9 Hz, 2H, Ar-*H*), 3.65 (s, 3H, OC$H_3$), 3.11–1.42 ppm (m, 9H, B*H*); **$^{11}$B NMR** (128 MHz, $CDCl_3$): δ=9.4 (s, 1B), −0.2 (d, $^1J_{BH}$=154 Hz, 1B), −6.9 (d, $^1J_{BH}$=151 Hz, 2B), −10.1 (br s, 6B) ppm; **$^{13}$C{$^1$H} NMR** (101 MHz, $CDCl_3$): δ=159.2, 136.0, 135.7, 130.9, 128.7, 128.6, 113.1, 53.4, 1.2 ppm; **$^{31}$P{$^1$H} NMR** (162 MHz, $CDCl_3$, AB spin system): δ=7.1 (d, $^3J_{P,P}$=122 Hz), 5.4 ppm (d, $^3J_{P,P}$=122 Hz); **HRMS (ESI+):** [$C_{33}H_{36}B_{10}OP_2$], m/z calculated: 620.3306 ([M+H]$^+$); found: 620.3310.

### 3.3.2.13 Synthesis and Characterization of 30

9-[4-(Dibenzylamino)phenyl]-*ortho*-carborane (**21**) (251 mg, 0.603 mmol) was dissolved in THF (10 ml) and the solution was cooled to −78 °C before *n*-butyllithium in *n*-hexane (0.82 ml, 1.27 mmol, 2.10 eq.) was added dropwise. The reaction mixture was slowly warmed to room temperature. After stirring for 30 min at room temperature, the reaction mixture was cooled to 0 °C, and $Ph_2PCl$ (0.23 ml, 1.27 mmol, 2.10 eq.) was added dropwise. The reaction mixture was

allowed to warm to room temperature and was stirred for further 20 h, then was cooled to 0 °C and quenched with degassed $H_2O$ (10 ml) and extracted with $Et_2O$ (3x20 ml). The organic layers were united and washed with $H_2O$ (3x20 ml) and brine (20 ml), dried over $MgSO_4$ and filtered. The remaining brown oil was purified by column chromatography (Biotage SNAP ULTRA 10 g, 90% hexanes, 10% ethyl acetate, silica gel) yielding 263 mg (0.335 mmol, 56%) of a colorless solid. Crystals suitable for XRD were obtained from dichloromethane and hexanes by slow evaporation.

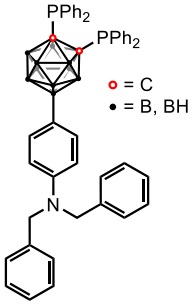


**$R_F$** (90% hexanes, 10% ethyl acetate) 0.32; **$^1$H NMR** (400 MHz, $CDCl_3$): δ=7.83 (m, 8H, PPh-*H*), 7.43 (m, 12H, PPh-*H),* 7.27 (m, 4H, $NCH_2$Ph-*H*), 7.22 (m, 6H, $NCH_2$Ph-*H*), 7.01 (d, $^3J_{H,H}$=9 Hz, 2H, Ar-*H*), 6.57 (br s, 2H, Ar-*H*), 4.56 (s, 4H, $NCH_2$), 2.89–1.86 ppm (m, 9H, B*H*); **$^{11}$B NMR** (128 MHz, $CDCl_3$): δ=10.0 (s, 1B), −0.2 (br s, 1B), −6.8 (d, $^1J_{BH}$=149 Hz, 2B), −10.2 ppm (br s, 6B); **$^{13}$C{$^1$H} NMR** (101 MHz, $CDCl_3$): δ=136.00, 135.74, 133.24, 130.81, 128.68, 128.60, 126.57, 60.54, 21.20, 14.35 ppm; **$^{31}$P{$^1$H} NMR** (162 MHz, $CDCl_3$ AB spin system): δ=7.2 (d, $^3J_{P,P}$=123 Hz), 5.4 ppm (d, $^3J_{P,P}$=123 Hz); **HRMS (ESI+):** [$C_{46}H_{47}B_{10}NP_2$], m/z calculated: 785.4256 ([M+H]$^+$); found: 785.4251.

### 3.3.2.14 Synthesis and Characterization of 31

Carboranylphosphine **28** (119 mg, 0.166 mmol, 1.00 eq.) was dissolved in THF (2 ml), hydrogen chloride in $Et_2O$ (3 mmol ml$^{-1}$, 1.0 ml, 3 mmol, 18.12 eq.) was added dropwise, and the mixture was stirred for 21 h at room temperature. The crude reaction mixture was poured into $Et_2O$ (20 ml) and the aqueous layer was extracted two more times with $Et_2O$ (2x20 ml). The united organic layers were washed with hydrochloric acid (1 M, 20 ml), $H_2O$ (20 ml), and brine (20 ml) and then dried over $MgSO_4$ and filtered. After evaporation of all solvents, a white solid was obtained and further purified by column chromatography (Biotage SNAP KP-Sil 25 g, 80% hexanes, 20% ethyl acetate, silica gel) yielding 95 mg (0.157 mmol, 95%) of a crystalline solid. Crystals suitable for XRD were grown from dichloromethane and *n*-pentane by slow evaporation.

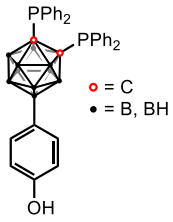


**$R_F$** (80% hexanes, 20% ethyl acetate) 0.36; **$^1$H NMR** (400 MHz, $CDCl_3$): δ=7.86 (m, 8H, PPh-*H*), 7.44 (m, 12H, PPh-*H),* 7.09 (d, $^3J_{H,H}$=8 Hz, 2H, Ar-*H*), 6.63 (d, $^3J_{H,H}$=8 Hz, 2H, Ar-*H*), 4.56 (s, 1H, O*H*), 2.96–1.26 (m, 9H, B*H*) ppm; **$^{11}$B NMR** (128 MHz, $CDCl_3$): δ=9.4 (s, 1B), −0.2 (d, $^1J_{BH}$=153 Hz, 1B), −6.8 (d, $^1J_{BH}$=150 Hz, 2B), −10.6 (m, 6B) ppm; **$^{13}$C{$^1$H} NMR** (101 MHz, $CDCl_3$): δ=154.9, 135.8 135.6, 133.6, 130.7, 128.5, 114.3, 25.6, 1.1, −3.1 ppm; **$^{31}$P{$^1$H} NMR** (162 MHz, $CDCl_3$ AB spin system): δ=7.1 (d, $^3J_{P,P}$=123 Hz), 5.5 ppm (d, $^3J_{P,P}$=123 Hz); **HRMS (ESI+):** [$C_{32}H_{34}B_{10}OP_2$], m/z calculated: 606.3148 ([M+H]$^+$); found: 606.3115.

### 3.3.2.15 Synthesis and Characterization of 32

Carborane derivative **19** (57 mg, 0.170 mmol, 1.00 eq.) was dissolved in THF (2 ml) and cooled to −78 °C before *n*-butyllithium in *n*-hexane (0.22 ml, 0.357 mmol, 2.10 eq.) was added dropwise. The reaction mixture was slowly warmed to room temperature. After stirring for 30 min at room temperature, the reaction mixture was cooled to 0 °C, and $Ph_2PCl$ (0.07 ml, 0.390 mmol, 2.30 eq.) was added dropwise. The reaction mixture was allowed to warm to room temperature and stirred for further 22 h. After reaction control by $^{31}P\{^1H\}$ NMR spectroscopy, more *n*-butyllithium in *n*-hexane (0.22 ml, 0.357 mmol, 2.10 eq.) and $Ph_2PCl$ (0.10 ml, 0.557 mmol, 3.28 eq.) were added as described above. After stirring for another 17 h, the reaction mixture was cooled to 0 °C and quenched with degassed $H_2O$ (5 ml) and stirred for 30 min. Then the aqueous layer was extracted with $Et_2O$ (4x40 ml). The organic layers were united and washed with $NaHCO_3$ (30 ml), dried over $MgSO_4$ and filtered. The remaining oil was purified by column chromatography (Biotage SNAP KP-Sil 10 g, 90% hexanes, 10% ethyl acetate, silica gel) yielding 17 mg (0.019 mmol, 11%) of a colorless solid.

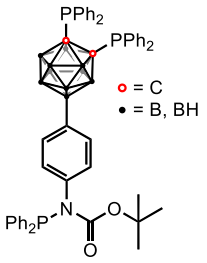


**$R_F$** (80% hexanes, 20% ethyl acetate) 0.53; **$^1$H NMR** (400 MHz, $CDCl_3$): δ=7.76 (m, 8H, PPh-*H*), 7.33 (m, 18H, PPh-*H* and NPPh-$H_{m,p}$), 7.19 (m, 4H, NPPh-$H_o$), 6.93 (d, $^3J_{H,H}$=8 Hz, 2H, Ar-*H*), 6.69 (d, $^3J_{H,H}$=8 Hz, 2H, Ar-*H*), 2.83–1.74 (m, 9H, B*H*), 1.16 (s, 9H, $CH_3$) ppm; **$^{11}$B NMR** (128 MHz, $CDCl_3$): δ=9.2 (s, 1B), −0.9 (d, $^1J_{BH}$=190 Hz, 1B), −7.0 (br s, 2B), −10.1 ppm (m, 6B); **$^{13}$C{$^1$H} NMR** (101 MHz, $CDCl_3$) δ=171.3, 156.3, 156.2, 141.7, 141.6, 137.3, 137.1, 136.0, 135.9, 135.7, 135.3, 135.1, 133.6, 133.5, 133.4, 133.2, 133.0, 132.8, 132.4, 132.2, 131.4, 130.9, 130.8, 129.1, 129.0, 128.7, 128.6, 128.1, 127.4, 81.7, 60.5, 28.1 ppm; **$^{31}$P{$^1$H} NMR** (162 MHz, $CDCl_3$, AB system): δ=58.5, 7.0 (d, $^3J_{P,P}$=122 Hz), 5.5 ppm (d, $^3J_{P,P}$=122 Hz); **HRMS (ESI+)** [$C_{49}H_{52}B_{10}NO_2P_3$], m/z calculated: 889.4285 ([M+H]$^+$), found: 889.4311.

### 3.3.2.16 Synthesis and Characterization of 33

Compound **33** was obtained as by-product during the column chromatographical purification of **22**. Single crystals suitable for XRD were obtained after several months by slow evaporation of a $CDCl_3$ solution at room temperature.

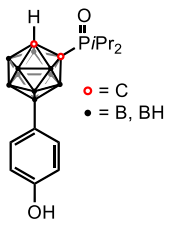


**$^1$H NMR** (400 MHz, $CDCl_3$): δ=7.22 (t, $^3J_{H,H}$=8 Hz, 2H, Ar-*H*), 6.75–6.65 (m, 2H, Ar-*H*), 3.61 (s, 1H, $C_{Cage}$-*H*), 3.49 (s, 1H, $C_{Cage}$-*H*), 3.26–1.67 (m, 9H, B*H*), 2.50 (dp, $^3J_{H,H}$=15, 7 Hz, 2H, C*H*($CH_3$)$_2$), 1.45–1.33 ppm (m, 12H, C*H*$_3$); O*H* was not observed; **$^{11}$B{$^1$H} NMR** (128 MHz, $CDCl_3$): δ=7.5 (s, 1B), −2.3 (s, 1B), −7.3 (s, 2B), −8.8 (s, 2B), −13.8 to −15.6 ppm (m, 6B); **$^{31}$P{$^1$H} NMR** (162 MHz, $CDCl_3$): δ=52.2 ppm; **HRMS (ESI+):** [$C_{14}H_{28}B_{10}O_2P$], m/z calculated: 368.2910 ([M+H]$^+$); not found.

### 3.3.2.17 Synthesis and Characterization of 34

This monophosphanyl carborane derivative was obtained from **24**. Single crystals suitable for XRD were obtained by layering *n*-pentane over an ethyl acetate solution of **34**.

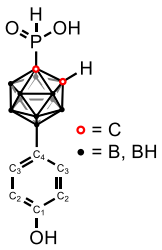


**$^{1}$H NMR** (400 MHz, $CDCl_3$): δ=7.25–7.20 (m, 2H, Ar-*H*), 6.74–6.67 (m, 2H, Ar-*H*), 3.97 (s, 1H, $C_{Cage}$-*H*), 3.85 (s, 1H, $C_{Cage}$-*H*), 3.31–1.68 ppm (m, 9H, B*H*), O*H* not observed; **$^{11}$B{$^{1}$H} NMR** (128 MHz, $CDCl_3$): δ=8.0 (s, 1B), −0.3 (s, 1B), −2.1 (s, 1B), −6.8 (s, 2B), −13.0 to−14.7 ppm (m, 5B); **$^{13}$C{$^{1}$H} NMR** (101 MHz, $CDCl_3$): δ=156.3–156.2 (Ar-COH), 133.5–133.4 (Ar-CH), 114.5 (Ar-CH), 60.1 ($C_{Cage}$-P), 53.3 ($C_{Cage}$-H), 48.5 ppm ($C_{Cage}$-H), $B_{Cage}$-C was not observed; **$^{31}$P{$^{1}$H} NMR** (162 MHz, $CDCl_3$): δ=32.8, 31.3 ppm; **HRMS (ESI+):** [$C_8H_{17}B_{10}O_3P$], m/z calculated: 301.1996 ($[M+H]^+$); not found.

### 3.3.2.18 Experimental details for 36, 37, 38

Carborane **17** (27.0 mg, 0.113 mmol, 6.09 eq.) and $K_2CO_3$ (40.4 mg, 0.292 mmol, 15.74 eq.) were suspended in acetone (3 ml) and heated to 40 °C before a solution of **1-G0** in THF (4.04 mg $ml^{-1}$, 1.60 ml, 0.019 mmol, 1.00 eq.) was added dropwise. The reaction mixture was stirred for 120 h before before the product was filtered and precipitated in *n*-pentane (5 ml). The crude mixture was washed with *n*-pentane (5 ml). The $^{31}$P{$^{1}$H} NMR spectrum showed an incomplete substitution. The white precipitate was redissolved in THF (4 ml), then more carborane **17** (8.9 mg, 0.037 mmol, 1.97 eq.) and $K_2CO_3$ (22.4 mg, 0.162 mmol, 8.52 eq.) were added. The reaction mixture was heated to 40 °C and stirred for another 72 h. All solvents were removed *in vacuo*. Dichloromethane (3 ml) was added to dissolve the product. The filtrate was precipitated in *n*-pentane (70 ml). The dissolving and precipitation process was repeated once and a mixture of **36** and **37** could be obtained as a white powder (19.0 mg). The $^{31}$P{$^{1}$H} NMR spectrum as well as the HRMS spectrum of the mixture of both compounds is shown in **Fig. 3.3.1** and **Fig. 3.3.2**.

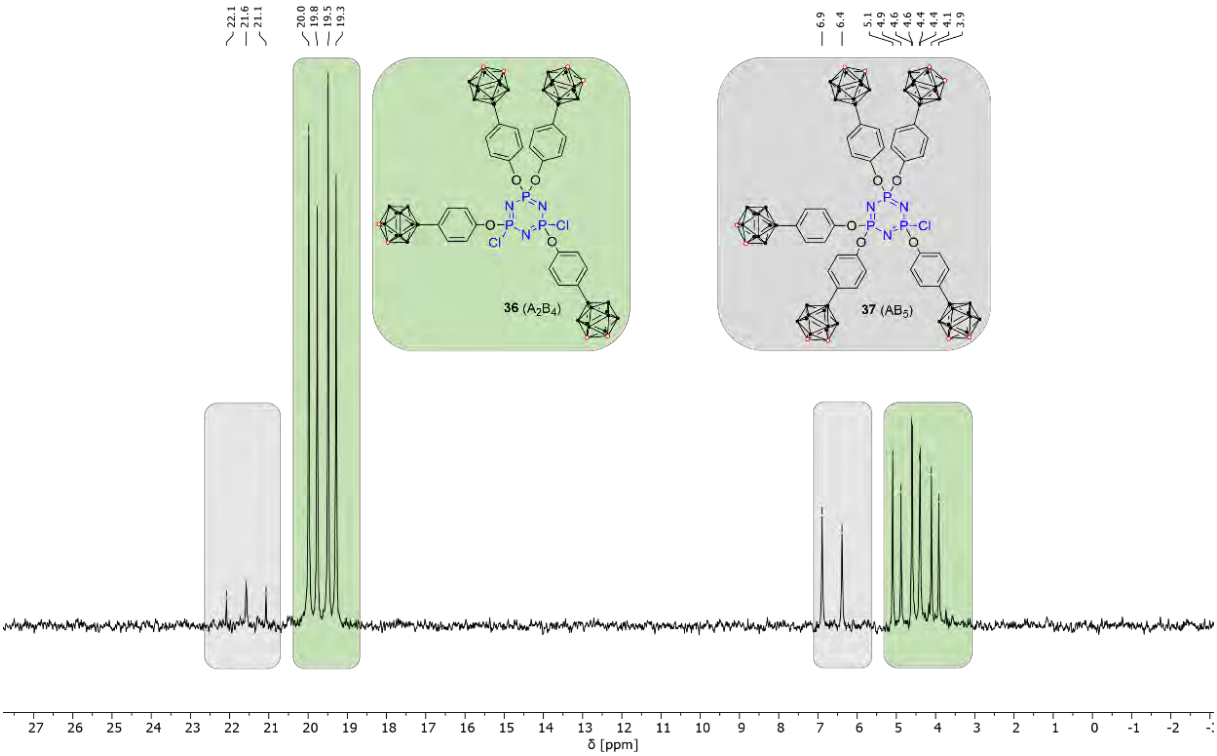


**Fig. 3.3.1.** $^{31}P\{^{1}H\}$ NMR spectrum of a mixture of **36** and **37** in $CDCl_3$.

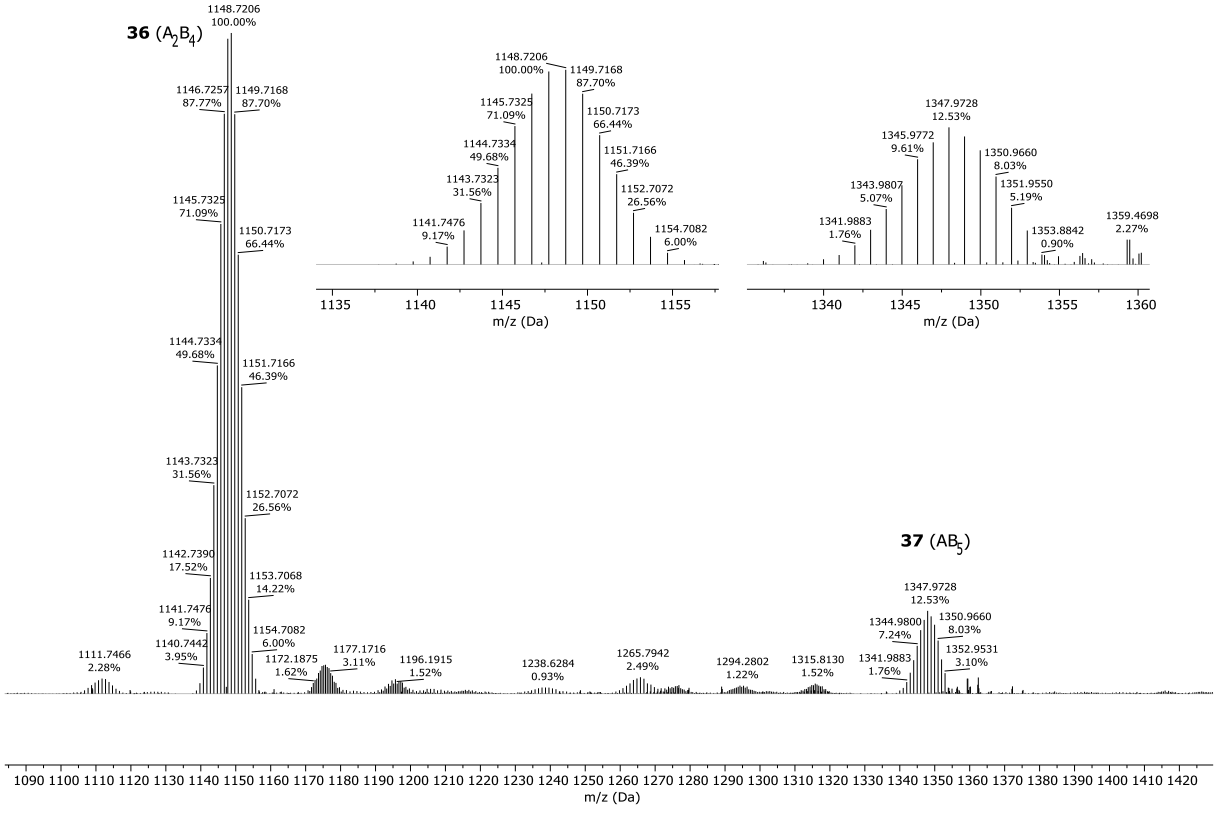


**Fig. 3.3.2.** HRMS (ESI+) spectrum of a mixture of **36** ($[C_{32}H_{60}B_{40}Cl_2N_3O_4P_3]$, m/z calculated: 1147.7262 ($[M+H]^+$); found: 1148.7206) and **37** ($[C_{40}H_{75}B_{50}ClN_3O_5P_3]$, m/z calculated 1347.9699 ($[M+H]^+$); found: 1347.9728).

A mixture of **37** and **38** was prepared by suspending carborane derivative **17** (62.7 mg, 0.263 mmol, 9.93 eq.) and $Cs_2CO_3$ (166.4 mg, 0.506 mmol, 19.11 eq.) in THF (8 ml) before a solution of **1-G0** in THF (15.6 mg $ml^{-1}$, 0.59 ml, 0.026 mmol, 1.00 eq.) was added at room temperature. The reaction mixture was stirred for four weeks before more carborane (**17**) (16.8 mg, 0.071 mmol, 2.66 eq.) and $Cs_2CO_3$ (48.6 mg, 0.148 mmol, 5.58 eq.) were added. The reaction mixture was stirred for another week at room temperature. All solvents were removed *in vacuo*. Dichloromethane (2 ml) was added to dissolve the product. The filtrate was precipitated in *n*-pentane (10 ml). The solving and precipitation process was repeated once and a mixture of **37** and **38** could be obtained as a white powder (71.4 mg). The $^{31}P\{^1H\}$ NMR spectrum as well as the HRMS spectrum of the mixture of both compounds is shown in **Fig. 3.3.3** and **Fig. 3.3.4**.

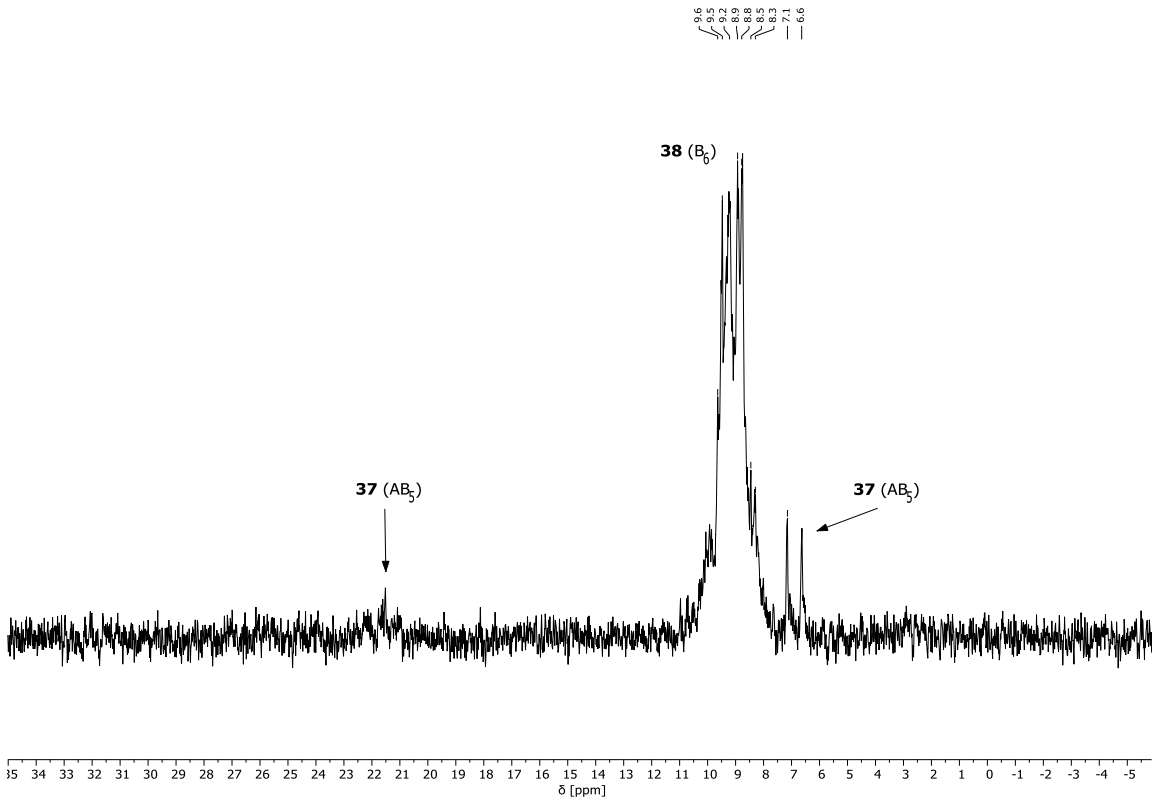


**Fig. 3.3.3.** $^{31}P\{^1H\}$ NMR spectrum of a mixture of **37** and **38** in ethyl acetate and spiked with $C_6D_6$.

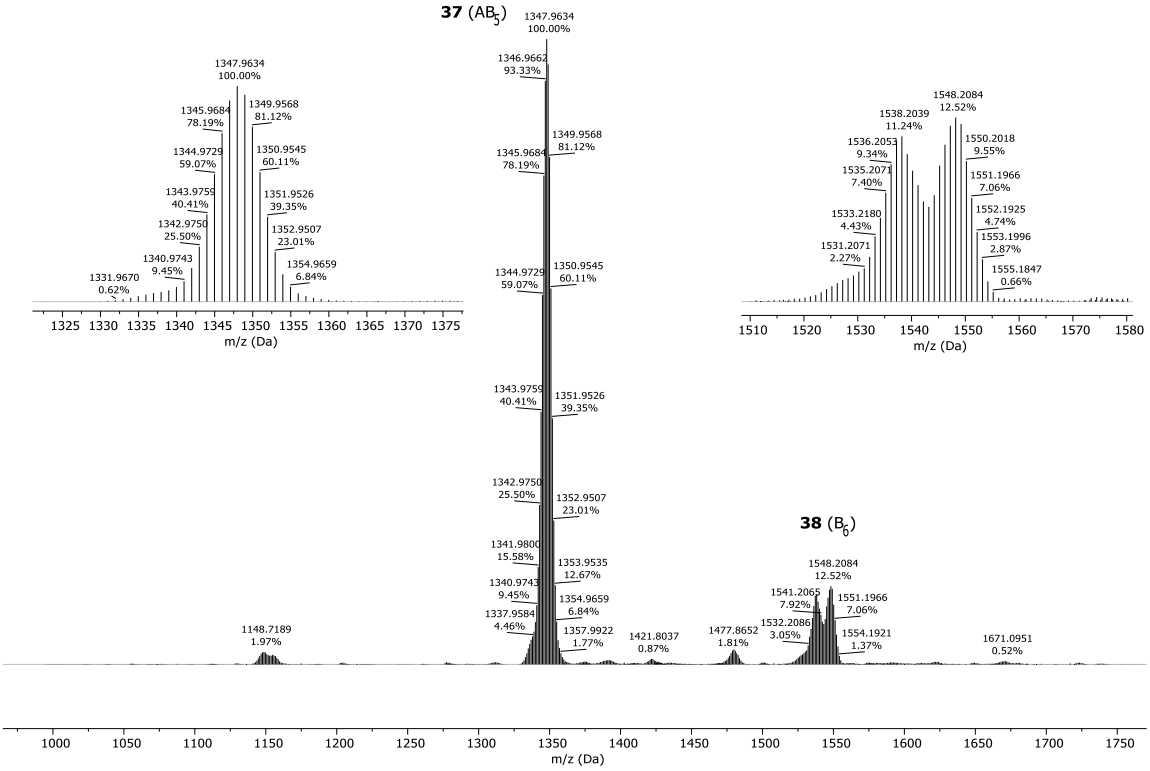


**Fig. 3.3.4.** HRMS (ESI+) spectrum of a mixture of **37** ([$C_{40}H_{75}B_{50}ClN_3O_5P_3$], m/z calculated: 1347.9699 ([M+H]$^+$); found: 1347.9634) and **38** ([$C_{48}H_{90}B_{60}N_3O_6P_3$], m/z calculated: 1548.2135 ([M+H]$^+$); found: 1548.2084). The sample was dissolved in $CH_2Cl_2$.

### 3.3.2.19 Synthesis and Characterization of 39

Carborane derivative **17** (34.2 mg, 0.145 mmol, 3.02 eq.) and $K_2CO_3$ (76.0 mg, 0.550 mmol, 11.46 eq.) were suspended in THF (2 ml) and a solution of $N_3P_3Cl_6$ (**1-G0**) in THF (20.2 mg ml$^{-1}$, 0.83 ml, 0.048 mmol, 1.00 eq.) was added dropwise. The reaction mixture was stirred for 72 h at room temperature, then the solvents were evaporated. Dichloromethane (2x2 ml) was added for extraction of the product. The product was precipitated with *n*-pentane (20 ml). The precipitate was isolated and dissolved in dichloromethane (1 ml) and again precipitated in *n*-pentane (20 ml). No further purification was needed to obtain **39** almost quantitively as a white solid (0.048 mmol).

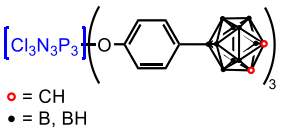


**$^1$H NMR** (400 MHz, $CDCl_3$): δ=7.25 (d, $^3J_{H,H}$=8 Hz, 6H, Ar-*H*), 6.71 (d, $^3J_{H,H}$=8 Hz, 6H, Ar-*H*), 3.61 (s, 3H, $C_{Cage}$-*H*), 3.50 (s, 3H, $C_{Cage}$-*H*)3.18–1.42 ppm (m, 27H, B*H*); Contains impurities of **17**. **$^{11}$B{$^1$H} NMR** (128 MHz, $CDCl_3$): δ=7.6 (1B), −2.2 (1B), −8.7 (2B), −13.8 to −15.4 (6B) ppm; **$^{13}$C{$^1$H} NMR** (101 MHz, $CDCl_3$): δ=155.3, 134.0, 125.2, 119.4 114.7, 114.4, 53.3, 48.6, 22.6, 14.3, 1.2 ppm; **$^{31}$P{$^1$H} NMR** (162 MHz, $CDCl_3$): δ=17.7 ppm (m); **HRMS (ESI+):** [$C_{24}H_{45}B_{30}Cl_3N_3O_3P_3$], m/z calculated: 948.4793 ([M+H]$^+$); found: 948.4766.

### 3.3.2.20 Synthesis and Characterization of 40

Carborane derivative **17** (40.0 mg, 0.168 mmol, 3.98 eq.) and $Cs_2CO_3$ (134 mg, 0.408 mmol, 9.72 eq) were suspended in THF (3 ml) and a solution of $P(S)Cl_3$ in THF (0.211 mmol $ml^{-1}$, 0.20 ml, 0.042 mmol, 2.10 eq.) was added dropwise to the suspension. The reaction mixture was stirred at room temperature for 96 h; then more **17** (18.8 mg, 0.079 mmol, 1.87 eq.) and $Cs_2CO_3$ (118 mg, 0.360 mmol, 8.53 eq) were added. The reaction mixture was stirred for another 45 h and was then heated for 24 h to 40 °C. The reaction progress was followed by $^{31}P\{^1H\}$ NMR spectroscopy. The reaction was stopped after obtaining only one phosphorus signal. The crude mixture was filtered and added into *n*-pentane (20 ml). The white precipitate was isolated by filtration, redissolved in THF (10 ml) and again precipitated with *n*-pentane (35 ml). After drying, the remaining white solid was purified by preparative thin-layer chromatography (99% dichloromethane, 1% ethyl acetate, 250 µm, silica gel) yielding 3.3 mg of a white solid (0.004 mmol, 3%).

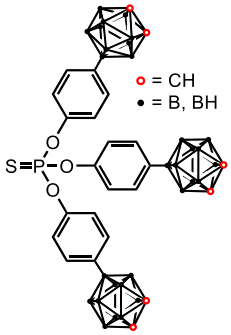


**$^1$H NMR** (400 MHz, $CDCl_3$): δ=7.73 (d, 2H, *J*=8 Hz, Ar-*H*), 7.08 (d, 2H, *J*=7 Hz, Ar-*H*), 3.62–3.59 (s, 1H, $C_{Cage}$-*H*), 3.52 ppm (s, 1H, $C_{Cage}$-*H*); The multiplet for the B*H* groups could not be observed; **$^{11}$B{$^1$H} NMR** (128 MHz, $CDCl_3$): δ=−2.1 (1B), −8.7 (1B), −14.3 ppm (8B); **$^{31}$P{$^1$H} NMR** (162 MHz, $CDCl_3$): δ=52.3 ppm; **HRMS (ESI+):** [$C_{24}H_{45}B_{30}O_3PS$] m/z calculated: 770.5898 ($[M+H]^+$); found: 770.5884.

### 3.3.2.21 Synthesis and Characterization of 41 and 42

Carborane **17** (24.1 mg, 0.101 mmol, 2.10 eq.) was dissolved in THF (5 ml) and DBU (1,8-diazabicyclo[2.4.0]undec-7-ene, 0.033 ml, 0.221 mmol, 4.60 eq.) was added and the reaction mixture was stirred for 1 h at room temperature. Then a solution of **35** in THF (13.3 mg $ml^{-1}$, 0.97 ml, 0.048 mmol, 1.00 eq.) was added dropwise. The reaction mixture was stirred at room temperature for 72 h, then the crude mixture was washed with distilled $H_2O$ (3x50 ml). The aqueous layer was once extracted with ethyl acetate (100 ml) and the organic layers were united, dried over $Na_2SO_4$ and filtered. The remaining product was purified by column chromatography (90% petroleum ether, 10% isopropanol, alumina), yielding 10.7 mg of **42** as a white solid (0.023 mmol, 48%) and 4.6 mg of **41** as white solid (0.07 mmol, 14%).

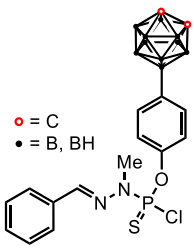


**$R_F$** (98% hexanes, 2% isopropanol) 0.69; **$^1$H NMR** (300 MHz, $CDCl_3$): δ=7.72 (m, 3H, PPh-$H_o$ and C*H*), 7.40 (m, 3H, PPh-$H_{m,p}$), 7.34 (d, $^3J_{H,H}$=8 Hz, 2H, Ar-*H*), 7.15 (dd, $^3J_{H,H}$=9, 2 Hz, 2H, Ar-*H*), 3.63 (s, 1H, $C_{Cage}$-*H*), 3.53 (s, 1H, $C_{Cage}$-*H*), 3.44 (s, 3H, 2.99–1.71 ppm (m, 9H, B*H*); **$^{11}$B{$^1$H} NMR** (96 MHz, $CDCl_3$): δ=7.3 (1B), −2.1 (1B), −8.6 (2B), −14.1 to −15.4 ppm (6B); **$^{31}$P{$^1$H} NMR** (121 MHz, $CDCl_3$):

δ=68.3 ppm; **HRMS (ESI+):** [$C_{16}H_{25}B_{10}ClN_2OPS$], m/z calculated: 468.2100 ([M+H]$^+$); found: 468.2103.

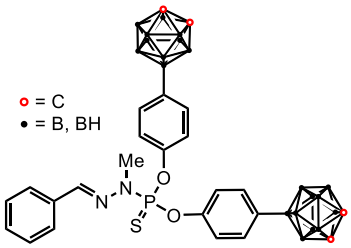


**$R_F$** (98% hexanes, 2% isopropanol) 0.37; **$^1$H NMR** (300 MHz, $CDCl_3$): δ=7.70 (m, 2H, PPh-*H$_o$*), 7.62 (s, 1H, C*H*), 7.38 (m, 3H, PPh-*H$_{m,p}$)*, 7.07 (dd, $^3J_{H,H=}$9, 2 Hz, 4H, Ar-*H*), 6.71 (m, 4H, Ar-*H*), 3.61 (s, 2H, $C_{Cage}$-*H*), 3.50 (s, 2H, $C_{Cage}$-*H*), 3.34 (d, $^3J_{H,H}$=11 3H, 2.63–1.85 ppm (m, 9H, B*H*); **$^{11}$B{$^1$H} NMR** (96 MHz, $CDCl_3$): δ=7.9 (1B), −2.1 (1B), −8.6 (1B), −14.1 to −15.4 ppm (6B); **$^{13}$C{$^1$H} NMR** was not obtained; **$^{31}$P{$^1$H} NMR** (121 MHz, $CDCl_3$): δ=62.1 ppm; **HRMS (ESI+):** [$C_{24}H_{40}B_{20}N_2O_2PS$], m/z calculated: 668.4538 ([M+H]$^+$); found: 668.4539.

### 3.3.2.22 Synthesis and Characterization of 43

Carborane derivative **17** (39.2 mg, 0.165 mmol, 6.11 eq.) and $Cs_2CO_3$ (100 mg, 0.304 mmol, 11.26 eq.) were suspended in THF (3 ml) and a solution of **1-G1** in THF (17.6 mg ml$^{-1}$, 2.8 ml, 0.027 mmol, 1.00 eq.) was added dropwise. The reaction mixture was stirred for 72 h at room temperature and then heated to 40 °C for further 72 h. After cooling to room temperature, the solvent was evaporated. Dichloromethane (3 ml) was added to dissolve the product. The product was precipitated with *n*-pentane (15 ml) and washed with *n*-pentane (2x5 ml). The dissolving and precipitation process was repeated once and **43** was obtained as a white powder (26.9 mg, 0.009 mmol, 30%).

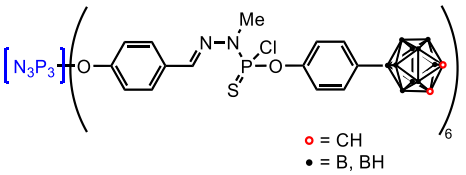


**$^1$H NMR** (400 MHz, $CDCl_3$): δ=7.56 (br s, 18H, **38**-Ph-*H*), 7.31 (d, $^3J_{H,H}$=8 Hz, 12H, Ar-*H*), 7.12 (d, $^3J_{H,H}$=8 Hz,12H, Ar-*H*), 6.98 (br s, 12H, **38**-Ph-*H*), 3.58 (s, 6H, $C_{Cage}$-*H*), 3.48 (s, 6H, $C_{Cage}$-*H*)3.09–1.45 ppm (m, 54H, B*H*); **$^{11}$B{$^1$H} NMR** (128 MHz, $CDCl_3$): δ=7.0 (1B), −2.2 (1B), −8.7 (2B), −14.2 to −15.4 ppm (6B); **$^{13}$C{$^1$H} NMR** (101 MHz, $CDCl_3$): δ=133.9, 128.7, 121.6, 53.5, 34.4, 22.6, 14.3, 0.2 ppm; **$^{31}$P{$^1$H} NMR** (162 MHz, $CDCl_3$): δ=67.7, 8.4 ppm; **HRMS (ESI+):** [$C_{96}H_{138}B_{60}Cl_6N_{15}O_{12}P_9S_6$], m/ calculated: 3028.0800 ([M+H]$^+$); not found.

### 3.3.2.23 Synthesis and Characterization of 44

Carborane **17** (19.7 mg, 0.083 mmol, 12.21 eq.) and $Cs_2CO_3$ (54.0 mg, 0.166 mmol, 24.41 eq.) were suspended in THF (4 ml) and a solution of **1-G1** in THF (17.6 mg ml$^{-1}$, 0.71 ml, 0.0068 mmol, 1.00 eq.) was added dropwise. The reaction mixture was stirred for 120 h at room temperature and then heated to 40 °C for further 24 h. After cooling to room temperature, the solvent was evaporated. Dichloromethane (4 ml) was added to dissolve the crude reaction mixture. The product was isolated by filtration and precipitated with *n*-pentane (20 ml), then washed with

*n*-pentane (4 ml). The dissolving and precipitation process was repeated once and **44** could be obtained as a white powder (6.3 mg, 0.002 mmol, 24%).

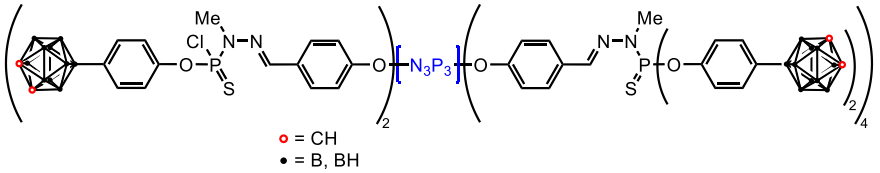


**$^{1}$H NMR** (400 MHz, $CDCl_3$): δ=7.56 (br s, 18H, **38**-Ph-*H*), 7.31 (d, 2H, *J*=8 Hz, Ar-*H*), 7.12 (d, 2H, *J*=8 Hz, Ar-*H*), 6.98 (br s, 12H, **38**-Ph-*H*), 3.58 (s, 6H, $C_{Cage}$-*H*), 3.48 (s, 6H, $C_{Cage}$-*H*)3.09–1.45 (m, 54H, B*H*) ppm; **$^{11}$B{$^{1}$H} NMR** (128 MHz, $CDCl_3$): δ=7.0 (1B), −2.2 (1B), −8.7 (2B), −14.2 to −15.4 (6B) ppm; **$^{13}$C{$^{1}$H} NMR** (101 MHz, $CDCl_3$, 25 °C): δ=133.9, 128.7, 121.6, 53.5, 34.4, 22.6, 14.3, 0.2 ppm; **$^{31}$P{$^{1}$H} NMR** (162 MHz, $CDCl_3$) δ=67.7, 8.4 ppm; **HRMS (ESI+):** $[C_{112}H_{168}B_{80}Cl_4N_{15}O_{14}P_9S_6]$, m/z calculated: 3427.5701 ($[M+H]^+$); not found.

### 3.3.2.24 Experimental details for the attempted synthesis of a three-fold substituted dendrimer 45

Carboranylphosphine **31** (46.6 mg, 0.077 mmol, 2.96 eq.) was suspended in THF (5 ml) and a solution of **1-G0** in THF (4.04 mg ml$^{-1}$, 2.2 ml, 0.026 mmol, 1.00 eq.) was added dropwise. The reaction mixture was stirred for 1 h before DBU (0.015 ml, 0.100 mmol, 3.87 eq.) was added. The reaction was stirred for 96 h, then all solvents were removed *in vacuo*. Dichloromethane (2 ml) was added to dissolve the cure reaction mixture. The product was precipitated in *n*-pentane (15 ml) and washed with *n*-pentane (2x4 ml). The dissolving and precipitation process was repeated once and different diastereomers of **45** together with other by-products could be observed by NMR spectroscopy as well as remaining DBU (see **Fig. 3.3.5**–**Fig. 3.3.8**).

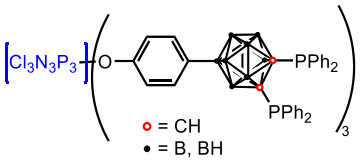


**$^{1}$H NMR** (400 MHz, $CDCl_3$): δ=7.85 (m, 24H, PPh*H*), 7.43 (m, 36H, PPh*H*), 7.10 (m, 12H, Ar-*H*), 7.00 (d, $^{3}J_{H,H}$=8 Hz, 12H, Ar-*H*), 6.79 (d, $^{3}J_{H,H}$=8 Hz, 12H, Ar-*H*), B*H* groups were not observed (overlapping signals of DBU); **$^{11}$B{$^{1}$H} NMR** (128 MHz, $CDCl_3$): δ=8.6 (1B), −0.1 (1B), −7.3 to −15.4 ppm (8B); **$^{13}$C{$^{1}$H} NMR** (101 MHz, $CDCl_3$): δ=166.2, 135.8, 135.6, 133.2, 133.0, 130.8, 128.6, 128.6, 128.5, 128.0, 127.8, 127.6, 114.9, 77.4, 77.1, 76.8, 54.4, 48.7, 37.9, 32.2, 29.0, 26.8, 24.1, 22.3, 19.5, 14.1, 1.0, 0.0 ppm; **$^{31}$P{$^{1}$H} NMR** (162 MHz, $CDCl_3$): δ=23.4–17.2, 7.7–5.0 ppm; **HRMS (ESI+):** $[C_{96}H_{97}B_{30}Cl_3N_3O_3P_9]$, m/z calculated: 2050.7334 ($[M+H]^+$); not found.

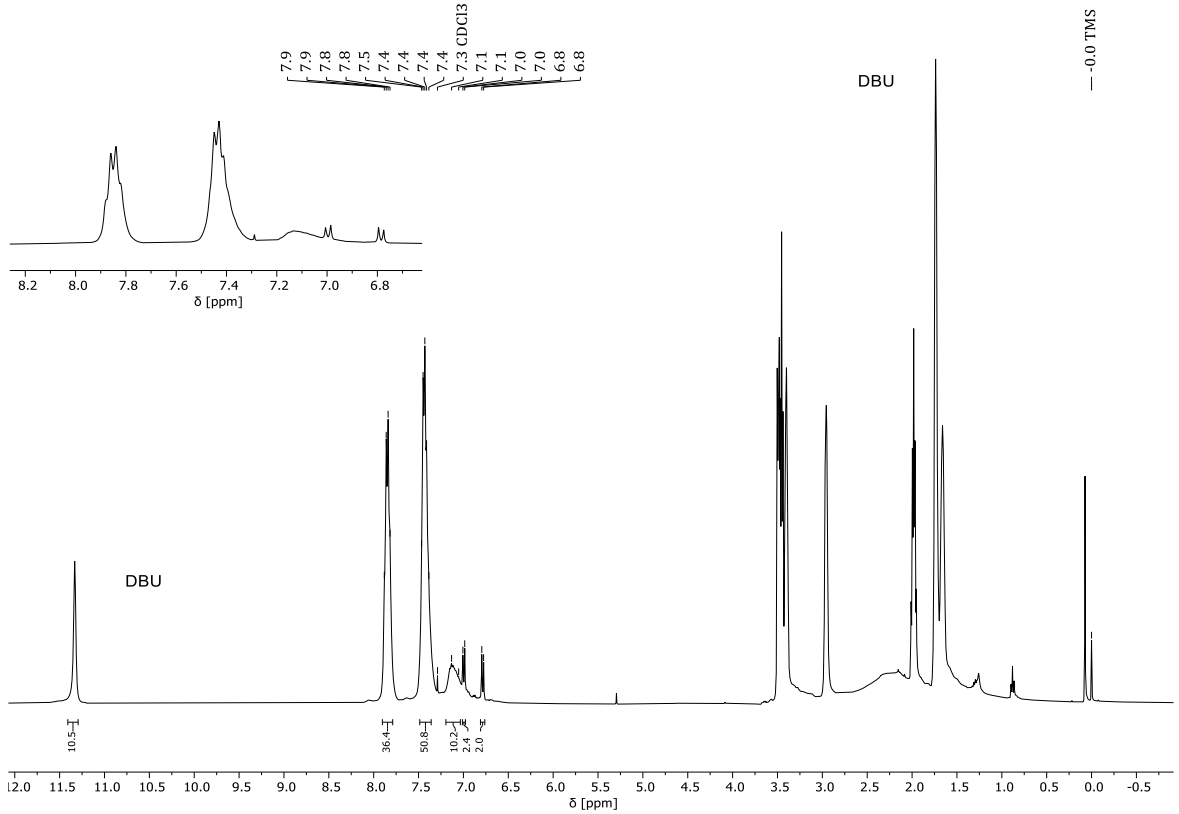


**Fig. 3.3.5.** $^{1}H$ NMR spectrum of **45** in $CDCl_3$. Remaining signals of DBU/$HDBU^+$ can be observed.

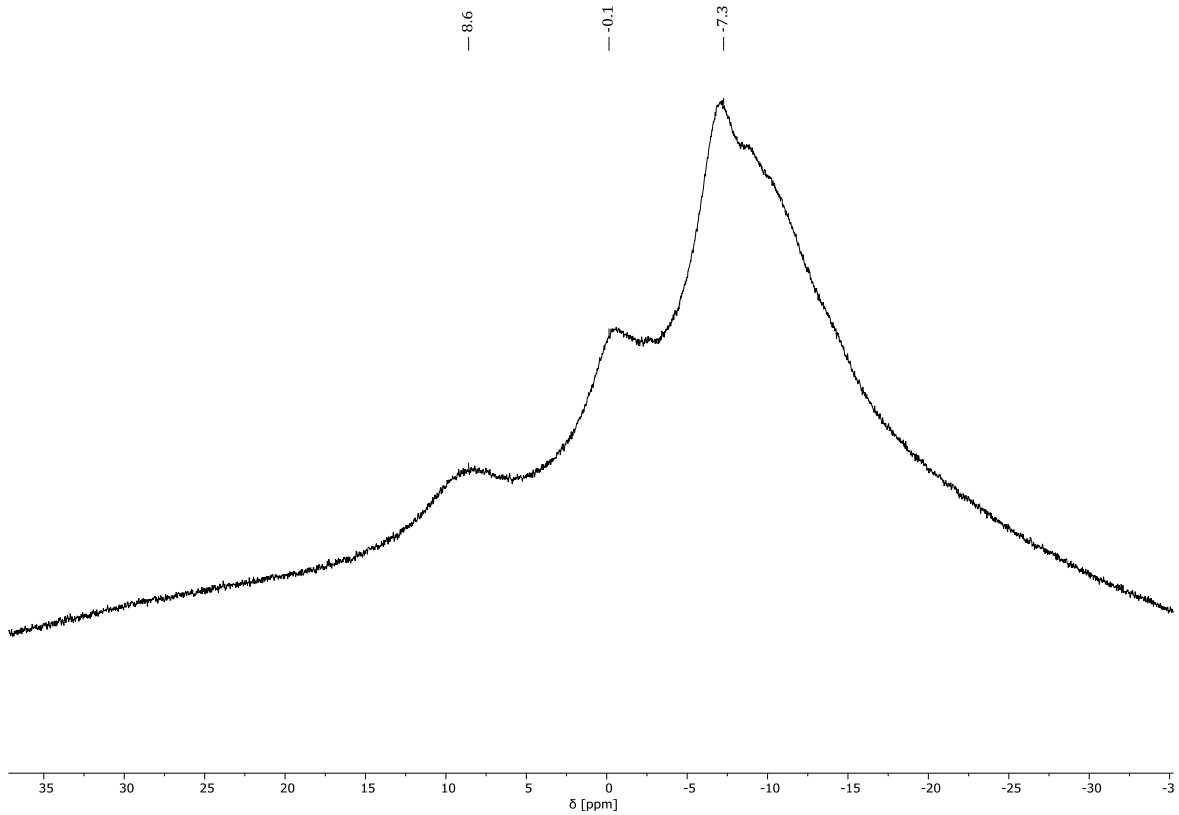


**Fig. 3.3.6.** $^{11}B\{^{1}H\}$ NMR spectrum of **45** in $CDCl_3$.

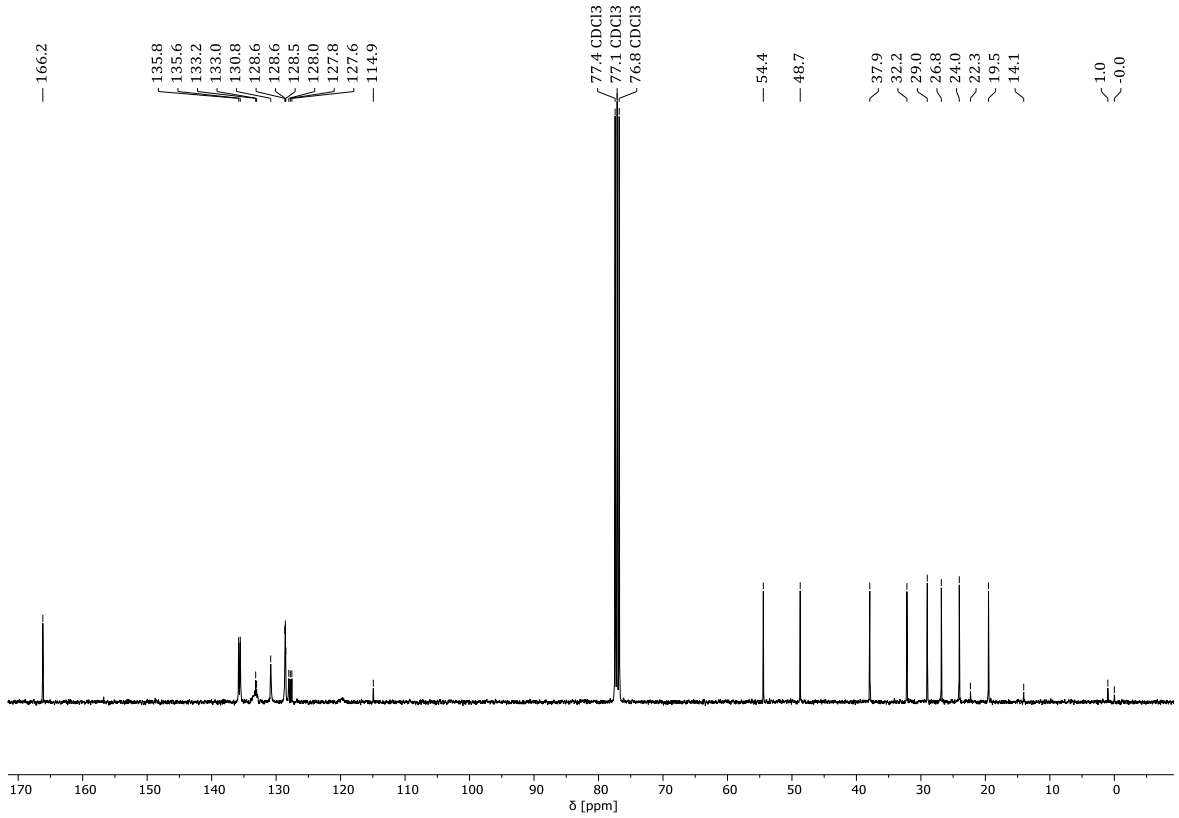


**Fig. 3.3.7.** $^{13}C\{^{1}H\}$ NMR spectrum of **45** in $CDCl_3$.

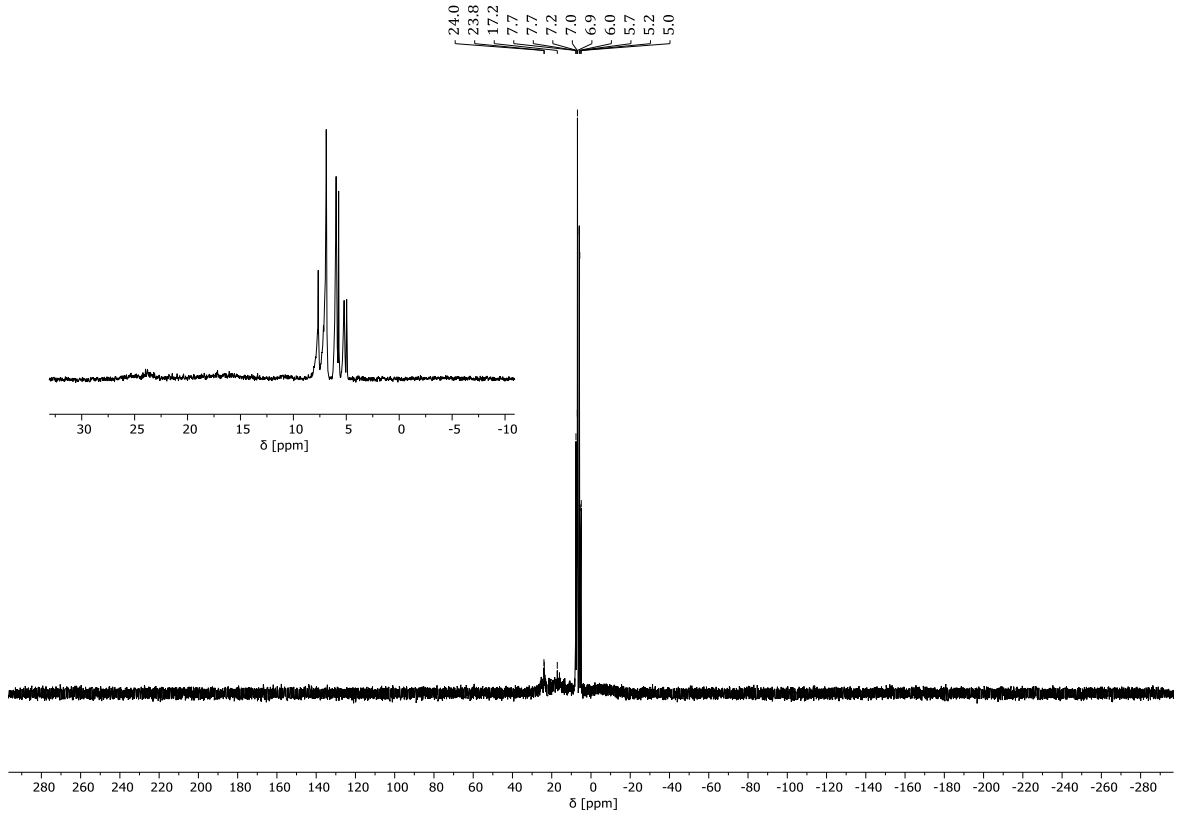


**Fig. 3.3.8.** $^{31}P\{^{1}H\}$ NMR spectrum of **45** in $CDCl_3$.

### 3.3.3 Single Crystal X-Ray Diffraction Analyses

The data were collected on a Gemini diffractometer (Rigaku Oxford Diffraction) using Mo-$K_\alpha$ radiation (λ=71.073 pm) and ω-scan rotation (**16**–**19** and **28**–**31**), on a Bruker Kappa Apex II diffractometer equipped with a 30 W air-cooled microfocus source, using Mo-$K_\alpha$ radiation (λ=71.073 pm), or on a Rigaku XtaLAB Synergy Dualflex diffractometer using a PhotonJet X-ray source (Cu, λ=1.54184 Å) with an Oxford Cryosystem Cryostream cooling device to collect the data at low temperature (100(2) K) (**25**, **33** and **34**). Data reduction was performed with CrysAlis Pro[93] and APEX3[56] including the program SCALE3 ABSPACK[57] and SADABS[56] for empirical absorption correction. The structures were solved by SHELXT (dual space method)[58] and all non-hydrogen atoms were refined anisotropically by means of least-squares procedures on $F^2$ with SHELXL.[59] With the exception of structures **17** and **18**, all carborane carbon atoms could be localized with a bond length and displacement parameter analysis. For **17** and **18** the electron density of all highly disordered solvent molecules had been removed with the SQUEEZE routine implemented in PLATON.[60] Excluding disordered regions and the methyl substituent C33 (**29**), all H atoms were located on difference Fourier maps calculated at the final stage of the structure refinement whereas for **25**, **33** and **34** generally all hydrogen atoms were calculated on idealized positions using a riding model. For **33** and **34**, the O-bound and P-bound H atoms were located in difference Fourier maps and freely refined for **33** and with O–H distances restrained to 0.84(2) Å for **34**. For **34**, the SQUEEZE function of PLATON[60] was used to eliminate the contribution of the electron density in the final refinement of highly disordered solvent. Structure figures were generated DIAMOND (version 4.6.5).[61]

CCDC deposition numbers given in **Table 3.3.1** contains the supplementary crystallographic data for this paper. The data can be obtained free of charge via https://summary.ccdc.cam.ac.uk/structure-summary-form (or from the Cambridge Crystallographic Data Centre, 12 Union Road, Cambridge CB2 1EZ, UK; fax: (+44)1223-336-033; or deposit@ccdc.cam.uk).

**Table 3.3.1.** Fundamental structure parameters.

| Compound | (**16**) | (**17**) | (**18**) | (**19**) |
|---|---|---|---|---|
| Empirical formula | $C_{14}H_{30}B_{10}OSi$ | $C_{8.33}H_{16.33}B_{10}ClO$ | $C_{8.25}H_{17.25}B_{10}Cl_{0.75}N$ | $C_{13}H_{25}B_{10}NO_2$ |
| Formula weight | 350.57 | 276.10 | 265.17 | 335.44 |
| Temperature [K] | 130(2) | 130(2) | 130(2) | 130(2) |
| Wavelength [pm] | 71.073 | 71.073 | 71.073 | 71.073 |
| Crystal system | Orthorhombic | Trigonal | Monoclinic | Monoclinic |
| Space group | P nma | R $\bar{3}$ | P $2_1/c$ | P $2_1/c$ |
| Unit cell dimensions | | | | |
| a [pm] | 1401.42(3) | 3487.5(1) | 1271.18(3) | 679.52(1) |
| b [pm] | 1189.75(3) | 3487.5(1) | 1731.22(3) | 2138.06(3) |
| c [pm] | 1283.73(3) | 658.82(4) | 1345.11(3) | 1322.05(2) |
| α [deg] | 90 | 90 | 90 | 90 |
| β [deg] | 90 | 90 | b= 91.923(2) | 90.932(1) |
| γ [deg] | 90 | 120 | 90 | 90 |
| Volume [$nm^3$] | 2.14041(9) | 6.9395(6) | 2.9585(1) | 1.92049(5) |
| Z | 4 | 18 | 8 | 4 |
| $\rho_{(calculated)}$ [$Mg/m^3$] | 1.088 | 1.189 | 1.191 | 1.160 |
| μ [$mm^{-1}$] | 0.110 | 0.229 | 0.189 | 0.066 |
| F(000) | 744 | 2544 | 1092 | 704 |
| Crystal size [$mm^3$] | 0.40 · 0.30 · 0.30 | 0.40 · 0.04 · 0.03 | 0.31 · 0.31 · 0.29 | 0.38 · 0.29 · 0.26 |
| $\Theta_{Min}$ / $\Theta_{Max}$ [deg] | 2.334 / 30.716 | 2.336 / 27.847 | 2.467 / 25.349 | 2.450 / 32.493 |
| Index ranges | −19 ≤ h ≤ 19 | −42 ≤ h ≤ 43 | −15 ≤ h ≤ 15 | −10 ≤ h ≤ 10 |
| Reflections collected | 21959 | 17391 | 27337 | 44563 |
| Indp. reflections ($R_{int}$) | 3256 (0.0470) | 3382 (0.0608) | 5412 (0.0345) | 6506 (0.0318) |
| Completeness ($\Theta_{Max}$) | 99.9 % (28.29°) | 99.9 % (25.35°) | 99.9 % (25.00°) | 100.0 % (30.51°) |
| $T_{Max}$ / $T_{Min}$ | 1.00000 / 0.97417 | 1.00000 / 0.99229 | 1.00000 / 0.98513 | 1.00000 / 0.97711 |
| Restraints / parameters | 0 / 197 | 0 / 173 | 600 / 477 | 0 / 335 |
| Gof on $F^2$ | 1.041 | 1.031 | 1.039 | 1.031 |
| R1 / wR2 (I>2σ(I)) | 0.0518 / 0.1259 | 0.0627 / 0.1443 | 0.0612 / 0.1528 | 0.0418 / 0.1009 |
| R1 / wR2 (all data) | 0.0687 / 0.1364 | 0.1138 / 0.1666 | 0.0818 / 0.1658 | 0.0543 / 0.1072 |
| Residual electron density [$e \cdot Å^{-3}$] | 0.410 / −0.247 | 0.170 / −0.242 | 0.293 / −0.166 | 0.356 / −0.227 |
| Comments | - | †[1] | †[2] | - |
| CCDC No | 2300964 | 2300965 | 2300966 | 2300967 |

**Table 3.3.1** continued.

| Compound | **(25)** | **(28)** | **(29)** | **(30)** |
|---|---|---|---|---|
| Empirical formula | $C_{22}H_{48}B_{10}OP_2Si$ | $C_{38}H_{48}B_{10}OP_2Si$ | $C_{33}H_{36}B_{10}OP_2$ | $C_{46}H_{47}B_{10}NP_2$ |
| Formula weight | 526.73 | 718.89 | 618.66 | 783.88 |
| Temperature [K] | 100(2) | 130(2) | 130(2) | 130(2) |
| Wavelength [pm] | 154.184 | 71.073 | 71.073 | 71.073 |
| Crystal system | Monoclinic | triclinic | monoclinic | monoclinic |
| Space group | P $2_1/c$ | $P\bar{1}$ | $P2_1/c$ | $P2_1/n$ |
| Unit cell dimensions | | | | |
| a [pm] | 772.16(3) | 1147.58(7) | 1131.80(2) | 1045.90(2) |
| b [pm] | 1259.34(7) | 1272.69(6) | 1260.10(2) | 1371.66(2) |
| c [pm] | 1612.71(7) | 1468.19(9) | 2366.12(3) | 2919.21(4) |
| α [deg] | 90 | 79.397(5) | 90 | 90 |
| β [deg] | 92.896(4) | 79.270(5) | 102.951(2) | 96.829(1) |
| γ [deg] | 90 | 78.406(5) | 90 | 90 |
| Volume [$nm^3$] | 1.56622(13) | 2.0398(2) | 3.28868(9) | 4.1582(1) |
| Z | 2 | 2 | 4 | 4 |
| $\rho_{(calculated)}$ [$Mg/m^3$] | 1.117 | 1.170 | 1.250 | 1.252 |
| μ [$mm^{-1}$] | 1.719 | 0.166 | 0.161 | 0.141 |
| F(000) | 564 | 756 | 1288 | 1640 |
| Crystal size [$mm^3$] | 0.10 0.08 0.02 | 0.20 · 0.10 · 0.05 | 0.37 · 0.33 · 0.20 | 0.40 · 0.35 · 0.30 |
| $\Theta_{Min}$ / $\Theta_{Max}$ [deg] | 2.743 / 76.496 | 2.247 / 29.065 | 2.394 / 32.356 | 2.460 / 28.208 |
| Index ranges | −9 ≤ h ≤ 9 | −15 ≤ h ≤ 14 | −16 ≤ h ≤ 16 | −13 ≤ h ≤ 13 |
| Reflections collected | 14794 | 17865 | 47322 | 44175 |
| Indp. reflections ($R_{int}$) | 4957 (0.1132) | 9353 (0.0367) | 10950 (0.0402) | 9504 (0.0440) |
| Completeness ($\Theta_{Max}$) | 99.3 % (67.68°) | 99.9 % (26.38°) | 100.0 % (30.51°) | 99.9 % (26.38°) |
| $T_{Max}$ / $T_{Min}$ | | 1.00000 / 0.99458 | 1.00000 / 0.99812 | 1.00000 / 0.99691 |
| Restraints / parameters | 54 / 353 | 0 / 661 | 179 / 695 | 106 / 743 |
| Gof on $F^2$ | 1.065 | 1.018 | 1.022 | 1.030 |
| R1 / wR2 (I>2σ(I)) | 0.0628 / 0.1497 | 0.0499 / 0.0993 | 0.0451 / 0.0990 | 0.0585 / 0.1314 |
| R1 / wR2 (all data) | 0.0897 / 0.1718 | 0.0889 / 0.1168 | 0.0661 / 0.1085 | 0.0834 / 0.1444 |
| Residual electron density [e·$Å^{-3}$] | 0.581 / −0.672 | 0.320 / −0.319 | 0.330 / −0.294 | 0.343 / −0.360 |
| Comments | - | - | †[3] | - |
| CCDC No | 2303300 | 2300968 | 2300969 | 2300970 |

**Table 3.3.1** continued.

| Compound | **(31)** | **(33)** | **(34)** |
|---|---|---|---|
| Empirical formula | $C_{32.25}H_{34.50}B_{10}Cl_{0.50}OP_2$ | $C_{14}H_{29}B_{10}O_2P$ | $C_8H_{17}B_{10}O_3P$ |
| Formula weight | 625.86 | 368.44 | 300.29 |
| Temperature [K] | 130(2) | 100(2) | 100(2) |
| Wavelength [pm] | 71.073 | 71.073 | 154.184 |
| Crystal system | triclinic | Monoclinic | Monoclinic |
| Space group | $P\bar{1}$ | P $2_1/c$ | P $2_1/n$ |
| Unit cell dimensions | | | |
| a [pm] | 1415.46(5) | 1218.4(9) | 1151.960(10) |
| b [pm] | 1550.54(6) | 1308.9(8) | 661.420(10) |
| c [pm] | 1557.59(6) | 1329.8(8) | 231.776(3) |
| α [deg] | 82.200(3) | 90 | 90 |
| β [deg] | 75.210(3) | 108.92(2) | 99.7020(10) |
| γ [deg] | 86.829(3) | 90 | 90 |
| Volume [$nm^3$] | 3.2739(2) | 2.006(2) | 1.74071(4) |
| Z | 4 | 4 | 4 |
| $\rho_{(calculated)}$ [$Mg/m^3$] | 1.270 | 1.220 | 1.146 |
| μ [$mm^{-1}$] | 0.202 | 0.144 | 1.364 |
| F(000) | 1298 | 776 | 616 |
| Crystal size [$mm^3$] | 0.45 · 0.35 · 0.15 | 0.12 · 0.08 · 0.04 | 0.12 · 0.08 · 0.04 |
| $\Theta_{Min}$ / $\Theta_{Max}$ [deg] | 2.545 / 30.571 | 1.767 / 25.485 | 3.870 / 79.985 |
| Index ranges | −20 ≤ h ≤ 18 | −14 ≤ h ≤ 14 | −11 ≤ h ≤ 14 |
| Reflections collected | 45156 | 36267 | 34556 |
| Indp. reflections ($R_{int}$) | 17927 (0.0490) | 3697 (0.0806) | 3775 / 0.0437 |
| Completeness ($\Theta_{Max}$) | 99.9 % (28.29°) | 100.0 % (25.24°) | 100.0 % |
| $T_{Max}$ / $T_{Min}$ | 1.00000 / 0.98358 | | |
| Restraints / parameters | 73 / 1127 | 0 / 256 | 2 / 216 |
| Gof on $F^2$ | 1.023 | 1.028 | 1.057 |
| R1 / wR2 (I>2σ(I)) | 0.0567 / 0.1182 | 0.0481 / 0.1101 | 0.0454 / 0.1223 |
| R1 / wR2 (all data) | 0.1013 / 0.1403 | 0.0686 / 0.1212 | 0.0495 / 0.1255 |
| Residual electron density [$e \cdot Å^{-3}$] | 0.458 / −0.431 | 0.424 / −0.383 | 0.388 / −0.391 |
| Comments | †[4] | - | - |
| CCDC No | 2300971 | 2303301 | 2303302 |

†[1]: Solvent molecules ($CDCl_3$) removed with SQUEEZE.[60] From the squeeze analysis we suggest to remove the electron density of approximately 6 poorly defined and diffuse oriented $CDCl_3$ molecules from the unit cell. The given formula ($C_8H_{16}B_{10}O{\cdot}1/3\ CHCl_3$) had been corrected for this solvent contribution. †[2]: Solvent molecules ($CDCl_3$) removed with SQUEEZE.[60] From the squeeze analysis we suggest to remove the electron density of approximately 2 poorly defined and diffuse oriented $CDCl_3$ molecules from the unit cell. The given formula ($C_8H_{17}B_{10}N \cdot 0.25\ CHCl_3$) had been corrected for this solvent contribution. †[3]: The complete molecule is marginally disordered with a ratio of: 0.929(1):0.071(1) (see **Fig. 3.3.9**). †[4]: Disordered phenyl substituent (C41 to C46) on two positions with a ratio of 0.75(2):0.25(2) and disordered solvent molecule ($CH_2Cl_2$) in the vicinity of a center of inversion.

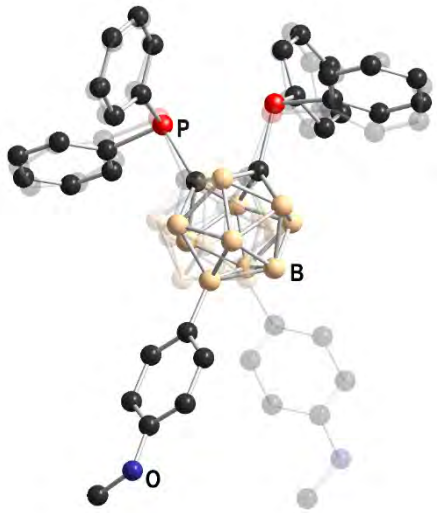


**Fig. 3.3.9.** Disordered molecule **29**. The 7% fraction is given in transparent mode.

### 3.3.4 Computational Studies

#### 3.3.4.1 Methods

Calculations have been carried out using the Gaussian16 suite of programs[62] at DFT level of theory with the B3LYP functional[63–65] combined with Grimme's D3 correction to account for dispersion effects.[66] The structures of **17***, **1-G0**, **TS1**, **G01**–**G06**, and **S01**–**S03** (**40**) were optimized in the experimentally employed solvents using the 6-31G(d,p) basis set for all the atoms (basis set BS1).[67,68] The solvents (dichloromethane, ε=8.930 or tetrahydrofuran, ε=7.4257) were described with the SMD (solvation model based on density) continuum model.[69] Frequency calculations were carried out for all the optimized geometries in order to characterize the stationary points as either minima or transition states. Connections between the transition state and the corresponding minima were checked by displacing in both directions, following the

transition vector, the geometry of the transition states, and subsequent geometry optimization until a minimum was reached.

Energies in solvent were refined by means of single-point calculations at the optimized BS1 geometries using and extended basis set (BS2). BS2 consists in the def2-TZVP basis set for all the atoms.[70,71] GIBBS energies in solvent were calculated adding to the BS2 energies in solvent the thermal and entropic corrections obtained with BS1. An additional correction of 1.9 kcal mol$^{-1}$ was applied to all GIBBS energies to change the standard state from the gas phase (1 atm) to the condensed phase (1 M) at 298.15 K ($\boldsymbol{\Delta G^{1atm\rightarrow 1M}}$).[72] In this way, all the energy values given in the article are GIBBS energies in solution calculated using the formula:

$$\boldsymbol{G = E(BS2) + G(BS1) - E(BS1) + \Delta G^{1atm\rightarrow 1M}}$$

### 3.3.4.2 Substitution of Cl by 17* in 1-G0

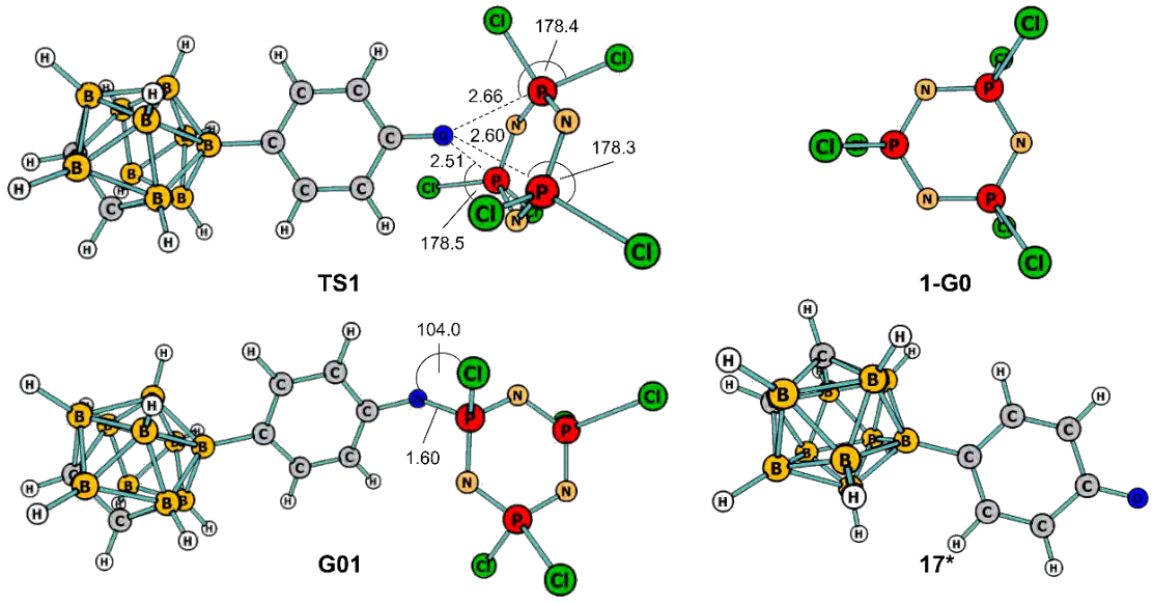


**Fig. 3.3.10.** Optimized structures of the starting material, the intermediates and transition states in the substitution of a Cl function by **17***. Selected bond lengths [Å] and angles [°] are displayed.

### 3.3.4.3 Substitution of multiple Cl by 17* in 1-G0

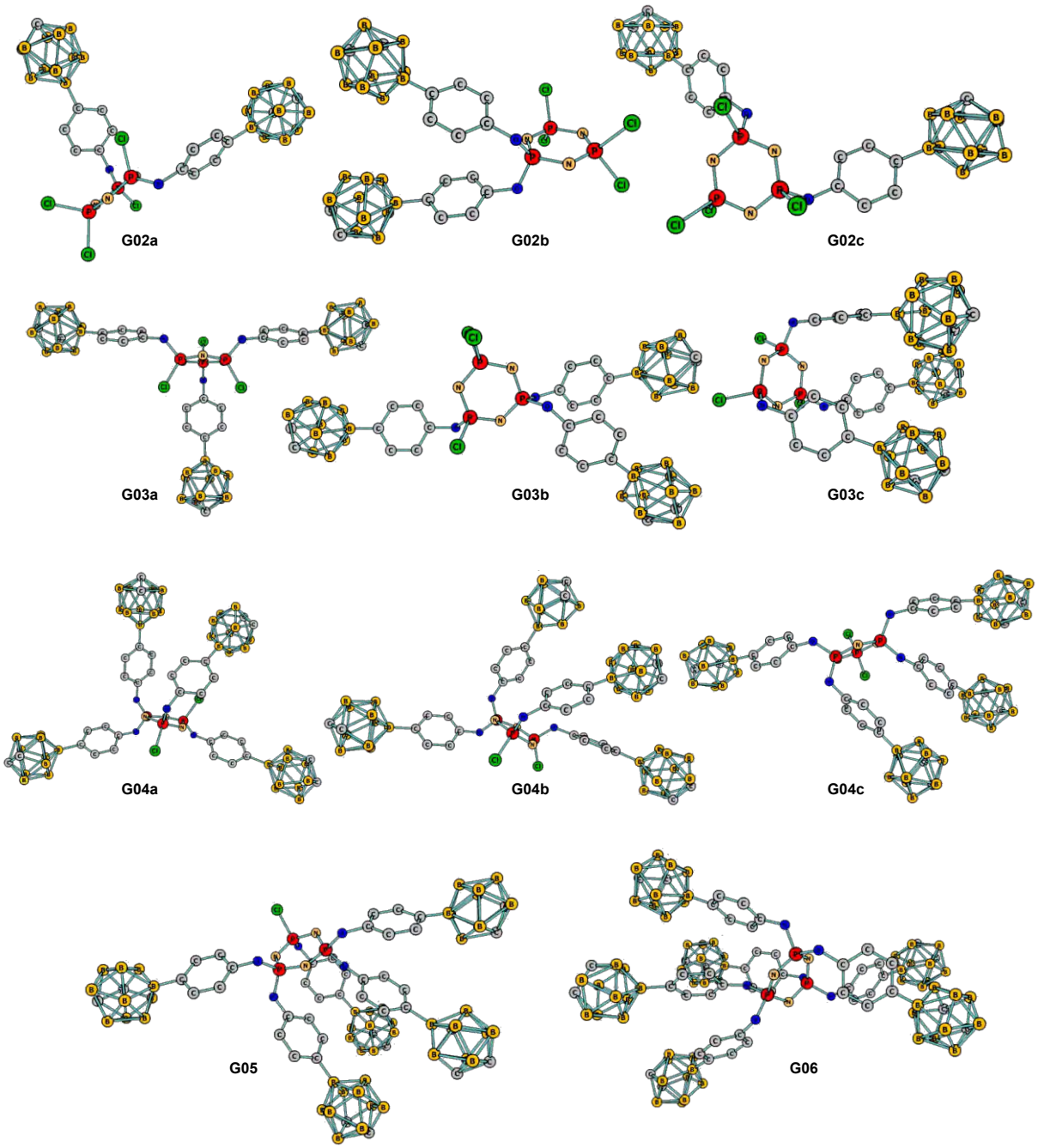


**Fig. 3.3.11.** Optimized structures of the products of the substitution of multiple Cl function by **17*** in **1-G0**.

### 3.3.4.4 Substitution of multiple Cl by 17* in 1-S0

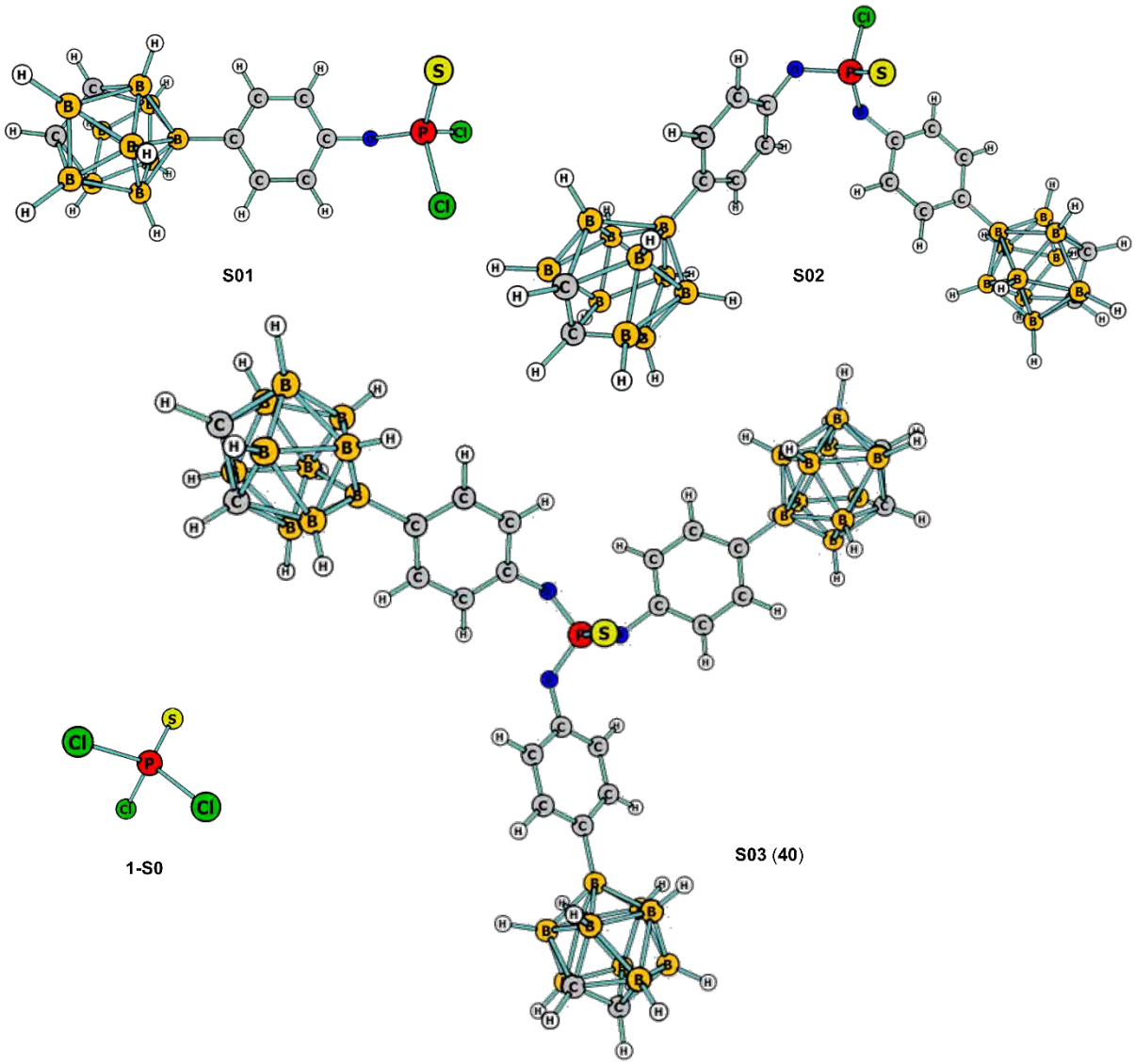


**Fig. 3.3.12.** Optimized structures of the products of the substitution of multiple Cl function by **17*** in **1-S0**.

### 3.3.4.5 Absolute energies of the calculated species (atomic units)

**Table 3.3.2.** Substitution of **1-G0** with **17*** in THF as solvent to form (multiple) substituted dendrimers **G01**–**G06**. Species shown in **Fig. 3.3.10** and **Fig. 3.3.11**.

| | E(acn)/BS1 | T,S correction | G(acn)/BS1 | E(acn)/BS2 | G(acn)/BS2 |
|---|---|---|---|---|---|
| **1-G0** | −3949.63568 | −0.01521 | −3949.65089 | −3950.09261 | −3950.10782 |
| **17*** | −637.930143 | 0.209542 | −637.720601 | −638.148658 | −637.939116 |
| **TS1** | −4587.59813 | 0.219746 | −4587.37839 | −4588.2519 | −4588.03215 |
| **G01** | −4127.29831 | 0.223271 | −4127.07504 | −4127.9195 | −4127.69623 |
| **$Cl^-$** | −460.345821 | −0.015023 | −460.360844 | −460.385498 | −460.400521 |
| **G02a** | −4304.963963 | 0.456827 | −4304.507137 | −4305.748562 | −4305.291735 |
| **G02b** | −4304.960109 | 0.455664 | −4304.504445 | −4305.745686 | −4305.290022 |
| **G02c** | −4304.963522 | 0.461037 | −4304.502484 | −4305.746962 | −4305.285925 |
| **G03a** | −4482.624438 | 0.694291 | −4481.930147 | −4483.573789 | −4482.879498 |
| **G03b** | −4482.625054 | 0.697006 | −4481.928048 | −4483.573001 | −4482.875995 |
| **G03c** | −4482.650641 | 0.703834 | −4481.946806 | −4483.592207 | −4482.888373 |
| **G04a** | −4660.295357 | 0.933583 | −4659.361774 | −4661.406043 | −4660.47246 |
| **G04b** | −4660.305095 | 0.937959 | −4659.367136 | −4661.412914 | −4660.474955 |
| **G04c** | −4660.295732 | 0.937321 | −4659.358411 | −4661.405311 | −4660.46799 |
| **G05** | −4837.970037 | 1.178351 | −4836.791686 | −4839.23873 | −4838.060379 |
| **G06** | −5015.641458 | 1.421954 | −5014.219504 | −5017.071243 | −5015.649289 |

**Table 3.3.3.** Substitution of **1-S0** with **17*** in THF as solvent to form (multiple) substituted dendrimers **S01**–**S03**. Species in the GIBBS energy profile of **Fig. 3.3.12**.

| | E(acn)/BS1 | T,S correction | G(acn)/BS1 | E(acn)/BS2 | G(acn)/BS2 |
|---|---|---|---|---|---|
| **1-S0** | −2120.191887 | −0.02502 | −2120.216907 | −2120.386775 | −2120.411795 |
| **S01** | −2297.851487 | 0.210006 | −2297.64148 | −2298.210797 | −2298.000791 |
| **S02** | −2475.51033 | 0.444792 | −2475.065538 | −2476.033656 | −2475.588864 |
| **S03** | −2653.167392 | 0.686874 | −2652.480518 | −2653.855516 | −2653.168642 |

## 3.4 Conclusion and Outlook

The syntheses of B9-substituted carboranes (**16**–**19**) and carboranylphosphines (**25**–**32**) in acceptable yields was demonstrated. Utilizing different protection and deprotection strategies suitable building blocks with enhanced reactivity for further grafting to different cores, namely **35**, **1-G0**, **1-S0** and **1-G1,** were obtained. Despite the lack of fully carboranylphosphine-substituted compounds, several carborane-substituted dendrimers were obtained. However, the separation of differently carborane-substituted dendrimers is challenging.

The potentially bidentate carboranylbisphosphines themselves, however, appear to be suitable ligands for metal complexes employed in homogeneous catalysis.[39] Furthermore, the selective grafting of a single carborane moiety per $P(S)Cl_2$ function in **1-G1** opens the way to

introducing additional functionalities by replacing the remaining Cl, for instance, with water-solubilizing functions, in view of biological experiments.[4]

## 3.5 References

[1] P. Stockmann, M. Gozzi, R. Kuhnert, M. B. Sárosi, E. Hey-Hawkins, *Chem. Soc. Rev.* **2019**, *48*, 3497–3512.

[2] A. F. Armstrong, J. F. Valliant, *Dalton Trans.* **2007**, 4240–4251.

[3] L. Ueberham, D. Gündel, M. Kellert, W. Deuther-Conrad, F.-A. Ludwig, P. Lönnecke, A. Kazimir, K. Kopka, P. Brust, R.-P. Moldovan, E. Hey-Hawkins, *J. Med. Chem.* **2023**, *66*, 5242–5260.

[4] A.-M. Caminade, M. Milewski, E. Hey-Hawkins, *Pharmaceutics* **2023**, *15*, 2117.

[5] K. Ohta, H. Yamazaki, Y. Endo, *J. Organomet. Chem.* **2009**, *694*, 1646–1651.

[6] I. B. Sivaev, M. Y. Stogniy, V. I. Bregadze, *Coord. Chem. Rev.* **2021**, *436*, 213795.

[7] M. Keener, C. Hunt, T. G. Carroll, V. Kampel, R. Dobrovetsky, T. W. Hayton, G. Ménard, *Nature* **2020**, *577*, 652–655.

[8] P. C. Andrews, M. J. Hardie, C. L. Raston, *Coord. Chem. Rev.* **1999**, *189*, 169–198.

[9] J. Li, J. Xu, L. Yan, C. Lu, H. Yan, *Dalton Trans.* **2021**, *50*, 8029–8035.

[10] A. Alconchel, O. Crespo, P. García-Orduña, M. C. Gimeno, *Inorg. Chem.* **2021**, *60*, 18521–18528.

[11] R. N. Grimes, *Carboranes: Third Edition*, Elsevier Inc., **2016**.

[12] A. V. Puga, F. Teixidor, R. Sillanpää, R. Kivekäs, M. Arca, G. Barberà, C. Viñas, *Chem. Eur. J.* **2009**, *15*, 9755–9763.

[13] R. P. Alexander, H. Schroeder, *Inorg. Chem.* **1963**, *2*, 1107–1110.

[14] F. Röhrscheid, R. H. Holm, *J. Organomet. Chem.* **1965**, *4*, 335–338.

[15] V. P. Balema, M. Pink, J. Sieler, E. Hey-Hawkins, L. Hennig, *Polyhedron* **1998**, *17*, 2087–2093.

[16] H.-S. Lee, J.-Y. Bae, J. Ko, Y. S. Kang, H. S. Kim, S.-J. Kim, J.-H. Chung, S. O. Kang, *J. Organomet. Chem.* **2000**, *614–615*, 83–91.

[17] F. Teixidor, C. Viñas, R. Benakki, R. Kivekäs, R. Sillanpää, *Inorg. Chem.* **1997**, *36*, 1719–1723.

[18] T. Lee, S. W. Lee, H. G. Jang, S. O. Kang, J. Ko, *Organometallics* **2001**, *20*, 741–748.

[19] A. R. Popescu, F. Teixidor, C. Viñas, *Coord. Chem. Rev.* **2014**, *269*, 54–84.

[20] P. Coburger, G. Kahraman, A. Straube, E. Hey-Hawkins, *Dalton Trans.* **2019**, *48*, 9625–9630.

[21] R. T. Baker, W. Tumas, *Science* **1999**, *284*, 1477–1479.

[22] R. Van Heerbeek, P. C. J. Kamer, P. W. N. M. Van Leeuwen, J. N. H. Reek, *Chem. Rev.* **2002**,

*102*, 3717–3756.

[23] J. Popp, A.-M. Caminade, E. Hey-Hawkins, *Eur. J. Inorg. Chem.* **2020**, *2020*, 1654–1669.

[24] A.-M. Caminade, A. Ouali, R. Laurent, C. O. Turrin, J. P. Majoral, *Chem. Soc. Rev.* **2015**, *44*, 3890–3899.

[25] S. Bauer, E. Hey-Hawkins in *Boron Science* (Ed.: N.S. Hosmane), CRC Press, **2011**, pp. 529–578.

[26] G. B. Gange, A. L. Humphries, D. E. Royzman, M. D. Smith, D. V. Peryshkov, *J. Am. Chem. Soc.* **2021**, *143*, 10842–10846.

[27] B. Wang, D. P. Shelar, X.-Z. Han, T.-T. Li, X. Guan, W. Lu, K. Liu, Y. Chen, W.-F. Fu, C.-M. Che, *Chem. Eur. J.* **2015**, *21*, 1184–1190.

[28] A. Pitto-Barry, *Polym. Chem.* **2021**, *12*, 2035–2044.

[29] A. H. Soloway, H. Hatanaka, M. A. Davis, *J. Med. Chem.* **1967**, *10*, 714–717.

[30] J. S. Andrews, J. Zayas, M. Jones, *Inorg. Chem.* **1985**, *24*, 3715–3716.

[31] A.-M. Spokoyny, T. C. Li, O. K. Farha, C. W. Machan, C. She, C. L. Stern, T. J. Marks, J. T. Hupp, C. A. Mirkin, *Angew. Chem. Int. Ed.* **2010**, *49*, 5339–5343, *Angew. Chem.* **2010**, *122*, 5467–5471

[32] M. Milewski, A.-M. Caminade, E. Hey-Hawkins, P. Lönnecke, *Acta Crystallogr. Sect. E Crystallogr. Commun.* **2022**, *78*, 1145–1150.

[33] L. I. Zakharkin, A. I. Kovredov, V. A. Ol'shevskaya, Z. S. Shaugumbekova, *J. Organomet. Chem.* **1982**, *226*, 217–222.

[34] P. Magnus, N. Sane, B. P. Fauber, V. Lynch, *J. Am. Chem. Soc.* **2009**, *131*, 16045–16047.

[35] G. R. Pettit, M. P. Grealish, M. K. Jung, E. Hamel, R. K. Pettit, J.-C. Chapuis, J. M. Schmidt, *J. Med. Chem.* **2002**, *45*, 2534–2542.

[36] S. E. Diltemiz, A. Ersöz, D. Hür, R. Keçili, R. Say, *Mater. Sci. Eng. C* **2013**, *33*, 824–830.

[37] N. Launay, M. Slany, A.-M. Caminade, J. P. Majoral, *J. Org. Chem.* **1996**, *61*, 3799–3805.

[38] R. Moumne, S. Lavielle, P. Karoyan, *J. Org. Chem.* **2006**, *71*, 3332–3334.

[39] S. D. Bull, S. G. Davies, C. Fenton, A. W. Mulvaney, R. Shyam Prasad, A. D. Smith, *J. Chem. Soc. Perkin Trans. 1* **2000**, 3765–3774.

[40] W. Wolfsberger, *J. Organomet. Chem.* **1986**, *317*, 167–173.

[41] O. Kühl (Ed.), *Phosphorus-31 NMR Spectroscopy*, Springer, Berlin, **2009**.

[42] G. A. Olah, C. W. McFarland, *J. Org. Chem.* **1969**, *34*, 1832–1834.

[43] J. B. Stothers, J. R. Robinson, *Can. J. Chem.* **1964**, *42*, 967–970.

[44] I. J. Bruno, J. C. Cole, P. R. Edgington, M. Kessler, C. F. Macrae, P. McCabe, J. Pearson, R. Taylor, *Acta Crystallogr. Sect. B Struct. Sci.* **2002**, *58*, 389–397 (ConQuest Version 2022.2.0).

[45] C. R. Groom, I. J. Bruno, M. P. Lightfoot, S. C. Ward, *Acta Crystallogr. Sect. B Struct. Sci. Cryst.*

*Eng. Mater.* **2016**, *72*, 171–179 (CSD Version 5.43 November 2021).

[46] G. Franc, E. Badetti, C. Duhayon, Y. Coppel, C.-O. Turrin, J.-P. Majoral, R.-M. Sebastián, A.-M. Caminade, *New J. Chem.* **2010**, *34*, 547–555.

[47] N. Launay, A.-M. Caminade, J. P. Majoral, *J. Organomet. Chem.* **1997**, *529*, 51–58.

[48] O. I. Kolodiazhnyi, A. Kolodiazhna, *Tetrahedron: Asym.* **2017**, *28*, 1651–1674.

[49] M. A. van Bochove, M. Swart, F. M. Bickelhaupt, *J. Am. Chem. Soc.* **2006**, *128*, 10738–10744.

[50] K. Roy, S. Kar, R. N. Das in *Understanding the Basics of QSAR for Applications in Pharmaceutical Sciences and Risk Assessment*, Elsevier, **2015**, pp. 1–46.

[51] R. F. Quijano-Quiñones, M. Quesadas-Rojas, G. Cuevas, G. J. Mena-Rejón, *Molecules* **2012**, *17*, 4661–4671.

[52] F. H. Stillinger, *Science* **1980**, *209*, 451–457.

[53] J.-E. Siewert, A. Schumann, C. Hering-Junghans, *Dalton Trans.* **2021**, *50*, 15111–15117.

[54] MestReNova (v. 14.1.0), Mestrelab Research S.L., **2019**.

[55] CrysAlis Pro: Data collection and data reduction software package, Rigaku Oxford Diffraction, (1995-2023), Rigaku Corporation, Wroclaw, Poland.

[56] Bruker, S*AINT* and *SADABS*, Bruker AXS Inc., Madison, Wisconsin, USA, **2008**.

[57] SCALE3 ABSPACK: Empirical absorption correction using spherical harmonics.

[58] G. M. Sheldrick, *Acta Crystallogr. Sect. A Found. Adv.* **2015**, *71*, 3–8.

[59] G. M. Sheldrick, *Acta Crystallogr. Sect. C Struct. Chem.* **2015**, *71*, 3–8.

[60] A. L. Spek, *Acta Crystallogr. Sect. C Struct. Chem.* **2015**, *71*, 9–18.

[61] K. Brandenburg, H. Putz, DIAMOND (v. 4.6.5), Crystal Impact GbR, Bonn, Germany **2006**.

[62] M. J. Frisch, G. W. Trucks, H. B. Schlegel, G. E. Scuseria, M. A. Robb, J. R. Cheeseman, G. Scalmani, V. Barone, G. A. Petersson, H. Nakatsuji, X. Li, M. Caricato, A. V. Marenich, J. Bloino, B. G. Janesko, R. Gomperts, B. Mennucci, H. P. Hratchian, J. V. Ortiz, A. F. Izmaylov, J. L. Sonnenberg, D. Williams-Young, F. Ding, F. Lipparini, F. Egidi, J. Goings, B. Peng, A. Petrone, T. Henderson, D. Ranasinghe, V. G. Zakrzewski, J. Gao, N. Rega, G. Zheng, W. Liang, M. Hada, M. Ehara, K. Toyota, R. Fukuda, J. Hasegawa, M. Ishida, T. Nakajima, Y. Honda, O. Kitao, H. Nakai, T. Vreven, K. Throssell, J. A. Montgomery, Jr., J. E. Peralta, F. Ogliaro, M. J. Bearpark, J. J. Heyd, E. N. Brothers, K. N. Kudin, V. N. Staroverov, T. A. Keith, R. Kobayashi, J. Normand, K. Raghavachari, A. P. Rendell, J. C. Burant, S. S. Iyengar, J. Tomasi, M. Cossi, J. M. Millam, M. Klene, C. Adamo, R. Cammi, J. W. Ochterski, R. L. Martin, K. Morokuma, O. Farkas, J. B. Foresman, and D. J. Fox, Gaussian 16, Revision C.01, Gaussian, Inc., Wallingford CT, **2016**.

[63] C. Lee, W. Yang, R. G. Parr, *Phys. Rev. B. Condens. Matter* **1988**, *37*, 785–789.

[64] B. Miehlich, A. Savin, H. Stoll, H. Preuss, *Chem. Phys. Lett.* **1989**, *157*, 200–206.

[65] A. D. Becke, *J. Chem. Phys.* **1993**, *98*, 5648–5652.

[66] S. Grimme, J. Antony, S. Ehrlich, H. Krieg, *J. Chem. Phys.* **2010**, *132*, 154104.

[67] W. J. Hehre, R. Ditchfield, J. A. Pople, *J. Chem. Phys.* **1972**, *56*, 2257–2261.

[68] M. M. Francl, W. J. Pietro, W. J. Hehre, J. S. Binkley, M. S. Gordon, D. J. DeFrees, J. A. Pople, *J. Chem. Phys.* **1982**, *77*, 3654–3665.

[69] A. V. Marenich, C. J. Cramer, D. G. Truhlar, *J. Phys. Chem. B* **2009**, *113*, 6378–6396.

[70] F. Weigend, R. Ahlrichs, *Phys. Chem. Chem. Phys.* **2005**, *7*, 3297–3305.

[71] F. Weigend, *Phys. Chem. Chem. Phys.* **2006**, *8*, 1057–1065.

[72] V. S. Bryantsev, M. S. Diallo, W. A. Goddard III, *J. Phys. Chem. B* **2008**, *112*, 9709–9719.

# Chapter 4: To be complexed or not – Carboranylphosphines as ligands for the complexation of transition metals used for homogeneous catalysis

# 4 To be complexed or not – Carboranylphosphines as ligands for the complexation of transition metals used for homogeneous catalysis

A plethora of transition metal complexes was synthesized in the past, utilizing *ortho*-carborane derivatives with various homo- or heterodonor atoms. This work, however, is limited to complexes formed from carboranylphosphines which were already studied for their potential use as catalysts for different reactions as described in Chapter 1. In particular, complexes of boron-substituted carboranylphosphines were investigated for which significantly fewer examples are known. Prior to the experimental investigations, DFT studies were carried out to find promising metal complex precursors with regard to their stability and geometry in complexes with boron-substituted carboranylphosphines. A few compounds were selected for preliminary catalytic tests.

## 4.1 DFT studies towards the complexation behavior of B9-functionalized carboranylphosphines

Computational approaches aided the experimental work that is discussed in detail in sections **4.2** to **4.4**. Structure optimizations were performed on already synthesized compounds like carboranes and carboranylphosphines, as well as on not yet synthesized carboranylphosphines and their transition metal complexes with palladium, copper, gold and rhodium (see **Scheme 4.1.1** and **Scheme 4.1.2**).

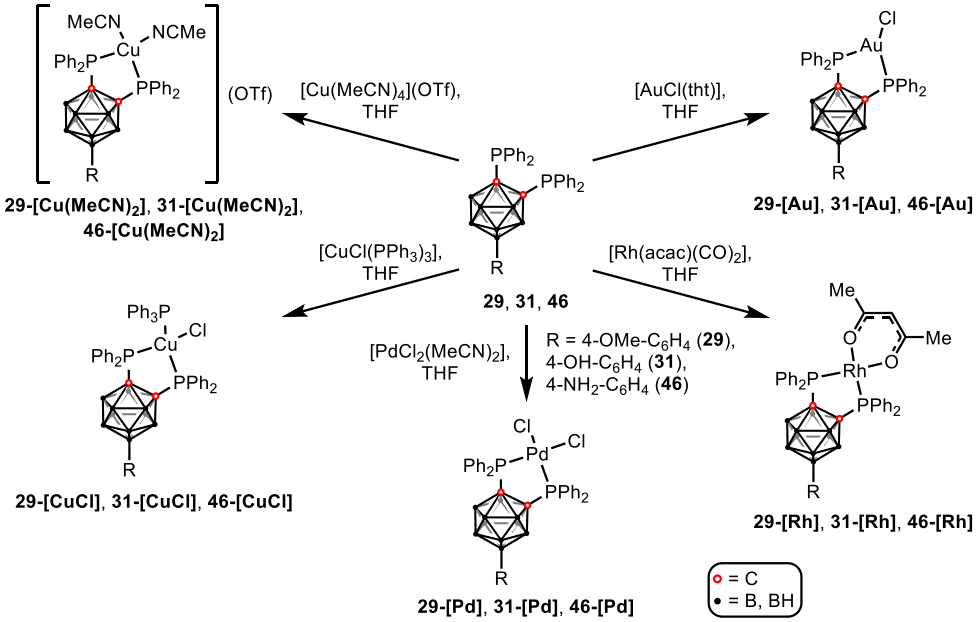


**Scheme 4.1.1.** Computed complexes formed from 9-R-1,2-bis(diphenylphosphino)- *ortho*-carborane derivatives **29**, **31** and **46** and different metal complex precursors. OTf = trifluoromethanesulfonate, acac = acetylacetonate, tht = tetrahydrothiophene.

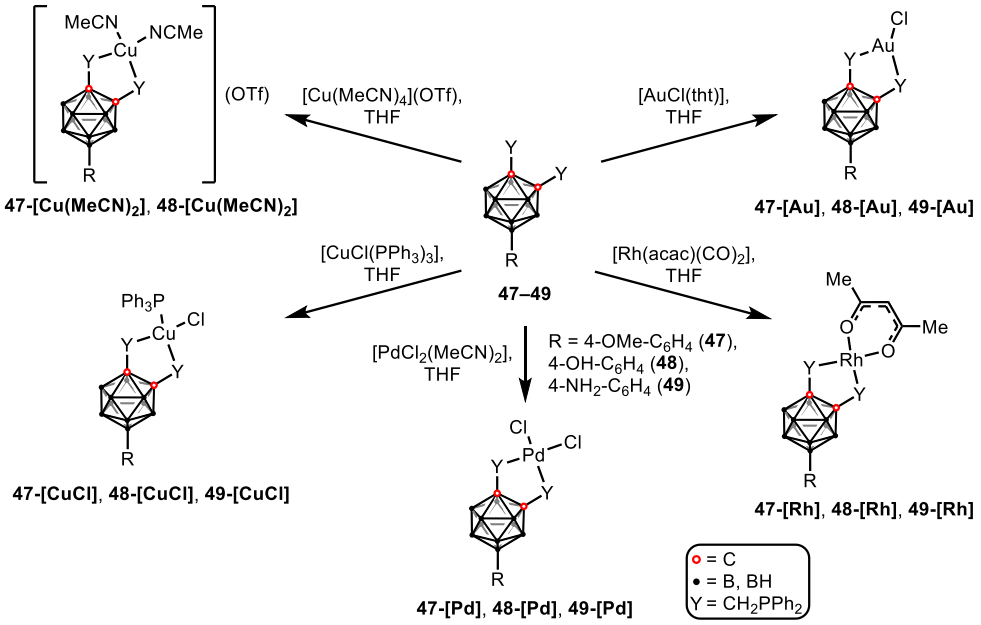


**Scheme 4.1.2.** Computed complexes formed from 9-R-1,2-bis-[(diphenylphosphino)methyl]-*ortho*-carborane derivatives **47**–**49** and different metal complex precursors.

The calculation of the GIBBS energy values of the transition metal complexes formed with different carboranylphosphine derivatives indicated that the addition of a flexible spacer ($CH_2$ group) between the carborane cluster and the phosphanyl group (**47**–**49**) leads to the formation of thermodynamically more favorable complexes (with a difference of at least 5 kcal $mol^{-1}$ to the complexes formed from **29**, **31** and **46**). Except for certain copper complexes, namely the complexes **29-[Cu(MeCN)$_2$]**, **31-[Cu(MeCN)$_2$]**, and **46-[Cu(MeCN)$_2$]** as well as **31-[CuCl]**, **46-[CuCl]**, and **47-[CuCl]**, all of the computed GIBBS energies exhibit negative values, indicating that the formation of the appropriate complexes relative to their starting materials is favored (see **Tab. 4.1.1**). In the following, only the optimized structure of the cationic complex $[Cu(MeCN)_2(L)]^+$ (L = **29**, **31**, **46**–**48**) will be displayed; since the triflate counter-anion was optimized independently, it will not be displayed. Comparing the complexes' GIBBS energy values estimated with and without the anion revealed comparable results ($[Cu(MeCN)_2(\mathbf{29})]^+ + (OTf)^-$ with +6.0 kcal $mol^{-1}$ vs. $[Cu(MeCN)_2(\mathbf{29})](OTf)$ with +6.6 kcal $mol^{-1}$ relative to the starting material). However, the anion has to be taken into account when calculating the GIBBS energies (as shown in Chapter **4.5.1**).

**Tab. 4.1.1.** Computed GIBBS energy values [kcal mol$^{-1}$] of complexes formed from ligands **29, 31, 46–49** and different metal precursors in THF or $CH_2Cl_2$ as solvent, respectively, relative to the starting materials.

| | Carboranylphosphine | 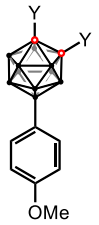 | 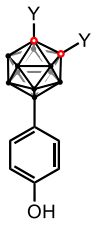 | 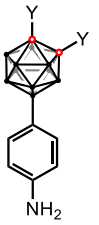 |
|---|---|---|---|---|
| | Metal complex precursor (solvent for calculation) | | | |
| **Y = PPh$_2$ (29, 31, 46)** | [AuCl(tht)] ($CH_2Cl_2$) | –13.2 | –14.3 | –14.1 |
| | [$PdCl_2(MeCN)_2$] (THF) | –42.0 | –42.1 | –20.9 |
| | [$Cu(MeCN)_4$](OTf) (THF) | +6.0 | +4.5 | +4.9 |
| | [$CuCl(PPh_3)_3$] (THF) | –0.2 | +0.4 | +0.1 |
| | [Rh(acac)$(CO)_2$] (THF) | –63.0 | –62.9 | –62.7 |
| **Y = CH$_2$PPh$_2$ (47–49)** | [AuCl(tht)] ($CH_2Cl_2$) | –24.7 | –23.5 | –25.2 |
| | [$PdCl_2(MeCN)_2$] (THF) | –42.4 | –41.9 | –42.5 |
| | [$Cu(MeCN)_4$](OTf) (THF) | +0.5 | –0.9 | not computed |
| | [$CuCl(PPh_3)_3$] (THF) | –10.3 | –9.4 | –9.2 |
| | [Rh(acac)$(CO)_2$] (THF) | –134.2 | –133.3 | –133.5 |

### 4.1.1 Computed complexes formed with 1,2-bis(diphenylphosphino)-*ortho*-carborane

To determine if the computed complexes correspond to previous developments, data for a variety of non-boron-substituted carboranylphosphine transition metal complexes will be compared to the optimized structures computed using ligands **29**, **31**, and **46**. All the complexes under consideration have one thing in common: the B9 substituent scarcely changes bond lengths and angles. A survey of the CSD (Cambridge Structural Database, version 5.43, November 2021) was performed with ConQuest® (version 2022.2.0) and bond lengths and angles of selected carboranylphosphine complexes were obtained.[1,2]

In **Fig. 4.1.1**, the structures of the computationally optimized Pd$^{II}$ complexes are shown. The carboranylphosphine derivatives **29**, **31**, and **46** serve as a bidentate ligand by interacting with the Pd$^{II}$ atom through the two phosphorus atoms. The remaining substituents occupy square-planar positions. When compared to values for a typical square-planar coordination geometry, the computed angles and bond lengths around Pd$^{II}$ are not significantly different. These hypothetical structures are in agreement with previously reported complexes of $(PPh_2)_2$-1,2-*ortho*-carborane derivatives, which have on average a P–Pd bond length of 2.25 Å, a C–C bond length of 1.69 Å, a

C–P–Pd bond angle of 108.2° and a P1–Pd–P2 bite angle of 91.0°. The dihedral angles between the planes formed by the atoms P1, P2, Pd and C1, C2, P1, P2 for **29-[Pd]** (23.7°), **31-[Pd]** (28.3°) and **46-[Pd]** (28.4°) are also in agreement.[3–5] The Pd–P bond lengths remain constant when the *trans*-ligands are similar matching the values seen for the corresponding distances in already reported complexes (2.21–2.33 Å).[3–5] The C1–C2 bond length decreases from 1.72 Å in the free ligand (mean value from carboranylphosphine derivatives **25**, **28**–**31**) to 1.67 Å owing to the metal coordination. On the contrary, the mean C–P bond length of 1.90 Å is moderately longer than in the free ligands (1.88 Å, refer to Chapter 3).

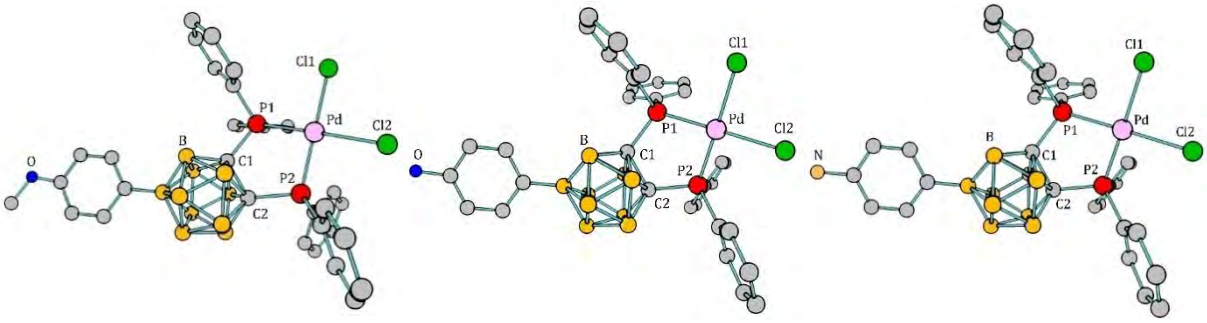


**29-[Pd]** **31-[Pd]** **46-[Pd]**

**Fig. 4.1.1.** Optimized structures of the computed complexes **29-[Pd]**, **31-[Pd]**, and **46-[Pd]**. Hydrogen atoms are omitted for clarity. Selected bond lengths [Å] and angles [°] of **29-[Pd]**: P···P 3.24, P–Pd 2.29, Cl–Pd 2.39, C1–C2 1.68, mean C–P–Pd 107.5, mean *trans*-P–Pd–Cl 176.0, mean *cis*-P–Pd–Cl 88.6, Cl–Pd–Cl 92.5, P–Pd–P 90.2; **31-[Pd]**: P···P 3.21, P–Pd 2.29, Cl–Pd 2.39, C1–C2 1.67, mean C–P–Pd 106.9, mean *trans*-P–Pd–Cl 175.9, mean *cis*-P–Pd–Cl 89.3, Cl–Pd–Cl 91.1, P–Pd–P 89.1; **49-[Pd]**: P···P 3.21, P–Pd 2.29, Cl–Pd 2.39, C1–C2 1.67, mean C–P–Pd 107.0, mean *trans*-P–Pd–Cl 175.6, mean *cis*-P–Pd–Cl 89.4, Cl–Pd–Cl 92.1, P–Pd–P 88.9.

TEIXIDOR and co-workers[6,7] prepared several $Cu^{I}$ carboranylphosphine complexes in an experimental setting using $[CuCl(PPh_3)_3]$ and either dppc, depc, doepc, or dipc as ligand. The stabilities of the complexes with ligands **29**, **31** and **46** were examined computationally in the context of this project, and the optimized structures (see **Fig. 4.1.2**) were compared with the reported complexes. In addition, $[Cu(MeCN)_4](OTf)$, another $Cu^{I}$ precursor, was studied for both practical (laboratory availability) and informational purposes (influence of solvation and counterions) to learn more about the impact of the leaving group.

Forming a complex with $[CuCl(PPh_3)_3]$, the bidentate carboranylphosphine, a $PPh_3$ group and a chlorido ligand are coordinated to the $Cu^{I}$ atom. The coordination sphere of $Cu^{I}$ is distorted tetrahedral with bond angles deviating considerably from the ideal tetrahedral angle of 109.5°. The limited bite angle of 95.4° of the bidentate ligands **29**, **31** and **46** and the other bond angles including the $Cu^{I}$ atom varying from 107.7° to 130.2° (exemplary in **29-[CuCl]**) are two factors that contribute to the distortion. The torsion angle P1–C1–C2–P2 (2.7°) is bigger than the mean torsion angle reported (2.0°). It is still demonstrating planarity for the four atoms as it can be seen

typically for P–$C_{Cage}$–$C_{Cage}$–P groups in bidentate 1,2-bisphosphino-*ortho*-carboranyl $Cu^{I}$ complexes.[6,8–10] The Cu cation lies above the P1–C1–C2–P2 plane by 8.3°, and therefore the chelate ring adopts an envelope shape. The P–Cu bond distances around $Cu^{I}$ are in good agreement with the average P–Cu bond length reported (2.25(2) Å and 2.26(2) Å) in different $Cu^{I}$ carboranylphosphine derivatives.[6,8–10] It is interesting that the computation predicts only a small difference between the GIBBS energies of the products and the starting material, indicating that there is no thermodynamical preference towards the formation of the desired products **29-[CuCl]**, **31-[CuCl]** and **46-[CuCl]**. It is quite the opposite for complexes formed with $[Cu(MeCN)_4](OTf)$ whose GIBBS energies are positive relative to the starting materials ($\Delta G > 4.5$ kcal $mol^{-1}$). The coordination sphere of $Cu^{I}$ is also distorted tetrahedral with bond angles deviating considerably from the ideal tetrahedral angle of 109.5°.

The C1–C2 bond length (1.73 Å in **29/31/46-[Cu(MeCN)$_2$]**, 1.78 Å in **29/31/46-[CuCl]**) and the mean C–P bond length (1.90 Å in **29/31/46-[Cu(MeCN)$_2$]**, 1.92 Å in **29/31/46-[CuCl]**) are both significantly longer than in the free ligands (1.72 Å for C1–C2 and 1.88 Å for C–P, refer to Chapter 3).

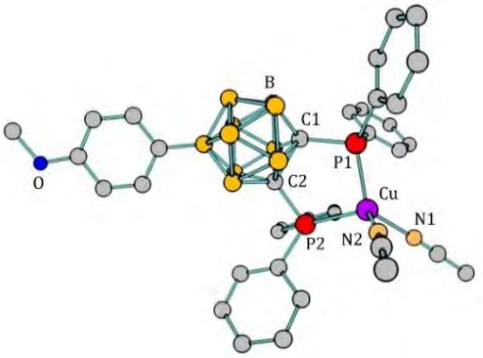


**29-[Cu(MeCN)$_2$]**

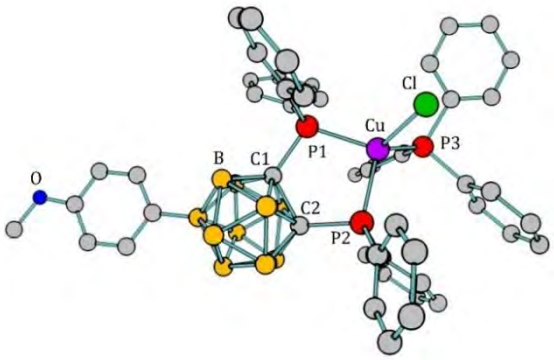


**29-[CuCl]**

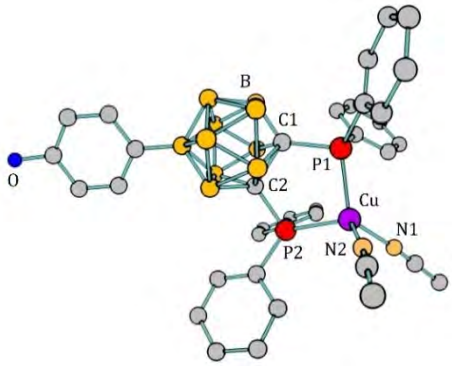


**31-[Cu(MeCN)$_2$]**

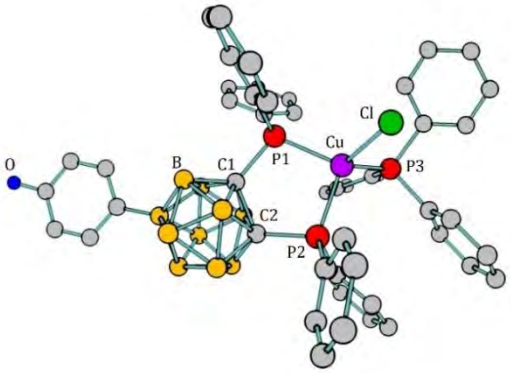


**31-[CuCl]**

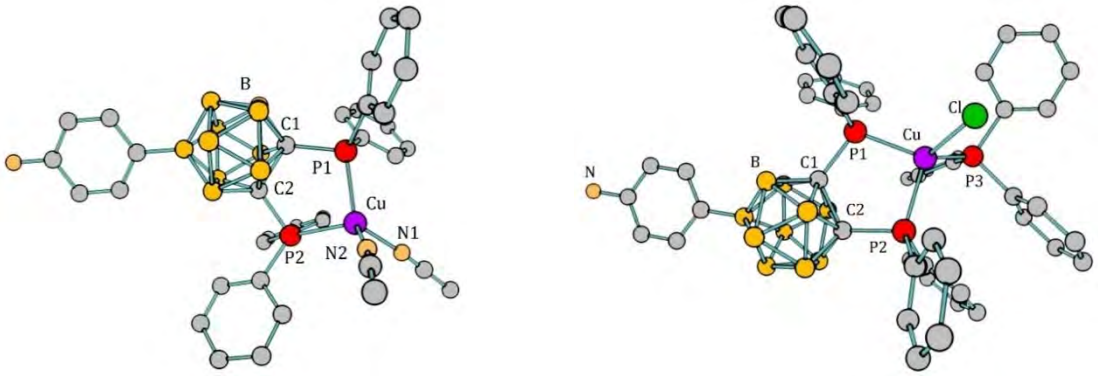


**46-[Cu(MeCN)$_2$]** **46-[CuCl]**

**Fig. 4.1.2.** Optimized structures of the computed complexes **29-[Cu(MeCN)$_2$]**, **31-[Cu(MeCN)$_2$]**, **46-[Cu(MeCN)$_2$]**, **29-[CuCl]**, **31-[CuCl]**, and **46-[CuCl]**. All hydrogen atoms are omitted for clarity. Selected bond lengths [Å] and angles [°] of **29-[Cu(MeCN)$_2$]**: P···P 3.34, P–Cu 2.31, N–Cu 2.05, C–C 1.73, P–C 1.90, mean C–P–Cu 102.4, P1–Cu–N1 120.8, P1–Cu–N2 116.8, P2–Cu–N1 116.4, P2–Cu–N2 111.0, N1–Cu–N2 100.2, P–Cu–P 92.4; **31-[Cu(MeCN)$_2$]**: P···P 3.35, P–Cu 2.31, N–Cu 2.05, C–C 1.73, P–C 1.90, mean C–P–Cu 102.6, P1–Cu–N1 121.2, P1–Cu–N2 114.7, P2–Cu–N1 113.3, P2–Cu–N2 113.2, N1–Cu–N2 101.9, P–Cu–P 93.1; **46-[Cu(MeCN)$_2$]**: P···P 3.35, P–Cu 2.31, N–Cu 2.05, C–C 1.73, P–C 1.90, mean C–P–Cu 102.7, P1–Cu–N1 121.1, P1–Cu–N2 114.6, P2–Cu–N1 113.4, P2–Cu–N2 113.2, N1–Cu–N2 101.9, P–Cu–P 93.1; **29-[CuCl]:** P···P 3.45, P–Cu 2.32, Cl–Cu 2.39, C1–C2 1.78, mean C–P1,2–Cu 106.1, P1–Cu–P2 95.4, P1–Cu–P3 130.2, P2–Cu–P3 109.8, P1–Cu–Cl 107.7, P2–Cu–Cl 115.8, P3–Cu–Cl 98.9; **31-[CuCl]:** P···P 3.44, P–Cu 2.32, Cl–Cu 2.39, C1–C2 1.78, mean C–P1,2–Cu 106.1, P1–Cu–P2 95.4, P1–Cu–P3 130.4, P2–Cu–P3 110.1, P1–Cu–Cl 107.8, P2–Cu–Cl 115.7, P3–Cu–Cl 98.5; **46-[CuCl]:** P···P 3.44, P–Cu 2.32, Cl–Cu 2.39, C1–C2 1.78, mean C–P1,2–Cu 106.0, P1–Cu–P2 95.5, P1–Cu–P3 130.2, P2–Cu–P3 109.8, P1–Cu–Cl 107.7, P2–Cu–Cl 115.8, P3–Cu–Cl 98.9.

The stability of another set of compounds formed from **29**, **31** and **46** with [AuCl(tht)] has been evaluated computationally. The optimized structures are given in **Fig. 4.1.3**. The Au$^{I}$ atom is coordinated in a trigonal planar geometry by the bidentate ligand and the chlorine atom and deviated from the P,P,Cl plane only by 0.018 Å. The restricted bite angle of 85.3° deviates significantly from the ideal geometry and from previously described gold complexes (90.9°).[11–19] It rather resembles a complex formed from a *nido*-carboranyl ligand and gold, namely [Au{(PPh$_2$)$_2$C$_2$B$_9$H$_{10}$}(PPh$_3$)] with a bite angle of 84.9°.[20] While the C1–P1–Au bond angle is 96.5°, the P2–Au–Cl bond is almost linear with a bond angle of 170.5° in the computed complex. The P1–Au (2.98 Å) and P2–Au bond lengths (2.28 Å) are likewise considerably different as a result of this (literature mean value: P–Au 2.38 Å). For the Au$^{I}$ complexes, there is a significant difference between the computed complexes and the data obtained for their crystal structures.[11–19] The mean C–P (1.91 Å) and C1–C2 bond lengths (1.75 Å) are both moderately longer than in the free ligands (1.72 Å for C1–C2 and 1.88 Å for C–P, refer to Chapter 3).

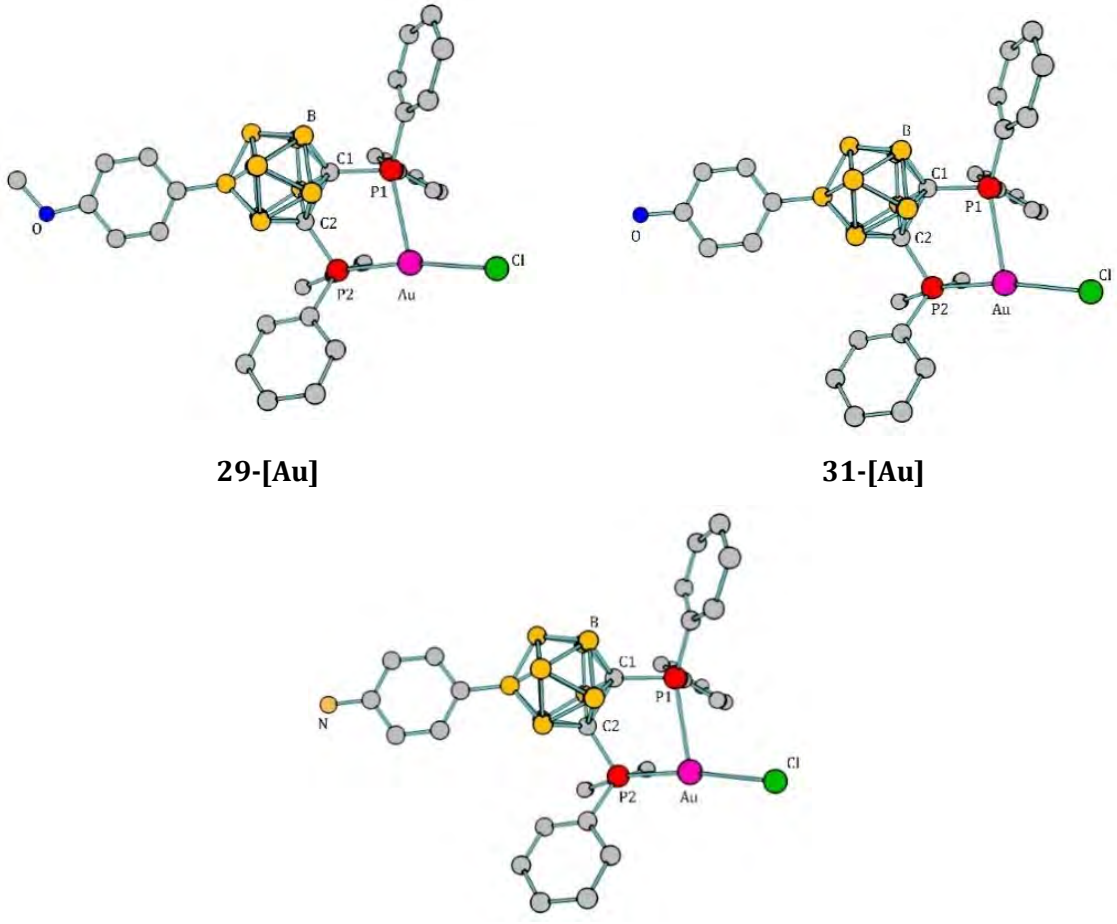


**29-[Au]** **31-[Au]**

**46-[Au]**

**Fig. 4.1.3.** Optimized structures of the computed complexes **29-[Au]**, **31-[Au]**, and **46-[Au]**. Hydrogen atoms are omitted for clarity. Selected bond lengths [Å] and angles [°] of **29-[Au]**: P···P 3.61, P1–Au 2.97, P2–Au 2.29, Cl–Au 2.38, C1–C2 1.75, P1–Au–Cl 104.0, P2–Au–Cl 170.0, C1–P1–Au 96.7, C2–P2–Au 110.0, P1–Au–P2 85.5; **31-[Au]**: P···P 3.61, P1–Au 2.99, P2–Au 2.29, Cl–Au 2.38, C1–C2 1.75, P1–Au–Cl 104.4, P2–Au–Cl 170.5, C1–P1–Au 96.4, C2–P2–Au 110.2, P1–Au–P2 85.1; **46-[Au]**: P···P 3.61, P1–Au 2.99, P2–Au 2.29, Cl–Au 2.38, C1–C2 1.75, P1–Au–Cl 104.4, P2–Au–Cl 170.5, C1–P1–Au 96.5, C2–P2–Au 110.2, P1–Au–P2 85.1.

The computed $Rh^{I}$ complexes shown in **Fig. 4.1.5** exhibited the best observed stability of complexes for which calculations were performed. The $Rh^{I}$ atom exhibits a rigid, nearly planar coordination sphere as a result of the two bidentate ligands. The dihedral angle between the P1–Rh–P2 plane and the O1–Rh–O2 plane is 0.93°. Compared to the metal complex precursor (Rh–O 2.04 Å),[21] the Rh–O bonds are slightly longer (2.08 Å). The calculated complexes compare well with similar $Rh^{I}$ complexes[22,23] as well as with the *nido*-carboranyl compound [Rh(7,8-$(PPh_2)_2$-7,8-$C_2B_9H_{10}$)(cod)],[24] and the cationic [Rh(diphos)($\eta^6$-benzene)]$^+$ complex.[25] The optimized structures show a similar P–Rh bond length (2.23 Å) as reported in the literature (2.14 Å, 2.29 Å,[24] and 2.23 Å[25]). The P–Rh–P bite angle also falls within the range of previously reported related compounds (88.8°).[22,23] Due to coordination, the C1–C2 bond length contracts

to 1.68 Å, although the C–P bond length (1.90 Å) is moderately longer than in the free ligand (1.72 Å for C1–C2 and 1.88 Å for C–P, refer to Chapter 3).

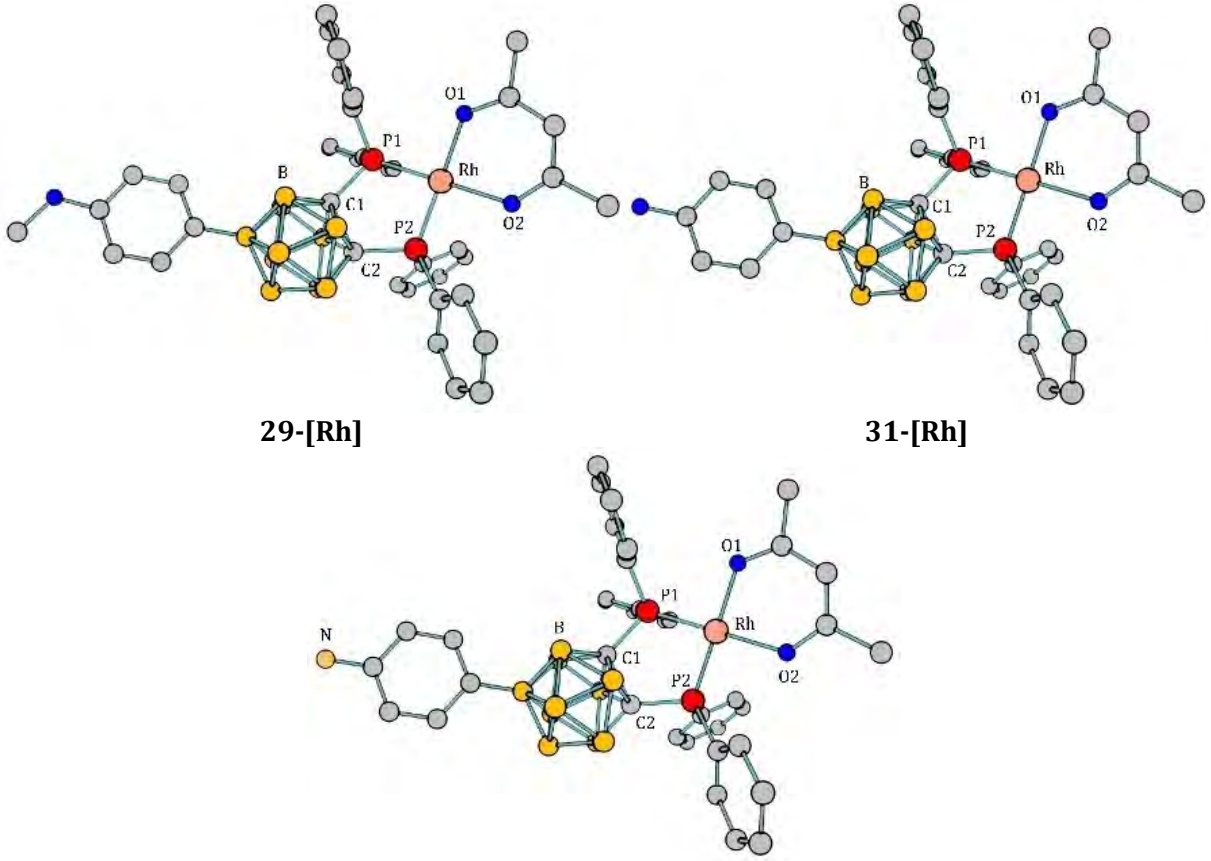


**29-[Rh]** **31-[Rh]**

**46-[Rh]**

**Fig. 4.1.4.** Optimized structures of the computed complexes **29-[Rh], 31-[Rh], and 46-[Rh]**. Hydrogen atoms are omitted for clarity. The B9 substituent does not alter the bond lengths and angles at all. Selected bond lengths [Å] and angles [°] of **29/31/46-[Rh]**: P···P 3.10, P–Rh 2.23, O–Rh 2.08, C–P 1.92, C1–C2 1.68, P1–Rh–O1 91.0, P2–Rh–O2 91.6, P1–Rh–O2 179.7, P2–Rh–O1 178.8, P1–Rh–P2 88.3.

Data obtained for non-boron-substituted compounds are being matched by the calculated optimized structures formed with the ligands **29**, **31** and **46**. The next stage was looking at compounds formed from the same metal precursors and phosphorus ligands **47**–**49**.

### 4.1.2 Computed complexes formed with 1,2-bis-[(diphenylphosphino)methyl]-*ortho*-carborane

So far, there are not many reports on 9-R-1,2-bis-[(diphenylphosphino)methyl]-*ortho*-carborane complexes. Therefore, both their computational investigation and, later, their synthetic preparation were targeted. Only the methoxyphenyl derivatives will be displayed and compared in the following (see **Fig. 4.1.5**) because bond lengths and angles are only slightly altered by the various B9 substituents. As mentioned earlier, the triflate anion will not be displayed since it was calculated separately from the cationic complex $[Cu(MeCN)_2(L)]^+$ (L = **29**, **31**, **46**–**49**).

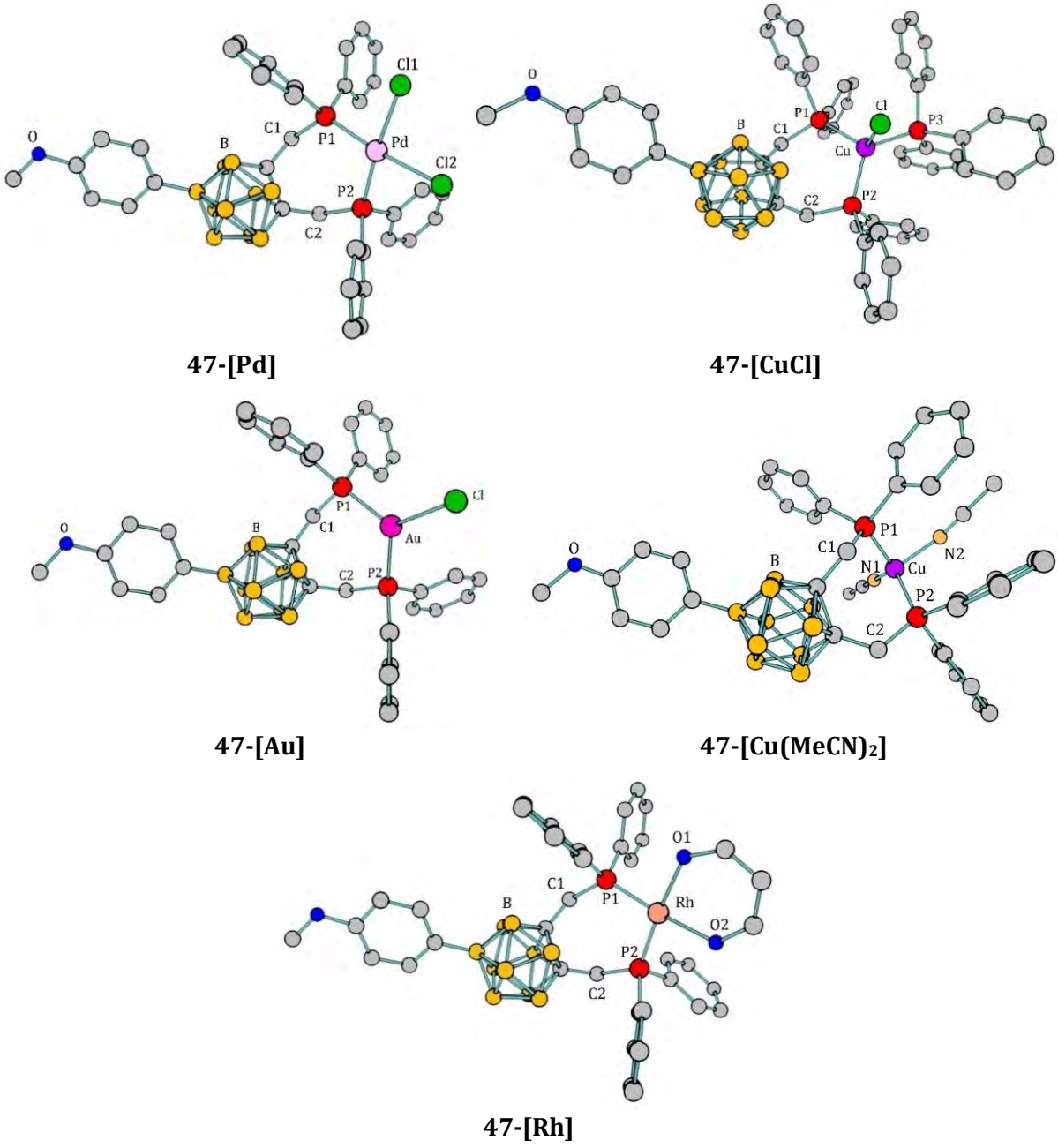


**Fig. 4.1.5.** Optimized structures of the computed complexes **47-[Pd]**, **47-[Au]**, **47-[CuCl]**, **47-[Cu(MeCN)$_2$]**, and **47-[Rh]**. Hydrogen atoms are omitted for clarity. Selected bond lengths [Å] and angles [°] of **47-[Pd]**: P···P 3.56, mean P–Pd 2.31, mean Cl–Pd 2.41, mean C–P 1.87, $C_{Cage}$–$C_{Cage}$ 1.65, mean C–$C_{Cage}$ 1.53, mean C–P–Pd 122.0, mean *trans*-P–Pd–Cl 174.2, mean *cis*-P–Pd–Cl 84.4, P1–Pd–P2 100.8, Cl1–Pd–Cl2 90.4; **47-[Au]**: P1–Au 2.38, P2–Au 2.39, Cl–Au 2.55, mean C–P 1.87, $C_{Cage}$–$C_{Cage}$ 1.69, mean C–$C_{Cage}$ 1.53, mean P–Au–Cl 122.5, C1–P1–Au 108.5, C2–P2–Au 111.7, P1–Au–P2 115.0; **47-[CuCl]**: P···P 3.72, mean P–Cu 2.33, Cl–Cu 2.45, $C_{Cage}$–$C_{Cage}$ 1.68, mean C–P 1.88, mean C1,2–P1,2–Cu 117.1, P1–Cu–P2 105.9, P1–Cu–P3 113.7, P2–Cu–P3 116.6, P1–Cu–Cl 110.9, P2–Cu–Cl 113.1, P3–Cu–Cl 96.7; **47-[Cu(MeCN)$_2$]**: P···P 3.59, mean P–Cu 2.29, N1–Cu 2.02, N2–Cu 2.15, $C_{Cage}$–$C_{Cage}$ 1.70, mean C–P 1.87, mean C–$C_{Cage}$ 1.53, C1–P1–Cu 108.8, C2–P2–Cu 118.4, P1–Cu–N1 121.5, P2–Cu–N 119.2, P1–Cu–N2 100.0, P2–Cu–N2 109.5, N1–Cu–N2 101.1, P1–Cu–P2 103.4; **47-[Rh]**: P···P 3.45, mean P–Rh 2.25, mean O–Rh 2.10, mean C–P 1.88, $C_{Cage}$–$C_{Cage}$ 1.66, mean C–$C_{Cage}$ 1.53, mean C–P–Rh 124.5, mean *trans*-P–Rh–O 174.6, mean *cis*-P–Rh–O 84.7, P1–Rh–P2 100.5, O1–Rh–O2 90.1.

A survey of the CSD (Cambridge Structural Database, version 5.43, November 2021) was performed with ConQuest® (version 2022.2.0) and no carboranylbis(methylenephosphines) or carboranylbis(methylenephosphine)-based complexes were found, i.e., only the bond lengths and angles of selected carboranylmono(methylenephosphines) and their complexes were obtained.[1,2] The $C_{Cage}$–C–P bond angles range from 108.0 to 127.2°. The carboranylmono-(methylenephosphines) analyzed showed a mean $C_{Cage}$–C bond length of 1.52 Å, a mean $C_{Cage}$–$C_{Cage}$ bond length of 1.68 Å and a mean C–P bond length of 1.85 Å.[26–34] Following complexation, ligand **47** exhibits comparable values for the bond angles and bond lengths listed above, which is consistent with previous research.

Since carboranylbis(methylenephosphine)-based complexes have not yet been reported, similar complexes were utilized as a benchmark. The $Pd^{II}$ atom in $[PdCl_2(1,2\text{-}C_6H_4(CH_2PPh_2)_2)]$[35] has a similar deformed square-planar coordination environment. The Pd–P (2.31 Å) and Pd–Cl (2.41 Å) bonds in **47-[Pd]** are slightly longer than in $[PdCl_2(1,2\text{-}C_6H_4(CH_2PPh_2)_2)]$ with Pd–P of 2.257(1) Å and Pd–Cl of 2.354(1) Å, respectively.[35] The P–Pd–P chelate angle of 100.04(6)° is in good accord with **47-[Pd]**.

For the $CH_2Cl_2$ solvate of the complex $[Au\{1,2\text{-}C_6H_4(CH_2PMe_2)_2\}_2]PF_6$,[35] two chelating ligands with Au–P bond lengths in the range of 2.40–2.43 Å form a distorted tetrahedral complex. These bond lengths are consistent with those for **47-[Au]**. In comparison to those found for **47-[Au]**, the bond angles of 103.62(2)° and 103.65(2)° around the $Au^{I}$ atom are significantly smaller.

In contrast to the complexes formed with **47**–**49**, those lacking the additional $CH_2$ linker between the P atoms and the carborane cage (**29**, **31**, **46**) had longer $C_{Cage}$–$C_{Cage}$ bonds. The lengthening may be due to a partial overlap between the tangentially oriented p atomic orbitals of the cluster CH and the appropriate-symmetry atomic orbitals of the exocluster phosphorus atom connected to the cluster carbon atom. A schematic representation of this reasoning is shown in **Fig. 4.1.6** for the substitution of aryl and sulfur atoms.[36] In the first case, an aromatic p orbital and a tangentially oriented p orbital partially overlap. In the second scenario, a d orbital with the right symmetry and energy partially overlaps. These interactions lead to a weakening and lengthening of the C–C bond. However, the C–C distance should not be affected when such overlap is not possible, such as for Si and $sp^3$-C atoms.[36]

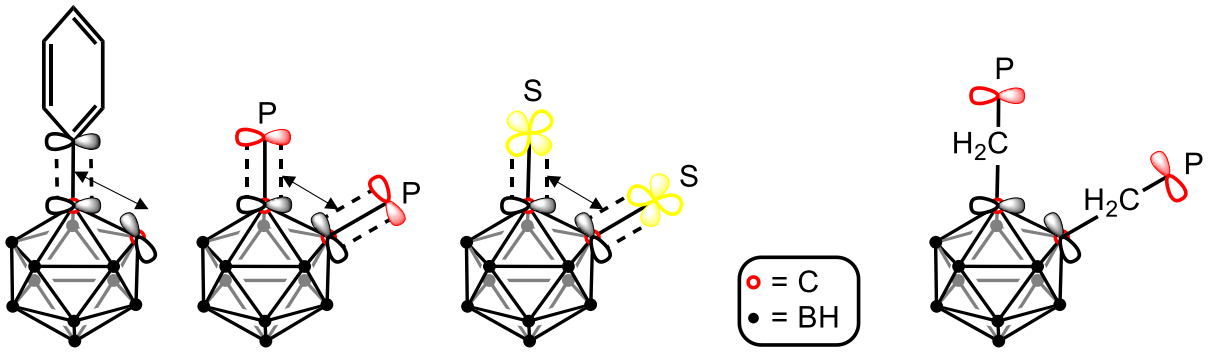


**Fig. 4.1.6.** C–C lengthening by partial overlap of appropriate atomic orbitals in the cluster and substituents.[36]

The C–P–M bond angles are much larger with the $CH_2$ linker present. The bite angles also increase. This could be a result of the flexibility that the $CH_2$ linker contributes to the backbone. The P–Pd–Cl bond angles of the complexes formed with either the carboranylbisphosphine derivatives **29, 31, 46** or carboranylbis(methylenephosphine) derivatives **47–49** are essentially the same. Since the two P–Au–Cl bond angles in **47-[Au]** are more similar, their geometry is more alike with the ideal trigonal-planar geometry. Still within the realm of a perfect tetrahedral structure are the P–Cu–Cl bond angles. In **47-[Cu(MeCN)$_2$]**, there are two sets of P–Cu–N bond angles. While the bond angles including P2 are relatively similar, those including P1 are notably different.

These overall results show that compounds **29, 31, 46–49**, acting as chelating bidentate ligands, are effective for the complexation of several transition metals. The inclusion of the carborane unit into the ligand backbone results in an increase in stiffness compared to the aliphatic ethylene backbone, a higher inclination to chelate, and coordination chemistry more similar to the rigid *ortho*-phenylene counterpart 1,2-$(PPh_2)_2$-$C_6H_4$. Another sign of these ligands' flexibility is the large range of P···P distances (3.10 Å for **29-[Rh]** to 3.72 Å for **47-[CuCl]**).

## 4.2 Addition of a $CH_2$ linker – Synthetic route for new carboranylphosphine

It has been discovered that complexes formed from ligands **47–49** are computationally more stable than complexes formed from ligands **29**, **31** and **46**. An approach similar to that used to synthesize other carboranylphosphines was thus attempted to obtain ligands **47–49** (refer to Chapter 3). First, chloromethyl diphenylphosphine (**50**) was synthesized according to reported methods.[37,38] *n*-Butyllithium was gradually added to a diphenylphosphine (**51**) solution in THF. The dropwise addition of $CH_2Cl_2$ to the *in situ* generated $LiPPh_2$ (**52**) yielded product **50** as could be seen by $^{31}P\{^1H\}$ NMR spectroscopy. The lithium salt **52** was used right away without further purification. To prevent degradation, the product was stored as toluene solution at −30 °C with exclusion of air (see **Scheme 4.2.1**). All solvents were dried and degassed prior to their use.

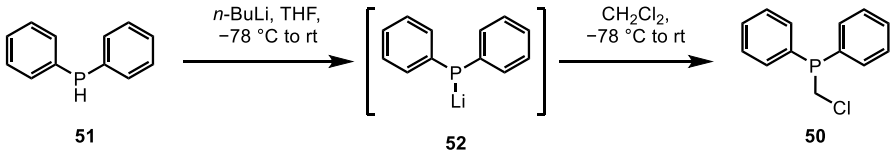


**Scheme 4.2.1.** Synthesis of chloromethyl diphenylphosphine (**50**).

Chloromethyl diphenylphosphine (**50**) was characterized by $^{31}P\{^{1}H\}$ NMR spectroscopy revealing a broad singlet at −9.4 ppm in $C_6D_6$, being in alignment with the literature.[38] In order to generate compound **53**, *n*-butyllithium was added to carborane derivative **16** at −78 °C to synthesize the dilithiocarborane. Phosphine **50** was then added dropwise (see **Scheme 4.2.2**).

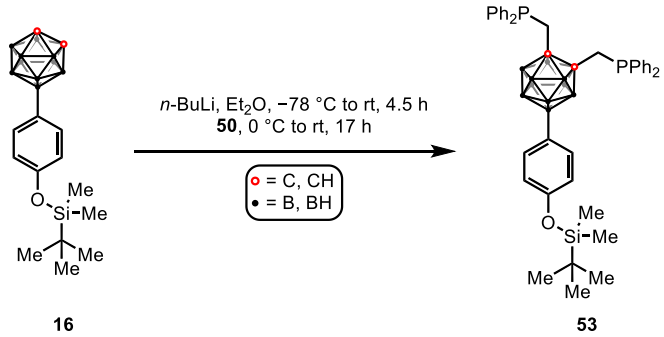


**Scheme 4.2.2.** Attempted synthetic approach to obtain carboranylphosphine derivative **53**.

The $^{31}P\{^{1}H\}$ NMR spectrum of the crude mixture showed a downfield shift of the signal by 0.4 ppm from −9.4 ppm (**50**) to −9.0 ppm (see **Fig. 4.2.1**). Comparing the obtained spectrum to previous $^{31}P$ NMR spectra of $Ph_2PCH_2X$ compounds (X = F,[39] I,[40] 4-H-$C_6H_4$,[41] 4-F-$C_6H_4$,[41] 4-Cl-$C_6H_4$,[41] 4-$CF_3$-$C_6H_4$),[41] it is evident that the chemical shift observed for product **53** is within the range of comparable compounds, with signals ranging from −26.6 ppm (X = I) to −7.3 ppm (X = 4-$CF_3$-$C_6H_4$). A similar chemical shift was further obtained for benzyldiphenylphosphine (X = 4-H-$C_6H_4$). In the case of bulkier X groups (X = 4-*t*Bu-$C_6H_4$, 18.7 ppm or 4-adamantyl-$C_6H_4$, 17.2 ppm)[41] a larger downfield shift is observed. Although the marginal shift of the signals in the $^{1}H$ and $^{11}B\{^{1}H\}$ NMR spectra relative to the starting material further hints on a reaction between **16** and chloromethyl diphenylphosphine (**50**), the analytic data obtained do not allow for a precise description of this suggested product.

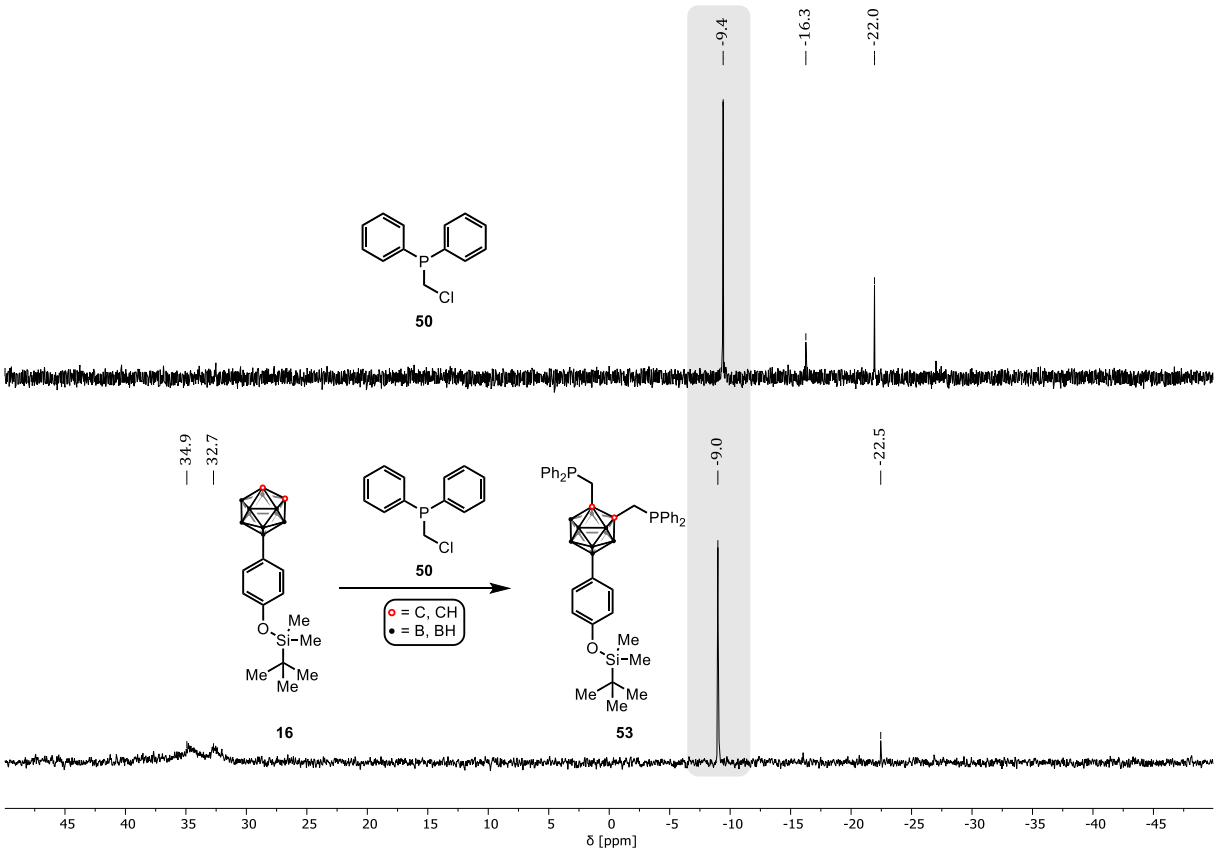


**Fig. 4.2.1.** $^{31}P\{^{1}H\}$ NMR spectra in $CDCl_3$ of **50** and the reaction mixture of **50** and carborane derivative **16**.

Additionally, compound **53** was not detectable with mass spectrometry following several purification attempts. There are a number of potential reasons, including the high sensitivity towards non-inert conditions, impure starting materials, and issues throughout the preparative procedures. For further investigation, the reaction should be repeated on a larger scale, in order to obtain conclusive results.

## 4.3 Complexation of different transition metals utilizing B9-substituted-1,2-bis(diphenylphosphino)-*ortho*-carboranes

The monomeric carboranylphosphine derivatives 9-(TBDMS)O-$C_6H_4$-1,2-$(PPh_2)_2$-$C_2B_{10}H_9$ (**28**) and 9-MeO-$C_6H_4$-1,2-$(PPh_2)_2$-$C_2B_{10}H_9$ (**29**) have been used for the first complexation experiments with a $Pd^{II}$, two $Cu^{I}$, an $Au^{I}$, a $Rh^{I}$, and a $Ru^{0}$ complex precursor. The silyl ether protected carboranylphosphine **28** was the most available of all compounds produced throughout the practical work of the dissertation and therefore used in the industrial context, where $Rh^{I}$ and $Ru^{0}$ or $Ru^{II}$ compounds were tested. (The dissertation project included a research stay of three months at a BASF SE site where some of the compounds synthesized could be tested for their catalytic application.) Furthermore, compound **28** is the precursor to the phenoxy derivative **31** which already had been used for the grafting to different macromolecules as demonstrated by CAMINADE

and co-workers.[42] The methoxyphenyl substituent in **29** mimics the phenoxy linker needed in immobilization reactions. It can be considered as the monomeric equivalent of the carboranyl-substituted dendrimers (as described in Chapter 3).

### 4.3.1 Palladium(II) complex precursor

The first series of B9-substituted carboranylphosphines was described by KALININ and co-workers in 2017.[43] Similar to their synthetic strategies, carboranylphosphine derivative **29** was reacted with $[PdCl_2(MeCN)_2]$ with the objective to yield the $Pd^{II}$ complex **29-[Pd]** (see **Scheme 4.3.1**).

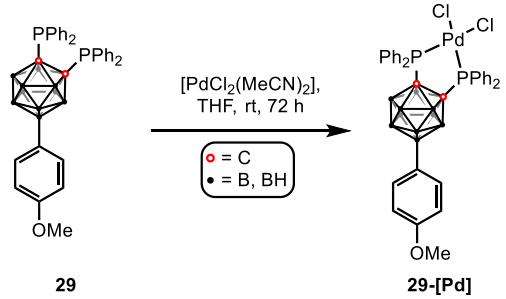


**29** **29-[Pd]**

**Scheme 4.3.1**. Synthetic approach for the complexation of $Pd^{II}$ by carboranylphosphine **29**.

The reaction progress was monitored by $^{31}P\{^1H\}$ NMR spectroscopy. Upon the addition of the $Pd^{II}$ complex precursor, the signals of the carboranylphosphine **29** (AB spin system, δ=7.1, 5.4 ppm) disappeared and two highly downfield shifted signals at 79.9 and 77.5 ppm could be observed. The downfield shift of the two new signals by 70 ppm is in good agreement with the $Pd^{II}$ complexes reported by KALININ and co-workers,[43] but might also be a sign of the formation of a phosphinito $Pd^{II}$ complex as described by MORALES-SERNA and co-workers.[44] Additionally a gray precipitate was formed during the reaction which could be only dissolved in DMSO-$d_6$. The $^{31}P\{^1H\}$ NMR spectrum showed two singlets at 85.5 and 85.1 ppm while the other signals observed before were absent. Also this downfield shift by 80 ppm aligns well with the $Pd^{II}$ complexes described by KALININ and co-workers.[43] The $^1H$ NMR spectrum obtained showed the expected signals for the desired complex **29-[Pd]** bearing an intact carboranylphosphine moiety. The $^{11}B\{^1H\}$ NMR spectrum obtained from the same solution further indicated the formation of *nido*-carboranyl species (−25.6, −33.9 ppm, see **Fig. 4.3.1**).

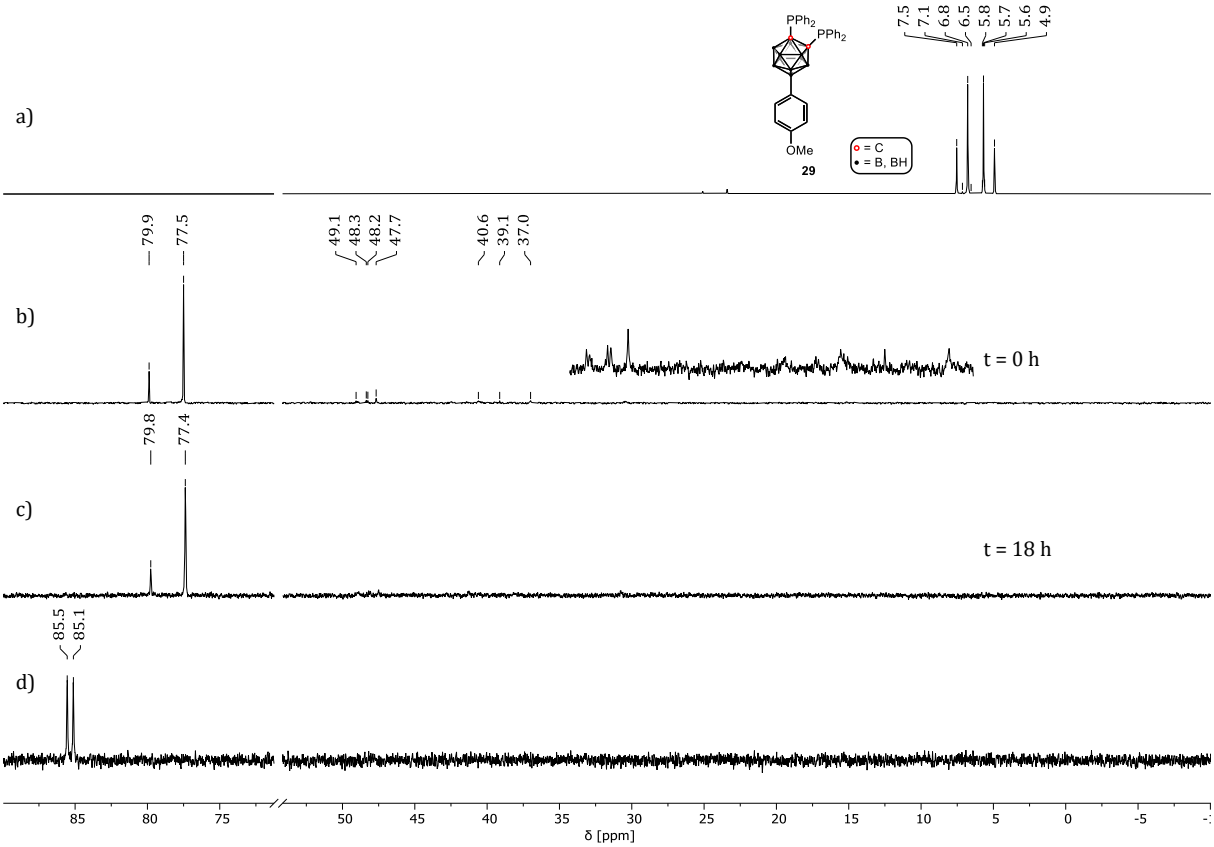


**Fig. 4.3.1.** $^{31}P\{^{1}H\}$ NMR spectra. (a) Carboranylphosphine derivative **29** in $CDCl_3$. (b) After complexation with $[PdCl_2(MeCN)_2]$ in $CD_3CN$. (c) After 18 hours in $CD_3CN$. (d) Gray residue dissolved in a few drops of DMSO-$d_6$ and $CD_3CN$.

To find out more about the species formed after DMSO-$d_6$ was added, the NMR solution was also used for a mass spectrometry analysis indicating the existence of two *nido*-carboranyl species **54** and **55** (deboronation in DMSO-$d_6$ over time, see **Fig. 4.3.2**).

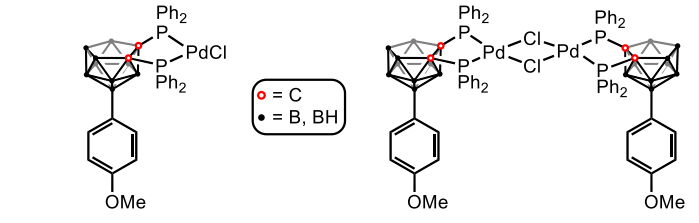


**54**

**HRMS (ESI+)**: $[C_{33}H_{36}B_9ClOP_2Pd]$, m/z calculated 750.1948 ($[M+H]^+$); found: 750.1963.

**55**

**HRMS (ESI+)**: $[C_{66}H_{72}B_{18}Cl_2O_2P_4Pd_2]$, m/z calculated: 1500.3827 ($[M+H]^+$); found: 1500.3777.

**Fig. 4.3.2.** Species detected by HRMS ESI(+) analysis of the gray residue dissolved in few drops of DMSO-$d_6$.

Crystallization from diethyl ether and toluene was attempted in an effort to learn more about the molecular compositions. Unexpectedly, an XRD analysis of the obtained crystals showed a completely different structure (complex **56**). Literature suggests that the hydrolysis of the dichlorophosphane complex **57** results in the formation of **56**.[44] Because toluene and diethyl

ether were not utilized as dry solvents, it is possible that once the required compound **29-[Pd]** was formed, it was hydrolyzed and transformed into **56**. This suggests that the palladium complex **29-[Pd]** may be very reactive and susceptible to hydrolysis, breaking the $C_{Cage}$–P bonds to yield **56** and carborane **20** as by-products. It might also be the reason that a deboronation occurs during the work-up (see **Scheme 4.3.2**.).

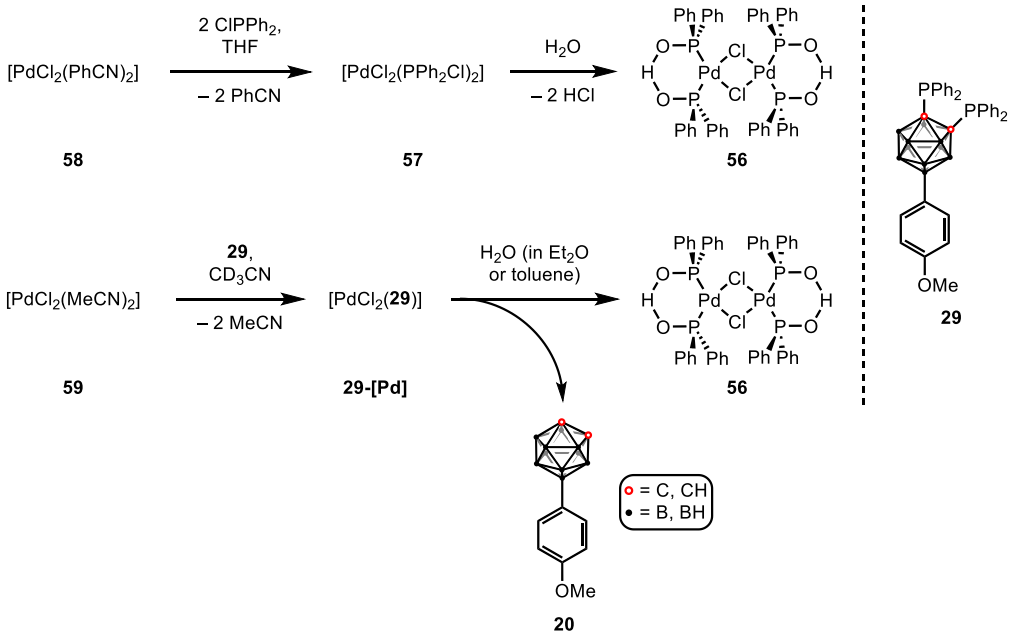


**Scheme 4.3.2.** Chemical structure and synthetic paths to obtain phosphinito complex **56**.[44] Hypothetical pathway for the formation of **56** during the attempted synthesis of **29-[Pd]** upon crystallization from diethyl ether and toluene.

The formation of the desired $Pd^{II}$ complex **29-[Pd]** could be demonstrated but its low stability towards moisture led to the decomposition and formation of different by-products. For future synthetic approaches, an exclusively inert operation is recommended.

### 4.3.2 Copper(I) complex precursor

Different mononuclear $Cu^{I}$ complexes were already successfully prepared by TEIXIDOR and co-workers from $[CuCl(PPh_3)_3]$ and depc, dipc, dppc, or doepc in refluxing EtOH.[6,7] In every instance, no deboronation was seen. For this reason, in an initial effort to form **29-[CuCl]**, $[CuCl(PPh_3)_3]$ was reacted with **29** under slightly varied reaction conditions (see **Scheme 4.3.3**).

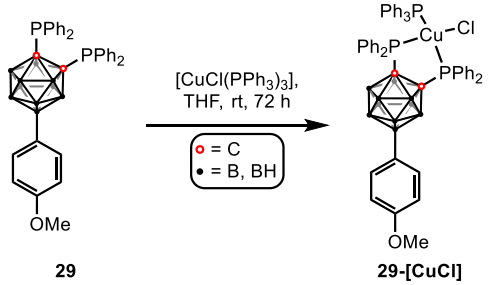


**Scheme 4.3.3.** Synthesis of the $Cu^{I}$ complex **29-[CuCl]**.

The reaction progress was monitored by $^{31}P\{^{1}H\}$ NMR spectroscopy. Upon addition of the $Cu^{I}$ complex, the $^{31}P\{^{1}H\}$ NMR signals of the starting material (AB spin system, δ=7.1, 5.4 ppm) disappeared and a more downfield shifted signal (18.9 ppm) could be observed. After the work-up, further spectroscopic investigation revealed an even more downfield shifted signal at 21.3 ppm. The difference between starting material and the formed compound of $\Delta\delta_P \sim 15$ ppm aligns well with the chemical shift difference reported for $Cu^{I}$ complexes in literature.[45] The broad signal at 11.9 ppm can be aligned with the coordinated $PPh_3$ group. Furthermore, a signal for liberated triphenylphosphine could be observed in the $^{31}P\{^{1}H\}$ NMR spectrum at −5.5 ppm. This proves the ligand exchange of **29** with two $PPh_3$ groups in the $Cu^{I}$ complex (see **Fig. 4.3.3**).

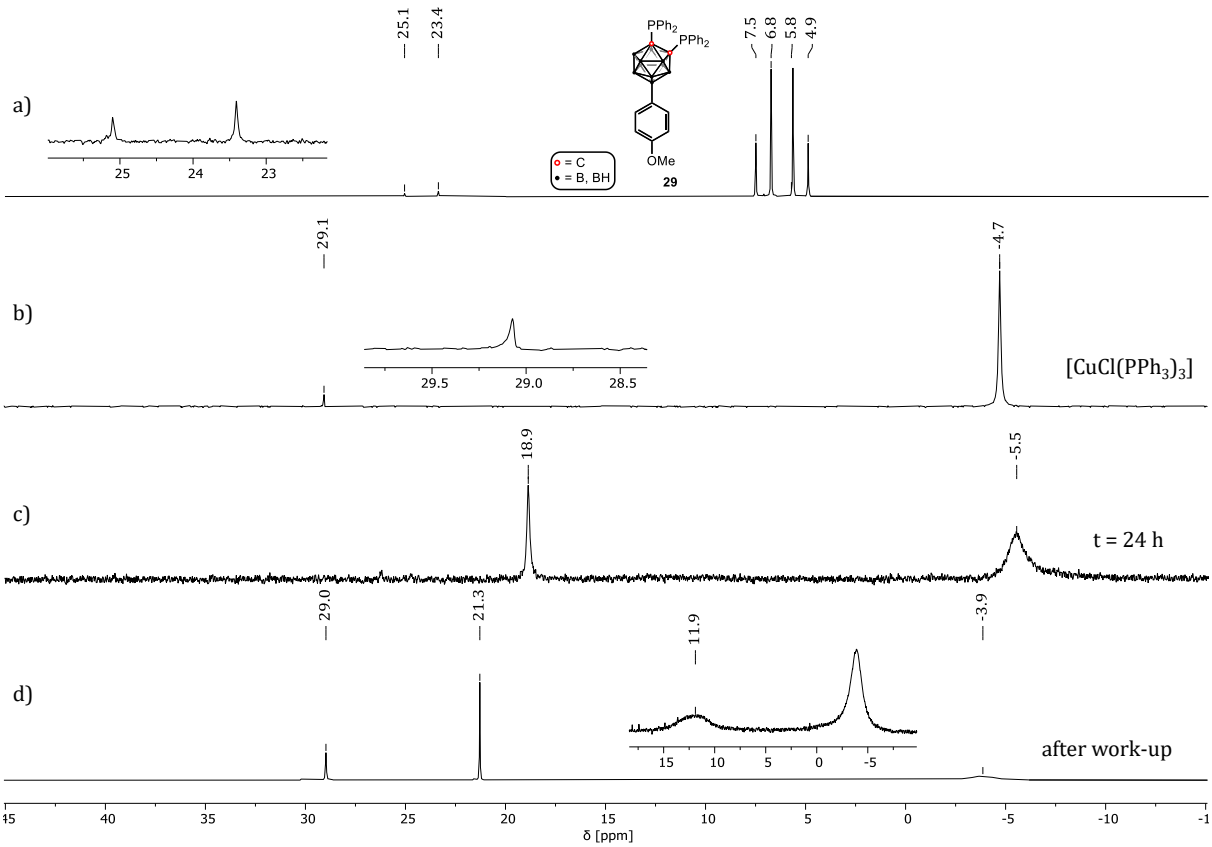


**Fig. 4.3.3.** $^{31}P\{^{1}H\}$ NMR spectra in $CDCl_3$. (a) Carboranylphosphine derivative **29**. (b) $[CuCl(PPh_3)_3]$. (c) After complexation of $[CuCl(PPh_3)_3]$ with **29**. (d) After purification.

Together with the $^{1}H$ and $^{11}B\{^{1}H\}$ NMR spectra obtained (no deboronation observed), the formation of **29-[CuCl]** could be confirmed. The obtained mass spectrum was further proof for the formation of the desired $Cu^{I}$ complex but also indicated that possibly also dimer **60** has been formed (see **Fig. 4.3.4**).

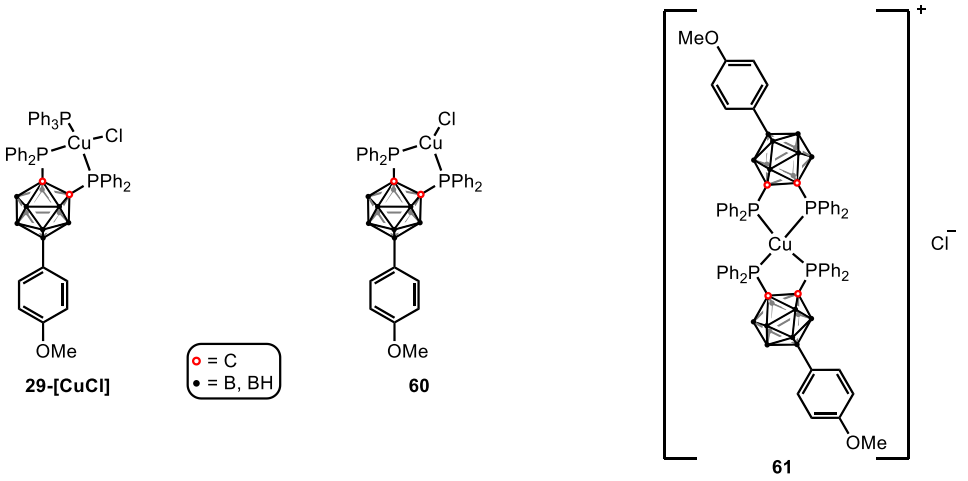


**HRMS (ESI+)**: $[C_{51}H_{51}B_{10}ClCuOP_3]$, m/z calculated: 944.3452 ($[M-Cl^-]^+$); found: 944.3454.

**HRMS (ESI+)**: $[C_{33}H_{36}B_{10}ClCuOP_2]$, m/z calculated: 682.2532 ($[M-Cl]^+$); found: 682.2554.

**HRMS (ESI+)**: $[C_{66}H_{72}B_{20}ClCuO_2P_4]$, m/z calculated: 1300.5797 ($[M-Cl]^+$); found: 1300.5781.

**Fig. 4.3.4.** Species observed by MS after ionization with an ESI source.

Based on the DFT calculation, the formation of complexes from **29** and $[Cu(MeCN)_4](OTf)$ should be thermodynamically less favored thenthe formation of complexes formed from $[CuCl(PPh_3)_3]$. However, for both practical (laboratory availability) and informational purposes (influence of solvation and counterions) to learn more about the impact of the leaving group carboranylphosphine **29** was reacted with $[Cu(MeCN)_4](OTf)$ in a second synthetic attempt and the reaction was monitored by $^{31}P\{^1H\}$ NMR spectroscopy (**Scheme 4.3.4**).

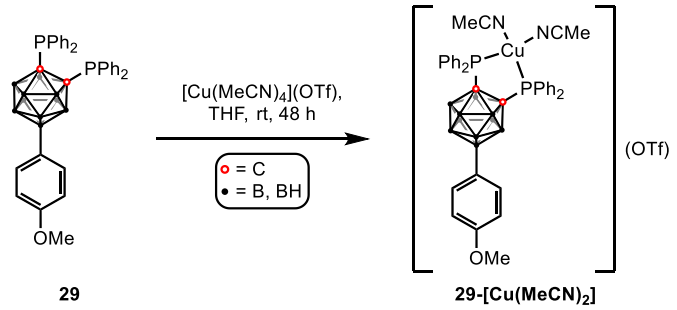


**Scheme 4.3.4.** Attempted synthesis of carboranylphosphine **29-[Cu(MeCN)$_2$]**.

Upon addition of the $Cu^I$ complex precursor, the $^{31}P\{^1H\}$ NMR signal of the starting material **29** (AB spin system, δ=7.1, 5.4 ppm) changed and a broad doublet at 5.8 ppm with a coupling constant of $^3J_{PP}$=89 Hz was observed. The $Cu^I$ complex formed from 1,2-bis(phenylphosphanyl)-*closo*-1,2-dicarba-*closo*-dodecaborane(12) reported by HEY-HAWKINS and co-workers has a comparable coupling constant.[45] The signals in the $^1H$ and $^{11}B\{^1H\}$ NMR spectra undergo a broadening which might be caused by the poor solubility of the compound in $CDCl_3$ and other solvents tested but are in alignment with the expected cationic product (see **Fig. 4.3.5**). Another reason for the broadening could be the formation of a paramagnetic $Cu^{II}$ complex.

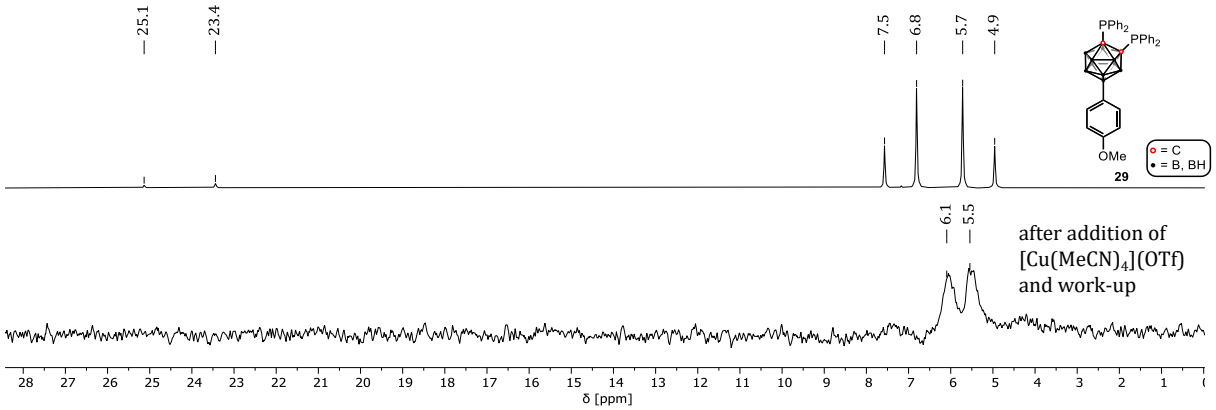


**Fig. 4.3.5:** $^{31}P\{^{1}H\}$ NMR spectra in $CDCl_3$. Top: Carboranylphosphine derivative **29.** Bottom: After the addition of $[Cu(MeCN)_4](OTf)$ and attempted purification.

Analysis by HRMS ESI(+) gave further proof for the formation of the desired complex (see **Fig. 4.3.6**). Any attempts to crystallize this compound failed.

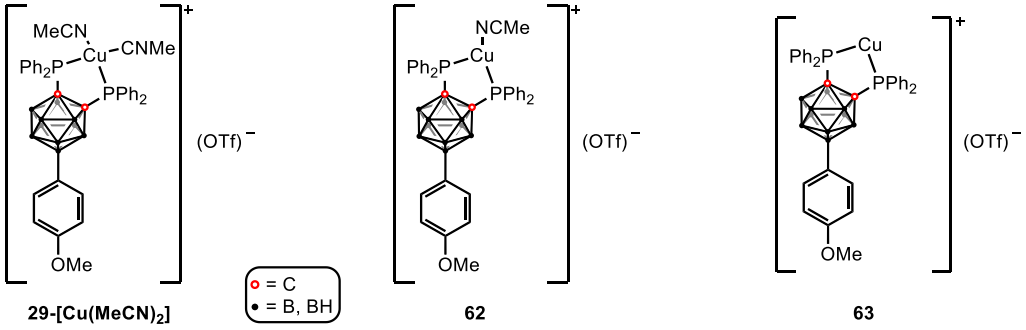


**HRMS (ESI+)**: $[C_{38}H_{42}B_{10}CuF_3N_2O_4P_2S]$, m/z calculated: 764.33065 ($[M-OTf]^+$), found: 764.3140.

**HRMS (ESI+)**: $[C_{36}H_{39}B_{10}CuF_3NO_4P_2S]$, m/z calculated: 723.2798 ($[M-OTf]^+$); found: 723.2862.

**HRMS (ESI+)**: $[C_{34}H_{36}B_{10}CuF_3O_4P_2S]$, m/z calculated: 682.2532 ($[M-OTf]^+$); found: 682.2590.

**Fig. 4.3.6:** Species observed by MS after ionization with an ESI source.

### 4.3.3 Gold(I) complex precursor

A variety of gold(I) complexes formed from dppc has already been described in literature.[11,46] To the best of our knowledge, no B9-substituted carboranylphosphine has been yet used for the complexation. For this reason, the suitability of carboranylphosphine derivative **29** for the complexation of $Au^{I}$ was investigated (see **Scheme 4.3.5**).

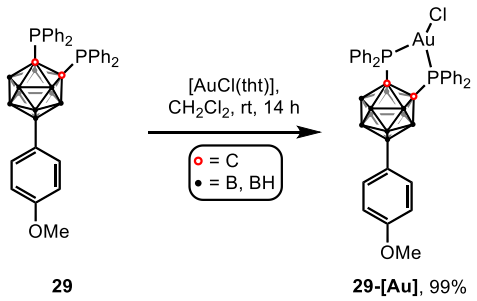


**29** **29-[Au]**, 99%

**Scheme 4.3.5.** Synthesis of gold(I) complex **29-[Au]**.

By using $^{31}P\{^{1}H\}$ NMR spectroscopy, a downfield shift of the signals of the starting material from 7.1 and 5.4 ppm to 49.7 and 49.4 ppm (both AB spin systems) could be tracked. The chemical shift difference of $\Delta\delta_P \sim 40$ ppm is a typical sign for the successful complexation.[11] The acquired $^{11}B\{^{1}H\}$ and $^{1}H$ NMR spectra provided additional evidence of the successful formation of a $Au^{I}$ complex with a 1:1 stoichiometry between $Au^{I}$ and **29**. Long-term storage of the reaction mixture in $CH_2Cl_2$ solution resulted in the appearance of a doublet at 94.0 ppm with a coupling constant of 144 Hz ($^{3}J_{PP}$). The $^{11}B\{^{1}H\}$ NMR spectrum indicated the formation of a *nido*-carboranyl species, i.e., it could be that [Au{(4-MeO-$C_6H_4$)-7,8-($PPh_2$)$_2$-$C_2B_9H_{10}$}(tht)] was formed.

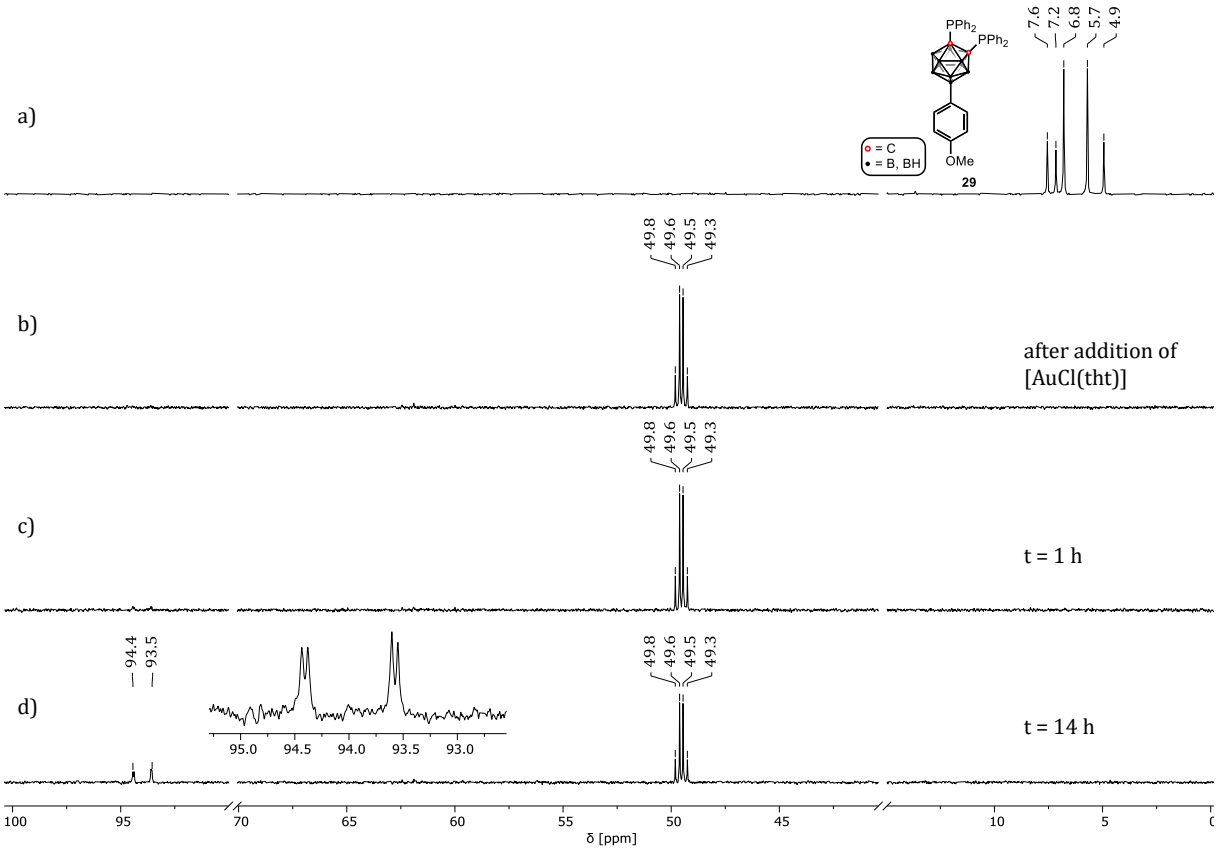


**Fig. 4.3.7.** $^{31}P\{^{1}H\}$ NMR spectra. (a) **29** in $CDCl_3$. (b) Upon complexation of [AuCl(tht)] with **29** in $CD_2Cl_2$. (c) After 1 h in $CD_2Cl_2$. (d) After stirring for 18 h in $CD_2Cl_2$.

Extremely small crystals were formed from $CH_2Cl_2$ and *n*-pentane in an effort to establish the molecular structure of **29-[Au]**. Unfortunately, only the existence of a gold *nido*-carboranyl species could be revealed. Unfortunately, the measured reflections were dispersed and broad. For this reason, only a disorder of the 4-MeO-$C_6H_4$ substituent and the decapping of the carbaborane could be revealed. An oxidation of gold(I) to gold(III) is suggested but the oxidation number of gold or any other definitive information could not be determined because all protons could only be calculated.

### 4.3.4 Rhodium(I) complex precursor

Different $Rh^I$ complexes have already been mentioned as potential candidates for a catalytic application.[47] According to the DFT calculations, among the compounds covered in this study, the $Rh^I$ complex precursor forms the most stable complexes with carboranylphosphine derivative **29** (highest negative GIBBS energies). Due to accessibility reasons, we shifted towards a more available carboranylphosphine **28** instead of the carboranylphosphine **29**. To learn more about the complexation behavior, carboranylphosphine **28** was therefore reacted with $[Rh(acac)(CO)_2]$ to obtain information about the complexation behavior with a $Rh^I$ species (see **Scheme 4.3.6**).

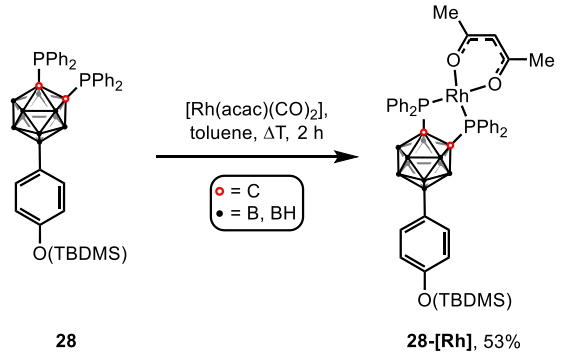


**28** **28-[Rh]**, 53%

**Scheme 4.3.6.** Synthesis of the rhodium(I) complex **28-[Rh]**.

By using $^{31}P\{^1H\}$ NMR spectroscopy, it was possible to observe a downfield shift of the signal of the starting material from 7.3 and 5.9 ppm (AB spin system) to 99.2 and 97.9 ppm (ABX system). The chemical shift difference of ~90 ppm is a typical sign for the successful complexation.[48] The coupling pattern further indicates the complexation of a $Rh^I$ atom. The two doublets observed for the starting material (AB system) evolved into two doublets of doublets (ABX system). This is the result of the chemical differences between the two phosphorus atoms and their coupling to $^{103}Rh$. Together with the $^1H$, $^{11}B\{^1H\}$, and $^{13}C\{^1H\}$ NMR spectra, the formation of compound **28-[Rh]** was confirmed (see **Fig. 4.3.8**).

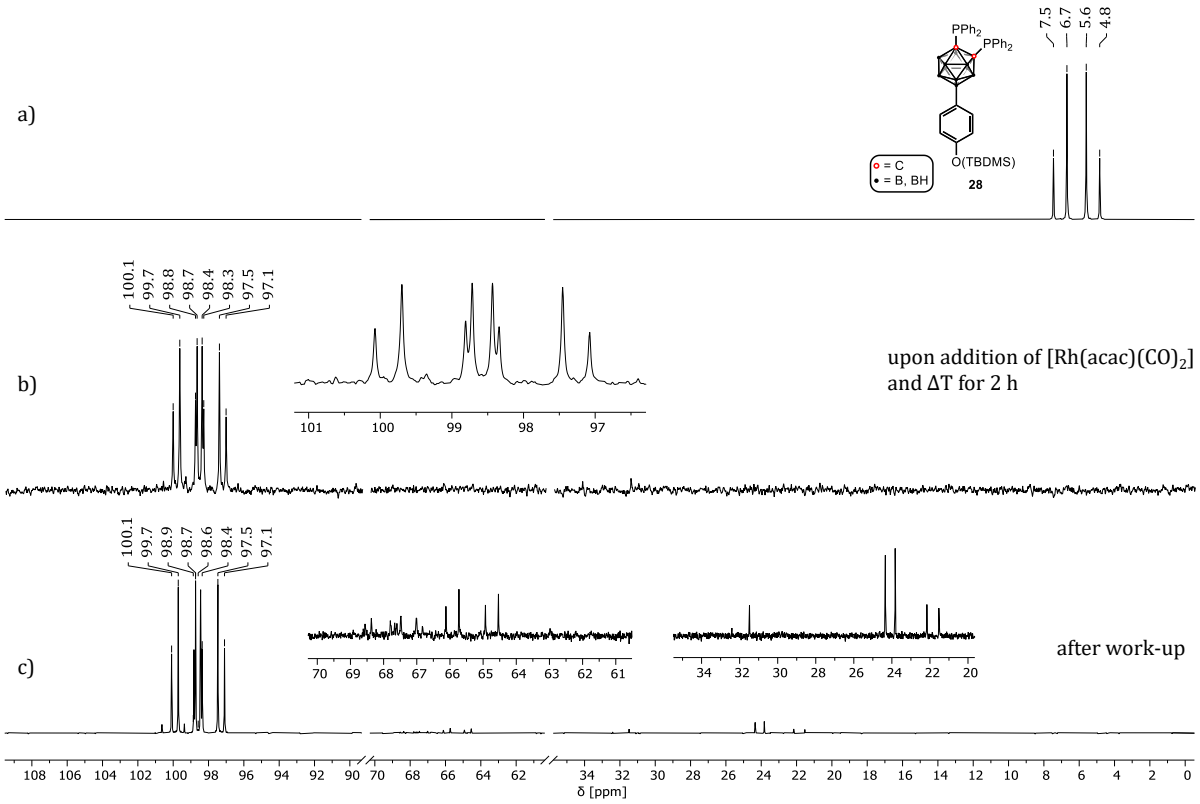


**Fig. 4.3.8.** $^{31}P\{^{1}H\}$ NMR spectra in $CDCl_3$. (a) Carboranyl derivative **28**. (b) Upon complexation of $[Rh(acac)(CO)_2]$ with **28**. (c) After purification.

The HRMS ESI(+) spectrum obtained after work-up further pointed to the existence of $Rh^{I}$ complex **64** in which two molecules of acetonitrile are coordinated to the $Rh^{I}$ atom instead of the acac ligand (see **Fig. 4.3.9**). This further proves the successful complexation of $Rh^{I}$ by carboranylphosphine derivative **28**.

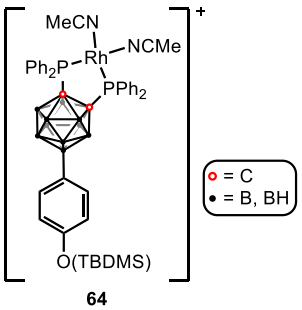


**HRMS (ESI+)**: $[C_{42}H_{54}B_{10}N_2OP_2RhSi]^+$,
m/z calculated: 904.3534 ($[M+H]^+$);
found: 904.3535

**Fig. 4.3.9.** Mass spectrum of the $Rh^{I}$ complex formed after ionization with an ESI source.

Learning more about the molecular structure of the complex formed would be extremely beneficial. Unfortunately, various attempts to grow crystals have failed thus far and pose a future challenge.

### 4.3.5 Ruthenium(0) complex precursor

Different ruthenium complexes, both neutral and cationic, were already prepared with dppc, depc, or doepc in refluxing EtOH.[49,50] Only dimeric structures have been observed thus far to have an intact *ortho*-carboranyl cage.[51] Especially, the cationic complexes were successfully used to catalyze cyclopropanation and KHARASCH addition reactions. Due to this, the complexation of $[Ru_3(CO)_{12}]$ was attempted in a similar way to the synthesis of the $Rh^I$ complex **28-[Rh]** (see **Scheme 4.3.7**).

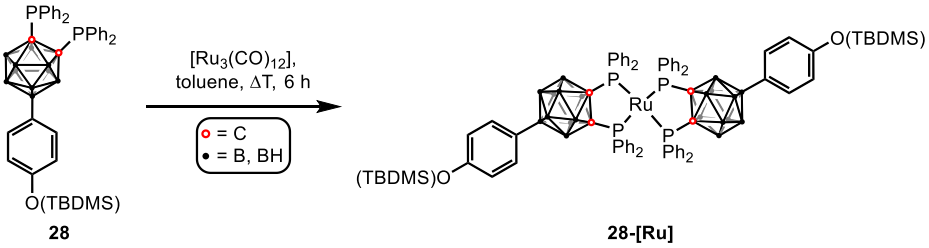


**Scheme 4.3.7.** Attempted synthesis of a ruthenium(0) complex.

The reaction progress was monitored by $^{31}P\{^1H\}$ NMR spectroscopy. Upon addition of $[Ru_3(CO)_{12}]$ and refluxing for 2 h, new signals emerged at 98.8–98.1 ppm. After adding an additional 2.0 eq. of $[Ru_3(CO)_{12}]$ to the refluxing reaction mixture, the latter signals remained while the signals for the starting material decreased and new signals at 87.7, 21.1–20.6 and 15.1–13.8 ppm appeared. After precipitation with *n*-pentane an orange solution and a solid precipitate was obtained. After filtration, all solvents were evaporated and the solid residue dissolved in $CDCl_3$. The $^{31}P\{^1H\}$ NMR spectrum showed multiple additional, unassignable signals. According to the evolution of the $^{31}P\{^1H\}$ NMR signals, it appears that different Ru species are formed over time. The signals at 98.8–98.1 ppm point to the formation of a $Ru^0$ complex; however, when the substance is left in solution, they disappear indicating the decomposition of the complex. Due to the overlap of signals from several Ru species, the obtained $^{11}B\{^1H\}$ NMR and $^1H$ NMR spectra were inconclusive.

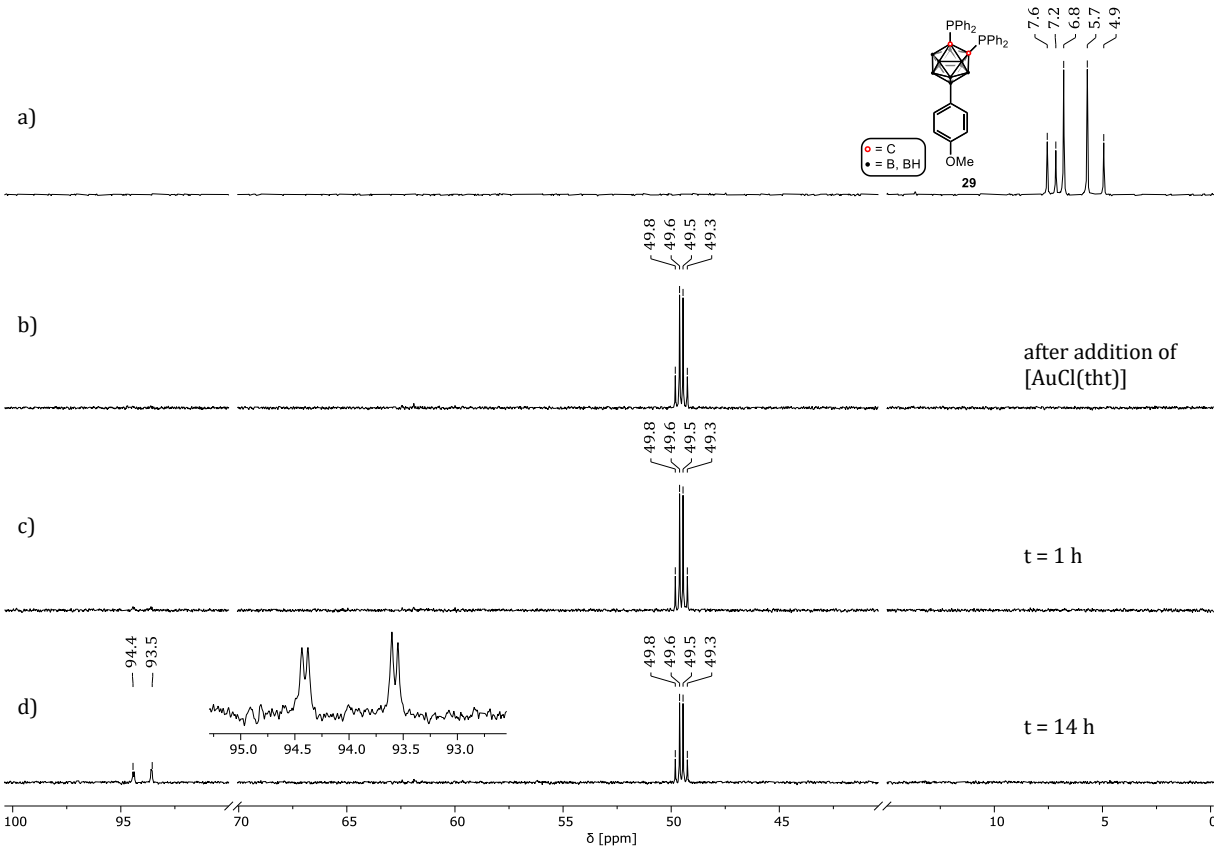


**Fig. 4.3.10.** $^{31}P\{^{1}H\}$ NMR spectra. (a) Carboranylphosphine **28** in $CDCl_3$. (b) After addition of 1.0 eq. $[Ru_3(CO)_{12}]$, no deuterated solvents. (c) After addition of further 2.0 eq. $[Ru_3(CO)_{12}]$, no deuterated solvent. (d) Removal of the precipitate and evaporation of the solvents; residue in $CDCl_3$.

HRMS ESI(+/−) analysis of the filtrate did not yield any conclusive information about the compounds formed. Attempts to crystallize any of the compounds were as well unsuccessful. For further investigation, the reaction should be repeated on a larger scale to obtain conclusive results.

### 4.3.6 Catalytic experiments with *in situ* generated complexes

The applicability of complexes made from $[RhCl(PPh_3)_3]$ and $[RhCl(CO)(PPh_3)_2]$ with dppc as hydrogenation and hydroformylation catalysts was first proven by HART and OWEN in 1985.[44] Reporting [RhCl(dppc)(CO)] as an effective hydroformylation catalyst under fairly mild conditions with some degree of unselectivity in regards of the products, and $[RhCl(dppc)PPh_3]$ as an effective hydrogenation catalyst but only at higher temperatures, we opted for the investigation how well our B9-substituted carboranylphosphines can compete.

In preliminary catalytic tests – the hydrogenation of oct-1-ene (**65**) and cyclohexene (**66**) as well as the hydroformylation of oct-1-ene – several metal complex precursors were investigated. Finding the right ratio of metal complex precursor and ligand as well as the reaction conditions requires many test reactions on a laboratory scale. An automated, parallel library

screening using the Chemspeed® platform (at BASF SE) was applied to solve this issue. Cyclohexene and oct-1-ene were hydrogenated at a pressure of 60 bar $H_2$ at temperatures of 70 °C and 100 °C, respectively, for 16 hours (see **Scheme 4.3.8**).

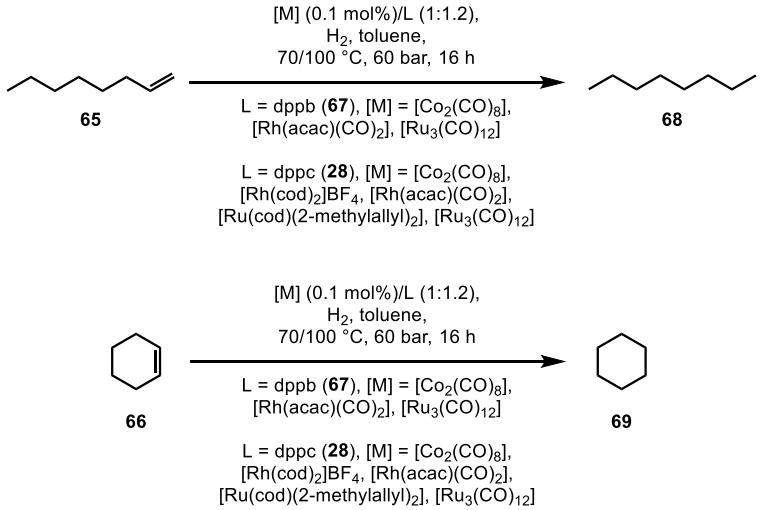


**Scheme 4.3.8.** Automated, parallel library screening using a Chemspeed® platform (at BASF SE) to find the best conditions for the hydrogenation of oct-1-ene and cyclohexene (dppb = 1,2-bis(di-phenylphosphino)benzene (**67**)).

Oct-1-ene was hydroformylated at a pressure of 10–20 bar $CO:H_2$ (1:1) and at temperatures of 70 °C and 100 °C, respectively, for 16 hours (see **Scheme 4.3.9**).

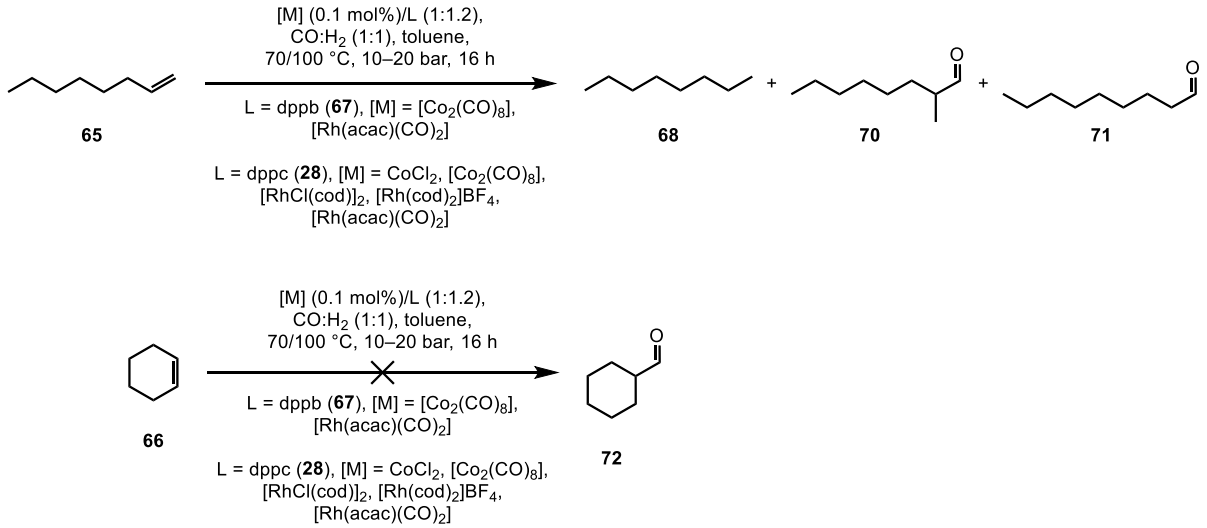


**Scheme 4.3.9.** Automated, parallel library screening using a Chemspeed® platform (at BASF SE) to find the best conditions for the hydroformylation of oct-1-ene and cyclohexene.

Samples were obtained and analyzed by GC (Agilent 6890 with GC814, length 30 m, column type: OV-1, diameter: 0.32 mm, film thickness D: 0.5 µm, heating program: start 50 °C, 5 min isothermic/20 °C $min^{-1}$/stop 300 °C). For the control studies, 1,2-bis(diphenylphosphino)-benzene (dppb, **67**) was utilized. It must be noted that the sole purpose of this preliminary

analysis is to determine whether or not a catalytic reaction occurs. The yields obtained from GC analysis are meaningless since it is feasible that the olefins, precursors, and solvents might become contaminated with one another while the reactors are being set up or heated. As the reactions were on a microgram scale, small variations in weight could further result in large variations in the yield.

Among the metal complex precursors of commercial importance – $CoCl_2$, $[Co_2(CO)_8]$, $[Rh(cod)_2]BF_4$, $[RhCl(cod)]_2$, $[Rh(acac)(CO)_2]$, $[Ru(cod)(2\text{-methylallyl})_2]$, and $[Ru_3(CO)_{12}]$ – $[Rh(acac)(CO)_2]$ and $[Ru_3(CO)_{12}]$ showed the best results and were thus studied in more detail.

Suitable reactions were upscaled and repeated under the same conditions in an autoclave (60 ml). $[Rh(acac)(CO)_2]$ and the phosphorus ligands **28**, dppb (**67**), and 1,2-bis(diphenyl-phosphino)-*ortho*-carborane (dppc, **73**), were tested for the hydrogenation of oct-1-ene (see **Scheme 4.3.10**, **Fig. 4.3.11**) while $[Ru_3(CO)_{12}]$ and the same phosphorus ligands were investigated for the hydrogenation of cyclohexene (see **Scheme 4.3.11**, **Fig. 4.3.12**). $[Rh(acac)(CO)_2]$ and the phosphorus ligands **28**, dppb (**67**), and dppc (**73**) were also tested for the hydroformylation of oct-1-ene (see **Scheme 4.3.12**, **Fig. 4.3.13**) All experimental work was conducted by Thomas Gaczensky at BASF SE in Ludwigshafen (refer to **4.4** for the experimental details).

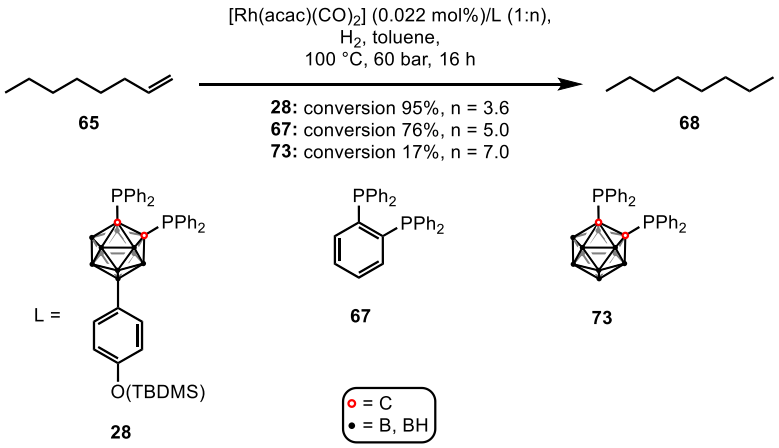


**Scheme 4.3.10.** Hydrogenation of oct-1-ene using $[Rh(acac)(CO)_2]$ and the phosphorus ligands **28**, **67** and **73**.

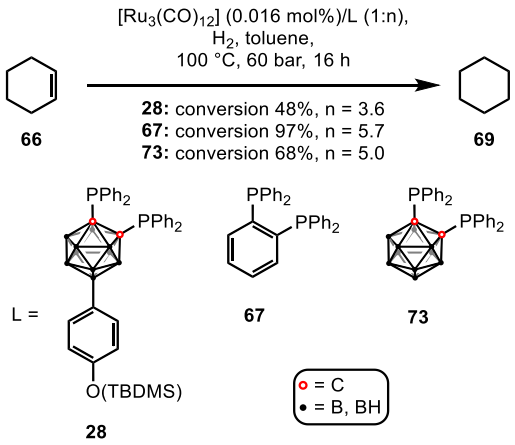


**Scheme 4.3.11.** Hydrogenation of cyclohexene using $[Ru_3(CO)_{12}]$ and the phosphorus ligands **28**, **67** and **73**.

For the hydrogenation of oct-1-ene conversions based on the GC analysis (after 16 h) of 95% (**28**), 76% (**67**) and 17% (**73**) were obtained. The following procedure was used to assess the gas kinetics: The initial gas was introduced at ambient temperature. The temperature rose to 90 °C during the course of 13 min, and after 20 min, it reached 100 °C. The yield for the three compounds was, interestingly, more similar when calculated based on the gas consumption (**28**: 94%, **67**: 87%, and **73**: 100%). The B9-substituted ligand performed at least 19% better than the two others on the basis of GC analysis and at least 7% better than dppb (**67**) based on the yield measured by gas-uptake. Comparing the results for obtaining the yield, it seems that there is a decrease of the yield over time (gas-uptake measured after 25 min vs. GC analysis after 16 h, see **Fig. 4.3.11**). To find out more about this, it would have been necessary to repeat the experiment and analyze what happened to the phosphorus ligand.

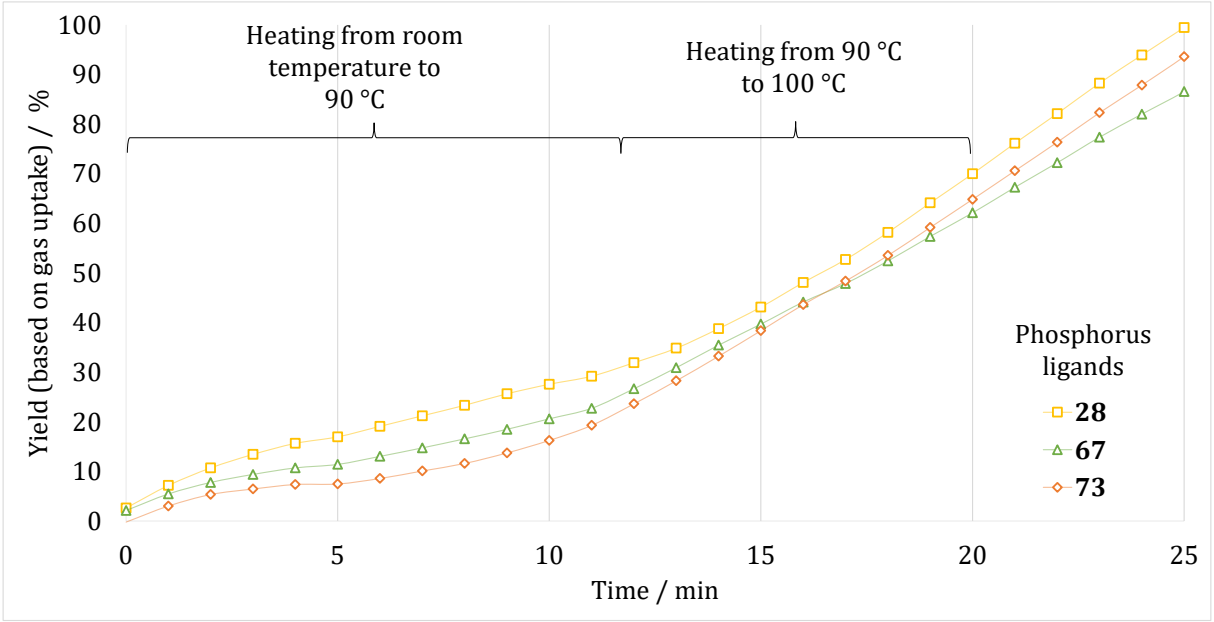


**Fig. 4.3.11.** Time-resolved comparison of the phosphorus ligands **28**, **67**, and **73** for the catalytic hydrogenation of oct-1-ene using $[Rh(acac)(CO)_2]$. Yields were determined by gas uptake.

For the hydrogenation of cyclohexene conversions of 48% (**28**), 97% (**67**), and 68% (**73**) were obtained after GC analysis. Gas kinetics were assessed using the following procedure: The initial gas was introduced at ambient temperature. The temperature rose to 90 °C during the course of 13 min, and after 20 min, it reached 100 °C. Interestingly, the yield determined by the amount of gas used after 25 minutes was more comparable for the three compounds (**28**: 52%, **67**: 55%, and **73**: 52%). The dppb ligand (**67**) outperformed both of the carboranylphosphine ligands indicating that neither **28** nor **73** can outdo other chelating bisphosphines when used with $[Ru_3(CO)_{12}]$. Comparing the results by obtained yields, it further appears that the carboranylphosphine-containing catalysts reach saturation at roughly 25 min, but the catalytic conversion of cyclohexene into cyclohexane continues with the dppb ligand (**67**). To find out more about this, it would have been necessary to repeat the experiment few times and analyze what happened to the catalysts during the reaction.

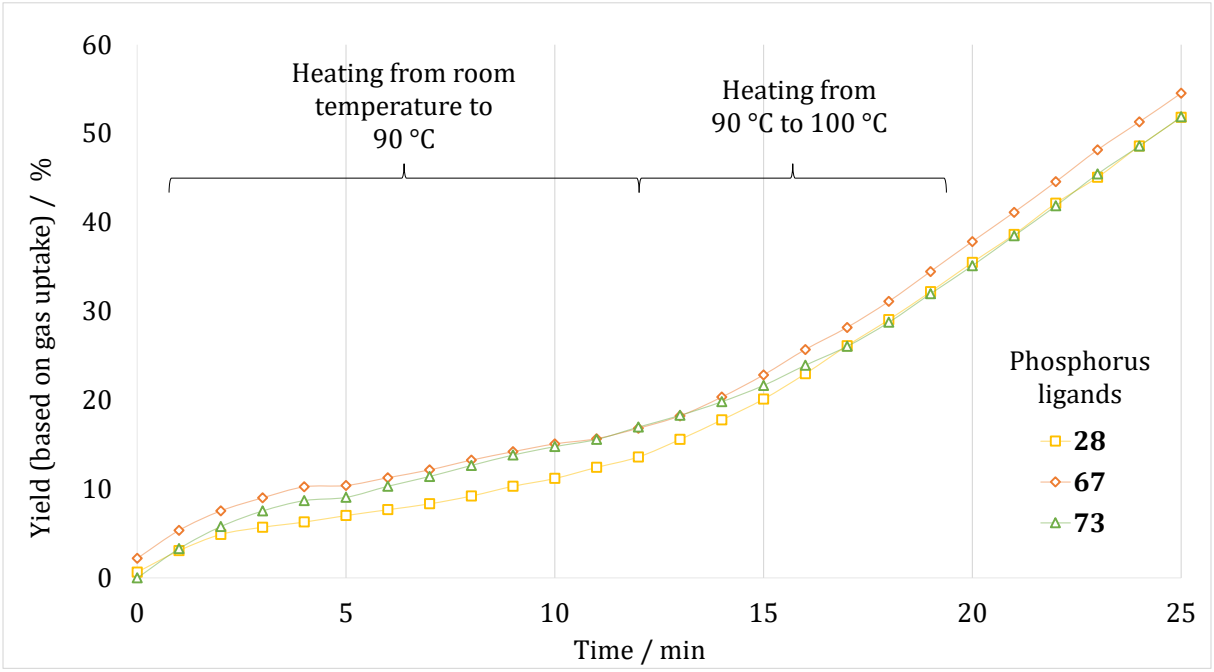


**Fig. 4.3.12.** Time-resolved comparison of the phosphorus ligands **28**, **67**, and **73** for the catalytic hydrogenation of cyclohexene with $[Ru_3(CO)_{12}]$**.** Yields were determined by gas uptake.

The catalytic hydroformylation of oct-1-ene with $[Rh(acac)(CO)_2]$ and the aforementioned phosphorus ligands was carried out in a similar manner using a syngas ($CO:H_2$, 1:1) pressure of 10 bar (see **Scheme 4.3.12**).

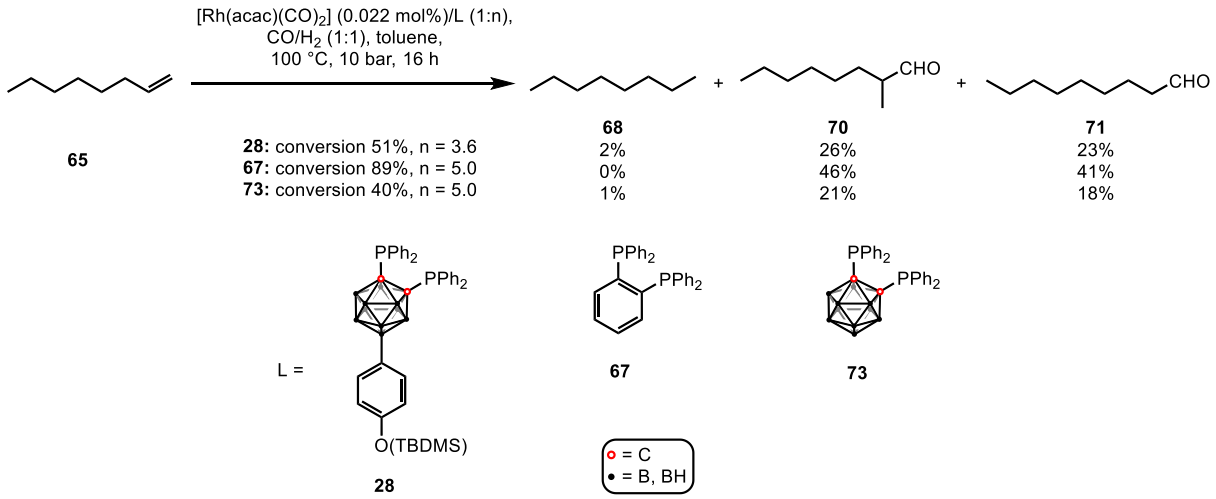


**Scheme 4.3.12.** Hydroformylation of oct-1-ene using [Rh(acac)(CO)$_2$] and the phosphorus ligands **28**, **67**, and **73**.

The hydroformylation of oct-1-ene yielded conversion rates measured by GC of 51% (**28**), 89% (**67**), and 40% (**73**). Additionally, the following procedure was used to assess the gas kinetics: The initial gas was introduced at ambient temperature. The temperature rose to 90 °C during the course of 13 min, and after 20 min, it reached 100 °C. Interestingly, the yield based on the gas consumption after 2 h was more similar for the three compounds (**28**: 56%, **67**: 43%, and **73**: 47%). Despite having the highest performance during the first 2 h based on the gas uptake, ligand **28** did not produce the same results in the GC. Octane, 2-methyloctanal, nonanal, and isomers of octene were formed throughout the catalytic run. The catalytic system therefore does not only hydroformylate but also isomerizes and hydrogenates the starting material. The lack of selectivity in the carbonylation is not surprising, as it was already reported before for similar compounds such as [RhCl(dppc)(CO)][44] and another chelate bisphosphine, [RhH(diphos)(CO)PPh$_3$].[52] Interestingly, the stationary point for dppb (**67**) is reached much later (after 180 min). A possible reason could be the treatment of the samples and the heating program used.

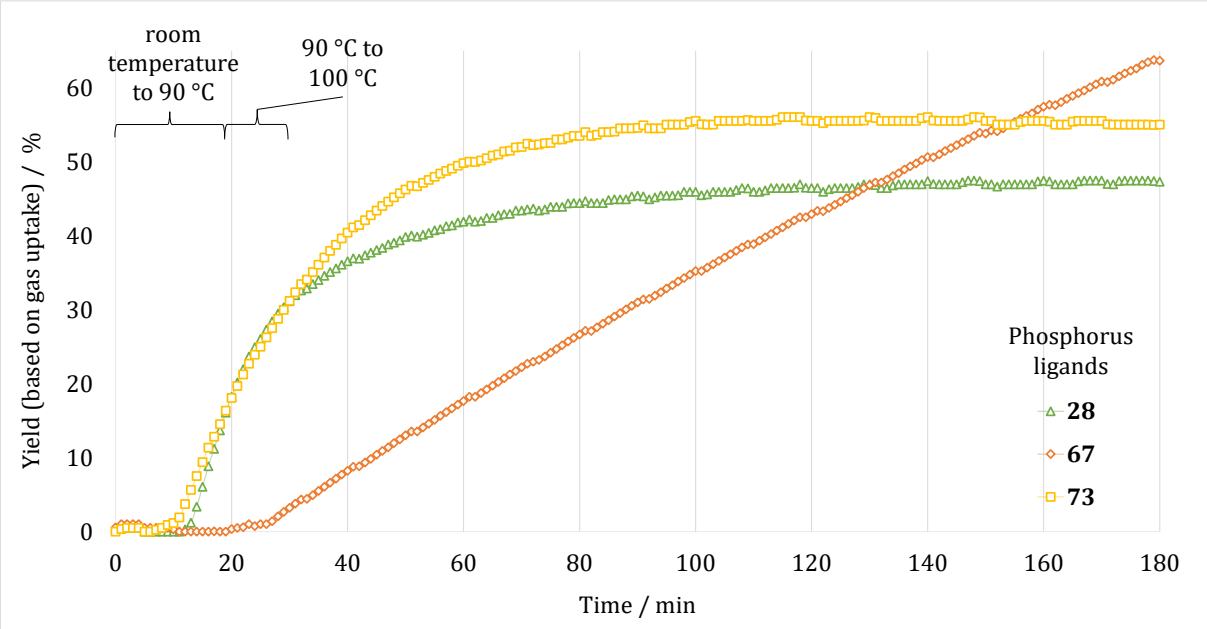


**Fig. 4.3.13.** Time-resolved comparison of the phosphorus ligands **28**, **67**, and **73** for the catalytic hydroformylation of oct-1-ene with $[Rh(acac)(CO)_2]$. Yields were determined by gas uptake.

Despite the fact that several of the reactions demonstrated good conversion, the selectivity is not perfect, hence these systems were not subjected to additional testing in an industrial setting. It should also be taken into account that all of the reactions in the autoclaves were performed only once. The results are therefore appropriate for preliminary studies but do not provide enough information to explain all the chemical processes going on. Additional experiments backed by computational analyses must be conducted in order to completely comprehend the formation of the catalytic species, its structure, and explain the selectivity of the process. It is necessary to contrast the outcomes of the reactions with an *in situ* formed catalyst with the results obtained where the metal carboranylphosphine complex was synthesized before (precatalyst). To learn more about the capabilities and restrictions of this catalytic system, tests with additional, more complicated substrates such hex-1-yne, allylbenzene, or 1-allyl-4-methoxybenzene as well as other phosphine ligands such as 9-(TBDMS)O-$C_6H_4$-doepc (**24**), 9-(TBDMS)O-$C_6H_4$-depc (**25**) or 9-(TBDMS)O-$C_6H_4$-dipc (**26**) might be conducted.

## 4.4 Experimental Section

### 4.4.1 General Procedures

*Materials:* Unless otherwise stated, all reactions requiring anhydrous conditions were conducted with oven-dried glassware under an atmosphere of nitrogen or argon using SCHLENK techniques. All glassware was dried at 120 °C for approximately 24 h before use. Anhydrous dichloromethane, diethyl ether, methanol, *n*-pentane, tetrahydrofuran and toluene were obtained using the MBRAUN solvent purification system MB SPS-800. Tetrahydrofuran was further dried over K and

distilled. If needed, deuterated solvents ($CD_3CN$, $C_6D_6$, $CDCl_3$, $CD_2Cl_2$, DMSO-$d_6$) were subjected to several freeze-pump-thaw cycles. All solvents were stored over 3 Å, 4 Å molecular sieves or K (for all non-chlorinated solvents), respectively, under an atmosphere of nitrogen or argon. Chloromethyl diphenylphosphine,[38] 9-phenoxy-(*tert*-butyl)dimethylsilyl-1,2-bis(diphenyl-phosphino)-*ortho*-carborane (**28**) and 9-methoxyphenyl-1,2-bis(diphenyl-phosphino)-*ortho*-carborane (**29**) (see Chapter 3), dichloridobis(acetonitrile)palladium(II),[53] [AuCl(tht)],[54] and 1,2-bis(diphenyl-phosphino)-*ortho*-carborane[55] were prepared according to literature. All other chemicals were purchased and used as received.

*Methods:* Thin-layer chromatography (TLC) with silica gel 60 $F_{254}$ on glass or aluminum available from Merck KGaA was used for monitoring the reactions. Eluted plates were visualized using a 254 nm UV lamp and/or by developing with a suitable stain following heating. This stain included an acidic 5–10% solution of $PdCl_2$ in methanol.

*NMR spectroscopy*: Proton ($^1$H), boron ($^{11}$B), carbon ($^{13}$C), and phosphorus ($^{31}$P) NMR spectra were recorded on a Bruker Avance III HD 400 MHz, Bruker Avance 400 MHz or Bruker Avance NEO 400 MHz NMR spectrometer at room temperature. NMR spectra were recorded at the following frequencies: $^1$H: 400.18 MHz, $^{13}$C: 100.64 MHz, $^{31}$P: 162.01 MHz (Avance III HD); $^1$H: 400.16 MHz, $^{13}$C: 100.63 MHz, $^{31}$P: 161.99 MHz (Avance 400 MHz) and $^1$H: 400.13 MHz, $^{13}$C: 100.62 MHz, $^{31}$P: 161.99 MHz (Avance NEO). All chemical shifts are reported in parts per million (ppm). NMR data were listed as follows: Chemical shift δ ppm (multiplicity, coupling constants, relative integral, assignment). NMR data were interpreted with MestReNova.[56]

*Electrospray ionization mass spectrometry* was performed with an ESI ESQUIRE 3000 PLUS spectrometer with an IonTrap-analyzer from Bruker Daltonics and an UPLC Xevo G2 QTOF spectrometer from Waters in negative or positive mode. Acetonitrile, dichloromethane, methanol or mixtures of these solvents were used.

### 4.4.2 Synthetic Procedures and Characterization

#### 4.4.2.1 Attempted synthesis of 29-[Pd]

Carboranylphosphine derivative **29** (12.0 mg, 0.019 mmol, 1.01 eq.) and [$PdCl_2(MeCN)_2$] (5.0 mg, 0.019 mmol, 1.00 eq.) were added to a YOUNG's NMR tube and dissolved in $CD_3CN$ (0.7 ml), then the sample was directly frozen in liquid $N_2$. After warming to room temperature, the reaction progress was monitored over 18 h by NMR spectroscopy. The orange suspension was filtered. The remaining gray solid residue was suspended in $CD_3CN$ and slowly dissolved by dropwise addition of DMSO-$d_6$. The NMR data obtained for **54** are reported in the following.

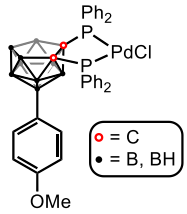


**$^{1}$H NMR** (400 MHz, $CD_3CN$/DMSO-$d_6$): δ=8.40 (t, $^{3}J_{H,H}$=10 Hz, 1H, Ph-*H*), 8.26–8.17 (m, 2H, Ph-*H*), 8.15–8.06 (m, 2H, Ph-*H*), 7.70–7.61 (m, 5H, Ph-*H*), 7.49–7.41 (m, 10H, Ph-*H*), 6.98 (d, $^{3}J_{H,H}$=8 Hz, 2H, Ar-*H*), 6.56 (d, $^{3}J_{H,H}$=8 Hz, 2H, Ar-*H*), 3.62 ppm (s, 3H, OC*H*$_3$), signals for all B were not observed; **$^{11}$B{$^{1}$H} NMR** (128 MHz, $CD_3CN$/DMSO-$d_6$): δ=26.2, 18.1, –2.9, –9.7, –11.6, –17.1, –26.3, –34.6 ppm; **$^{31}$P{$^{1}$H} NMR** (162 MHz, $CD_3CN$/DMSO-$d_6$): δ=85.5, 85.1 ppm; **HRMS (ESI+):** [$C_{33}H_{36}B_9ClOP_2Pd$], m/z calculated: 750.1948 ([M$^{1}$+H]$^{+}$); found: 750.1963; [$C_{66}H_{72}B_{18}Cl_2O_2P_4Pd_2$] m/z calculated: 1500.3827 ([M$^{2}$+H]$^{+}$); found: 1500.3777.

### 4.4.2.2 Synthesis of 29-[CuCl]

Carboranylphosphine derivative **29** (20.1 mg, 0.032 mmol, 1.04 eq.) and [$CuCl(PPh_3)_3$] (29.6 mg, 0.033 mmol, 1.00 eq.) were dissolved in THF (3 ml) and the reaction mixture was stirred at room temperature for 72 h. After a control by $^{31}$P{$^{1}$H} NMR spectroscopy, all solvents were removed *in vacuo* and the residue redissolved in THF (2 ml). Different attempts were made to crystallize the product from mixtures of *n*-pentane/THF, toluene/THF, and *n*-hexane/THF. The NMR data obtained for **29-[CuCl]** are reported in the following.

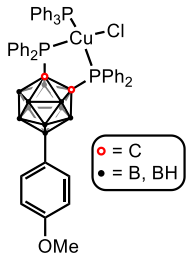


**$^{1}$H NMR** (400 MHz, $CDCl_3$): δ=7.84 (br s, ), 7.67–7.54 (m, 8H, Ph-*H*), 7.53–7.25 (m, 12H, Ph-*H*), 7.23–7.15 (m, 9H, $PPh_3$-*H*), 7.15–7.08 (m, 6H, $PPh_3$-*H*), 7.05 (d, $^{3}J_{H,H}$=8 Hz, 2H, Ar–*H*), 6.62 (d, $^{3}J_{H,H}$=8 Hz, 2H, Ar-*H*), 3.62 (s, 3H, OC*H*$_3$), 3.21–1.60 ppm (m, 9H, B*H*); **$^{11}$B{$^{1}$H} NMR** (128 MHz, $CDCl_3$): δ=9.9, –0.8, –4.3, –8.9 to –12.0 ppm; **$^{31}$P{$^{1}$H} NMR** (162 MHz, $CDCl_3$): δ=21.3, 11.9 ppm; **HRMS (ESI+):** [$C_{66}H_{72}B_{20}ClCuO_2P_4$], m/z calculated: 1300.5797 ([M$^{1}$–Cl]$^{+}$); found: 1300.5781; [$C_{51}H_{51}B_{10}ClCuOP_3$], m/z calculated 944.3452 ([M$^{2}$–Cl]$^{+}$); found: 944.3454; [$C_{33}H_{36}B_{10}ClCuOP_2$], m/z calculated 682.2532 ([M$^{3}$–Cl]$^{+}$); found: 682.2554.

### 4.4.2.3 Synthesis of 29-[Au]

Carboranylphosphine derivative **29** (16.4 mg, 0.027 mmol, 1.00 eq.) and [AuCl(tht)] (8.53 mg, 0.027 mmol, 1.00 eq.) were added to a Young's NMR tube and dissolved in $CD_2Cl_2$ (0.7 ml), then the sample was directly frozen in liquid $N_2$. After warming to room temperature, the reaction progress was monitored over 14 h by NMR spectroscopy. The yellow solution was filtered into a Schlenk and the remaining dark red solid was washed with $CH_2Cl_2$ (3x1 ml). The filtrate was dried *in vacuo* and the residue extracted with $Et_2O$ (5 ml). After filtration, all solvents were removed *in vacuo* and 27.7 mg (0.033 mmol, quantitative) of a crystalline product was obtained. Crystals too small for a complete XRD of **29-[Au]** were obtained from a mixture of $CH_2Cl_2$ and *n*-pentane. The NMR data obtained for **29-[Au]** are reported in the following.

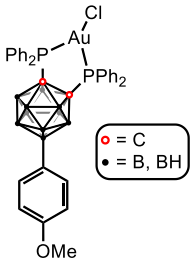


**$^{1}$H NMR** (400 MHz, $CD_2Cl_2$): δ=8.04–7.93 (m, 8H, Ph-*H*), 7.65–7.55 (m, 4H, Ph-*H*), 7.53–7.43 (m, 8H, Ph-*H*), 6.97 (d, $^{3}J_{H,H}$=9 Hz, 2H, Ar-*H*), 6.68 (d, $^{3}J_{H,H}$=9 Hz, 2H, Ar-*H*), 3.70 (s, 3H, OC$H_3$), 3.58–1.44 ppm (m, 9H, B*H*); **$^{11}$B{$^{1}$H} NMR** (128 MHz, $CD_2Cl_2$): δ=12.4 (1B), 1.5 (2B), –6.1 (br s, 3B), –9.2 ppm (br s, 4B); **$^{13}$C{$^{1}$H} NMR** (101 MHz, [D$_2$]dichloromethane): δ=136.0, 135.9, 133.5, 132.9, 129.5, 129.3, 113.0, 54.9, 38.6, 30.5 ppm; **$^{31}$P{$^{1}$H} NMR** (162 MHz, $CD_2Cl_2$, AB spin system): δ=49.7 (d, $^{2}J_{P,P}$=32 Hz), 49.4 ppm (d, $^{2}J_{P,P}$=32 Hz).

#### 4.4.2.4 Synthesis of 28-[Rh]

Carboranylphosphine derivative **28** (40.1 mg, 0.056 mmol, 1.00 eq.) was dissolved in toluene (3 ml) and heated to reflux. [Rh(acac)(CO)$_2$] (14.7 mg, 0.057 mmol, 1.02 eq.) was added in one portion. The yellow reaction mixture was stirred for another 2 h under reflux conditions. After cooling to room temperature overnight, the yellow solution was added to *n*-pentane (20 ml) to precipitate the crude product that was further isolated by filtration. After drying *in vacuo*, toluene (1 ml) was used to redissolve the brown oily residue. Upon addition of *n*-pentane (8 ml) a brown solid precipitated and was separated by filtration. The red-brown filtrate was dried yielding 27 mg (0.029 mmol, 53%) of **28-[Rh]**.

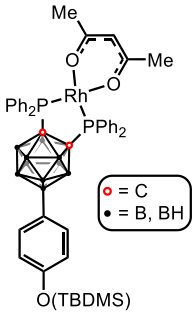


**$^{1}$H NMR** (400 MHz, $CDCl_3$): δ=8.28–8.18 (m, 8H, Ph-*H*), 7.48–7.35 (m, 12H, Ph-*H*), 7.07 (d, $^{3}J_{H,H}$=H Hz, 2H, Ar-*H*), 6.63 (d, $^{3}J_{H,H}$=8 Hz, 2H, Ar-*H*), 5.31 (s, 1H, acac-*H*), 3.22–1.91 (m, 9H, B*H*), 2.37 (s, 6H, acac-C$H_3$), 0.95 (s, 9H, *t*Bu-*H*), 0.15 ppm (s, 6H, SiC$H_3$); **$^{11}$B{$^{1}$H} NMR** (128 MHz, $CDCl_3$): δ=8.9 (2B), –1.5 (2B), –4.0 (2B), –11.2 ppm (4B); **$^{13}$C{$^{1}$H} NMR** (101 MHz, $CDCl_3$): δ=185.3–185.2 (C=O), 155.2 (C–O), 137.9, 135.6–135.3 (Ph), 133.3 (Ar), 132.6, 132.3–132.2, 131.9, 130.8–130.7 (Ph), 129.0, 128.8, 128.2, 128.0, 127.6–127.5 (Ph), 125.3, 118.9 (Ar), 99.6 (acac-CH), 86.8–86.6 ($C_{Cage}$), 81.7–81.5 ($C_{Cage}$), 77.2, 25.7 (*t*Bu), 21.5 (acac–$CH_3$), 18.1, 1.0, –4.4 ppm (Si$CH_3$); **$^{31}$P{$^{1}$H} NMR** (162 MHz, $CDCl_3$, ABX system): δ=99.2 ($^{2}J_{P,P}$=61 Hz, $^{1}J_{P,Rh}$=205 Hz), 97.9 ppm ($^{2}J_{P,P}$=61 Hz, $^{1}J_{P,Rh}$=205 Hz); **HRMS (ESI+):** [$C_{42}H_{54}B_{10}N_2OP_2RhSi$], m/z calculated: 904.3534 ([M+H]$^{+}$); found: 904.3535.

### 4.4.3 Preliminary studies using the Chemspeed® platform at BASF SE

Amounts of precursor between 0.3 and 1.6 mg ([$Co_2(CO)_8$], [RhCl(cod)]$_2$, [Rh(acac)(CO)$_2$], [Ru(2-methylallyl)$_2$(cod)], and [$Ru_3(CO)_{12}$]) and of 0.9 and 5.6 mg of the phosphorus ligands (**28**, **67**) were weighed separately from each other and dissolved in toluene. $CoCl_2$ and [Rh(cod)$_2$]$BF_4$ were weighed by the Chemspeed® system. After installing vials containing the olefins (cyclohexene, oct-1-ene) and toluene, the system was purged and sealed. Step by step, precursor, olefins and toluol were added by the system to the different reactors before the gas was introduced and

heating was applied. The following conditions were tested: 60 bar $H_2$, 70 °C, 16 h; 60 bar $H_2$, 100 °C, 16 h; 10–20 bar CO:$H_2$, 70 °C, 16 h, 10–20 bar CO:$H_2$, 100 °C, 16 h.

### 4.4.4 Hydrogenation Catalysis

#### 4.4.4.1 General Procedure

The defined amounts of precursor [Rh(acac)$(CO)_2$] for oct-1-ene or [$Ru_3(CO)_{12}$] for cyclohexene and the phosphorus ligand (**28**, **67**, **73**) were weighed separately from each other and dissolved in toluene. The solutions were then transferred into the autoclave (60 ml) which was stored inside a glovebox. The olefin (5.0 g) was added, the heating bath was attached and the hydrogen gas (60 bar) was introduced. The first gas uptake happened at room temperature. After 13 min, the bath temperature had increased to 90 °C. After 20 min, the temperature reached 100 °C and the solution was stirred for 16 h. A reaction sample was taken after 16 h and analyzed by GC (Agilent 6890 with GC814, length 30 m, column type: Optima 1, diameter: 0.32 mm, film thickness D: 0.5 μm). The integrals of the peak areas were used to determine the yield by GC.

#### 4.4.4.2 Input and results

[$Ru_3(CO)_{12}$] (6.3 mg, 0.0099 mmol), dppb (**67**) (25.4 mg, 0.0569 mmol), cyclohexene (5.0 g, 0.0609 mol), toluene (5.0 g, 5.8 ml), GC: 96.5% conversion to cyclohexane, 3.5% unreacted cyclohexene

[$Ru_3(CO)_{12}$] (6.3 mg, 0.0099 mmol), dppc (**73**) (25.4 mg, 0.0496 mmol), cyclohexene (5.0 g, 0.0609 mol), GC: 47.7% conversion to cyclohexane, 52.3% unreacted cyclohexene

[$Ru_3(CO)_{12}$] (6.3 mg, 0.0099 mmol), **28** (25.4 mg, 0.0353 mmol), cyclohexene (5.0 g, 0.0609 mol), GC: 68.3% conversion to cyclohexane, 31.7% unreacted cyclohexene

[Rh(acac)$(CO)_2$] (2.55 mg, 0.0099 mmol), dppb (**67**) (22.2 mg, 0.0497 mmol), oct-1-ene (5.0 g, 0.0446 mol), toluene (5.0 g, 5.8 ml), GC: 76.3% conversion to octane, 19.0% unreacted oct-1-ene, 4.7% isomers of oct-1-ene

[Rh(acac)$(CO)_2$] (2.55 mg, 0.0099 mmol), dppc (**73**) (35.5 mg, 0.0693 mmol), oct-1-ene (5.0 g, 0.0446 mol), toluene (5.0 g, 5.8 ml), GC: 94.8% conversion to octane, 3.1% unreacted oct-1-ene, 2.1% isomers of oct-1-ene

[Rh(acac)$(CO)_2$] (2.55 mg, 0.0099 mmol), **28** (25.4 mg, 0.0353 mmol), oct-1-ene (5.0 g, 0.0446 mol), toluene (5.0 g, 5.8 ml), GC: 73.3% conversion to octane, 16.6% unreacted oct-1-ene, 10.4% isomers of oct-1-ene

### 4.4.5 Hydroformylation Catalysis

#### 4.4.5.1 General Procedure

The defined amounts of precursor [Rh(acac)$(CO)_2$] and the phosphorus ligand were weighed in separately from each other and dissolved in toluene. The solutions were then transferred into the autoclave (60 ml) which was stored inside a glovebox. Oct-1-ene (5.0 g, 0.045 mol) was added, the heating bath was attached and the gas ($CO:H_2$, 10 bar) was introduced. The first gas uptake happened at room temperature. After 13 min, the bath temperature had increased to 90 °C. After 20 min, the temperature reached 100 °C and the solution was stirred for 16 h. A reaction sample was taken after 16 h and analyzed by GC (Agilent 6890 with GC814, length 30 m, column type: Optima 1, diameter: 0.32 mm, film thickness D: 0.5 µm). The integrals of the peak areas were used to determine the yield by GC.

#### 4.4.5.2 Input and Results

[Rh(acac)$(CO)_2$] (2.55 mg, 0.0099 mmol), dppb (**67**) (22.2 mg, 0.0497 mmol), oct-1-ene (5.0 g, 0.0446 mol), toluene (5.0 g, 5.8 ml), GC: 88.9% conversion to 1.7% isomers of oct-1-ene, 46.2% *iso*-nonanal, 40.9% *n*-nonanal, 11.1% unreacted oct-1-ene

[Rh(acac)$(CO)_2$] (2.55 mg, 0.0099 mmol), dppc (**73**) (25.4 mg, 0.0496 mmol), oct-1-ene (5.0 g, 0.0446 mol), toluene (5.0 g, 5.8 ml), GC: 42.0% conversion to 1.3% octane, 1.7% isomers of oct-1-ene, 20.6% *iso*-nonanal, 18.4% *n*-nonanal, 58.0% unreacted oct-1-ene

[Rh(acac)$(CO)_2$] (2.55 mg, 0.0099 mmol), **28** (25.4 mg, 0.0353 mmol), oct-1-ene (5.0 g, 0.0446 mol), toluene (5.0 g, 5.8 ml), GC: 53.3% conversion to 1.8% octane, 2.5% isomers of oct-1-ene, 26.0% *iso*-nonanal, 23.0% *n*-nonanal, 46.7% unreacted oct-1-ene

## 4.5 Computational Studies

### 4.5.1 Methods

Calculations have been carried out using the Gaussian16 suite of programs[57] at DFT level of theory with the B3LYP functional[58–60] combined with Grimme's D3 correction to account for dispersion effects.[61] The structures of **29-[Pd]**, **31-[Pd]**, **46–49-[Pd]**, **29-[CuCl]**, **31-[CuCl]**, **46–49-[CuCl]**, **29-[Cu(MeCN)$_2$]**, **31-[Cu(MeCN)$_2$]**, **46–48-[Cu(MeCN)$_2$]**, **29-[Au]**, **31-[Au]**, **46–49-[Au]**, **29-[Rh]**, **31-[Rh]**, **46–49-[Rh]** as well as the metal complex precursor and reaction products were optimized in the experimentally employed solvents, using the basis set BS1 including the 6-31G(d,p) basis set for the main group elements,[62,63] and the scalar relativistic Stuttgart-Dresden SDD pseudopotential and its associated double-z basis set,[64] complemented with a set of *f* polarization functions,[65] for the transition metal atoms (palladium, copper, gold and rhodium). The solvents (dichloromethane, ε=8.930 or tetrahydrofuran, ε=7.4257) were described with the SMD (solvation model based on density) continuum model.[66] Frequency calculations were carried out for all the optimized geometries in order to characterize the stationary points as either minima or transition states. Connections between the transition state and the corresponding minima were checked by displacing in both directions, following the transition vector, the geometry of the transition states, and subsequent geometry optimization until a minimum was reached.

Energies in solvent were refined by means of single-point calculations at the optimized BS1 geometries using and extended basis set (BS2). BS2 consists of the def2-TZVP basis set for the main group atoms and and the quadruple-ζ def2-QZVP basis set for transition metal atoms.[67,68] GIBBS energies in solvent were calculated adding to the BS2 energies in solvent the thermal and entropic corrections obtained with BS1. An additional correction of 1.9 kcal/mol was applied to all GIBBS energies to change the standard state from the gas phase (1 atm) to the condensed phase (1 M) at 298.15 K ($\boldsymbol{\Delta G^{1atm\rightarrow 1M}}$).[69] In this way, all the energy values given in the article are GIBBS energies in solution calculated using the formula:

$$\boldsymbol{G = E(BS2) + G(BS1) - E(BS1) + \Delta G^{1atm\rightarrow 1M}}$$

### 4.5.2 Optimized structures of the calculated species

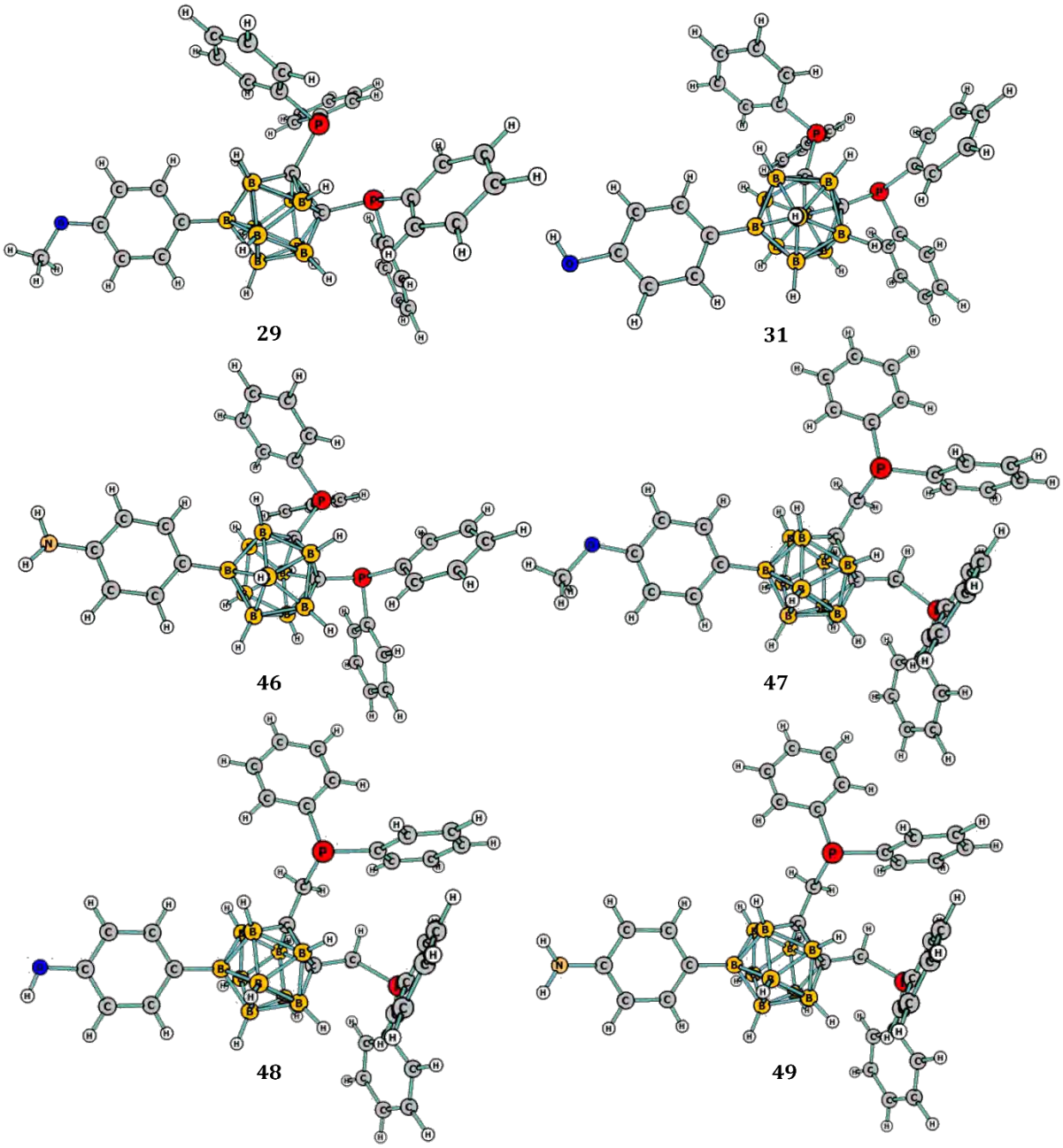


**Fig. 4.5.1.** Optimized structures of the carboranylphosphine ligands **29**, **31** and **46–49**. The structures look the same and are not dependent on the solvent used for the calculation.

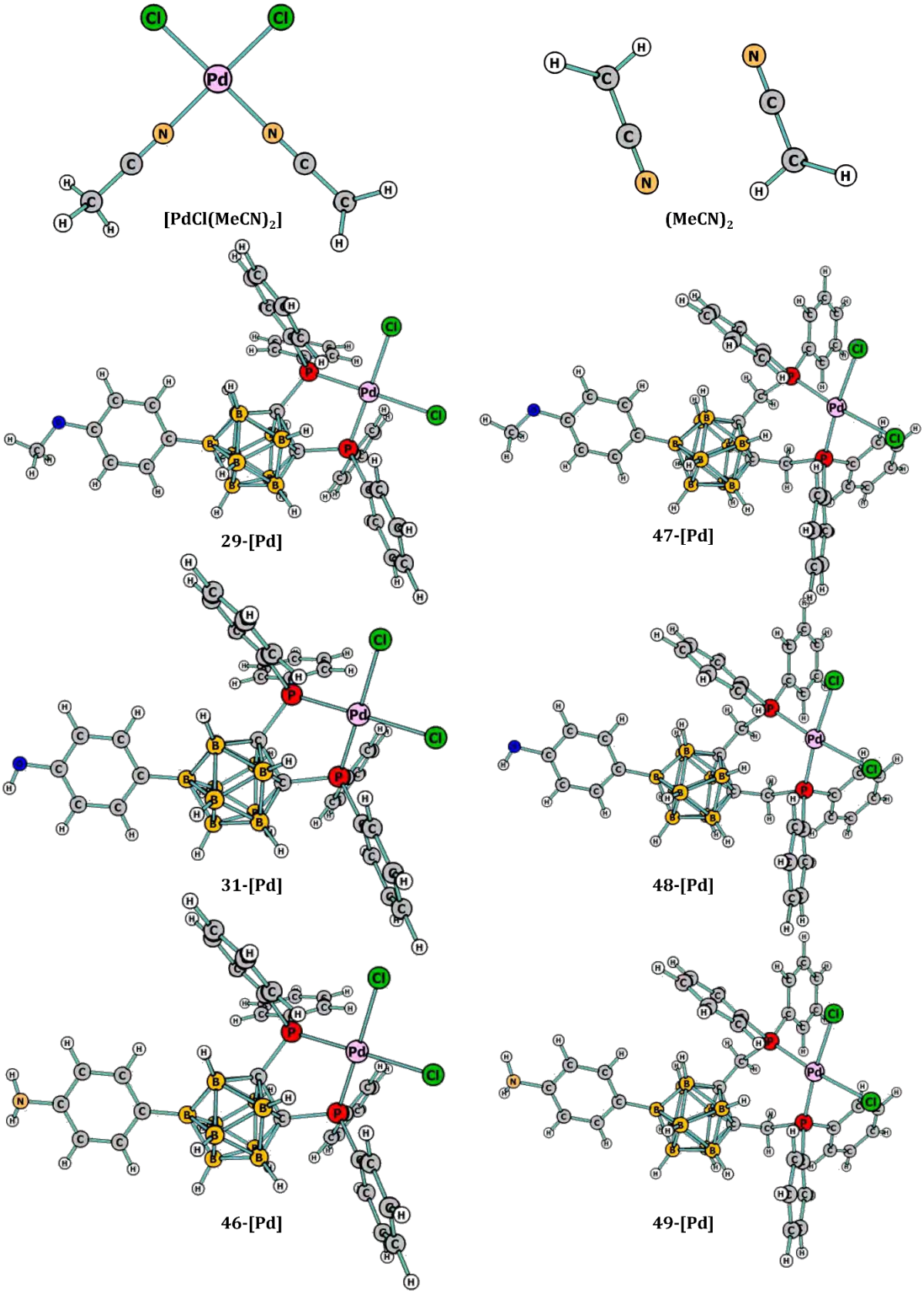


**Fig. 4.5.2.** Optimized structures of the precursor and complexes formed from $[PdCl_2(MeCN)_2]$ and ligands **29**, **31** and **46–49**.

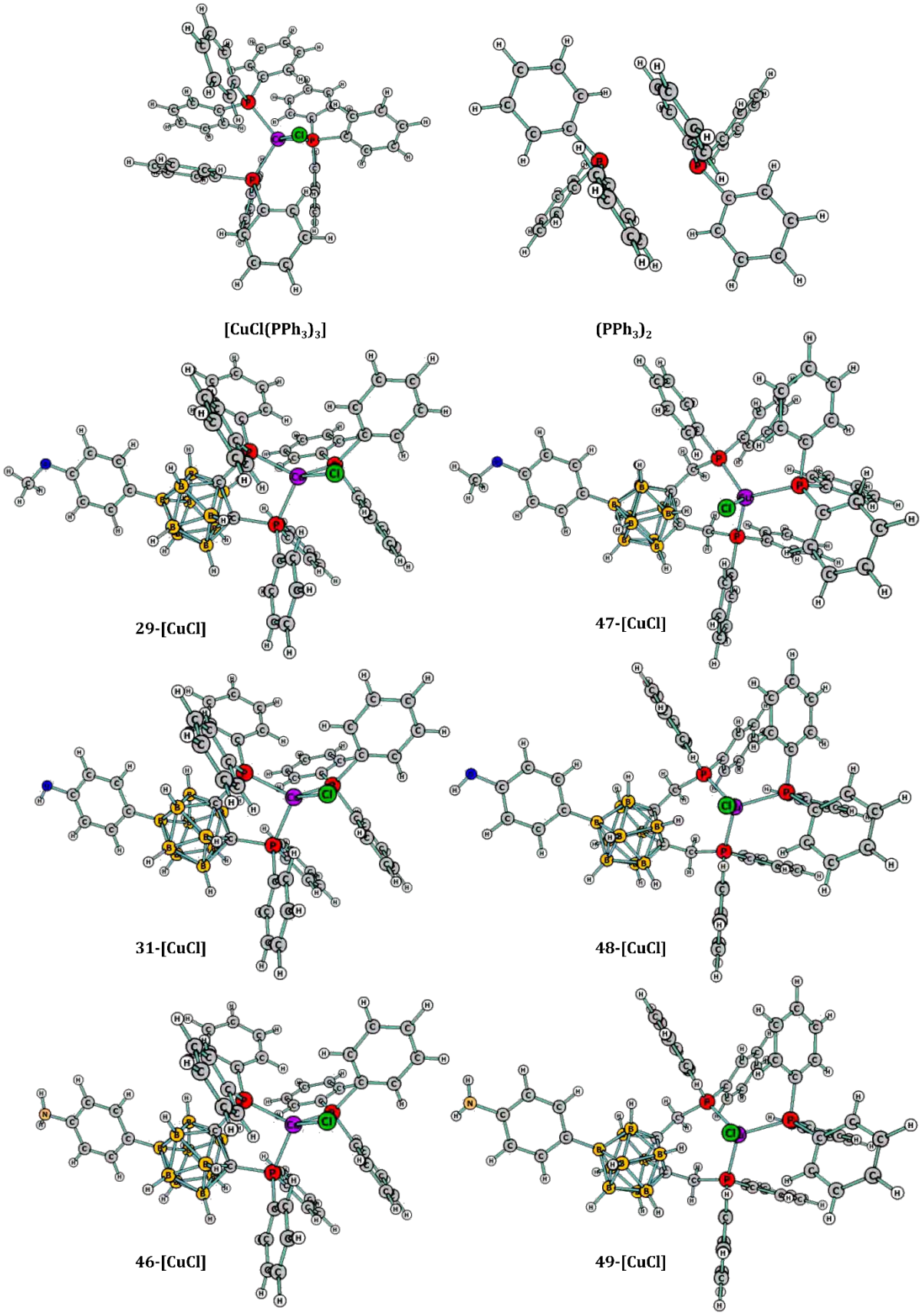


**Fig. 4.5.3.** Optimized structures of the precursor and complexes formed from [CuCl(PPh$_3$)$_3$] and ligands **29**, **31** and **46–49**.

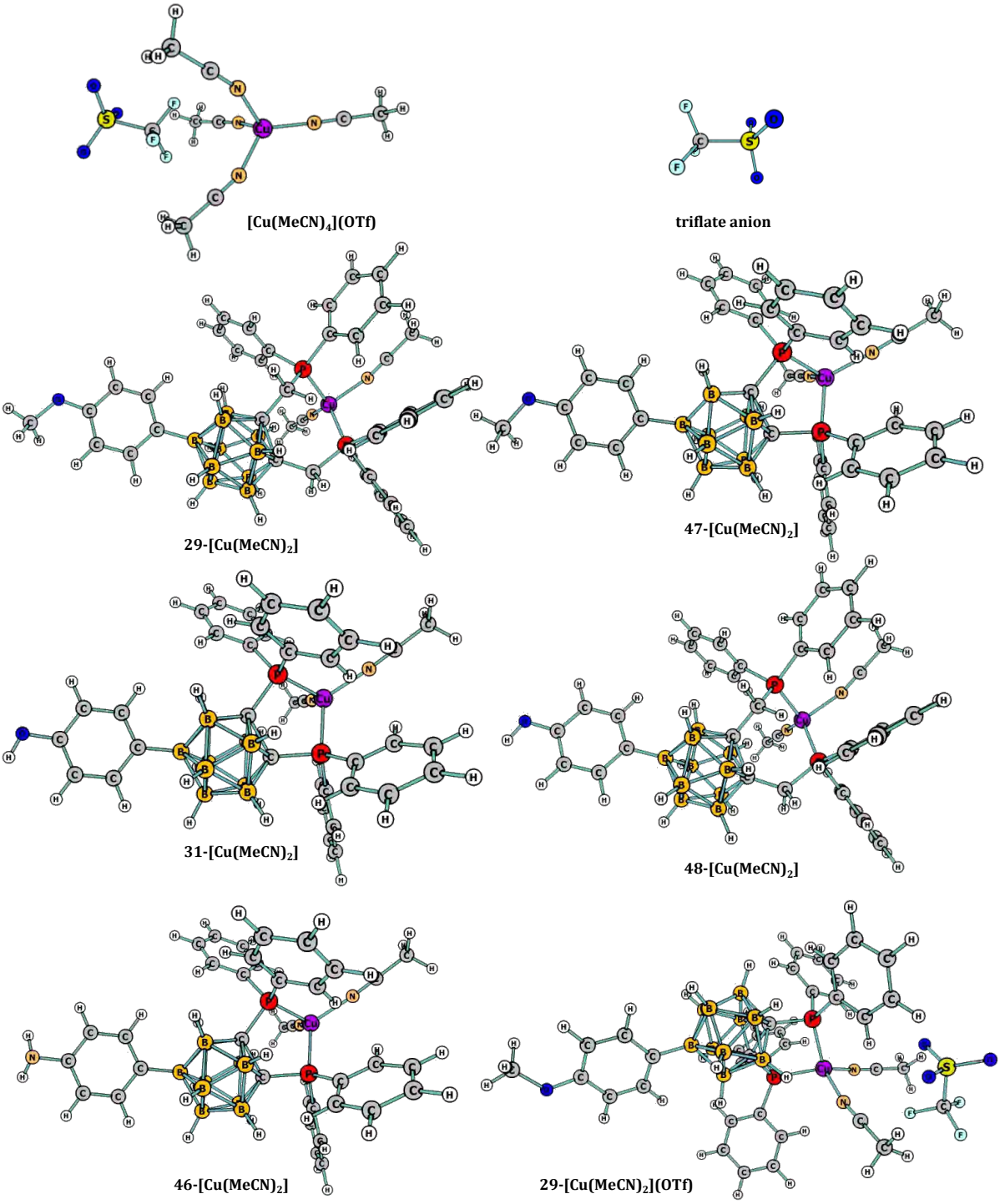


**Fig. 4.5.4.** Optimized structures of the precursor and complexes formed from $[Cu(MeCN)_4](OTf)$ and ligands **29**, **31** and **46**–**48**.

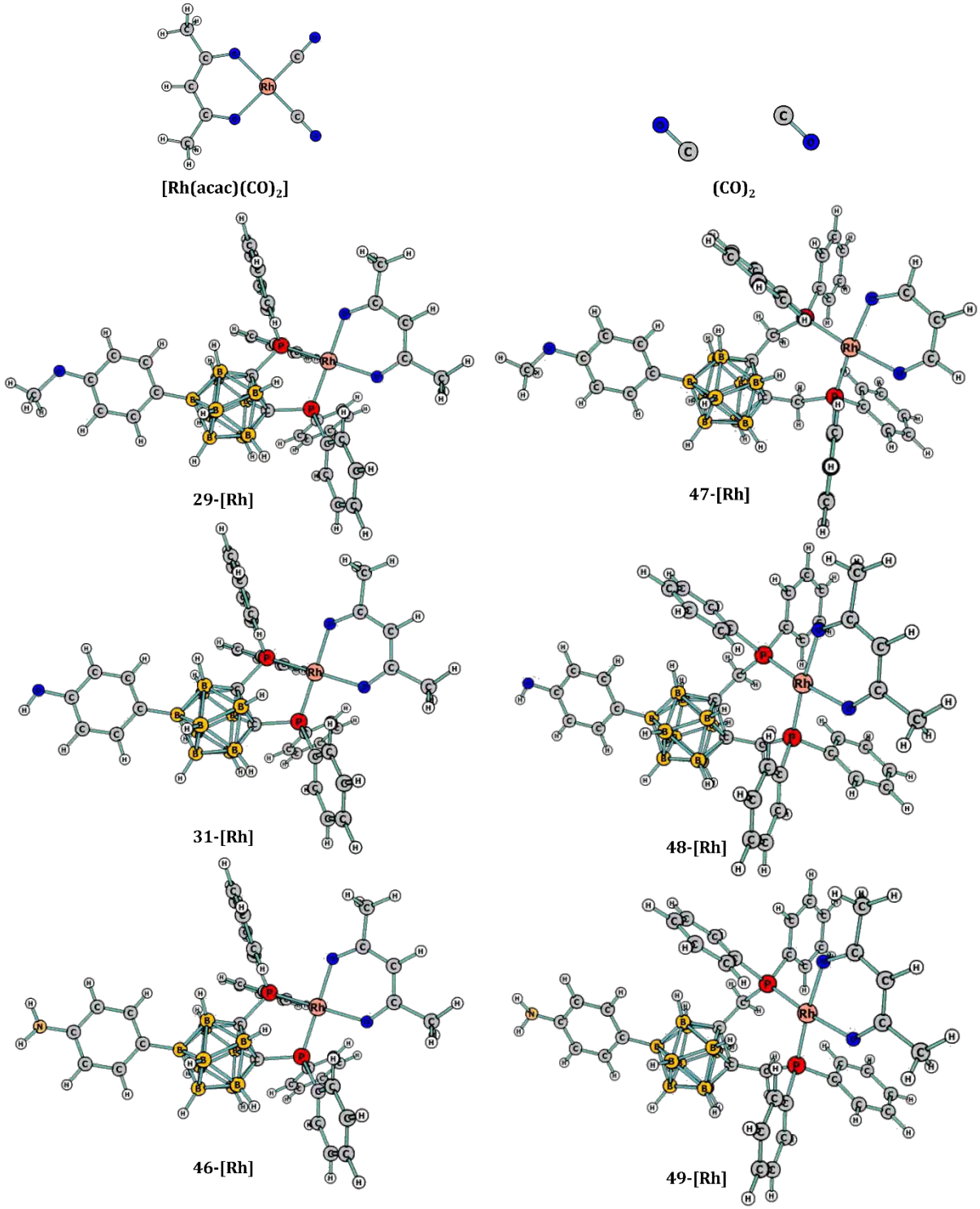


**Fig. 4.5.5.** Optimized structures of the precursor and complexes formed from [Rh(acac)(CO)$_2$] and ligands **29**, **31** and **46–49**.

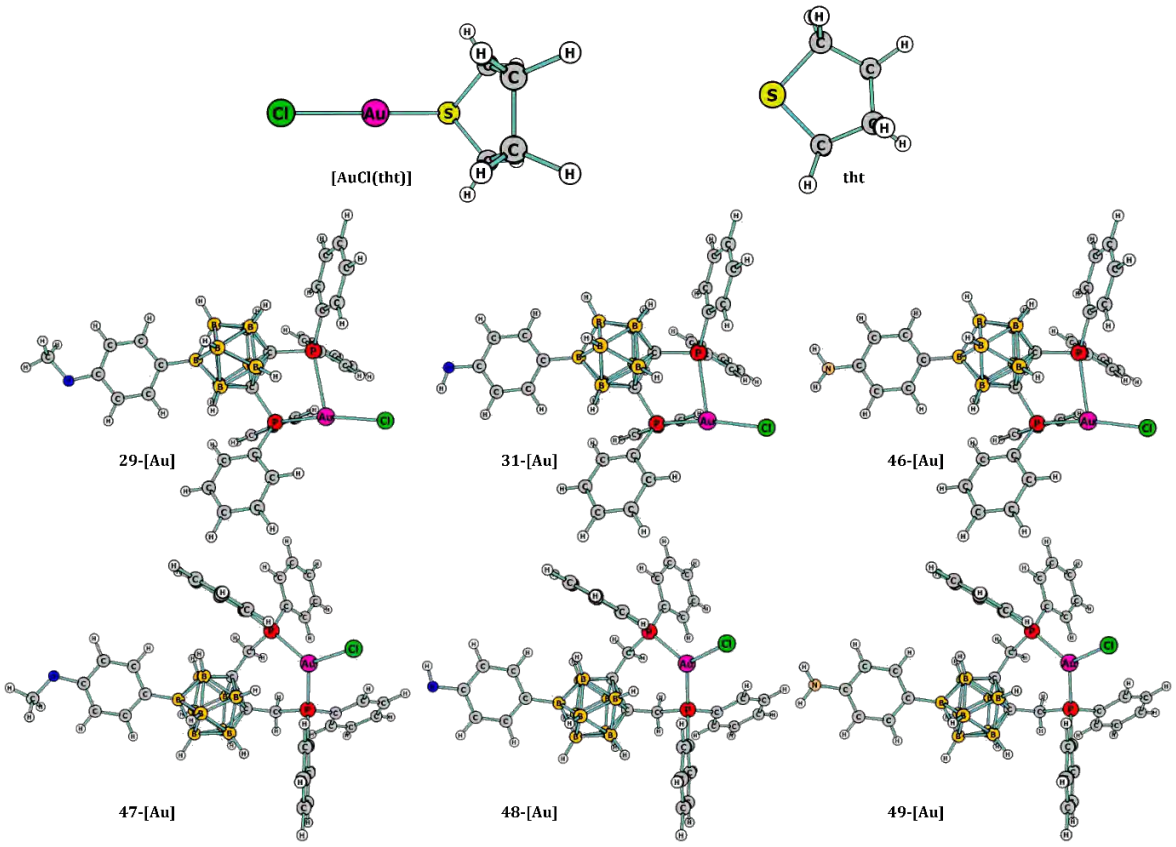


**Fig. 4.5.6.** Optimized structures of the precursor and complexes formed from [AuCl(tht)] and ligands **29**, **31** and **46–49**.

### 4.5.3 Absolute energies of the calculated species (atomic units)

**Tab. 4.5.1:** Complexation of different metal precursors with **29**, **31**, **46–49** in THF as solvent. Species shown in **Fig. 4.5.1**, **Fig. 4.5.2, Fig. 4.5.3**, **Fig. 4.5.4** and **Fig. 4.5.5**.

| | E(acn)/BS1 | T,S correction | G(acn)/BS1 | E(acn)/BS2 | G(acn)/BS2 |
|---|---|---|---|---|---|
| **29** | −2285.917496 | 0.565082 | −2285.357659 | −2286.519575 | −2285.954493 |
| **31** | −2246.617776 | 0.538425 | −2246.07935 | −2247.20435 | −2246.665925 |
| **46** | −2226.757007 | 0.550418 | −2226.206589 | −2227.330859 | −2226.780441 |
| **47** | −2364.56653 | 0.621508 | −2363.945022 | −2365.187406 | −2364.565898 |
| **48** | −2325.261535 | 0.594124 | −2324.667411 | −2325.872154 | −2325.27803 |
| **49** | −2305.400724 | 0.60683 | −2304.793893 | −2305.998606 | −2305.391776 |
| **$[PdCl_2(MeCN)_2]$** | −1313.981192 | 0.05239 | −1313.928802 | −1314.188627 | −1314.136237 |
| **$(MeCN)_2$** | −265.535247 | 0.055787 | −265.479460 | −265.643294 | −265.587507 |
| **29-[Pd]** | −3334.433476 | 0.566095 | −3333.867382 | −3335.133289 | −3334.567194 |
| **31-[Pd]** | −3295.128717 | 0.539291 | −3294.589426 | −3295.818071 | −3295.27878 |
| **46-[Pd]** | −3275.268136 | 0.55198 | −3274.716155 | −3275.944738 | −3275.392758 |
| **47-[Pd]** | −3413.08318 | 0.624694 | −3412.458486 | −3413.80681 | −3413.182116 |
| **48-[Pd]** | −3373.778203 | 0.598019 | −3373.180184 | −3374.491575 | −3373.893556 |
| **49-[Pd]** | −3353.9174 | 0.60988 | −3353.307519 | −3354.618054 | −3354.008174 |
| **$[CuCl(PPh_3)_3]$** | −3766.817318 | 0.736350 | −3766.080968 | −5210.929736 | −5210.193386 |

**Tab. 4.5.1** continued.

| | | | | | |
|---|---|---|---|---|---|
| **$(PPh_3)_2$** | −2072.721110 | 0.476761 | −2072.244349 | −2073.268594 | −2072.791833 |
| **29-[CuCl]** | −3980.012239 | 0.820812 | −3979.191427 | −5424.174232 | −5423.353420 |
| **31-[CuCl]** | −3940.707229 | 0.795193 | −3939.912036 | −5384.858998 | −5384.063805 |
| **46-[CuCl]** | −3920.846461 | 0.806710 | −3920.039751 | −5364.985509 | −5364.178799 |
| **47-[CuCl]** | −4058.671462 | 0.874427 | −4057.797035 | −5502.858232 | −5501.983805 |
| **48-[CuCl]** | −4019.366543 | 0.848446 | −4018.518098 | −5463.543039 | −5462.694593 |
| **49-[CuCl]** | −3999.505609 | 0.86148 | −3998.64413 | −5443.669408 | −5442.807928 |
| **$[Cu(MeCN)_4](OTf)$** | −1689.97118 | 0.146383 | −1689.824797 | −3133.834092 | −3133.687709 |
| **OTf** | −961.564283 | −0.005328 | −961.569611 | −961.933827 | −961.939155 |
| **29-$[Cu(MeCN)_2]$** | −2748.794377 | 0.650030 | −2748.144347 | −4192.753059 | −4192.103029 |
| **29-$[Cu(MeCN)_2](OTf)$** | −3710.396932 | 0.664917 | −3709.732015 | −5154.709075 | −5154.044158 |
| **31-$[Cu(MeCN)_2]$** | −2709.48962 | 0.62129 | −2708.86833 | −4153.438076 | −4152.816786 |
| **46-$[Cu(MeCN)_2]$** | −2689.62904 | 0.634183 | −2688.994857 | −4133.564788 | −4132.930605 |
| **47-$[Cu(MeCN)_2]$** | −1689.97118 | 0.146383 | −1689.824797 | −3133.834092 | −3133.687709 |
| **48-$[Cu(MeCN)_2]$** | −2788.14168 | 0.675968 | −2787.465712 | −4232.113485 | −4231.437517 |
| **$Rh(acac)(CO)_2$** | −682.578856 | 0.087247 | −682.491609 | −682.6275153 | −682.5402683 |
| **$(CO)_2$** | −226.609365 | −0.020255 | −226.629619 | −226.718016 | −226.738271 |
| **29-[Rh]** | −2741.873551 | 0.668912 | −2741.204639 | −2742.634491 | −2741.965579 |
| **31-[Rh]** | −2702.568609 | 0.642486 | −2701.926124 | −2703.319269 | −2702.676783 |
| **46-[Rh]** | −2682.707835 | 0.654826 | −2682.053009 | −2683.445784 | −2682.790958 |
| **47-[Rh]** | −2820.521013 | 0.724169 | −2819.796844 | −2821.305929 | −2820.58176 |
| **48-[Rh]** | −2781.216055 | 0.698229 | −2780.517825 | −2781.990731 | −2781.292502 |
| **49-[Rh]** | −2761.355221 | 0.710676 | −2760.644545 | −2762.117159 | −2761.406483 |

**Tab. 4.5.2** Complexes of **29**, **31**, **46**–**49** formed with [AuCl(tht)] in $CH_2Cl_2$ as solvent. Species shown in **Fig. 4.5.1** and **Fig. 4.5.6**.

| | **E(acn)/BS1** | **T,*S* correction** | **G(acn)/BS1** | **E(acn)/BS2** | **G(acn)/BS2** |
|---|---|---|---|---|---|
| **29** | −2285.931061 | 0.564332 | −2285.366729 | −2286.527880 | −2285.963548 |
| **31** | −2246.62652 | 0.538821 | −2246.087699 | −2247.213108 | −2246.674287 |
| **46** | −2226.765837 | 0.550448 | −2226.215389 | −2227.339668 | −2226.78922 |
| **47** | −2364.574996 | 0.62147 | −2363.953527 | −2365.195888 | −2364.574418 |
| **48** | −2325.270325 | 0.59426 | −2324.676065 | −2325.880991 | −2325.286731 |
| **49** | −2305.409665 | 0.608304 | −2304.80136 | −2306.007598 | −2305.399294 |
| **[AuCl(tht)]** | −1151.531381 | 0.078528 | −1151.452853 | −1151.660804 | −1151.582276 |
| **tht** | −555.4591474 | 0.085543 | −555.373604 | −555.5431972 | −555.4576542 |
| **29-[Au]** | −2882.032335 | 0.563729 | −2881.468606 | −2882.669949 | −2882.106220 |
| **31-[Au]** | −2842.727406 | 0.536118 | −2842.191288 | −2843.354766 | −2842.818648 |
| **46-[Au]** | −2822.86707 | 0.548425 | −2822.318644 | −2823.481666 | −2822.933241 |
| **47-[Au]** | −2960.689606 | 0.613951 | −2960.075655 | −2961.352336 | −2960.738385 |
| **48-[Au]** | −2921.384858 | 0.588663 | −2920.796195 | −2922.037391 | −2921.448728 |
| **49-[Au]** | −2901.524383 | 0.600037 | −2900.924345 | −2902.164143 | −2901.564106 |

## 4.6 Conclusion

This chapter focused on the complexation of different B9-substituted carboranylphosphines. The first goal was the DFT calculation of the most stable and therefore promising metal complexes formed from carboranylphosphine derivatives **29**, **31** and **46–49**. Once the computations were completed, the results had to be transferred into the laboratory.

According to the DFT calculations, the formation of different complexes synthesized from the ligands **29**, **31** and **46–49** and $Pd^{II}$, $Cu^{I}$, $Au^{I}$ and $Rh^{I}$ complexes should be mostly thermodynamically favored. The insertion of a $CH_2$ linker (ligands **47–49**) between the carborane cage and the phosphorus atoms further results in the formation of even more stable complexes.

Based on the computational results, experiments were conducted to synthesize the proposed complexes. Rhodium(I) complex **28-[Rh]**, gold(I) complex **29-[Au]**, and copper(I) complex **29-[CuCl]** could all be synthesized. Additionally, it was possible to proof the formation of Pd complex **29-[Pd]**, but due to its high reactivity, an isolation was not feasible. Unfortunately, no crystal structures for the complexes could be obtained, which would have helped to confirm the findings and, in some cases, aid to identify the reaction products.

Using an automated parallel library screening system at BASF SE, preliminary catalytic studies for the hydrogenation and hydroformylation of oct-1-ene and cyclohexene were conducted with various rhodium and ruthenium complex precursors and carboranylphosphine derivative **28**. The most promising systems were then transferred into an autoclave to test the reactions under reproducible conditions. All of those reactions could only be carried out once in the industrial setting. To get more significant results, more runs would have been required. Investigation of the catalytic species produced *in situ* from the metal complexes and ligands would have been required as well.

It would be essential to repeat several catalytic studies, look into the scope and limitations of the performed hydrogenation and hydroformylation, and further develop better catalytic systems in order to better comprehend the results.

## 4.7 References

[1] I. J. Bruno, J. C. Cole, P. R. Edgington, M. Kessler, C. F. Macrae, P. McCabe, J. Pearson, R. Taylor, *Acta Crystallogr. Sect. B Struct. Sci.* **2002**, *58*, 389–397.

[2] C. R. Groom, I. J. Bruno, M. P. Lightfoot, S. C. Ward, *Acta Crystallogr. Sect. B Struct. Sci. Cryst. Eng. Mater.* **2016**, *72*, 171–179.

[3] S. Paavola, R. Kivekäs, F. Teixidor, C. Viñas, *J. Organomet. Chem.* **2000**, *606*, 183–187.

[4] S. Paavola, F. Teixidor, C. Viñas, R. Kivekäs, *J. Organomet. Chem.* **2002**, *657*, 187–193.

[5] J.-M. Dou, D.-P. Zhang, D.-C. Li, D.-Q. Wang, *Polyhedron* **2007**, *26*, 719–724.

[6] R. Kivekäs, R. Sillanpää, F. Teixidor, C. Viñas, M. M. Abad, *Acta Chem. Scand.* **1996**, *50*, 499–504.

[7] F. Teixidor, C. Viñas, M. M. Abad, R. Kivekäs, R. Sillanpää, *J. Organomet. Chem.* **1996**, *509*, 139–150.

[8] A. Sterzik, E. Rys, S. Blaurock, E. Hey-Hawkins, *Polyhedron* **2001**, *20*, 3007–3014.

[9] D. Zhang, J. Dou, S. Gong, D. Li, D. Wang, *Appl. Organomet. Chem.* **2006**, *20*, 632–637.

[10] A. Alconchel, O. Crespo, P. García-Orduña, M. C. Gimeno, *Inorg. Chem.* **2021**, *60*, 18521–18528.

[11] O. Crespo, M. C. Gimeno, A. Laguna, P. G. Jones, *J. Chem. Soc. Dalton Trans.* **1992**, 1601–1605.

[12] O. Crespo, M. C. Gimeno, P. G. Jones, A. Laguna, *Inorg. Chem.* **1994**, *33*, 6128–6131.

[13] O. Crespo, M. C. Gimeno, P. G. Jones, A. Laguna, M. D. Villacampa, *Angew. Chem. Int. Ed. Engl.* **1997**, *36*, 993–995.

[14] M. Joost, A. Zeineddine, L. Estévez, S. Mallet–Ladeira, K. Miqueu, A. Amgoune, D. Bourissou, *J. Am. Chem. Soc.* **2014**, *136*, 14654–14657.

[15] M. Joost, L. Estévez, S. Mallet-Ladeira, K. Miqueu, A. Amgoune, D. Bourissou, *Angew. Chem. Int. Ed.* **2014**, *53*, 14512–14516, *Angew. Chem.* **2014**, *52*, 14740-14744.

[16] M. Joost, L. Estévez, K. Miqueu, A. Amgoune, D. Bourissou, *Angew. Chem. Int. Ed.* **2015**, *54*, 5236–5240.

[17] A. Zeineddine, F. Rekhroukh, E. D. Sosa Carrizo, S. Mallet-Ladeira, K. Miqueu, A. Amgoune, D. Bourissou, *Angew. Chem. Int. Ed.* **2018**, *57*, 1306–1310, *Angew. Chem.* **2018**, *5*, 1320–1324.

[18] M. Navarro, A. Toledo, M. Joost, A. Amgoune, S. Mallet-Ladeira, D. Bourissou, *Chem. Commun.* **2019**, *55*, 7974–7977.

[19] M. Navarro, A. Toledo, S. Mallet-Ladeira, E. D. Sosa Carrizo, K. Miqueu, D. Bourissou, *Chem. Sci.* **2020**, *11*, 2750–2758.

[20] O. Crespo, M. Concepción Gimeno, P. G. Jones, A. Laguna, *Inorg. Chem.* **1996**, *35*, 1361–1366.

[21] F. Huq, A. C. Skapski, *J. Cryst. Mol. Struct.* **1974**, *4*, 411–418.

[22] S. Bauer, S. Tschirschwitz, P. Lönnecke, R. Frank, B. Kirchner, M. L. Clarke, E. Hey-Hawkins,

*Eur. J. Inorg. Chem.* **2009**, *2009*, 2776–2788.

[23] S. Bauer, I. Maulana, P. Coburger, S. Tschirschwitz, P. Lönnecke, M. B. Sárosi, R. Frank, E. Hey-Hawkins, *ChemistrySelect* **2017**, *2*, 7407–7416.

[24] F. Teixidor, C. Viñas, M. M. Abad, C. Whitaker, J. Rius, *Organometallics* **1996**, *15*, 3154–3160.

[25] C. Fischer, R. Thede, H. J. Drexler, A. König, W. Baumann, D. Heller, *Chem. Eur. J.* **2012**, *18*, 11920–11928.

[26] L. I. Zakharkin, M. G. Meiramov, V. A. Antonovich, A. V. Kazantsev, A. I. Yanovsky, Y. T. Struchkov, *Zhurnal Obs. Khimii* **1983**, *53*, 90–97.

[27] A. V. Polyakov, A. I. Yanovsky, Y. T. Struchkov, V. N. Kalinin, A. V. Usatov, L. I. Zakharkin, *Russ. J. Coord. Chem.* **1988**, *14*, 1278.

[28] D.-H. Kim, L. Heung-Sae, J. Ko, K. Park, S.-I. Cho, J.-I. Shon, S. O. Kang, *Bull. Korean Chem. Soc.* **1999**, *20*, 600–604.

[29] T. Lee, S. W. Lee, H. G. Jang, S. O. Kang, J. Ko, *Organometallics* **2001**, *20*, 741–748.

[30] H.-S. Lee, J.-Y. Bae, D.-H. Kim, H. S. Kim, S.-J. Kim, S. Cho, J. Ko, S. O. Kang, *Organometallics* **2002**, *21*, 210–219.

[31] A. S. King, G. Ferguson, J. F. Britten, J. F. Valliant, *Inorg. Chem.* **2004**, *43*, 3507–3513.

[32] R. E. Marsh, *Acta Crystallogr. Sect. B Struct. Sci.* **2004**, *60*, 252–253.

[33] J.-D. Lee, J. Ko, M. Cheong, S. O. Kang, *Organometallics* **2005**, *24*, 5845–5852.

[34] T. Kim, J. Lee, S. U. Lee, M. H. Lee, *Organometallics* **2015**, *34*, 3455–3458.

[35] M. D. Brown, W. Levason, G. Reid, R. Watts, *Polyhedron* **2005**, *24*, 75–87.

[36] R. Kivekäs, R. Sillanpää, F. Teixidor, C. Viñas, R. Nunez, *Acta Crystallogr. Sect. C Cryst. Struct. Commun.* **1994**, *50*, 2027–2030.

[37] N. Braussaud, T. Rüther, K. J. Cavell, B. W. Skelton, A. H. White, *Synthesis* **2001**, *2001*, 0626–0632.

[38] S. Burck, S. G. A. Van Assema, B. Lastdrager, J. C. Slootweg, A. W. Ehlers, J. M. Otero, B. Dacunha-Marinho, A. L. Llamas-Saiz, M. Overhand, M. J. Van Raaij, K. Lammertsma, *Chem. Eur. J.* **2009**, *15*, 8134–8145.

[42] N. Launay, M. Slany, A.-M. Caminade, J. P. Majoral, *J. Org. Chem.* **1996**, *61*, 3799–3805.

[43] E. V. Oleshkevich, E. G. Rys, V. V. Bashilov, P. V. Petrovskii, V. A. Ol'shevskaya, S. K. Moiseev, A. B. Ponomaryov, V. N. Kalinin, *Russ. J. Gen. Chem.* **2017**, *87*, 2589–2595.

[44] R. E. Islas, J. Cárdenas, R. Gaviño, E. García-Ríos, L. Lomas-Romero, J. A. Morales-Serna, *RSC Adv.* **2017**, *7*, 9780–9789.

[45] V. P. Balema, F. Somoza, E. Hey-Hawkins, *J. Inorg. Chem* **1998**, 651–656.

[46] S. Al-Baker, W. E. Hill, C. A. McAuliffe, *J. Chem. Soc. Dalton Trans.* **1985**, 1387–1390.

[47] F. A. Hart, D. W. Owen, *Inorg. Chim. Acta* **1985**, *103*, L1–L2.

[48] G. Dyer, R. M. Wharf, W. E. Hill, *Inorg. Chim. Acta* **1987**, *133*, 137–140.

[49] A. Demonceau, F. Simal, A. F. Noels, C. Viñas, R. Nuñez, F. Teixidor, *Tetrahedron Lett.* **1997**, *38*, 4079–4082.

[50] F. Simal, S. Sebille, A. Demonceau, A. F. Noels, R. Nuñez, M. Abad, F. Teixidor, C. Viñas, *Tetrahedron Lett.* **2000**, *41*, 5347–5351.

[51] I. B. Sivaev, M. Y. Stogniy, V. I. Bregadze, *Coord. Chem. Rev.* **2021**, *436*, 213795.

[52] C. U. Pittman, A. Hirao, *J. Org. Chem.* **1978**, *43*, 640–646.

[53] J. C. Carretero, R. G. Arrayás in *Encyclopedia of reagents for organic synthesis* (Ed.: L. A. Paquette), Wiley, New York, Chichester, **1995**.

[54] R. Uson, A. Laguna, M. Laguna, D. A. Briggs, H. H. Murray, J. P. Fackler, John Wiley & Sons, Ltd, **1989**, pp. 85–91.

[55] M. Keener, C. Hunt, T. G. Carroll, V. Kampel, R. Dobrovetsky, T. W. Hayton, G. Ménard, *Nature* **2020**, *577*, 652–655.

[56] MestReNova (v. 14.1.0), Mestrelab Research S.L., **2019**.

[57] M. J. Frisch, G. W. Trucks, H. B. Schlegel, G. E. Scuseria, M. A. Robb, J. R. Cheeseman, G. Scalmani, V. Barone, G. A. Petersson, H. Nakatsuji, X. Li, M. Caricato, A. V. Marenich, J. Bloino, B. G. Janesko, R. Gomperts, B. Mennucci, H. P. Hratchian, J. V. Ortiz, A. F. Izmaylov, J. L. Sonnenberg, D. Williams-Young, F. Ding, F. Lipparini, F. Egidi, J. Goings, B. Peng, A. Petrone, T. Henderson, D. Ranasinghe, V. G. Zakrzewski, J. Gao, N. Rega, G. Zheng, W. Liang, M. Hada, M. Ehara, K. Toyota, R. Fukuda, J. Hasegawa, M. Ishida, T. Nakajima, Y. Honda, O. Kitao, H. Nakai, T. Vreven, K. Throssell, J. A. Montgomery, Jr., J. E. Peralta, F. Ogliaro, M. J. Bearpark, J. J. Heyd, E. N. Brothers, K. N. Kudin, V. N. Staroverov, T. A. Keith, R. Kobayashi, J. Normand, K. Raghavachari, A. P. Rendell, J. C. Burant, S. S. Iyengar, J. Tomasi, M. Cossi, J. M. Millam, M. Klene, C. Adamo, R. Cammi, J. W. Ochterski, R. L. Martin, K. Morokuma, O. Farkas, J. B. Foresman, and D. J. Fox, Gaussian 16, Revision C.01, Gaussian, Inc., Wallingford CT, **2016**.

[58] C. Lee, W. Yang, R. G. Parr, *Phys. Rev. B. Condens. Matter* **1988**, *37*, 785–789.

[59] B. Miehlich, A. Savin, H. Stoll, H. Preuss, *Chem. Phys. Lett.* **1989**, *157*, 200–206.

[60] A. D. Becke, *J. Chem. Phys.* **1993**, *98*, 5648–5652.

[61] S. Grimme, J. Antony, S. Ehrlich, H. Krieg, *J. Chem. Phys.* **2010**, *132*, 154104.

[62] W. J. Hehre, R. Ditchfield, J. A. Pople, *J. Chem. Phys.* **1972**, *56*, 2257–2261.

[63] M. M. Francl, W. J. Pietro, W. J. Hehre, J. S. Binkley, M. S. Gordon, D. J. DeFrees, J. A. Pople, *J. Chem. Phys.* **1982**, *77*, 3654–3665.

[64] D. Andrae, U. Häußermann, M. Dolg, H. Stoll, H. Preuß, *Theor. Chim. Acta* **1990**, *77*, 123–141.

[65] A. W. Ehlers, M. Böhme, S. Dapprich, A. Gobbi, A. Höllwarth, V. Jonas, K. F. Köhler, R. Stegmann, A. Veldkamp, G. Frenking, *Chem. Phys. Lett.* **1993**, *208*, 111–114.

[66] A. V. Marenich, C. J. Cramer, D. G. Truhlar, *J. Phys. Chem. B* **2009**, *113*, 6378–6396.

[66] A. V. Marenich, C. J. Cramer, D. G. Truhlar, *J. Phys. Chem. B* **2009**, *113*, 6378–6396.

[67] F. Weigend, R. Ahlrichs, *Phys. Chem. Chem. Phys.* **2005**, *7*, 3297–3305.

[68] F. Weigend, *Phys. Chem. Chem. Phys.* **2006**, *8*, 1057–1065.

[69] V. S. Bryantsev, M. S. Diallo, W. A. Goddard III, *J. Phys. Chem. B* **2008**, *112*, 9709–9719.

# Chapter 5: Summary and future perspectives

# 5 Summary and future perspectives

This dissertation project aimed at preparing, characterizing, and utilizing a new ligand system for challenging catalytic transformations. The system was built on two chemical building blocks: a PPH dendritic framework (Chapter 2), already known for its catalytic application and carboranylphosphine monomeric units (Chapter 3), already investigated towards their interesting complexation behavior[1,2] and a few catalytic applications.[3] To combine both constructs, first a synthetic strategy for the suitable functionalization of the B9 position of the carboranylphosphines for anchoring them to supports, namely dendrimers, was developed. The second step was the investigation of different methods of linking them to the dendritic backbone. With respect to the work of CAMINADE and co-workers on PPH dendrimers,[4–6] different dendritic phosphorus-containing scaffolds including symmetrical and unsymmetrical PPH dendrimers were chosen as the starting point for an anchoring. Based on previous work of HART and OWEN[7] and the HEY-HAWKINS group[8] on carboranylphosphines and their complexes, 1,2-bis(di-phenylphosphino)-*ortho*-carborane was chosen as a suitable monomeric unit for further investigations (see **Scheme 5.1**).

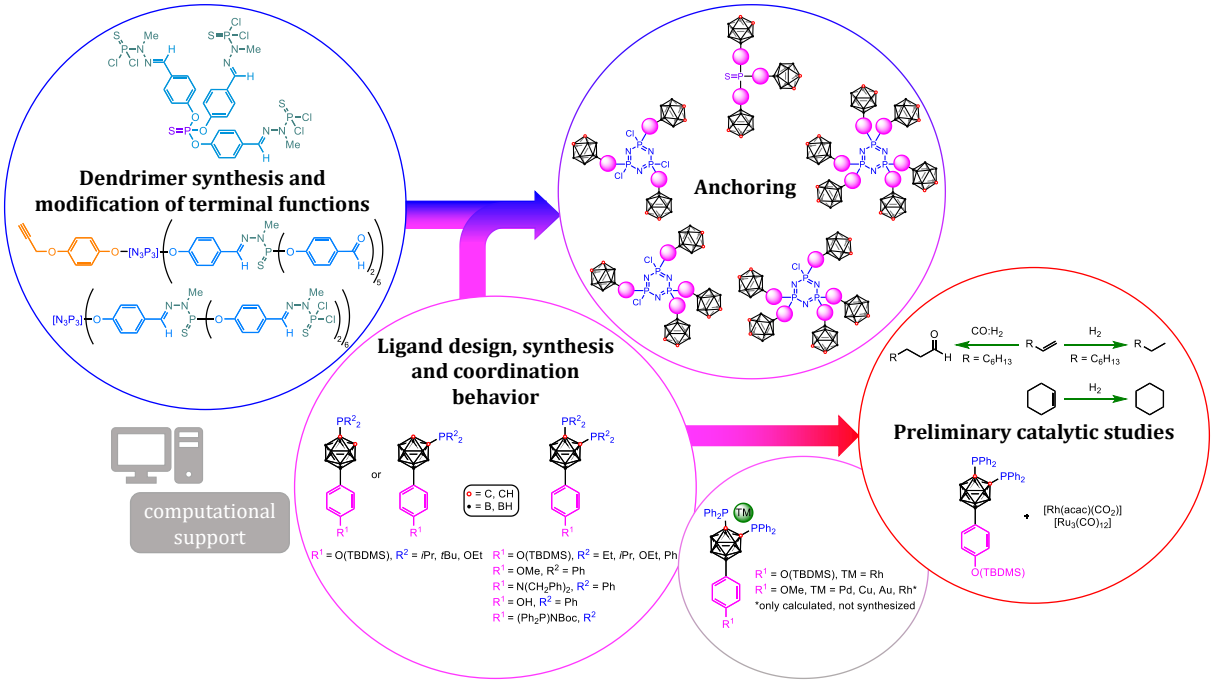


**Scheme 5.1.** Schematic overview of the major results obtained in the doctoral project. TM = transition metal.

## 5.1 Preparation of the monomers and dendrimers

The synthesis of different dendritic compounds starting from a $P(S)Cl_3$ (**1-S0**) or an $N_3P_3Cl_6$ core (**1-G0**) was performed (Chapter 2). Several classical dendrimers were obtained in good yields (62–98%) and acceptable purities up to generation **1-G2** or **2-S1**, respectively (see **Scheme 5.1.1**). The reiterative synthetic process, which entails a condensation reaction with the

phosphorhydrazide $H_2NNMeP(S)Cl_2$ and a substitution reaction with 4-hydroxybenzaldehyde, was applied, but it could be shown that the established protocols are vulnerable.

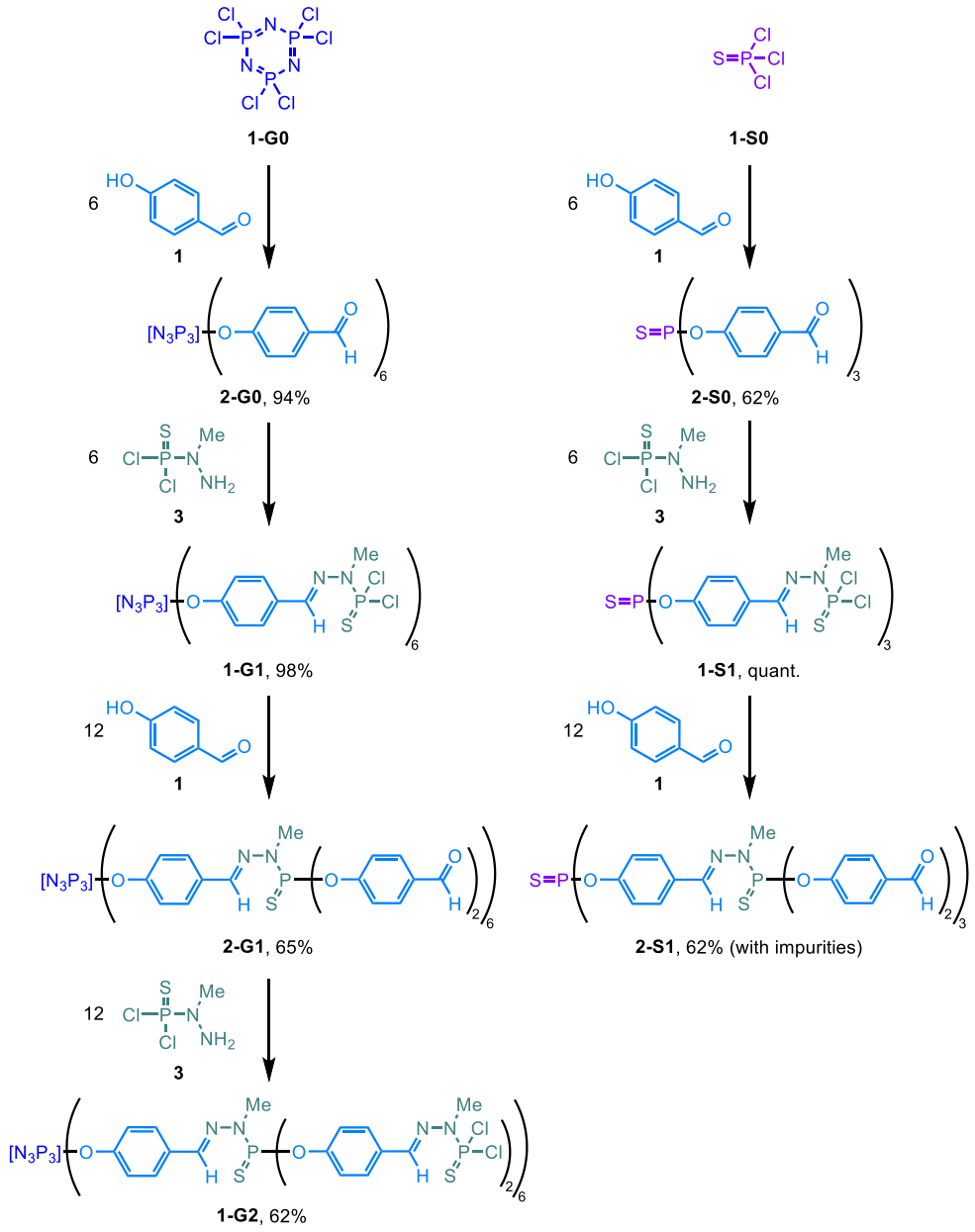


**Scheme 5.1.1.** Overview of the synthetic steps yielding various classical dendrimers and dendritic phosphorus-containing scaffolds in the doctoral project.

Although the terminal functions of PPH dendrimers are often similar, having two different types of terminal functions can be advantageous. For this reason, a specific functionalization of the $N_3P_3$ core was targeted, with at least one function different from the others. Different unsymmetrical $AB_5$ monomers and dendrimers, with one function distinct from the others up to generation **$AB_5$-2-G1** (A = 4-(prop-2-yn-1-yloxy)phenol, B = 4-hydroxybenzaldehyde, see **Scheme 5.1.2**) have been prepared. Additionally, to the synthesis of the unsymmetrical $AB_5$ dendrimers, also a specific functionalization of only half of the terminal P–Cl groups in **1-G0** and **1-G1** was targeted to obtain

further dendritic backbones for the anchoring of different carboranes and carboranylphosphines. Problems were particularly evident during the stochastic monofunctionalization and purification of typical dendrimers.

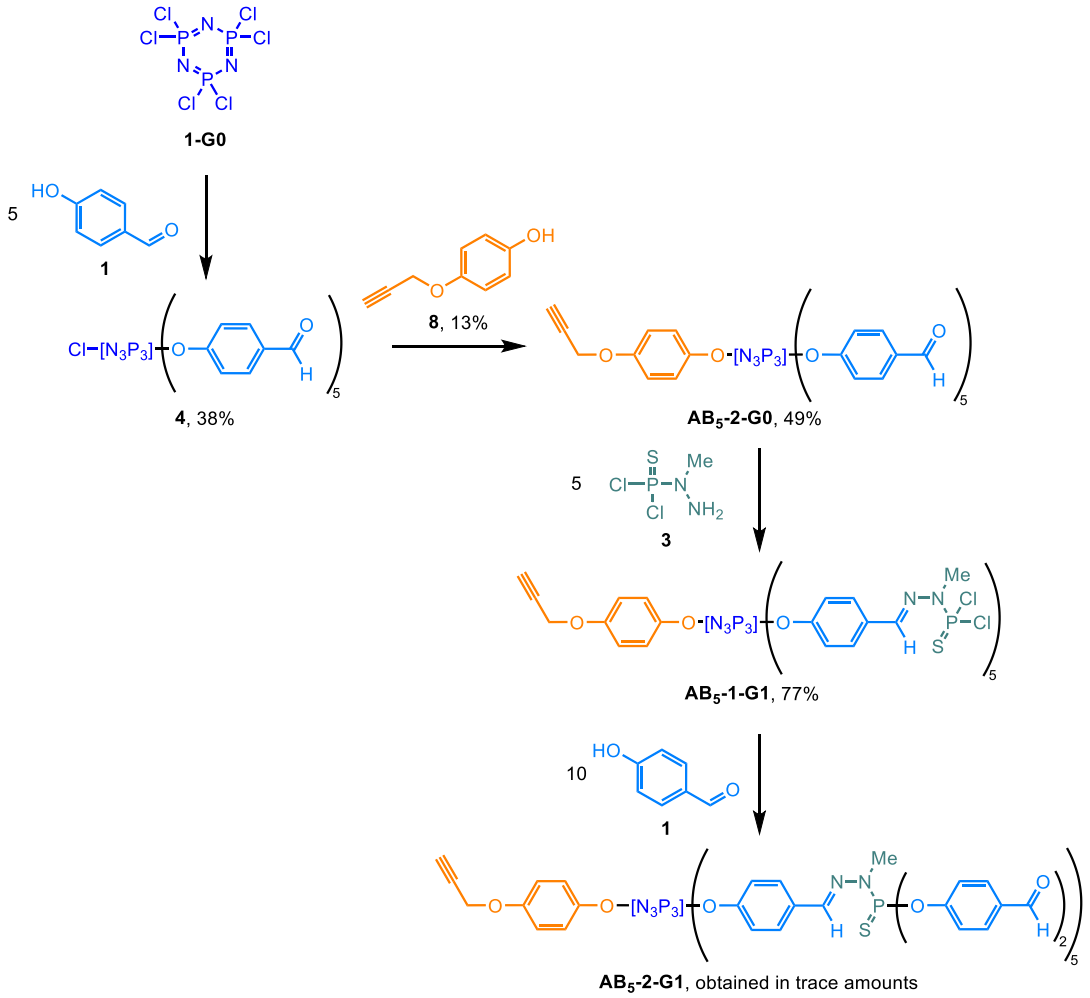


**Scheme 5.1.2.** Overview of the synthetic steps yielding various unsymmetrical $AB_5$ monomers and dendrimers in the doctoral project.

Starting from 1,2-dicarba-*closo*-dodecaboranes(12) (*ortho* isomer, **14**) a selection of different B9-substituted carboranes has been prepared. An adaption of the synthetic phosphorylation protocol of ALEXANDER and SCHROEDER[9] that had been used to prepare 1,2-phosphanyl-substituted carborane derivatives in the past was applied and modified yielding novel 1- or 1,2-phosphanyl-substituted carborane derivatives in low to excellent yields (7–95%, see **Scheme 5.1.3**).

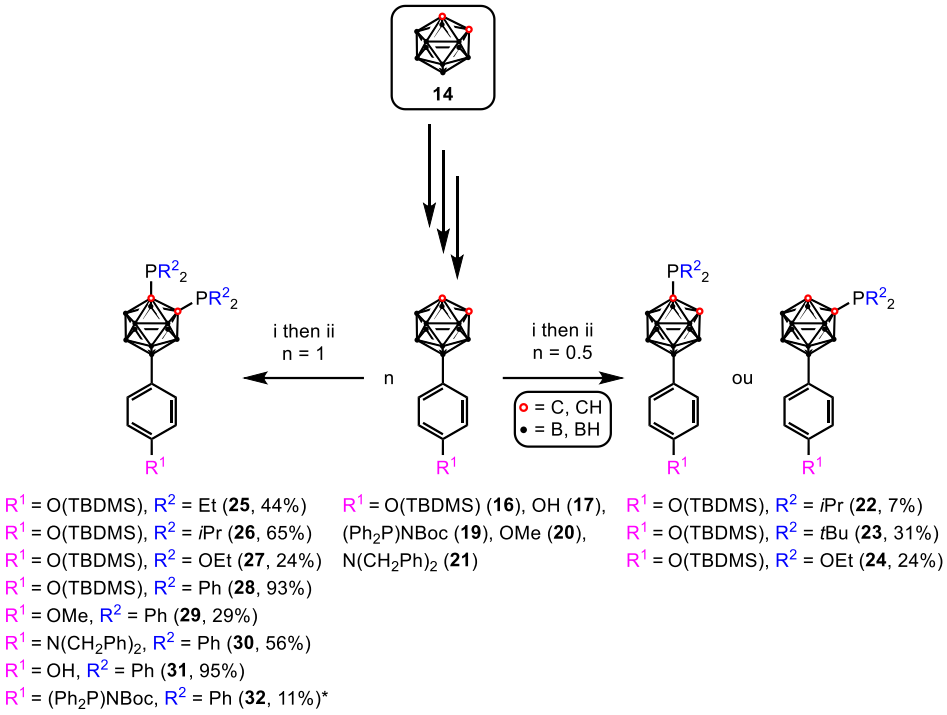


**Scheme 5.1.3.** Synthesis of B9-substituted carboranylphosphines. (i) *n*-butyllithium, $Et_2O$ or THF, −78 °C to rt; (ii) $PR^2_2Cl$, $Et_2O$ or THF, −78 °C / 0 °C to rt. *The NH group in **19** was also substituted by $PPh_2$.

While isolated side products revealed the highly stoichiometry-dependent nature of the phosphorylation step, which in the future could be used to more easily access unsymmetrically substituted phosphines, these crystalline materials frequently allowed for the elucidation of their solid-state structures (see **Fig. 5.1.1** and **Fig. 5.1.2**). The synthesized carboranes and carboranylphosphines have C1–C2 ($C_{Cage}$–$C_{Cage}$) bond lengths that are comparable to other known compounds. The electronic and steric impact of the substituents on the P atoms causes a considerable increase in bond length in disubstituted compounds. The mean C–P bond lengths and P···P distances of the carboranylphosphines are consistent with previously described compounds. The obtained results revealed that various substituents in the B9 position have only a minimal effect on the C1–C2 and C–P bond lengths, whereas the substituents at the phosphorus atom have a significant influence. Only a few examples of the functionalized B9-position in carboranylphosphines have previously been documented.[2] This project led to new synthetic protection and deprotection strategies to modify the carborane cage further.

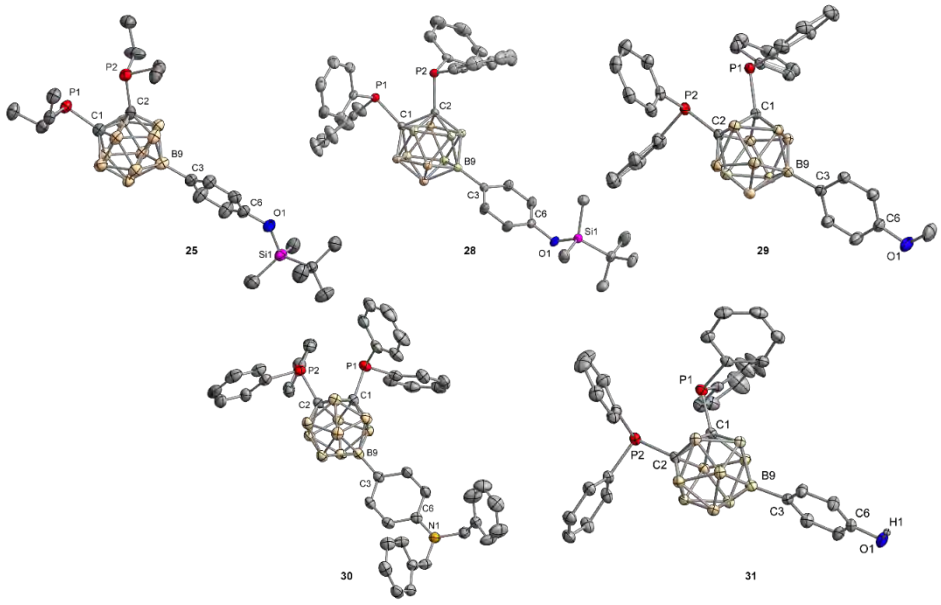


**Fig. 5.1.1.** Molecular structures of carboranylphosphines **25** and **28**–**31** in the solid state with thermal ellipsoids drawn at the 50% probability level. Hydrogen atoms other than OH in **31** are omitted for clarity.

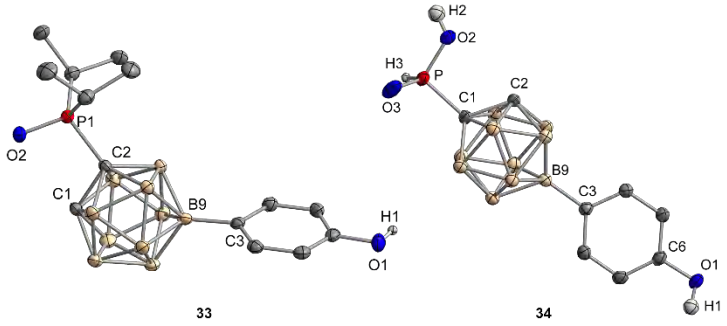


**Fig. 5.1.2.** Molecular structures of carboranylphosphines **33** and **34** in the solid state with thermal ellipsoids drawn at the 50% probability level. Hydrogen atoms other than OH and PH are omitted for clarity.

## 5.2 Coordination behavior

Bearing two phosphorus groups in close proximity, the new carboranylphosphines resemble already known bidentate phosphines and might be promising ligands for the complexation of different transition metals useful for homogeneous catalysis.

Especially, the tunability of the steric and electronic properties of the carboranylphosphines allowed the synthesis of new ligands needed for the complexation of different transition metals (Pd, Cu, Au, Rh, Ru). Prompted by the close proximity of both phosphorus atoms when directly attached to the carborane cage (similar to an ethylene or *ortho*-phenylene moiety), the capability to accommodate different transition metals in a 1:1 coordination mode was investigated. According to DFT calculations performed with different B9-substituted carboranylphosphines (**29, 31** and **46**–**49**), in most cases the formation of transition metal complexes from these ligands and different complex precursors should be

thermodynamically favored (see **Tab. 5.2.1** and **Fig. 5.2.1**). More stable complexes can be formed after a $CH_2$ linker is inserted between the carborane cage and the phosphorus atoms. Experiments were carried out to find synthetic proof. Unfortunately, it was not possible to form any complexes with the ligands **47–49** or **53**.

**Tab. 5.2.1.** Computed GIBBS energies [kcal mol$^{-1}$] of complexes formed with ligands **29, 31, 46–49** and different metal complex precursors in THF or $CH_2Cl_2$ as solvents, relative to the starting materials.

| | Carboranylphosphine | 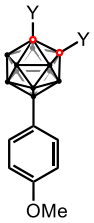 | 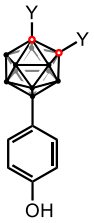 | 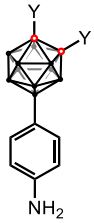 |
|---|---|---|---|---|
| | Metal complex precursor (solvent for calculation) | OMe | OH | $NH_2$ |
| **Y = $PPh_2$ (29, 31, 46)** | [AuCl(tht)] ($CH_2Cl_2$) | –13.2 | –14.3 | –14.1 |
| | [$PdCl_2(MeCN)_2$] (THF) | –42.0 | –42.1 | –20.9 |
| | [$Cu(MeCN)_4$](OTf) (THF) | +6.0 | +4.5 | +4.9 |
| | [$CuCl(PPh_3)_3$] (THF) | –0.2 | +0.4 | +0.1 |
| | [$Rh(acac)(CO)_2$] (THF) | –63.0 | –62.9 | –62.7 |
| **Y = $CH_2PPh_2$ (47–49)** | [AuCl(tht)] ($CH_2Cl_2$) | –24.7 | –23.5 | –25.2 |
| | [$PdCl_2(MeCN)_2$] (THF) | –42.4 | –41.9 | –42.5 |
| | [$Cu(MeCN)_4$](OTf) (THF) | +0.5 | –0.9 | not computed |
| | [$CuCl(PPh_3)_3$] (THF) | –10.3 | –9.4 | –9.2 |
| | [$Rh(acac)(CO)_2$] (THF) | –134.2 | –133.3 | –133.5 |

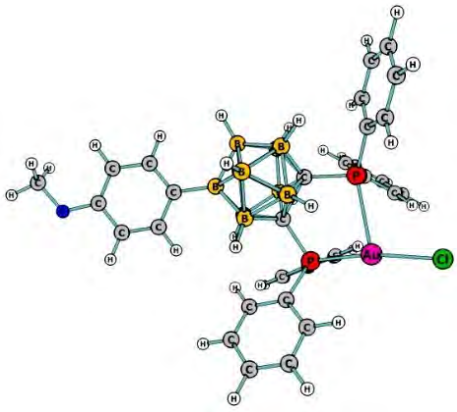

**29-[Au]**

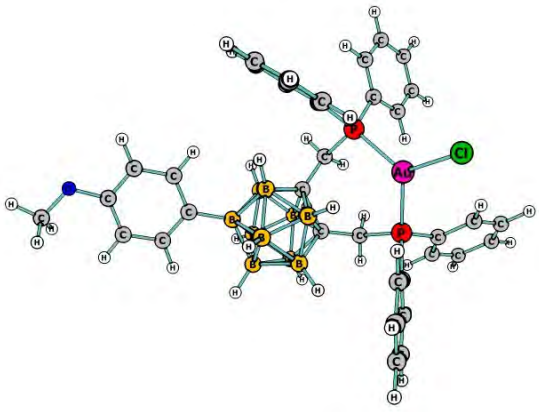

**47-[Au]**

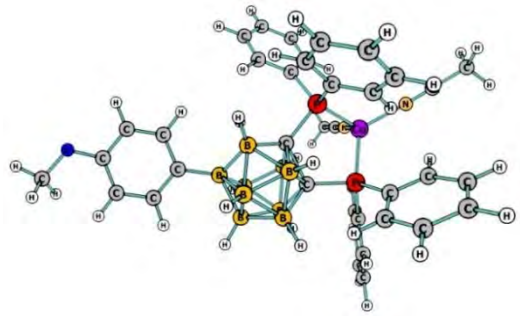

**29-[Cu(MeCN)$_2$]**

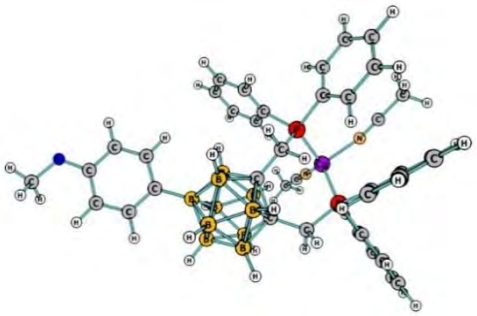

**47-[Cu(MeCN)$_2$]**

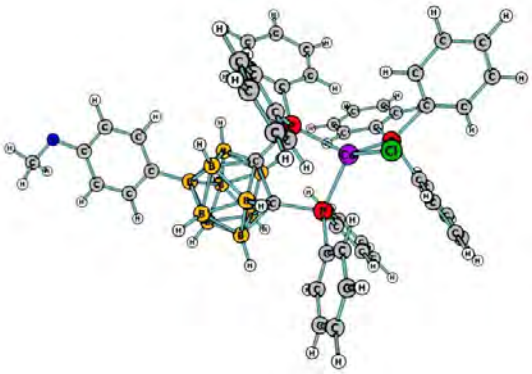

**29-[CuCl]**

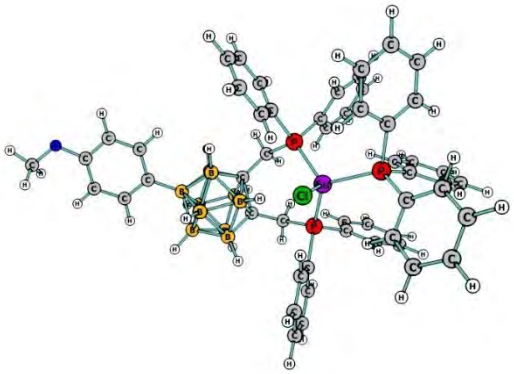

**47-[CuCl]**

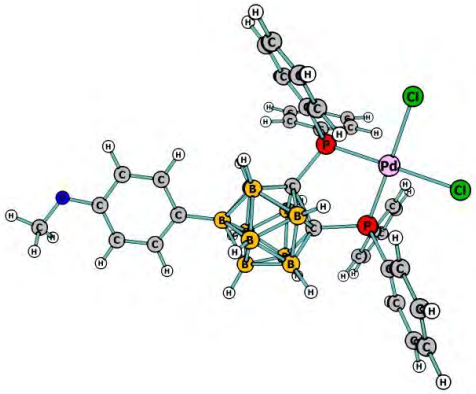

**29-[Pd]**

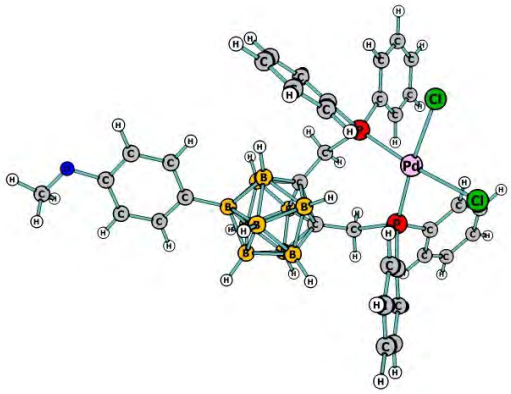

**47-[Pd]**

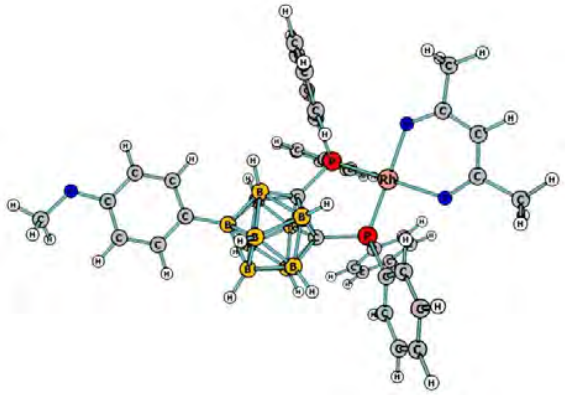

**29-[Rh]**

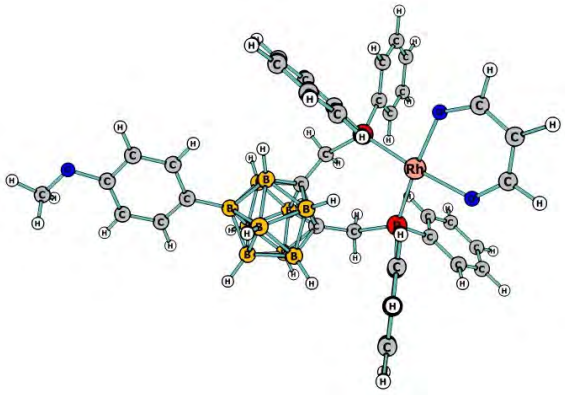

**47-[Rh]**

**Fig. 5.2.1.** Computed complexes formed from 9-(4-MeO-$C_6H_4$)-1,2-bis(diphenylphosphino)- (**29**) and 9-(4-MeO-$C_6H_4$)-1,2-bis[(diphenylphosphino)methyl]-*ortho*-carborane (**47**) and different metal complex precursors. All hydrogen atoms are omitted for clarity. The triflate anion in **29-** and **47-[Cu(MeCN)$_2$]** was optimized separately. The optimized structures obtained for other B9 substituents are not displayed.

For this reason, only the monomeric carboranylphosphine derivatives 9-(TBDMS)O-$C_6H_4$-1,2-$(PPh_2)_2$-$C_2B_{10}H_9$ (**28**) and 9-(4-MeO-$C_6H_4$)-1,2-$(PPh_2)_2$-$C_2B_{10}H_9$ (**29**) have been used for the first complexation experiments with a $Pd^{II}$, two $Cu^{I}$, an $Au^{I}$, a $Rh^{I}$, and a $Ru^{0}$ complex precursor. The silyl ether protected carboranylphosphine **28** was the most available of all compounds produced throughout the practical work of the dissertation. The methoxyphenyl substituent in **29** mimics the phenoxy linker needed in immobilization reactions. It can be considered as the monomeric equivalent of the carboranyl-substituted dendrimers (as described in Chapter 3). Rhodium(I) complex **28-[Rh]**, gold(I) complex **29-[Au]**, and copper(I) complex **29-[CuCl]** could be synthesized and characterized by NMR spectroscopy and mass spectrometry. Additionally, it was possible to proof the formation of $Pd^{II}$ complex **29-[Pd]**, but due to its high reactivity, an isolation was not feasible. Instead the dimeric hydrolysis product, $Pd^{II}$ complex **56**, was isolated (see **Fig. 5.2.1**).

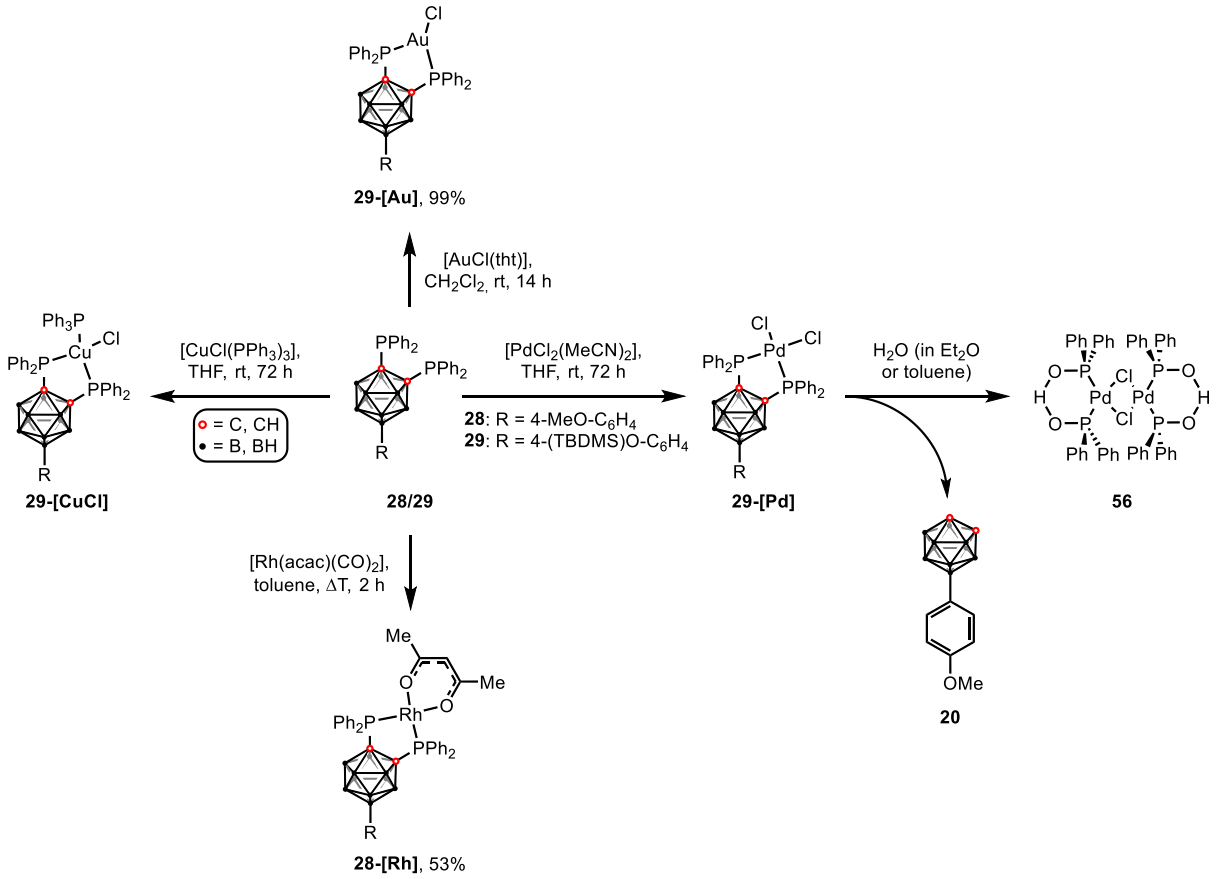


**Scheme 5.2.1.** Overview of the synthesis of different carboranylphosphine transition metal complexes.

## 5.3 Preliminary catalytic investigations

Using an automated parallel library screening system at BASF SE, preliminary catalytic studies for the hydrogenation and hydroformylation of oct-1-ene and cyclohexene were conducted with various rhodium and ruthenium complex precursors and 9-(4-TBDMSO-$C_6H_4$)-1,2-$(PPh_2)_2$-$C_2B_{10}H_9$ (**28**). The most promising systems were then transferred into an autoclave to test the

reactions under reproducible conditions. Ligand **28** showed the best performance for the hydrogenation of oct-1-ene with $[Rh(acac)(CO)_2]$ performing better than already known systems. It further showed a better conversion in the hydrogenation of cyclohexene with $[Ru_3(CO)_{12}]$ than the non-substituted carboranylphosphine derivative 1,2-bis(diphenylphosphino)-*ortho*-carborane (dppc, **73**), but worked not as good as a simple bisphosphine, namely 1,2-bis(diphenylphosphino)-benzene (dppb, **67**). Despite the fact that several of the reactions demonstrated good conversion, the selectivity is not superior to other known systems; hence these systems were not subjected to additional testing in an industrial setting. However, to get more significant results, further runs would have been required. Investigation of the catalytic species produced *in situ* from the metal complexes and ligands would have been required as well. It would be essential to repeat several catalytic studies, look into the scope and limitations of the performed hydrogenation and hydroformylation, and further develop better catalytic systems in order to better comprehend the results.

## 5.4 Anchoring of carboranes and polyphosphorhydrazone dendrimers

Various dendritic compounds were evaluated for their suitability of being grafted to various new phenol-linked carboranes and carboranylphosphines. DFT calculations have proven that the reaction proceeds similar to an $S_N2$ reaction, with the nucleophilic phenoxide **17*** approaching the electrophilic phosphorus center of the $N_3P_3Cl_6$ core opposite to the leaving group $Cl^-$. Products of multiple substitution reactions with **17*** were also optimized to computationally check the stability of such products. It could be shown that the six-fold substitution of **1-G0** forms a product with greater stability by 194.5 kcal $mol^{-1}$ relative to the starting material (see **Scheme 5.4.1**).

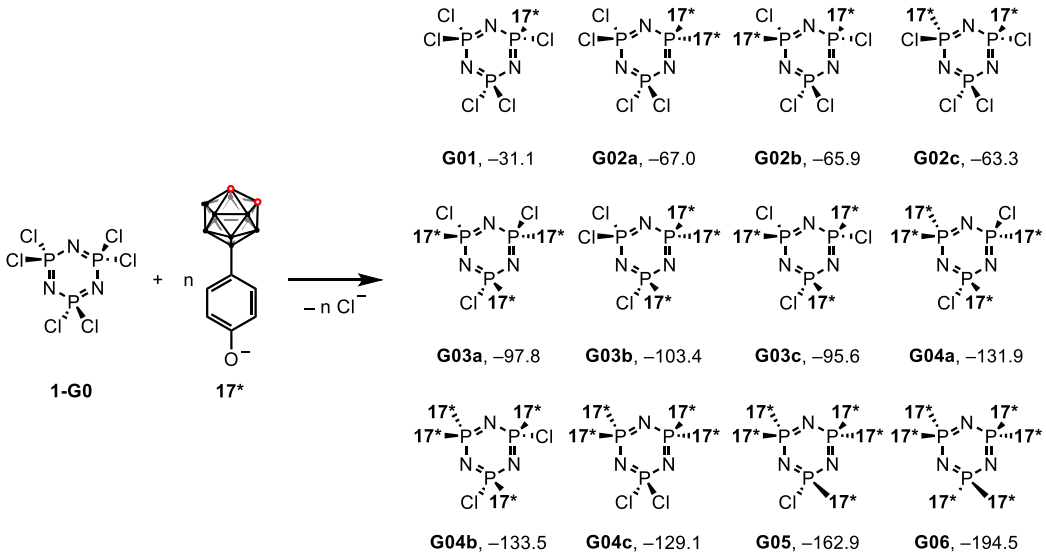


**Scheme 5.4.1.** Computed GIBBS energy values in THF as solvent (in kcal $mol^{-1}$) for the substitution of **1-G0** with n equivalents of **17*** relative to the starting material.

As calculations support the possibility of multiple substitution of chloride centers in $N_3P_3Cl_6$ by carboranyl groups, this hypothesis was experimentally checked (see **Scheme 5.4.2**).

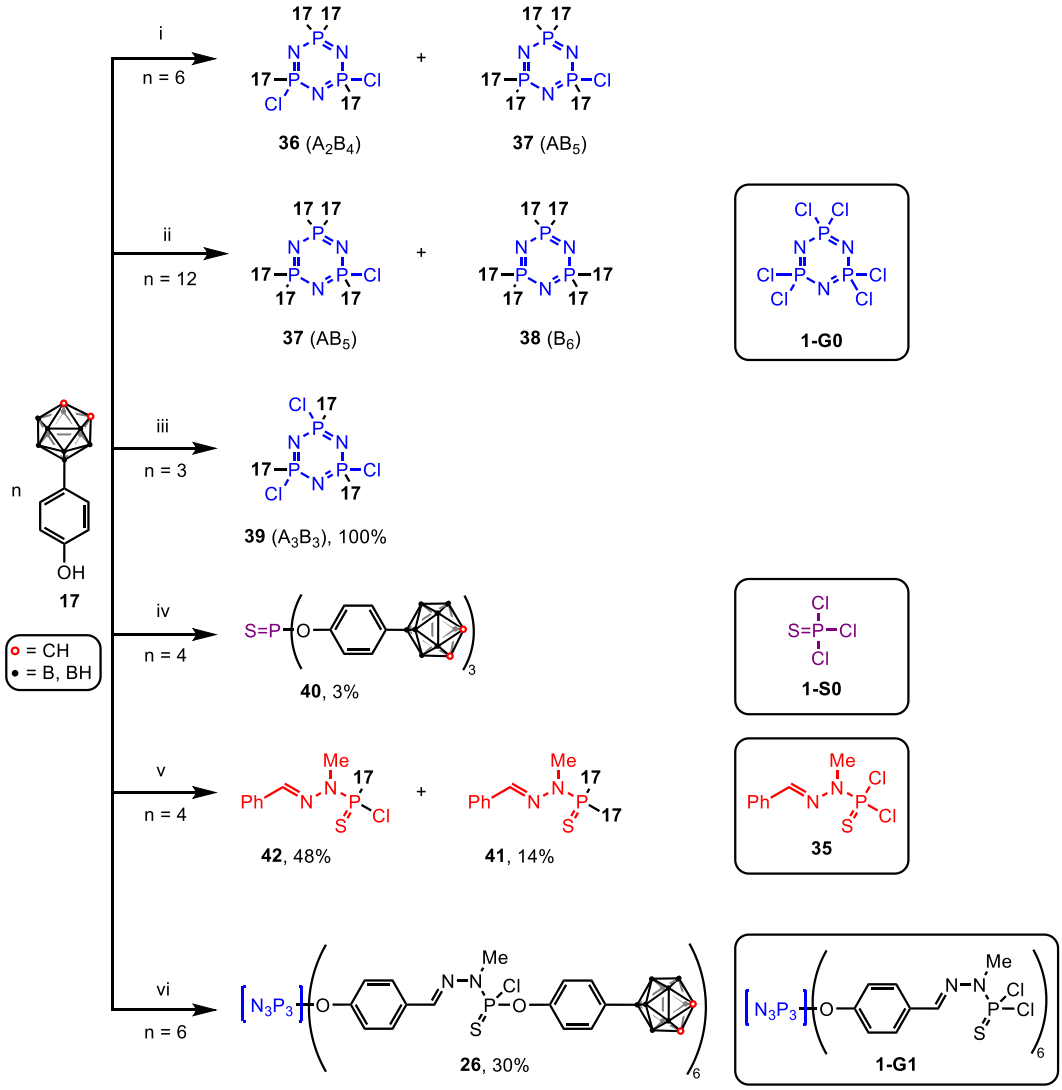


**Scheme 5.4.2.** Reaction of different equivalents of **17** with the $N_3P_3Cl_6$ core **1-G0**, $P(S)Cl_3$ **1-S0** and model molecule **35**. Conditions: (i) **1-G0**, $K_2CO_3$, acetone, 40 °C for 120 h, then rt for 72 h; (ii) **1-G0**, $C_2CO_3$, THF, rt, 25 d; (iii) **1-G0**, $K_2CO_3$, acetone, rt, 72 h; (iv) **1-S0**, $Cs_2CO_3$, THF, 40 °C, 96 h; (v) **35**, DBU, THF, rt, 72 h; (vi) **1-G1**, $Cs_2CO_3$, THF, rt for 72 h, then 40 °C for 23 h. All compounds were analyzed by NMR spectroscopy and ESI-MS. Only one isomer of the incompletely substituted dendrimers ($A_3B_3$, $A_2B_4$) is displayed.

A grafting to the model molecule **35**, to different phosphorus-containing compounds **1-G0** and **1-S0** as well as to dendrimer **1-G1** was tested. Despite the lack of a full substitution with a carboranylphosphine, novel carborane-substituted dendritic compounds were synthesized. Further, the selective grafting of a single carborane per $P(S)Cl_2$ function was investigated yielding a monofunctionalized dendrimer **43** (**Fig. 5.4.1**).

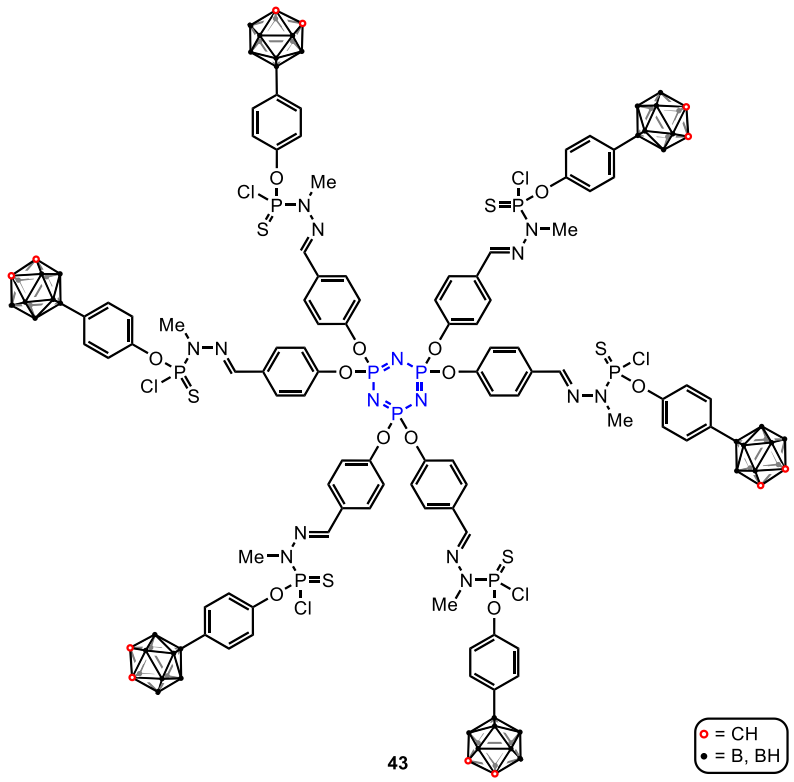


**Fig. 5.4.1.** Full structure of dendrimer **43**.

Yet, the separation process of differently carborane-substituted dendrimers is still a focus of investigation. Also, the selective grafting of a single carborane per $P(S)Cl_2$ function should be investigated for other generations of dendrimers because it will open the way to the grafting of additional functionalities to replace the remaining Cl, for instance with water-solubilizing functions, in view of biological experiments.[10]

## 5.5 In a nutshell

Several *ortho*-carboranes bearing a phenoxy or a phenylamino group in the B9 position were prepared employing various protection and deprotection strategies. Furthermore, the synthetic access to novel 1- or 1,2-phosphanyl-substituted carborane derivatives was developed in this dissertation project. The resulting diethyl-, diisopropyl-, di-*tert*-butyl-, diphenyl- or diethoxyphosphines bearing a tunable *ortho*-carborane moiety are intriguing ligands for future applications in homogeneous catalysis or the medicinal sector. The ligand framework has shown a distinctive coordination behavior to different transition metals in a 1:1 coordination mode by the chelating carboranylbisphosphines. A catalyst generated *in situ* from a mixture of Rh or Ru complex precursors and carboranylbisphosphine derivative **28** could be used for the hydrogenation and hydroformylation of unsaturated olefins.

Following established protocols, dendritic compounds were synthesized from a hexachlorocyclotriphosphazene or thiophosphoryl chloride core, and possible anchoring options for the B9-substituted *ortho*-carboranes were investigated experimentally and theoretically

(DFT). In spite of the synthetic challenges, different carborane-containing dendrimers could be obtained and the results should open the door to the synthesis of carboranylphosphine-containing dendrimers in order to improve the catalytic performance and exploring new reaction pathways. Following studies on differently substituted carboranylphosphines as well as other catalytic applications would be highly interesting. So far, only electron-deficient C–P carboranylphosphines were utilized for the anchoring. Changing the system to electron-rich B–P carboranylphosphines (similar to the work of SPOKOYNY and co-workers)[11] linking the carboranes *via* their $C_{Cage}$ atoms to the dendrimers could be an interesting switch. It is obvious that the research in this field is not exhausted, and depending on the approach chosen, a lot of interesting results can certainly be obtained.

## 5.6 References

[1] I. B. Sivaev, M. Y. Stogniy, V. I. Bregadze, *Coord. Chem. Rev.* **2021**, *436*, 213795.

[2] E. V. Oleshkevich, E. G. Rys, V. V. Bashilov, P. V. Petrovskii, V. A. Ol'shevskaya, S. K. Moiseev, A. B. Ponomaryov, V. N. Kalinin, *Russ. J. Gen. Chem.* **2017**, *87*, 2589–2595.

[3] S. Bauer, E. Hey-Hawkins in *Boron Science* (Ed.: N. S. Hosmane), CRC Press, **2011**, pp. 529–578.

[4] N. Launay, A.-M. Caminade, R. Lahana, J.-P. Majoral, *Angew. Chem. Int. Ed. Engl.* **1994**, *33*, 1589–1592.

[5] N. Launay, A.-M. Caminade, J. P. Majoral, *J. Organomet. Chem.* **1997**, *529*, 51–58.

[6] E. Cavero, M. Zablocka, A.-M. Caminade, J. P. Majoral, *Eur. J. Org. Chem.* **2010**, 2759–2767.

[7] F. A. Hart, D. W. Owen, *Inorg. Chim. Acta* **1985**, *103*, L1–L2.

[8] P. Coburger, G. Kahraman, A. Straube, E. Hey-Hawkins, *Dalton Trans.* **2019**, *48*, 9625–9630.

[9] R. P. Alexander, H. Schroeder, *Inorg. Chem.* **1963**, *2*, 1107–1110.

[10] A.-M. Caminade, M. Milewski, E. Hey-Hawkins, *Pharmaceutics* **2023**, *15*, 2117.

[11] A. M. Spokoyny, C. D. Lewis, G. Teverovskiy, S. L. Buchwald, *Organometallics* **2012**, *31*, 8478–8481.

# Chapter 6: Résumé et perspectives

# 6 Résumé et perspectives

Ce projet de thèse visait à préparer, caractériser et utiliser un nouveau système de ligands pour des réactions catalytiques en milieu homogène, jusqu'ici difficiles.Le système a été construit à partir de deux composants chimiques de base : un support dendritique polyphosphorhydrazone (Chapitre 2), déjà connu pour ses applications en catalyse, lorsqu'ils sont fonctionnalisés en surface par des complexes de métaux de transition,[1–13] et des carboranylphosphines (Chapitre 3), déjà étudiées pour leurs propriétés de complexation de métaux de transition intéressantes,[14,15] et leurs possibles applications en catalyse.[16] Dans ce travail, la fonction attendue pour le dendrimère est de jouer le rôle de support de fonctions périphériques capables de catalyser les réactions ciblées. Pour combiner ces deux composants, une stratégie de synthèse a été mise en place pour fonctionnaliser judicieusement la position B9 des carboranylphosphines afin d'augmenter leur réactivité vis-à-vis du support dendrimère. La deuxième étape a consisté à étudier différentes méthodes pour les lier au squelette dendritique. En tenant compte du travail antérieur du groupe de CAMINADE et de ses collaborateurs sur les dendrimères polyphosphorhydrazone,[17–19] différents squelettes dendritiques contenant du phosphore, y compris des dendrimères polyphosphorhydrazone symétriques et asymétriques, ont été choisis comme point de départ pour l'ancrage des carboranylphosphines. Sur la base des travaux antérieurs de HART et OWEN[20] et du groupe HEY-HAWKINS[21] sur les carboranylphosphines et leurs complexes, le 1,2-bis(diphénylphosphino)-*ortho*-carborane a été choisi comme unité monomère appropriée pour des investigations ultérieures (voir **Schéma 6.1**).

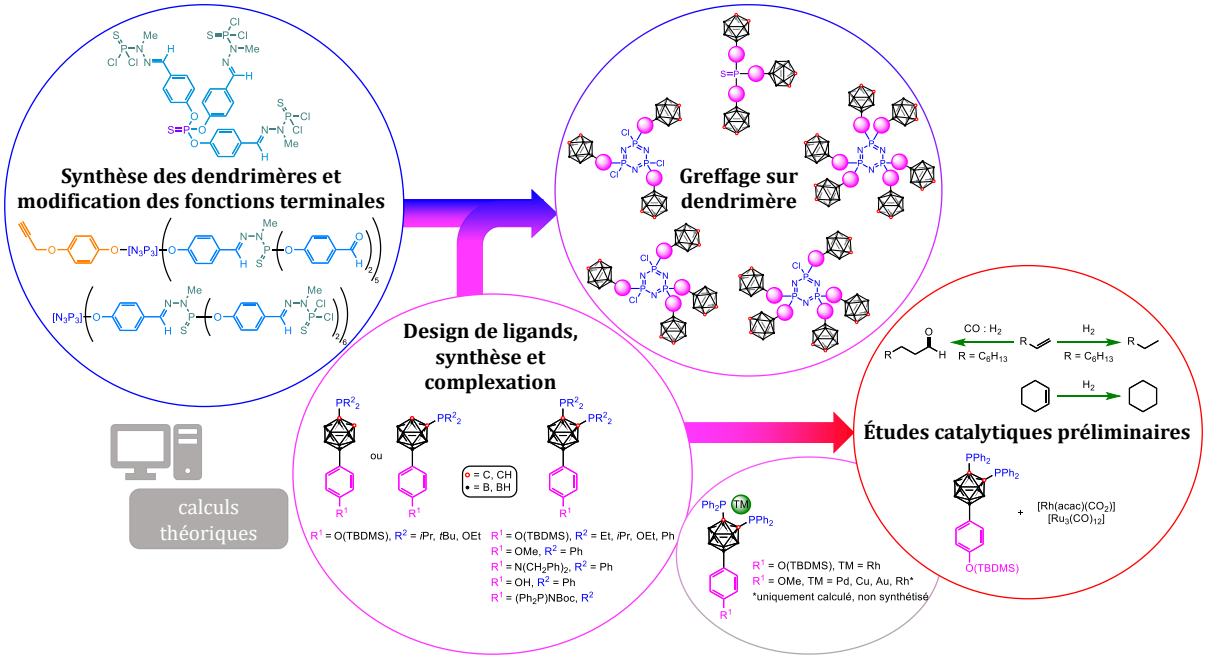


**Schéma 6.1.** Aperçu schématique des principaux résultats obtenus tout au long du projet de doctorat. TM = métal de transition.

## 6.1 Préparation des monomères et des dendrimères

La synthèse de différents composés dendritiques à partir d'un noyau $P(S)Cl_3$ (**1-S0**) ou d'un noyau $N_3P_3Cl_6$ (**1-G0**) a été réalisée (Chapitre 2). Plusieurs dendrimères classiques ont été obtenus avec de bons rendements (62–98%) et des puretés acceptables jusqu'à la génération **1-G2** et **2-S1**, respectivement (voir **Schéma 6.1.1**). Le processus synthétique répétitif impliquant une réaction de condensation avec le phosphorhydrazide $H_2NNMeP(S)Cl_2$ et une réaction de substitution avec le 4-hydroxybenzaldéhyde, a été appliqué mais il s'est avéré délicat.

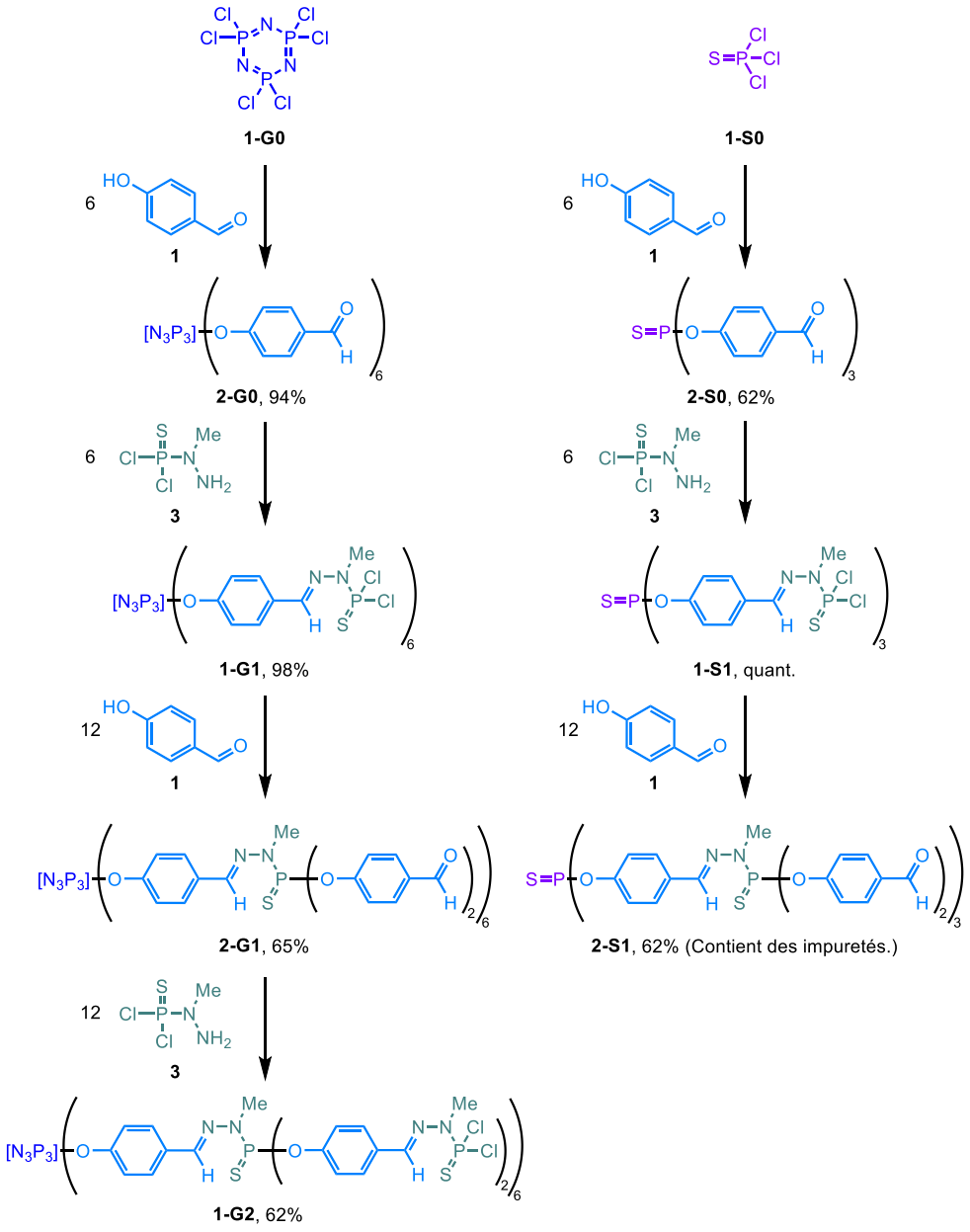


**Schéma 6.1.1.** Etapes de synthèse des dendrimères phosphorés classiques utilisés au projet de doctorat.

Bien que la surface des dendrimères polyphosphorhydrazone soit souvent fonctionnalisée par un seul type de substituants, le fait d'avoir deux types de fonctions différentes peut présenter des avantages. Pour cette raison, une fonctionnalisation spécifique du noyau $N_3P_3$ a été ciblée, avec au

moins une fonction différente des autres. Différents monomères $AB_5$ et dendrimères, présentant une fonction différente des autres au niveau du cœur ont été préparés jusqu'à la génération **$AB_5$-2-G1** (A = 4-(prop-2-yn-1-yloxy)phénol, B = 4-hydroxybenzaldéhyde, voir **Schéma 6.1.2**). De plus, des dendrimères asymétriques **1-G0** et **1-G1** dont seulement la moitié des atomes de chlore des groupes terminaux $P(S)Cl_2$ sont substitués ont été visés afin d'obtenir d'autres squelettes dendritiques pour l'ancrage de différents carboranes et carboranylphosphines. Des problèmes sont particulièrement apparus lors de la monofonctionnalisation stochastique et la purification des dendrimères classiques.

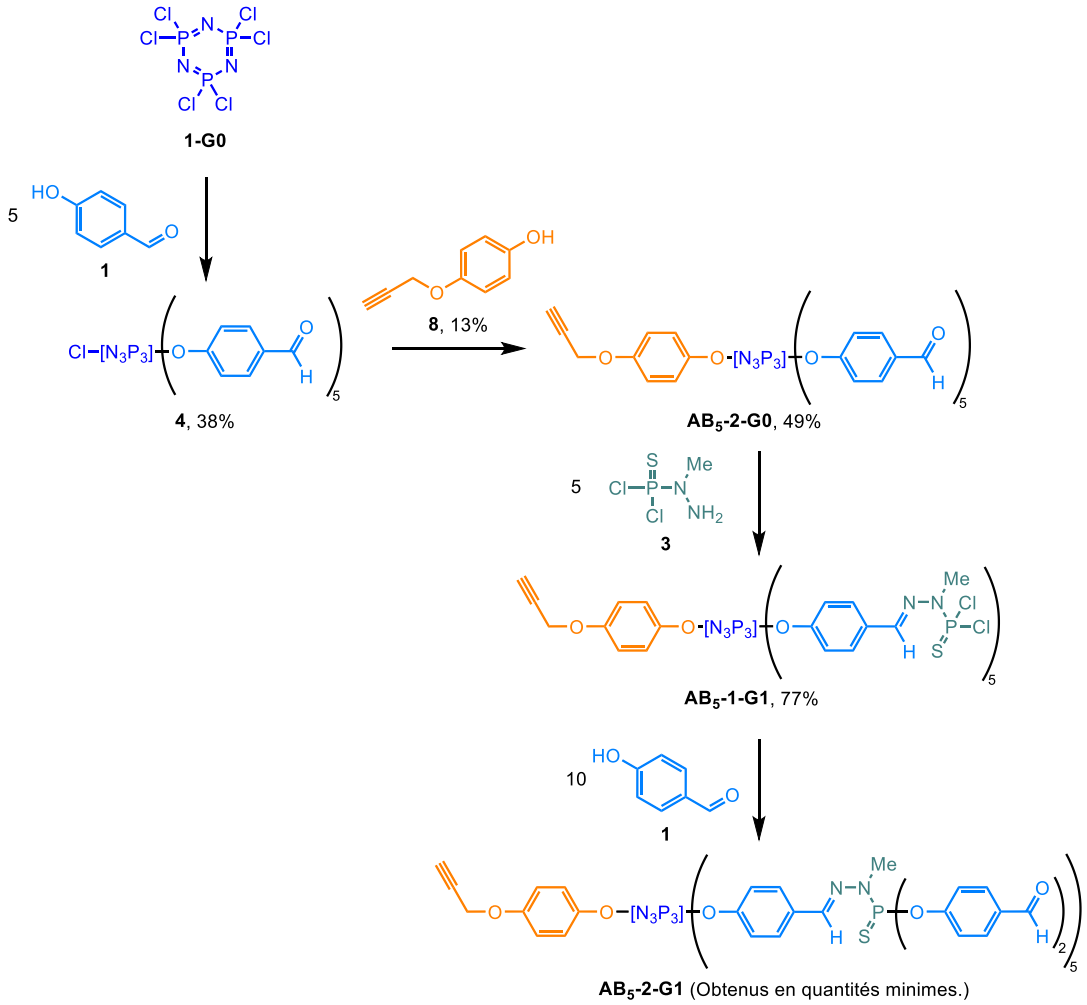


**Schéma 6.1.2.** Etapes de synthèse des divers monomères $AB_5$ et dendrimères asymétriques.

À partir de 1,2-dicarba-closo-dodécaboranes(12) (*ortho*-isomère, **14**), une sélection de différents carboranes substitués en position B9 a été préparée. Une adaptation du protocole synthétique de phosphorylation d'ALEXANDER et SCHROEDER,[22] qui avait été utilisé par le passé pour préparer des dérivés de carboranes substitués en position 1,2-phosphanyl, a été appliquée et modifiée pour produire de nouveaux dérivés de carboranes substitués en position 1- ou 1,2-phosphanyl avec des rendements allant de faibles à excellents (7-95 %, voir **Schéma 6.1.3**).

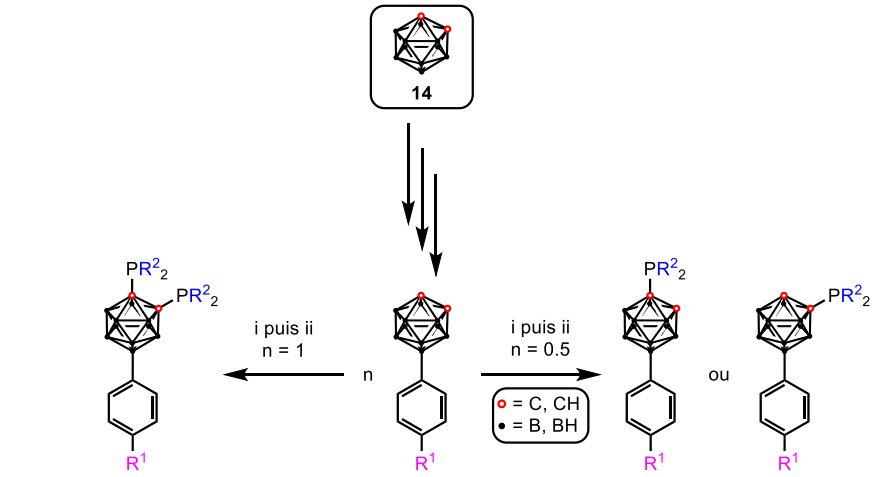


**Schéma 6.1.3.** Synthèse de carboranylphosphines substituées en B9. (i) *n*-butyllithium, $Et_2O$ ou THF, de –78 °C à température ambiante ; (ii) $PR^2{}_2Cl$, $Et_2O$ ou THF, de –78 °C / 0 °C à température ambiante. *Le groupe NH dans le composé **19** a également été substitué par $PPh_2$.

Les produits secondaires isolés ont révélé la forte influence de la stœchiométrie sur l'étape de phosphorylation, ce qui pourrait à l'avenir faciliter l'accès aux phosphines substituées de manière asymétrique. La plupart des molécules obtenues ont pu être caractérisées à l'état solide par diffraction des rayons-X sur monocristaux (voir **Fig. 3.2.1**, **Fig. 3.2.2** and **Fig. 3.2.3**). Les carboranes et carboranylphosphines synthétisés présentent des longueurs de liaison C1–C2 ($C_{Cage}$–$C_{Cage}$) comparables à celles d'autres composés connus. L'impact électronique et stérique des substituants sur les atomes de phosphore induit une augmentation considérable de la longueur de liaison dans les composés disubstitués. Les longueurs moyennes des liaisons C–P et les distances P···P des carboranylphosphines sont cohérentes avec les composés précédemment décrits. Les résultats obtenus révèlent que divers substituants en position B9 n'ont qu'un effet minimal sur les longueurs de liaison C1–C2 et C–P, tandis que les substituants au niveau de l'atome de phosphore ont une influence significative. Seuls quelques exemples de carboranylphosphines ayant la position B9 fonctionnalisée avaient été précédemment rapportés.[15] Ce projet a permis de développer des stratégies de protection et de déprotection synthétiques donnant accès à de nouvelles modifications de la cage carborane.

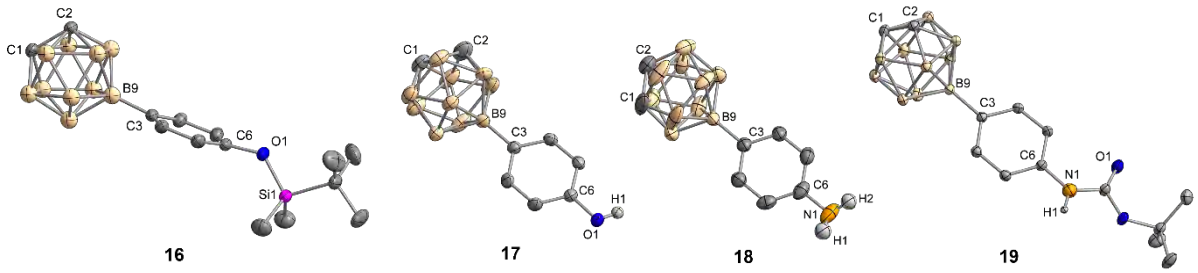


**Fig. 6.1.1.** Structures moléculaires des carboranes **16**–**19** à l'état solide avec des ellipsoïdes thermiques dessinés au niveau de probabilité de 50%. Les atomes d'hydrogène autres que OH et NH sont omis pour des raisons de clarté. Longueurs de liaison sélectionnées [Å] **16** : C1–C2 1.620(3) ; **17** : C1–C2 1.623(3) ; **18** : C1–C2 1.596(4) ; **19** : C1–C2 1.625(1).

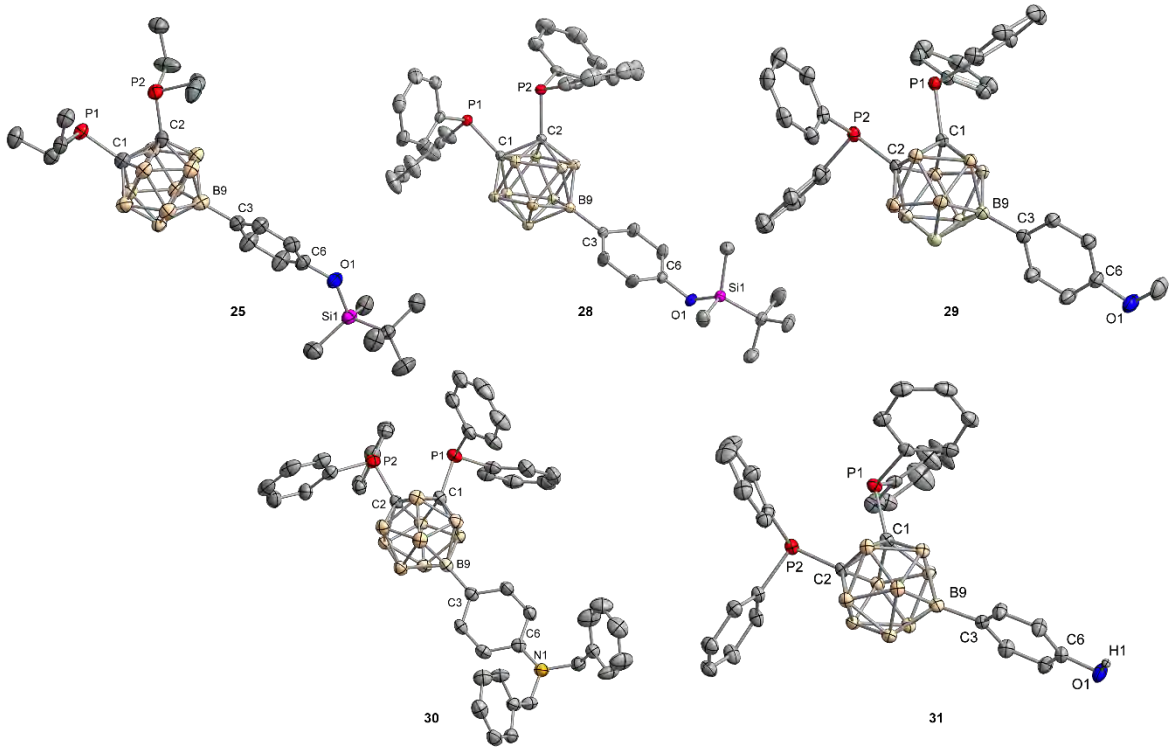


**Fig. 6.1.2.** Structures moléculaires des carboranylphosphines **25** et **28**–**31** à l'état solide avec des ellipsoïdes thermiques dessinés au niveau de probabilité de 50 %. Les atomes d'hydrogène autres que OH dans **31** sont omis pour des raisons de clarté. Longueurs de liaison sélectionnées [Å] **25** : C1–C2 1.717(10), moyenne P–C 1.879(1), P1···P2 3.280(2) ; **28** : C1–C2 1.717(3), moyenne P–C 1.882(7), P1···P2 3.195(8) ; **29** : C1–C2 1.717(3), moyenne P–C 1.881(7), P1···P2 3.224(7); **30**: C1–C2 1.716(2), moyenne P–C 1.883(7), P1···P2 3.130(1) ; **31** : C1–C2 1.706(3), moyenne P–C 1.883(2), P1···P2 3.1827(9).

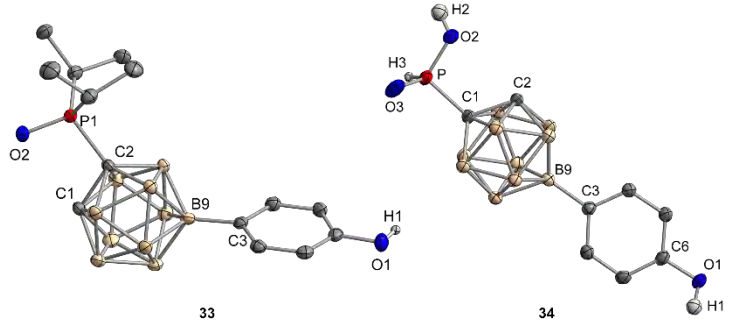


**Fig. 6.1.3.** Structures moléculaires des carboranylphosphines **33** et **34** à l'état solide avec des ellipsoïdes thermiques dessinés au niveau de probabilité de 50%. Les atomes d'hydrogène autres que OH et PH sont omis pour des raisons de clarté. Longueurs de liaison sélectionnées [Å] **33** : C1–C2 1.657(3), C2–P 1.867(3) ; **34** : C1–C2 1.641(2), C1–P 1.825(2).

## 6.2 Complexation

Portant deux substituants phosphine en proximité étroite, les nouvelles carboranylphosphines ressemblent à des phosphines bidentées déjà connues et pourraient être des ligands prometteurs pour la complexation de différents métaux de transition utiles en catalyse homogène. En particulier, la capacité d'ajuster les propriétés stériques et électroniques des carboranylphosphines a permis la synthèse de nouveaux ligands pouvant être envisagés pour complexer différents métaux de transition (Pd, Cu, Au, Rh, Ru). Motivés par la proximité des deux atomes de phosphore lorsqu'ils sont directement fixés à la cage carborane (similaire à un groupement éthylène ou *ortho*-phénylène), la capacité à complexer différents métaux de transition dans un mode de coordination 1 : 1 a été étudiée. Selon les calculs effectués en utilisant la théorie de la fonctionnelle de la densité (DFT) sur différentes carboranylphosphines substituées en position B9 (**29**, **31** et **46–49**), dans la plupart des cas, la formation de complexes de métaux de transition de ces ligands avec différents précurseurs organométalliques devrait être thermodynamiquement favorisée (voir **Tab. 6.2.1** et **Fig. 5.2.1**). De plus, les calculs prédisent la possibilité de complexes plus stables obtenus après l'insertion d'un lien $CH_2$ entre la cage de carborane et les atomes de phosphore. Cependant, il n'a pas encore été possible de confirmer ce résultat théorique par l'expérience, la synthèse des ligands **47–49** ou **53** n'ayant pas été réalisée à ce jour.

**Tab. 6.2.1.** Énergies de GIBBS calculées [kcal mol$^{-1}$] pour les complexes formés à partir des ligands **29**, **31**, **46–49** et différents précurseurs métalliques dans le THF ou le $CH_2Cl_2$ en tant que solvants, par rapport aux matériaux de départ.

| | Carboranylphosphine | 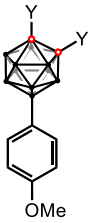 | 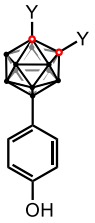 | 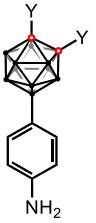 |
|---|---|---|---|---|
| | Précurseur organométallique (solvent pour le calcul) | | | |
| **Y = $PPh_2$ (29, 31, 46)** | [AuCl(tht)] ($CH_2Cl_2$) | –13.2 | –14.3 | –14.1 |
| | [$PdCl_2(MeCN)_2$] (THF) | –42.0 | –42.1 | –20.9 |
| | [$Cu(MeCN)_4$](OTf) (THF) | +6.0 | +4.5 | +4.9 |
| | [$CuCl(PPh_3)_3$] (THF) | –0.2 | +0.4 | +0.1 |
| | [$Rh(acac)(CO)_2$] (THF) | –63.0 | –62.9 | –62.7 |
| **Y = $CH_2PPh_2$ (47–49)** | [AuCl(tht)] ($CH_2Cl_2$) | –24.7 | –23.5 | –25.2 |
| | [$PdCl_2(MeCN)_2$] (THF) | –42.4 | –41.9 | –42.5 |
| | [$Cu(MeCN)_4$](OTf) (THF) | +0.5 | –0.9 | non calculé |
| | [$CuCl(PPh_3)_3$] (THF) | –10.3 | –9.4 | –9.2 |
| | [$Rh(acac)(CO)_2$] (THF) | –134.2 | –133.3 | –133.5 |

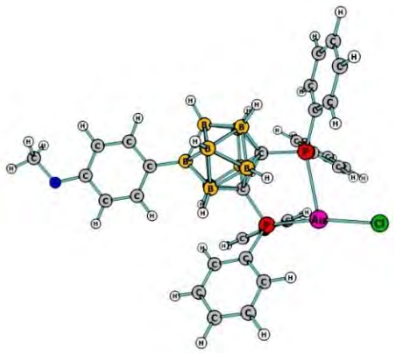

**29-[Au]**

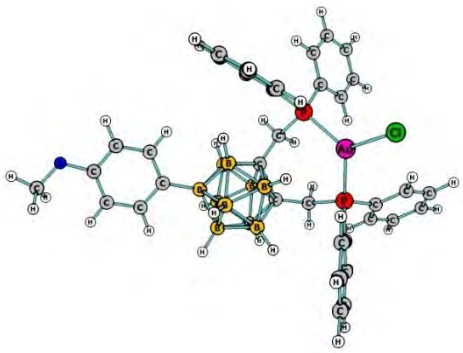

**47-[Au]**

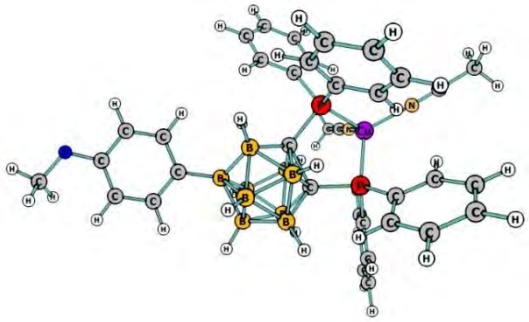

**29-[Cu(MeCN)$_2$]**

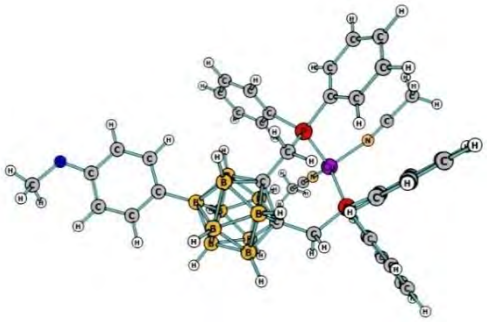

**47-[Cu(MeCN)$_2$]**

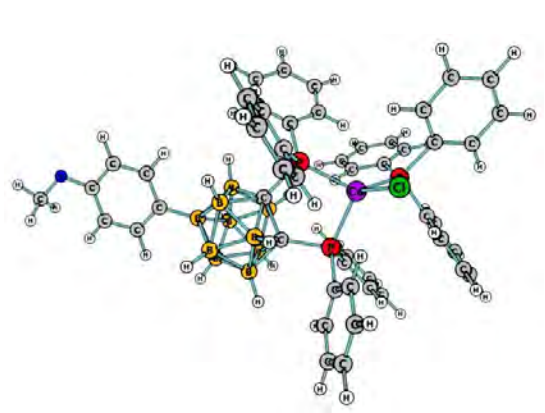

**29-[CuCl]**

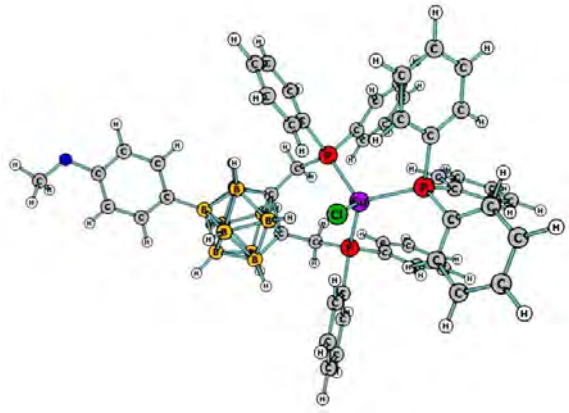

**47-[CuCl]**

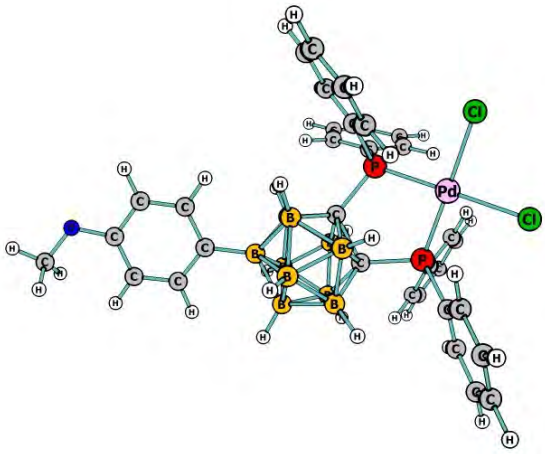

**29-[Pd]**

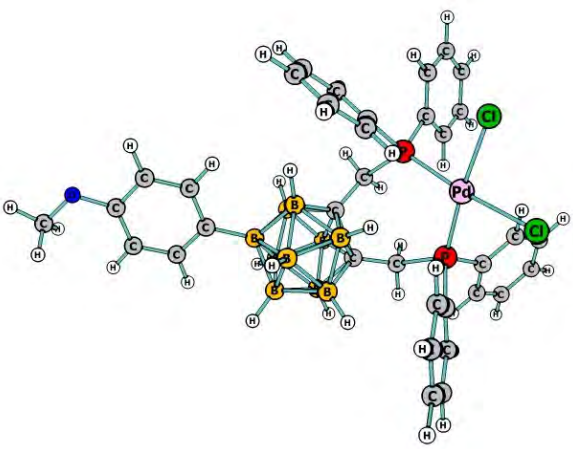

**47-[Pd]**

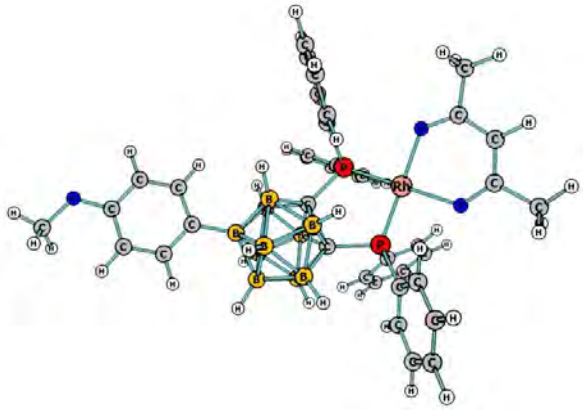

**29-[Rh]**

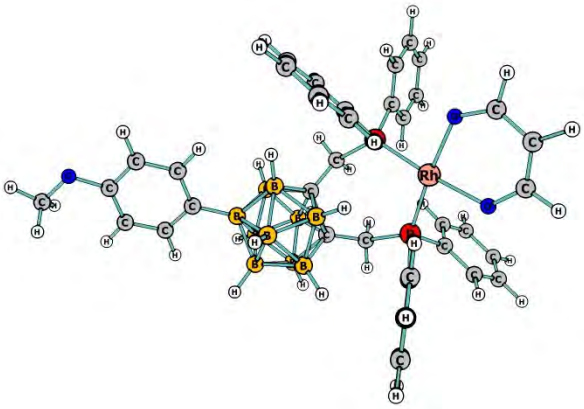

**47-[Rh]**

**Fig. 6.2.1.** Complexes calculés formés à partir de 9-(4-MeO-$C_6H_4$)-1,2-bis(diphénylphosphino) (**29**) et de 9-(4-MeO-$C_6H_4$)-1,2-bis[(diphénylphosphino)méthyl]-*ortho*-carborane (**47**) avec différents précurseurs organométalliques. Tous les atomes d'hydrogène ont été omis pour plus de clarté. L'anion triflate dans **29**- et **47-[Cu(MeCN)$_2$]** a été optimisé séparément. Les structures optimisées obtenues pour d'autres substituants en position B9 ne sont pas montrées.

Seuls les monomères de carboranylphosphine 9-(TBDMS)O-$C_6H_4$-1,2-$(PPh_2)_2$-$C_2B_{10}H_9$ (**28**) et 9-(4-MeO-$C_6H_4$)-1,2-$(PPh_2)_2$-$C_2B_{10}H_9$ (**29**) ont été utilisés pour les premières expériences de complexation avec un précurseur de $Pd^{II}$, deux précurseurs de $Cu^{I}$, un précurseur d'$Au^{I}$, un

précurseur de $Rh^{I}$ et un précurseur de $Ru^{0}$. La carboranylphosphine protégée par un éther silylé **28** est la plus disponible (plus grande quantité, plus facile à synthétiser) parmi tous les composés produits tout au long du travail expérimental de la thèse. Le substituant méthoxyphényle dans le composé **29** imite le lien phénoxy nécessaire dans les réactions de greffage sur dendrimère. Il peut donc être considéré comme un bon représentant monomère des dendrimères substitués par des carboranes (comme décrit au Chapitre 3). Le complexe de rhodium(I) **28-[Rh]**, le complexe d'or(I) **29-[Au]** et le complexe de cuivre(I) **29-[CuCl]** ont pu être synthétisés et caractérisés par spectroscopie de résonance magnétique nucléaire et spectrométrie de masse. Il a également été possible de mettre en évidence la formation du complexe de palladium **29-[Pd]**, même s'il n'a pas pu être isolé en raison de sa grande réactivité induisant la formation du complexe dimère du palladium (**59**) et du méthoxyphénylcarborane (**20**) qui ont été isolés (voir **Schéma 6.2.1**).

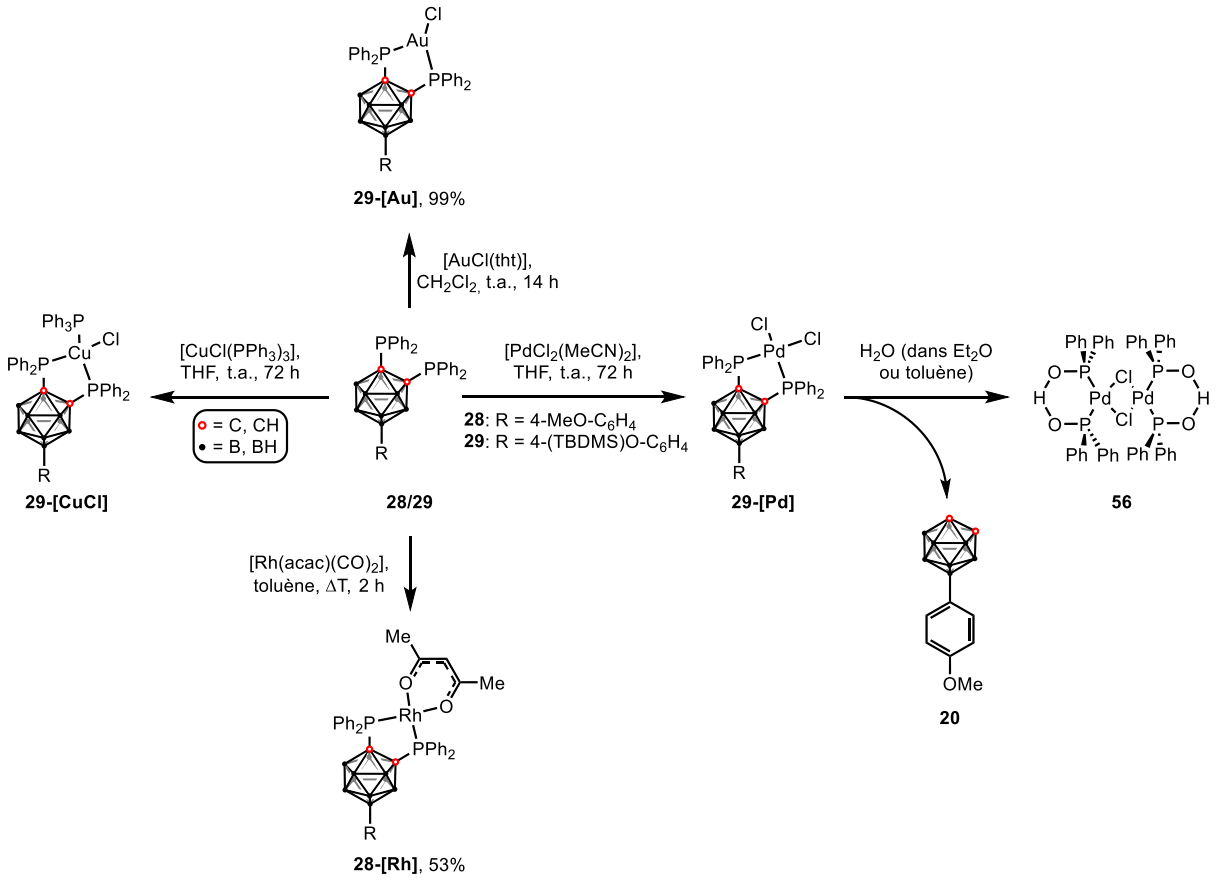


**Schéma 6.2.1.** Synthèse des différents complexes de métaux de transition contenant des carboranylphosphines.

## 6.3 Tests catalytiques préliminaires

À l'aide d'un automate de synthèse en parallèle chez BASF SE, des études catalytiques préliminaires pour l'hydrogénation et l'hydroformylation de l'oct-1-ène et du cyclohexène ont été menées avec divers complexes de rhodium et de ruthénium en présence du ligand carboranylphosphine 9-(4-TBDMSO-$C_6H_4$)-1,2-$(PPh_2)_2$-$C_2B_{10}H_9$ (**28**). Les systèmes les plus

prometteurs ont ensuite été transférés dans un autoclave pour tester les réactions dans des conditions reproductibles. Le ligand **28** en présence de [Rh(acac)$(CO)_2$] a montré les meilleures performances pour l'hydrogénation de l'oct-1-ène, plus performants que les systèmes déjà connus. Le ligand (**28**) a également montré une meilleure conversion dans la réaction d'hydrogénation du cyclohexène avec le complexe [$Ru_3(CO)_{12}$] par rapport au dérivé non substitué 1,2-bis(diphénylphosphino)-*ortho*-carborane (dppc, **73**), mais n'a pas été aussi performant qu'une simple bisphosphine, à savoir le 1,2-bis(diphénylphosphino)benzène (dppb, **67**). Malgré le fait que plusieurs des réactions aient montré une bonne conversion, la sélectivité n'a pas été améliorée par rapport à d'autres systèmes connus, justifiant que ces systèmes n'aient pas été soumis à des tests supplémentaires en conditions industrielles. Cependant, pour obtenir des résultats plus significatifs, quelques séries d'essais complémentaires auraient été nécessaires. Il aurait également été intéressant d'étudier les espèces catalytiques produites *in situ* à partir des sels métalliques et des ligands.

Il apparait essentiel de compléter ces études catalytiques, d'explorer la portée et les limitations des réactions d'hydrogénation et d'hydroformylation effectuées, et de développer d'autres systèmes catalytiques afin de mieux comprendre les résultats obtenus.

## 6.4 Ancrage des carboranes sur les dendrimères polyphosphorhydrazone

Divers composés dendritiques ont été évalués quant à leur aptitude à être substitués par divers carboranes et carboranylphosphines liés au phénol. Des calculs théoriques réalisés en utilisant la théorie de la fonctionnelle de la densité ont montré que la réaction se déroule par un mécanisme de type $S_N2$ dans lequel le phénolate nucléophile **17*** approche le centre phosphoré électrophile $N_3P_3Cl_6$ (**1-G0**) par le côté opposé au groupe partant $Cl^-$. Les différents produits de réactions de polysubstitution avec **17*** ont été optimisés théoriquement pour en évaluer la stabilité. Il a été montré que le produit hexasubstitué **G06** est plus stable de 194.5 kcal $mol^{-1}$ que le produit de départ **1-G0** (voir **Schéma 6.4.1**).

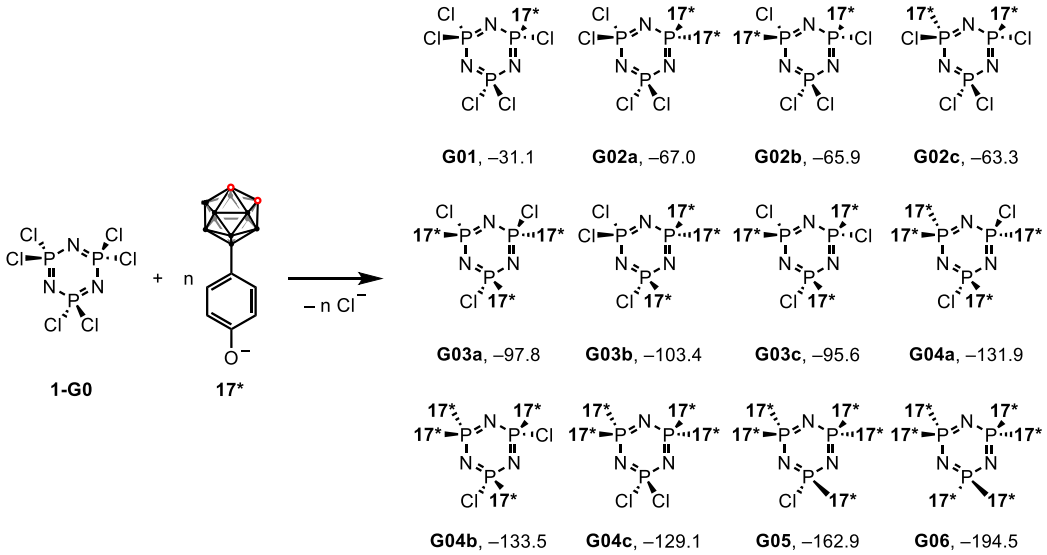


**Schéma 6.4.1.** Valeurs calculées des énergies de GIBBS dans le THF en tant que solvant (en kcal mol$^{-1}$) pour la substitution de **1-G0** par n équivalents de **17*** par rapport au matériau de départ.

Comme les calculs confirment la possibilité de substitution multiple des atomes de chlore de $N_3P_3Cl_6$ par des groupes carboranyle, cette hypothèse a été vérifiée expérimentalement (voir **Schéma 6.4.2**).

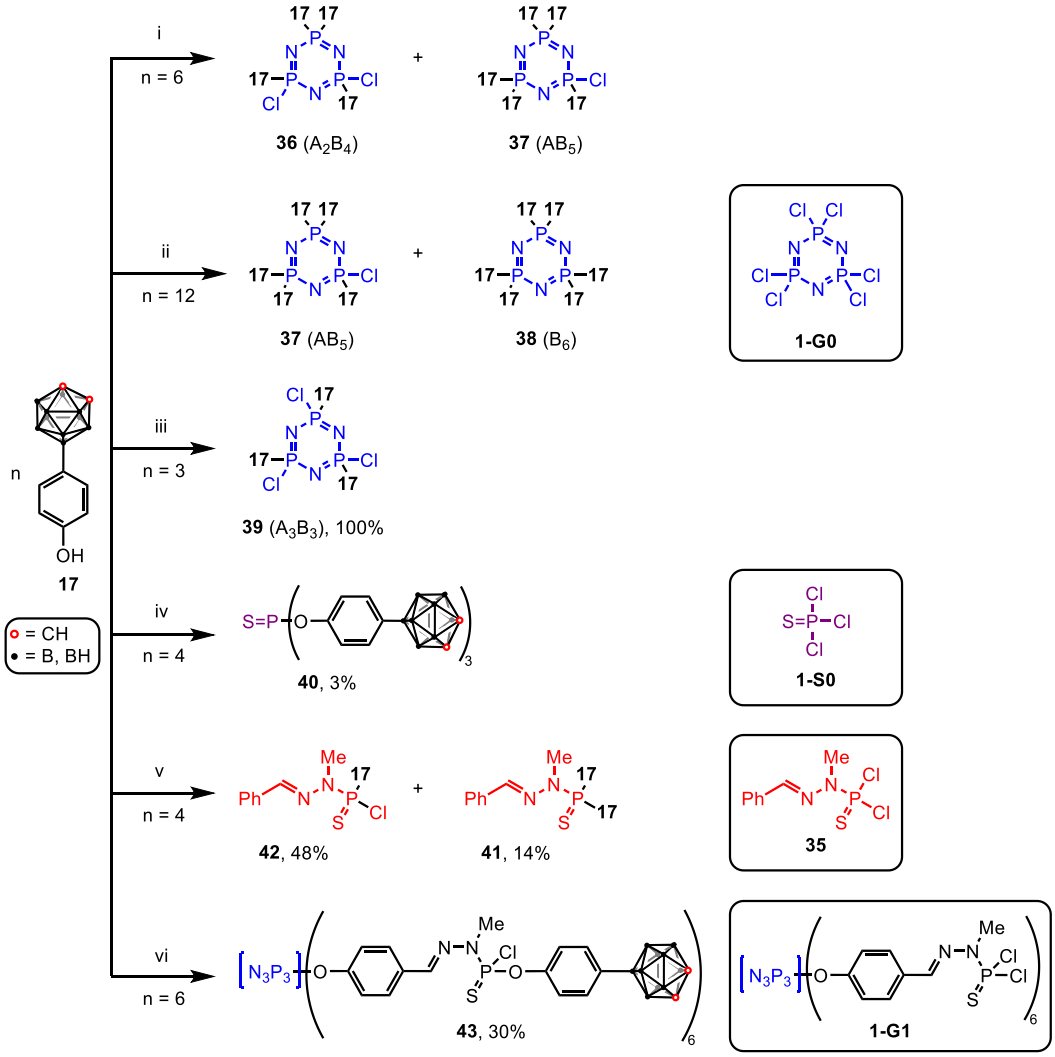


**Schéma 6.4.2.** Réaction de différentes quantités de **17** avec $N_3P_3Cl_6$ (**1-G0**), $P(S)Cl_3$ (**1-S0**) et la molécule modèle **35**. Conditions : (i) **1-G0**, $K_2CO_3$, acétone, 40 °C pendant 120 h puis à température ambiante pendant 72 h ; (ii) **1-G0**, $Cs_2CO_3$, THF, température ambiante, 25 jours ; (iii) **1-G0**, $K_2CO_3$, acétone, température ambiante, 72 h ; (iv) **1-S0**, $Cs_2CO_3$, THF, 40 °C, 96 h ; (v) **35**, DBU, THF, température ambiante, 72 h ; (vi) **1-G1**, $Cs_2CO_3$, THF, à température ambiante pendant 72 h, puis à 40 °C pendant 23 h. Toutes les structures ont été analysées par spectroscopie résonance magnétique nucléaire et par spectrométrie de masse avec ionisation par électro-nébulisation.

Le greffage du phénolcarborane (**17**) sur la molécule modèle **35**, sur différents composés phosphorés **1-G0** et **1-S0**, ainsi que sur le dendrimère **1-G1** a été testé. Malgré l'absence de substitution complète par une carboranylphosphine, de nouveaux composés dendritiques substitués par des carboranes ont été synthétisés. En particulier, le greffage sélectif d'un seul carborane par fonction $P(S)Cl_2$ a été étudié avec succès, conduisant au dendrimère monofonctionnalisé sur chaque fonction $P(S)Cl_2$ **43** (voir **Fig. 6.4.1**).

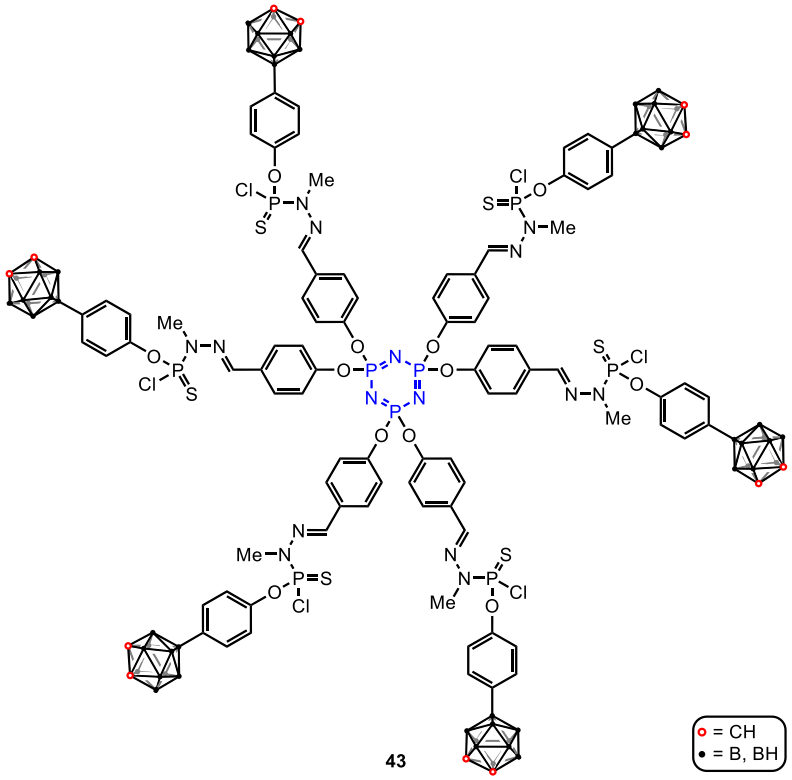


**Fig. 6.4.1**. Structure du dendrimère **43**.

Cependant, l'étape de séparation des dendrimères substitués par un nombre différent de carboranes demeure un défi à relever. De plus, la substitution sélective d'un seul atome de chlore de chaque extrémité $P(S)Cl_2$ par un carborane devrait être étudiée pour d'autres générations de dendrimères, car cela ouvrirait la voie au greffage de fonctionnalités supplémentaires pour remplacer les atomes de Cl restants, par exemple de fonctions permettant de solubiliser les dendrimères dans l'eau, en vue d'applications dans le domaine de la biologie.[23]

## 6.5 En résumé

Plusieurs *ortho*-carboranes portant un groupe phénoxy ou phénylamino en position B9 ont été préparés en utilisant diverses stratégies de protection et de déprotection. De plus, l'accès synthétique à de nouveaux carboranes substitués en position 1- ou 1,2-phosphanyl a été développé dans le cadre de ce projet de thèse. Les phosphines résultantes, telles que la diisopropyl-, la diéthyl-, la di-*tert*-butyl-, la diphényl- ou la diéthoxyphosphine portant un motif *ortho*-carborane modulable, apparaissent comme des ligands intéressants pour des applications futures en catalyse homogène ou dans le domaine médical. Les ligands ont montré un mode de coordination 1 : 1 avec les différents métaux de transition grâce aux carboranylphosphines chélatantes. Un catalyseur généré *in situ* à partir d'un mélange de précurseurs de $Rh^{I}$ ou $Ru^{0}$ et de la carboranylphosphine **28** a pu être utilisé pour l'hydrogénation et l'hydroformylation d'oléfines insaturées.

Suivant des méthodes de synthèse classiques, des dendrimères phosphorés ont été synthétisés à partir d'un cœur hexachlorocyclotriphosphazène ou de chlorure de thiophosphoryle, et différentes méthodes de greffage des *ortho*-carboranes substitués en position B9 ont été étudiées expérimentalement et théoriquement (théorie de la fonctionnelle de la densité). Malgré les défis synthétiques, plusieurs dendrimères portant des carboranes en périphérie ont pu être obtenus, et les résultats devraient ouvrir la voie à la synthèse de dendrimères contenant également des carboranylphosphines, afin d'étudier leurs performances catalytiques et d'explorer de nouvelles voies de synthèse. Des études supplémentaires sur les carboranylphosphines portant divers substituants, ainsi que d'autres applications catalytiques, mériteraient d'être menées. Jusqu'à présent, seules les carboranylphosphines C–P déficientes en électrons ont été envisagées. L'utilisation de carboranylphosphines B–P riches en électrons (similaire au travail de SPOKOYNY et de ses collègues),[24] reliant les carboranes aux dendrimères *via* leurs atomes de la cage $C_{Cage}$, pourrait être une variation intéressante à considérer. Il est évident que beaucoup de découvertes restent à faire dans ce domaine de recherche.

Ce projet de thèse visait à développer un nouveau système de ligands pour des réactions catalytiques difficiles. Pour ce faire, deux composants chimiques ont été combinés : une structure dendritique polyphosphorhydrazone, connue pour ses applications en catalyse, et des motifs carboranylphosphine, déjà étudiés pour leur capacité de complexation et leurs applications possibles en catalyse. Les principales étapes de ce projet peuvent être résumées comme suit :

1. Préparation des dérivés carboranylphosphines et des dendrimères : Différents composés dendritiques ont été synthétisés à partir de noyaux $P(S)Cl_3$ ou $N_3P_3Cl_6$, produisant des dendrimères classiques avec de bons rendements jusqu'à la génération **1-G2** ou **2-S1**.
2. Synthèse de carboranes substitués : plusieurs carboranes substitués en position B9 ont été préparés, en utilisant diverses stratégies de protection et de déprotection, donnant des rendements variables. Les structures à l'état solide de ces composés ont été déterminées par diffraction des rayons X.
3. Chimie de coordination : les nouvelles carboranylphosphines, portant deux groupes phosphorés proches, ont montré une capacité de complexation intéressante envers différents métaux de transition. Des calculs théoriques ont montré que la formation de complexes de métaux de transition devrait être thermodynamiquement favorable dans la plupart des cas.
4. Tests catalytiques préliminaires : des tests catalytiques préliminaires ont été menés pour les réactions d'hydrogénation et d'hydroformylation de composés organiques. La carboranylphosphine **28** a montré des performances prometteuses pour l'hydrogénation de l'oct-1-ène.

5. Greffage des carboranes sur des dendrimères polyphosphorhydrazone : divers dendrimères ont été envisagés comme supports pour le greffage de carboranes et de carboranylphosphines portant une fonction phénol. Les réactions de substitution se sont déroulées suivant un mécanisme de type $S_N2$. La substitution sélective d'un seul atome de chlore des extrémités $P(S)Cl_2$ par des carboranes a également été étudiée, conduisant à un dendrimère dont la moitié de ses atomes de chlore sont encore disponibles pour une deuxième fonctionnalisation.

## 6.6 Références


[1] A.-M. Caminade, R. Laurent, *Coord. Chem. Rev.* **2019**, *389*, 59–72.

[2] V. Maraval, R. Laurent, A.-M. Caminade, J.-P. Majoral, *Organometallics* **2000**, *19*, 4025–4029.

[3] M. Keller, A. Hameau, G. Spataro, S. Ladeira, A.-M. Caminade, J.-P. Majoral, A. Ouali, *Green Chem.* **2012**, *14*, 2807–2815.

[4] M. Keller, V. Collière, O. Reiser, A.-M. Caminade, J.-P. Majoral, A. Ouali, *Angew. Chem. Int. Ed.* **2013**, *52*, 3626–3629; *Angew. Chem*. **2013**, *125*, 3714–3717.

[5] P. Servin, R. Laurent, A. Romerosa, M. Peruzzini, J.-P. Majoral, A.-M. Caminade, *Organometallics* **2008**, *27*, 2066–2073.

[6] N. G. García-Peña, A.-M. Caminade, A. Ouali, R. Redón, C.-O. Turrin, *RSC Adv.* **2016**, *6*, 64557–64567.

[7] P. Servin, R. Laurent, L. Gonsalvi, M. Tristany, M. Peruzzini, J. P. Majoral, A.-M. Caminade, *Dalton Trans.* **2009**, 4432–4434.

[8] P. Neumann, H. Dib, A.-M. Caminade, E. Hey-Hawkins, *Angew. Chem. Int. Ed.* **2015**, *54*, 311–314; *Angew. Chem.* **2015**, *127*, 316-319.

[9] M. Petrucci-Samija, V. Guillemette, M. Dasgupta, A. K. Kakkar, *J. Am. Chem. Soc.* **1999**, *121*, 1968–1969.

[10] P. Servin, R. Laurent, H. Dib, L. Gonsalvi, M. Peruzzini, J. P. Majoral, A.-M. Caminade, *Tetrahedron Lett.* **2012**, *53*, 3876–3879.

[11] A. Ouali, R. Laurent, A.-M. Caminade, J. P. Majoral, M. Taillefer, *J. Am. Chem. Soc.* **2006**, *128*, 15990–15991.

[12] A. Gissibl, C. Padié, M. Hager, F. Jaroschik, R. Rasappan, E. Cuevas-Yañez, C. O. Turrin, A.-M. Caminade, J. P. Majorai, O. Reiser, *Org. Lett.* **2007**, *9*, 2895–2898.

[13] M. Keller, M. Ianchuk, S. Ladeira, M. Taillefer, A.-M. Caminade, J. P. Majoral, A. Ouali, *Eur. J. Org. Chem.* **2012**, *2012*, 1056–1062.

[14] I. B. Sivaev, M. Y. Stogniy, V. I. Bregadze, *Coord. Chem. Rev.* **2021**, *436*, 213795.

[15] E. V. Oleshkevich, E. G. Rys, V. V. Bashilov, P. V. Petrovskii, V. A. Ol'shevskaya, S. K. Moiseev, A. B. Ponomaryov, V. N. Kalinin, *Russ. J. Gen. Chem.* **2017**, *87*, 2589–2595.

[16] S. Bauer, E. Hey-Hawkins *dans Boron Science* (Ed. : N. S. Hosmane), CRC Press, **2011**, pp. 529–578.

[17] N. Launay, A.-M. Caminade, R. Lahana, J.-P. Majoral, *Angew. Chem. Int. Ed. Engl.* **1994**, *33*, 1589–1592.

[18] N. Launay, A.-M. Caminade, J. P. Majoral, *J. Organomet. Chem.* **1997**, *529*, 51–58.

[19] E. Cavero, M. Zablocka, A.-M. Caminade, J. P. Majoral, *Eur. J. Org. Chem.* **2010**, 2759–2767.

[20] F. A. Hart, D. W. Owen, *Inorg. Chim. Acta* **1985**, *103*, L1–L2.

[21] P. Coburger, G. Kahraman, A. Straube, E. Hey-Hawkins, *Dalton Trans.* **2019**, *48*, 9625–9630.

[22] R. P. Alexander, H. Schroeder, *Inorg. Chem.* **1963**, *2*, 1107–1110.

[23] A.-M. Caminade, M. Milewski, E. Hey-Hawkins, *Pharmaceutics* **2023**, *15*, 2117.

[24] A. M. Spokoyny, C. D. Lewis, G. Teverovskiy, S. L. Buchwald, *Organometallics* **2012**, *31*, 8478–8481.

# Chapter 7: Zusammenfassung und Ausblick

# 7 Zusammenfassung und Ausblick

Ziel des Dissertationsprojektes war die Synthese, Charakterisierung und Anwendung eines neuen Ligandensystems für anspruchsvolle homogene katalytische Reaktionen. Das Ligandensystem besteht dabei aus zwei chemisch sehr unterschiedlichen Bausteinen: Einem polyphosphorhydrazone-basierten dendritischen Gerüsts (Kapitel 2), welches, wenn es mit den entsprechenden terminalen Funktionen oberflächenfunktionalisiert wird, bereits für seine Anwendungen in der Katalyse bekannt ist,[1–13], und diversen Carboranylphosphanen (Kapitel 3), die bereits für ihre interessanten Eigenschaften bei der Komplexierung von Übergangsmetallen[14,15] und der potenziellen Anwendungen in der Katalyse untersucht wurden.[16] In dieser Arbeit soll das Dendrimer als Träger für periphere Carboranylfunktionen dienen, die gezielte Reaktionen katalysieren können.

Um diese beiden Komponenten zu kombinieren, wurde eine Synthesestrategie verfolgt, bei der zunächst die B9-Position der Carboranylphosphane gezielt funktionalisiert wurden, um ihre Reaktivität für die Reaktion mit dem dendritischen Träger zu erhöhen. Der zweite Schritt bestand darin, verschiedene Methoden zu erforschen, um die funktionalisierten Monomere mit dem dendritischen Gerüst zu verknüpfen. Unter Berücksichtigung früherer Arbeiten von CAMINADE et al. an polyphosphorhydrazonhaltigen Dendrimeren[17–19] wurden verschiedene dendritische Strukturen, einschließlich symmetrischer und asymmetrischer Dendrimere, als Ausgangspunkte für die Verankerung der Carboranylphosphane ausgewählt.

Basierend auf den Arbeiten von HART und OWEN[20] sowie HEY-HAWKINS et al.[21] zu Carboranylphosphanen und deren Komplexen wurde das 1,2-Bis(diphenylphosphino)-*ortho*-carboran als Startpunkt und damit geeignete monomere Einheit für weitere Untersuchungen ausgewählt (siehe **Schema 7.1**).

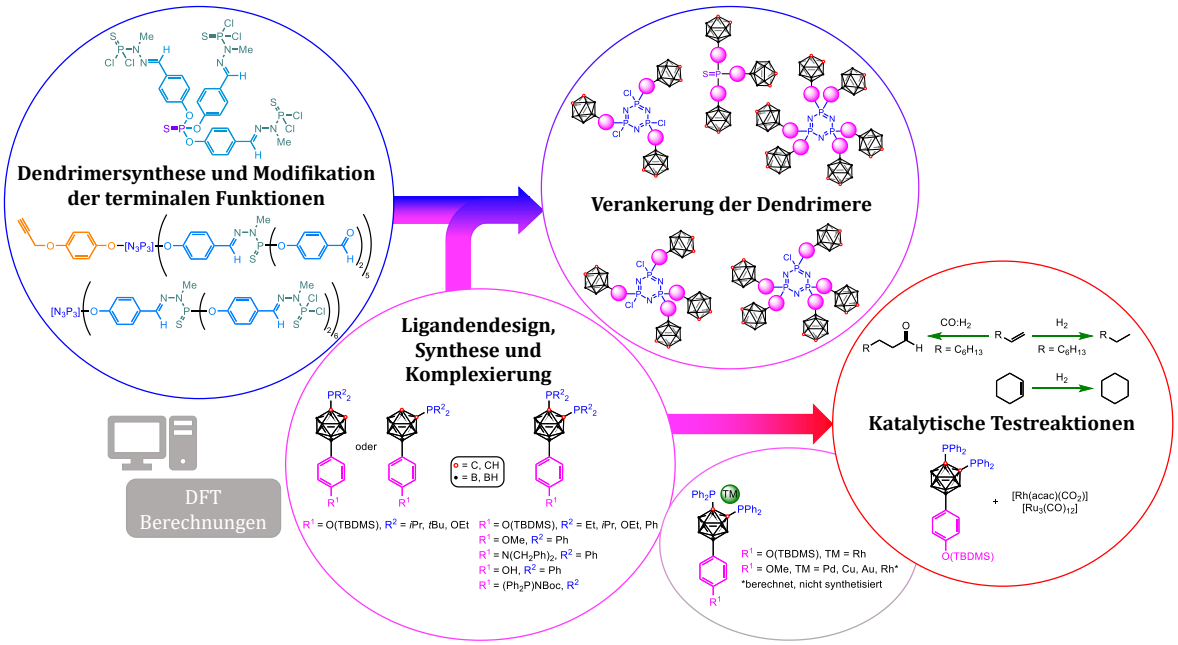


**Schema 7.1.** Schematische Darstellung der Gesamtergebnisse des Projektes. TM = Übergangsmetall.

## 7.1 Herstellung von Monomeren und Dendrimeren

Die Synthese verschiedener dendritischer Verbindungen ausgehend von einem $P(S)Cl_3$-Kern (**1-S0**) oder einem $N_3P_3Cl_6$-Kern (**1-G0**) wurde durchgeführt (Kapitel 2). Mehrere klassische Dendrimere wurden mit guten Ausbeuten (62–98%) und akzeptabler Reinheit bis zur Generation **1-G2** bzw. **2-S1** erhalten (siehe **Schema 7.1.1**). Ein sich wiederholender synthetische Prozess, der eine Kondensationsreaktion mit dem Phosphorhydrazid $H_2NNMeP(S)Cl_2$ und eine Substitutionsreaktion mit 4-Hydroxybenzaldehyd umfasste, wurde angewandt, erwies sich in der Reproduktion jedoch als eher anspruchsvoll.

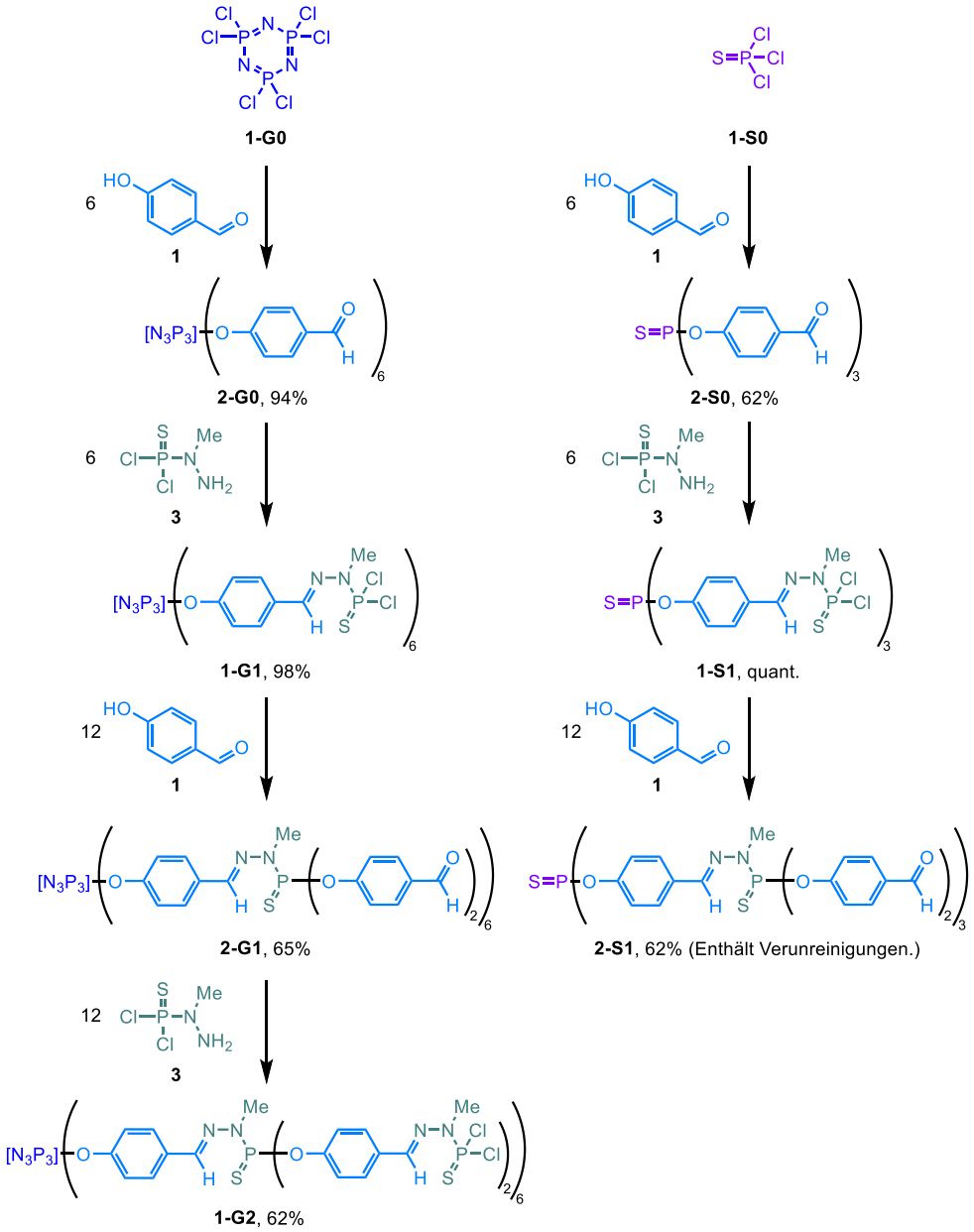


**Schema 7.1.1.** Synthesestufen für die Synthese eines klassischen phosphorhaltigen Dendrimers genutzt für dieses Projekt.

Obwohl die Oberfläche von polyphosphorhydrazonhaltigen Dendrimeren häufig durch einen einzigen Typ von Substituenten funktionalisiert ist, kann das Vorhandensein von zwei verschiedenen Funktionen Vorteile bieten. Aus diesem Grund wurde eine spezifische Funktionalisierung des $N_3P_3$-Kerns angestrebt, mit mindestens einer Funktion, die sich von den anderen unterscheidet. Unterschiedliche $AB_5$-Monomere und Dendrimere mit einer Funktion, die sich auf Kernebene von den anderen unterscheidet, wurden bis zur Generation **$AB_5$-2-G1** (A = 4-(prop-2-yn-1-yloxy)phenol, B = 4-Hydroxybenzaldehyd, siehe **Schema 7.1.2**) hergestellt. Zudem wurde die Synthese asymmetrischer Dendrimere ausgehend von **1-G0** und **1-G1** angestrebt, bei denen nur die Hälfte der Chloratome der terminalen $P(S)Cl_2$-Gruppen substituiert ist, um andere dendritische Strukturen für die Verankerung verschiedener Carborane und Carboranylphosphane zu erhalten. Insbesondere traten Probleme bei der stochastischen Monofunktionalisierung und Reinigung klassischer Dendrimere auf.

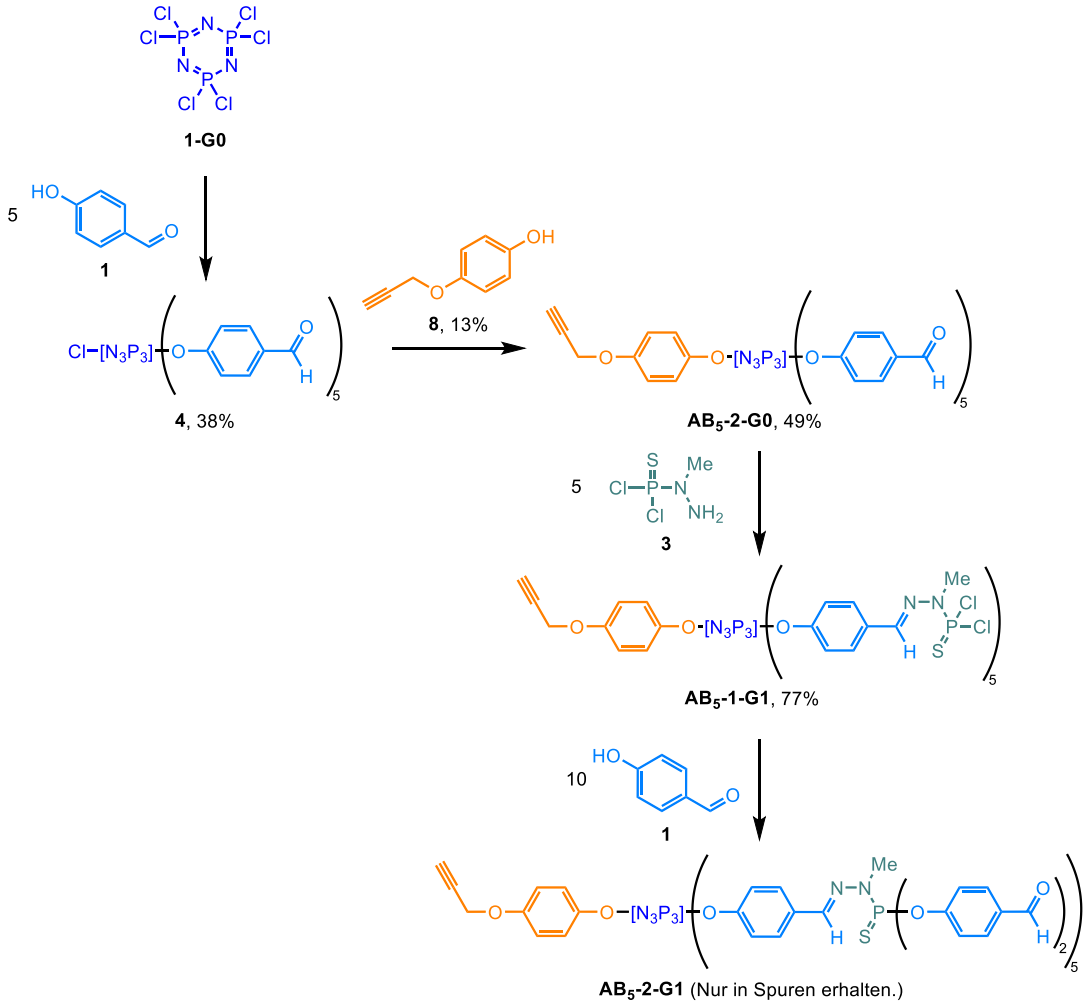


**Schema 7.1.2.** Synthesestufen für die Synthese diverse Ab5-Monomere und asymmetrischer Dendrimere, welche in diesem Projekt synthetisiert wurden.

Ausgehend von 1,2-Dicarba-*closo*-dodecaboranen(12) (*ortho*-Isomer, **14**) wurde eine Auswahl verschiedener substituierter Carborane an Position B9 hergestellt. Eine Anpassung des

synthetischen Phosphorylierungsprotokolls von ALEXANDER und SCHROEDER,[22] das in der Vergangenheit zur Herstellung von substituierten 1,2-phosphanylierten Carboranderivaten an verwendet wurde, wurde angewendet und modifiziert, um neue substituierte 1- oder 1,2-phosphanylierte Carboranderivate in niedrigen bis hervorragenden Ausbeuten (7-95 %, siehe **Schema 7.1.3**) herzustellen.

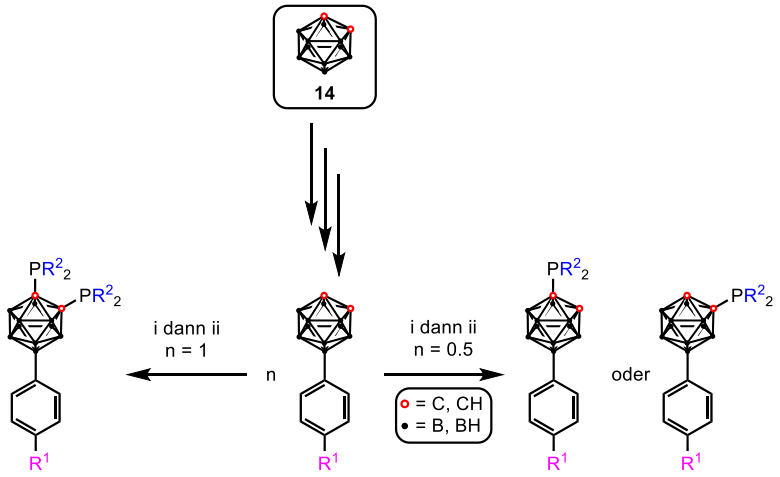


$R^1$ = O(TBDMS), $R^2$ = Et (**25**, 44%)
$R^1$ = O(TBDMS), $R^2$ = *i*Pr (**26**, 65%)
$R^1$ = O(TBDMS), $R^2$ = OEt (**27**, 24%)
$R^1$ = O(TBDMS), $R^2$ = Ph (**28**, 93%)
$R^1$ = OMe, $R^2$ = Ph (**29**, 29%)
$R^1$ = $N(CH_2Ph)_2$, $R^2$ = Ph (**30**, 56%)
$R^1$ = OH, $R^2$ = Ph (**31**, 95%)
$R^1$ = $(Ph_2P)NBoc$, $R^2$ = Ph (**32**, 11%)*

$R^1$ = O(TBDMS) (**16**), OH (**17**), $(Ph_2P)NBoc$ (**19**), OMe (**20**), $N(CH_2Ph)_2$ (**21**)

$R^1$ = O(TBDMS), $R^2$ = *i*Pr (**22**, 7%)
$R^1$ = O(TBDMS), $R^2$ = *t*Bu (**23**, 31%)
$R^1$ = O(TBDMS), $R^2$ = OEt (**24**, 24%)

**Schema 7.1.3.** Synthese von B9-substituierten Carboranylphosphanen. (i) *n*-Butyllithium, $Et_2O$ oder THF,–78 °C bis Raumtemperatur ; (ii) $PR^2{}_2Cl$, $Et_2O$ oder THF,–78 °C / 0 °C bis Raumtemperatur. *Die NH-Gruppe der Verbindung **19** wurde ebenfalls phosphanyliert mit $PPh_2$.

Die isolierten Nebenprodukte zeigten einen starken Einfluss der Stöchiometrie zwishcen Carboran, *n*-Butyllithium und Phosphan auf den Phosphorylierungsschritt, was in Zukunft den Zugang zu asymmetrisch substituierten Phosphanen erleichtern könnte. Die meisten erhaltenen Moleküle konnten im Festkörperzustand durch Röntgenstrukturanalyse charakterisiert werden (siehe **Fig. 7.1.1**, **Fig. 7.1.2** und **Fig. 7.1.3**). Die synthetisierten Carborane und Carboranylphosphane zeigten C–C-Bindungslängen ($C_{Carboran}$–$C_{Carboran}$) vergleichbar mit anderen bekannten Verbindungen. Die elektronische und sterische Auswirkung der Substituenten auf die Phosphoratome führte zu einer deutlichen Verlängerung der Bindungslängen bei den disubstituierten Verbindungen. Die mittleren Längen der C–P-Bindungen und die P···P-Abstände der Carboranylphosphane entsprechen den zuvor beschriebenen Verbindungen. Die erzielten Ergebnisse zeigen, dass verschiedene Substituenten in Position B9 nur minimale Auswirkungen auf die C1–C2- und C–P-Bindungslängen haben, während Substituenten auf Phosphoratomniveau einen signifikanten Einfluss haben. Es wurden nur wenige Beispiele für Carboranylphosphane mit

funktionalisierter B9-Position zuvor beschrieben.[15] Dieses Projekt hat dazu beigetragen, synthetische Schutz- und Entschützungsstrategien zu entwickeln, die den Zugang zu neuen Modifikationen des Carborankäfigs ermöglichen.

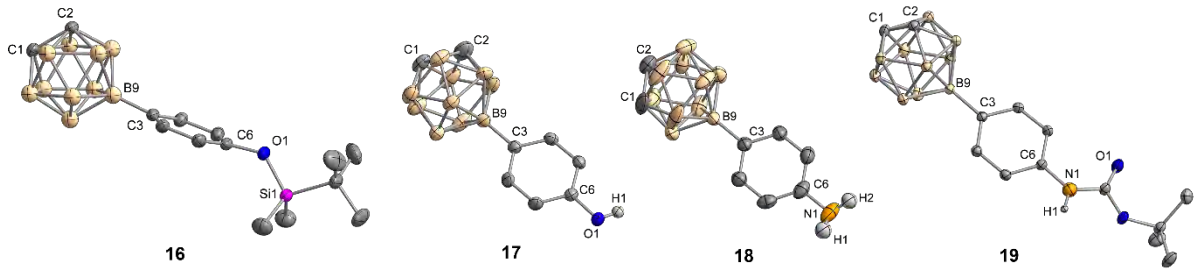


**Fig. 7.1.1.** Molekülstruktur der Carborane **16**–**19** im Festkörperzustand. Die Position der thermalen Ellipsoide ist mit einer Wahrscheinlichkeit von 50% dargestellt. Die Wassterstoffatome sind der Übersichtlichkeit halber ausgeblendet, außer für OH und NH. Ausgewählte Bindungslängen [Å] **16:** C1–C2 1.620(3); **17**: C1–C2 1.623(3); **18**: C1–C2 1.596(4); **19**: C1–C2 1.625(1).

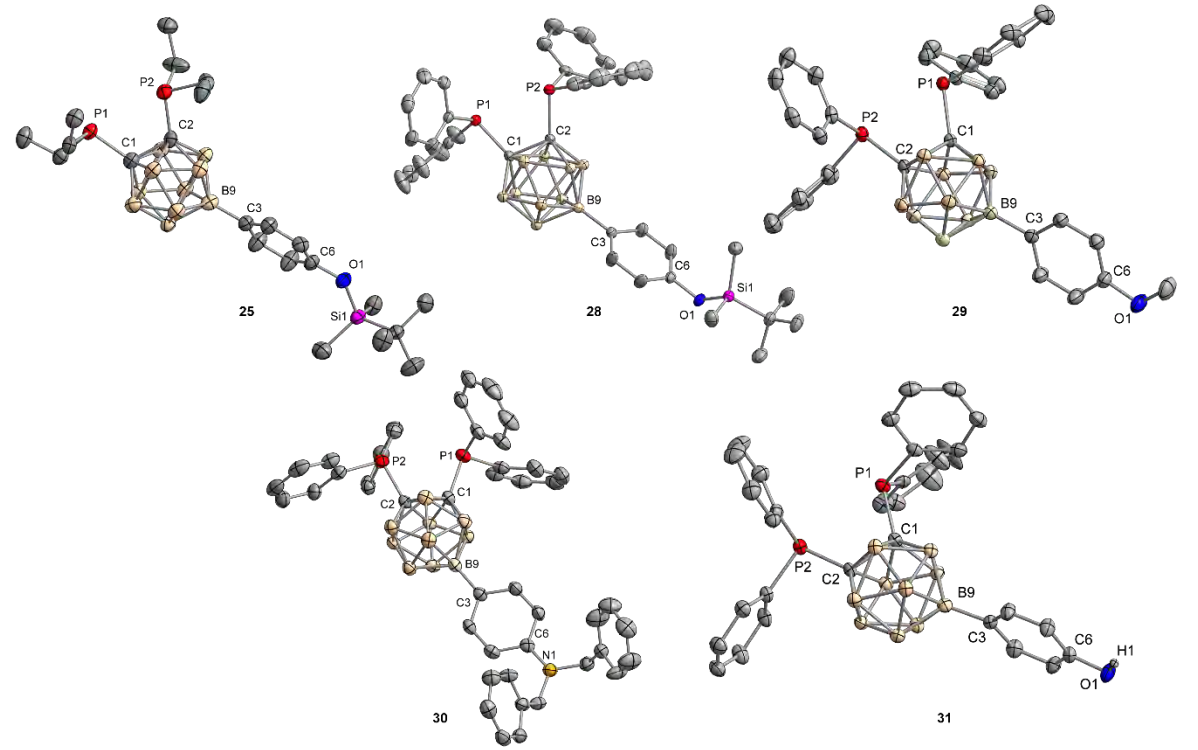


**Fig. 7.1.2.** Molekülstruktur der Carboranylphosphane **25** und **28**–**31** im Festkörperzustand. Die Position der thermalen Ellipsoide ist mit einer Wahrscheinlichkeit von 50% dargestellt. Die Wassterstoffatome sind der Übersichtlichkeit halber ausgeblendet, außer für OH in Verbindung **31**. Ausgewählte Bindungslängen [Å] **25**: C1–C2 1.717(10), Durchschnitt P–C 1.879(1), P1···P2 3.280(2) ; **28** : C1–C2 1.717(3), Durchschnitt P–C 1.882(7), P1···P2 3.195(8); **29**: C1–C2 1.717(3), moyenne P–C 1.881(7), P1···P2 3.224(7); **30**: C1–C2 1.716(2), Durchschnitt P–C 1.883(7), P1···P2 3.130(1); **31**: C1–C2 1.706(3), Durchschnitt P–C 1.883(2), P1···P2 3.1827(9).

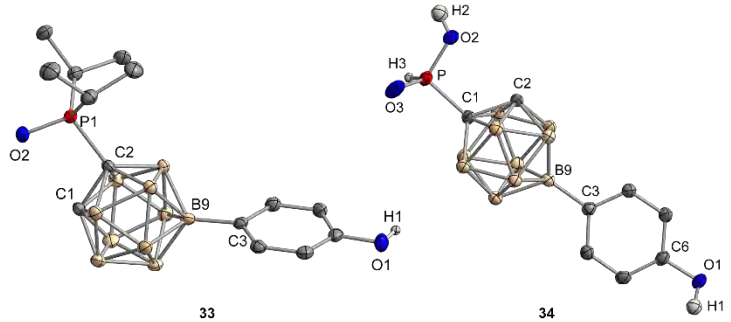


**Fig. 7.1.3.** Molekülstruktur der Carboranylphosphane **33** und **34** im Festkörperzustand. Die Position der thermalen Ellipsoide ist mit einer Wahrscheinlichkeit von 50% angegeben. Die Wassterstoffatome sind der Übersichtlichkeit halber ausgeblendet, außer OH und PH. Ausgewählte Bindungslängen [Å] **33**: C1–C2 1.657(3), C2–P 1.867(3); **34**: C1–C2 1.641(2), C1–P 1.825(2).

## 7.2 Komplexierung

Mit zwei räumlich nah beieinander liegenden Phosphansubstituenten ähneln die neuen Carboranylphosphane bekannten zweizähnigen Phosphanen und könnten vielversprechende Liganden für die Komplexierung verschiedener Übergangsmetalle sein, die in der homogenen Katalyse nützlich sind. Insbesondere die Fähigkeit, die sterischen und elektronischen Eigenschaften der Carboranylphosphane anzupassen, ermöglichte die Synthese neuer Liganden, die für die Komplexierung verschiedener Übergangsmetalle (Pd, Cu, Au, Rh, Ru) in Betracht gezogen werden können. Angeregt durch die Nähe der beiden Phosphoratome, wenn sie direkt an den Carborankäfig gebunden sind (ähnlich einer Ethylen- oder *ortho*-Phenylengruppe), wurde die Fähigkeit untersucht, verschiedene Übergangsmetalle in einem 1:1-Koordinationsmodus zu komplexieren. Nach Berechnungen mit Hilfe der Dichtefunktionaltheorie (DFT) für verschiedene B9-substituierte Carboranylphosphane (**29**, **31** und **46**–**49**) zeigt sich in den meisten Fällen, dass die Bildung von Übergangsmetallkomplexen mit verschiedenen organometallischen Vorläufern durch diese Liganden thermodynamisch begünstigt sein sollte (siehe **Tab. 7.2.1** und **Fig. 7.2.1**). Zusätzlich prognostizieren die Berechnungen die Möglichkeit, dass stabilere Komplexe entstehen könnten, nachdem eine $CH_2$-Verbindung zwischen dem Carborankäfig und den Phosphoratomen eingeführt wurde. Allerdings konnte dieses theoretische Ergebnis bisher nicht experimentell bestätigt werden, da die Synthese der Liganden **47**–**49** oder **53** bis dato noch nicht erfolgreich durchgeführt wurde.

**Tab. 7.2.1.** Berechnete GIBBS Energien [kcal mol$^{-1}$] für die Komplexe gebildet mit den Carboranylphosphanen **29**, **31**, **46–49** und verschiedenen Metallpräkursoren in THF oder $CH_2Cl_2$ als Lösungsmittels im Vergleich zu den Startmaterialien.

| Carboranylphosphan | | 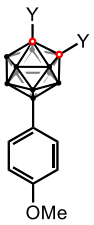 | 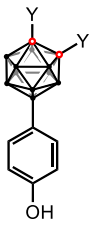 | 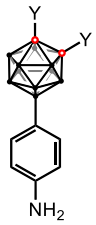 |
|---|---|---|---|---|
| Organometallischer Präkursor (Lösungsmittel für die Berechnung) | | | | |
| **Y = $PPh_2$ (29, 31, 46)** | [AuCl(tht)] ($CH_2Cl_2$) | –13.2 | –14.3 | –14.1 |
| | [$PdCl_2(MeCN)_2$] (THF) | –42.0 | –42.1 | –20.9 |
| | [$Cu(MeCN)_4$](OTf) (THF) | +6.0 | +4.5 | +4.9 |
| | [$CuCl(PPh_3)_3$] (THF) | –0.2 | +0.4 | +0.1 |
| | [$Rh(acac)(CO)_2$] (THF) | –63.0 | –62.9 | –62.7 |
| **Y = $CH_2PPh_2$ (47–49)** | [AuCl(tht)] ($CH_2Cl_2$) | –24.7 | –23.5 | –25.2 |
| | [$PdCl_2(MeCN)_2$] (THF) | –42.4 | –41.9 | –42.5 |
| | [$Cu(MeCN)_4$](OTf) (THF) | +0.5 | –0.9 | nicht berechnet |
| | [$CuCl(PPh_3)_3$] (THF) | –10.3 | –9.4 | –9.2 |
| | [$Rh(acac)(CO)_2$] (THF) | –134.2 | –133.3 | –133.5 |

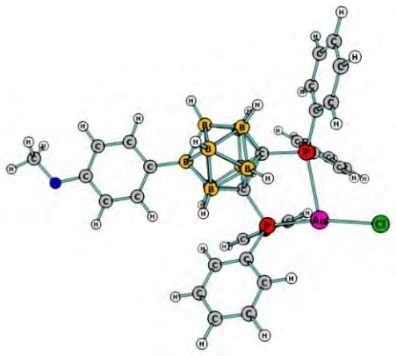

**29-[Au]**

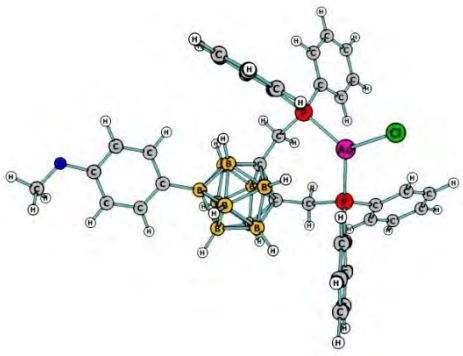

**47-[Au]**

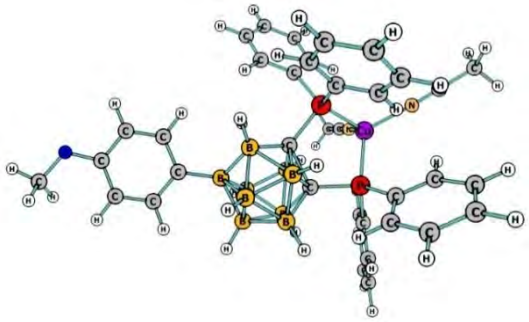

**29-[Cu(MeCN)$_2$]**

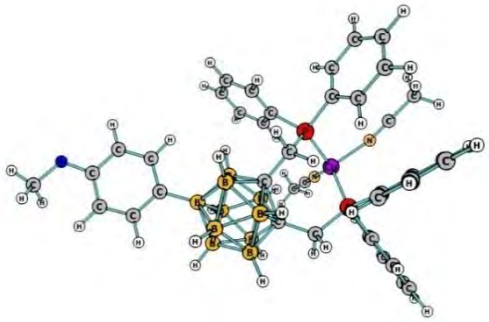

**47-[Cu(MeCN)$_2$]**

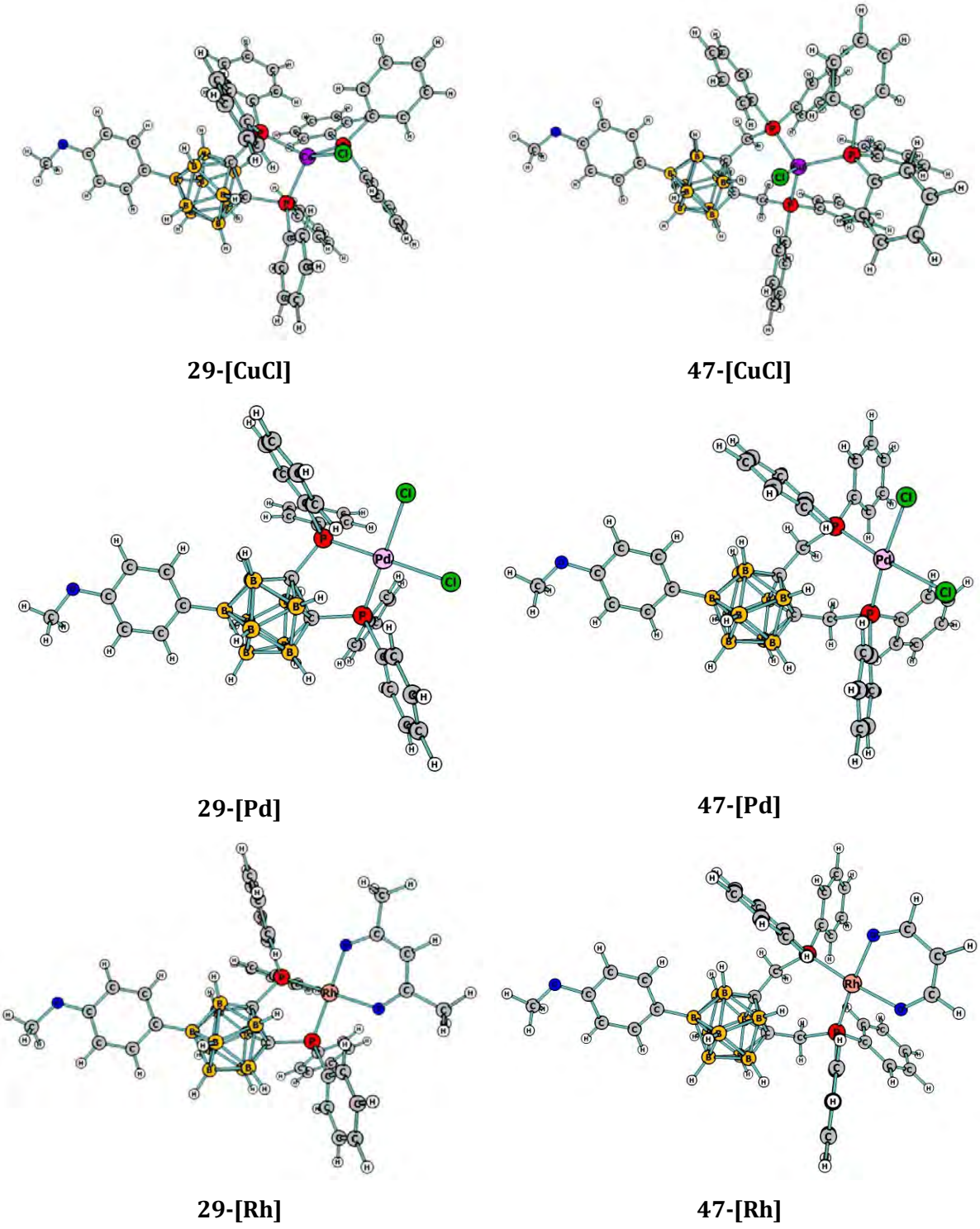


**Fig. 7.2.1.** Berechnete Komplexe, die aus 9-(4-MeO-$C_6H_4$)-1,2-bis(diphénylphosphino)- (**29**) und 9-(4-MeO-$C_6H_4$)-1,2-bis[(diphenylphosphino)methyl]-*ortho*-carboran mit verschiedenen metallorganischen Vorläufern gebildet wurden. Alle Wasserstoffatome wurden der Übersichtlichkeit halber weggelassen. Das Triflatanion in **29**- und **47-[Cu(MeCN)$_2$]** wurde separat optimiert. Die optimierten Strukturen, die für andere Substituenten in B9-Position erhalten wurden, sind nicht gezeigt.

Nur die Monomere der Carboranylphosphine 9-(TBDMS)O-$C_6H_4$-1,2-$(PPh_2)_2$-$C_2B_{10}H_9$ (**28**) und 9-(4-MeO-$C_6H_4$)-1,2-$(PPh_2)_2$-$C_2B_{10}H_9$ (**29**) wurden für die ersten Komplexierungsversuche mit

einem $Pd^{II}$-Vorläufer, zwei $Cu^{I}$-Vorläufern, einem $Au^{I}$-Vorläufer, einem $Rh^{I}$-Vorläufer und einem $Ru^{0}$-Vorläufer verwendet. Die durch ein Silylether geschützte Carboranylphosphin-Verbindung 28 ist die am weitesten verfügbare (größere Menge, einfacher zu synthetisieren) unter allen während der experimentellen Arbeit der Dissertation hergestellten Verbindungen. Der Methoxyphenylsubstituent in Verbindung **29** ahmt die erforderliche Phenoxybindung notwendig für das Graften an Dendimere nach. Es kann daher als eine gute repräsentative Monomerverbindung für durch Carborane substituierte Dendrimere betrachtet werden (wie im Kapitel 3 beschrieben). Der Rhodium(I)-Komplex **28-[Rh]**, der Gold(I)-Komplex **29-[Au]** und der Kupfer(I)-komplex **29-[CuCl]** konnten durch Kernresonanzspektroskopie und Massenspektrometrie synthetisiert und charakterisiert werden. Es war auch möglich, die Bildung des Palladium-Komplexes **29-[Pd]** nachzuweisen, obwohl er aufgrund seiner hohen Reaktivität nicht isoliert werden konnte, da es zur Bildung des Palladium-Dimerkomplexes (**59**) und des Methoxyphenylcarborans (**20**) kam, die wiederum isoliert wurden (siehe **Schema 7.2.1**).

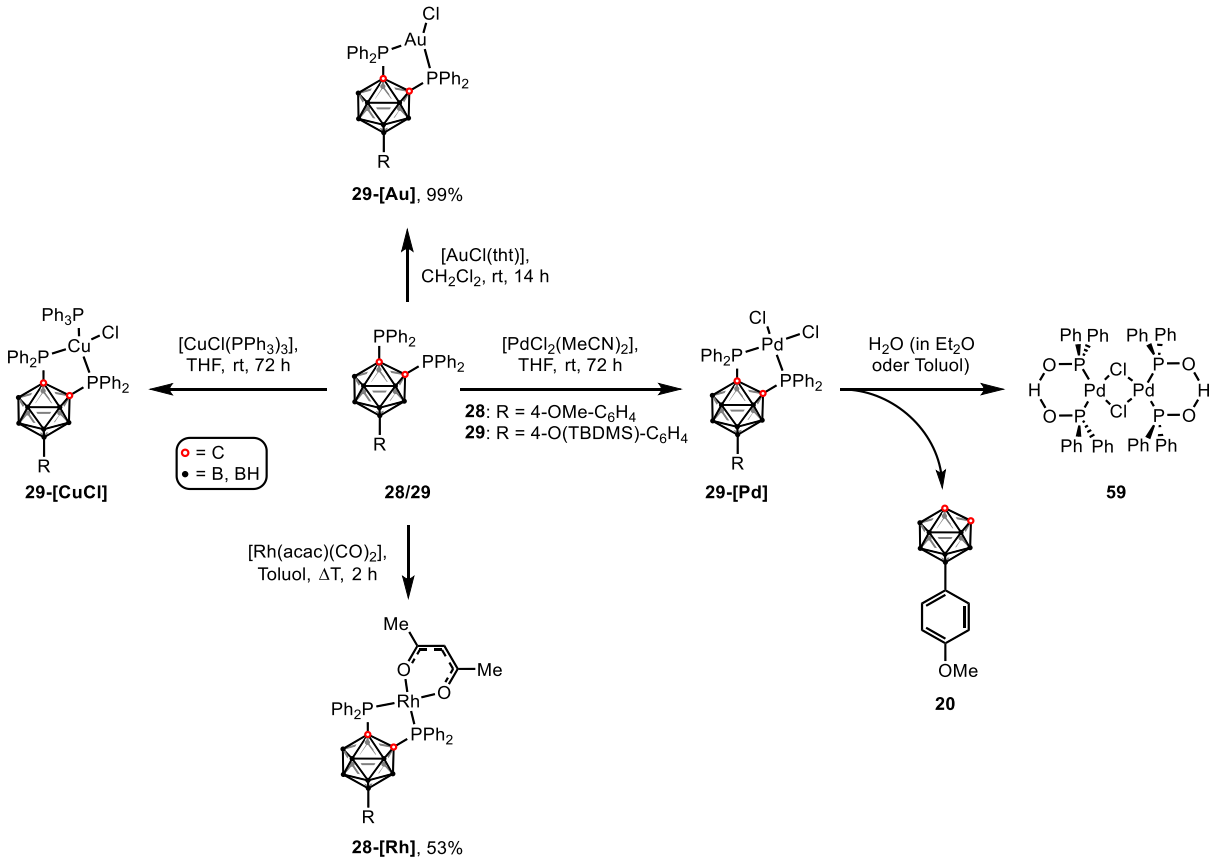


**Schema 7.2.1.** Herstellung verschiedener Übergangsmetallkomplexe mit Carboranylphosphanen.

## 7.3 Vorläufige katalytische Experimente

Mit Hilfe eines Syntheseautomaten bei der BASF SE wurden vorläufige katalytische Studien zur Hydrierung und Hydroformylierung von Oct-1-en und Cyclohexen mit verschiedenen Rhodium- und Rutheniumkomplexen in Gegenwart des Carboranylphosphanliganden

9-(4-(TBDMS)O-$C_6H_4$)-1,2-($PPh_2$)$_2$-$C_2B_{10}H_9$ (**28**) durchgeführt. Die vielversprechendsten Systeme wurden dann in einem Autoklaven unter reproduzierbaren Bedingungen auf ihre Reaktionsfähigkeit getestet. Der Ligand **28** in Gegenwart von [Rh(acac)$(CO)_2$] zeigte die besten Leistungen bei der Hydrierung von Oct-1-en, besser als bekannte Systeme. Der Ligand (**28**) zeigte auch eine bessere Umwandlung in der Cyclohexen-Hydrierungsreaktion mit dem Komplex [$Ru_3(CO)_{12}$] im Vergleich zum unsubstutierten Derivat 1,2-Bis(diphenylphosphino)-*ortho*-Carboran (dppc, **73**), war jedoch nicht so leistungsfähig wie eine einfache Bisphosphan, nämlich 1,2-Bis(diphenylphosphino)benzol (dppb, **67**). Obwohl viele Reaktionen eine gute Umwandlung zeigten, wurde die Selektivität im Vergleich zu anderen bekannten Systemen nicht verbessert, was erklärt, warum diese Systeme nicht weiteren Tests unter industriellen Bedingungen unterzogen wurden. Jedoch wären einige zusätzliche Testreihen notwendig gewesen, um signifikantere Ergebnisse zu erzielen. Es wäre auch interessant gewesen, die in situ gebildeten katalytischen Spezies aus den Metallsalzen und Liganden zu untersuchen.

Es erscheint entscheidend, diese katalytischen Studien zu vervollständigen, den Umfang und die Grenzen der durchgeführten Hydrierungs- und Hydroformylierungsreaktionen zu erkunden und andere katalytische Systeme zu entwickeln, um die erhaltenen Ergebnisse besser zu verstehen.

## 7.4 Verankerung von Carboranen an Polyphosphorhydrazon-Dendrimeren

Verschiedene dendritische Verbindungen wurden auf ihre Eignung hin untersucht, durch verschiedene Carborane und Carboranylphosphane, welche einen Phenolsubstituenten trugen, substituiert zu werden. Theoretische Berechnungen unter Verwendung der Dichtefunktionaltheorie zeigten, dass die Reaktion über einen $S_N2$-ähnlichen Mechanismus verläuft, bei dem das nukleophile Phenolat **17*** den elektrophilen Phosphorzentrum $N_3P_3Cl_6$ (**1-G0**) von der Seite des abgehenden $Cl^-$-Ions angreift. Die verschiedenen Reaktionsprodukte der Polysubstitution mit **17*** wurden theoretisch optimiert, um deren Stabilität zu bewerten. Es wurde gezeigt, dass das hexasubstituierte Produkt **G06** um 194,5 kcal $mol^{-1}$ stabiler ist als das Ausgangsprodukt **1-G0** (siehe **Schema 7.4.1**).

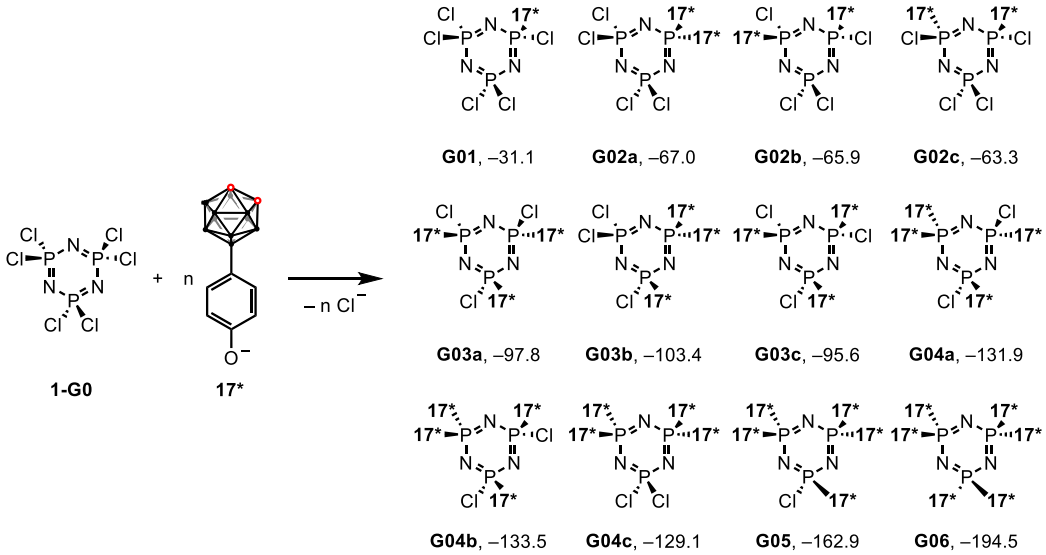


**Schema 7.4.1.** Berechnete GIBBS-Energien in THF als Lösungsmittel (in kcal mol$^{-1}$) für die Substitution von **1-G0** durch n Äquivalente von **17*** im Vergleich zum Ausgangsmaterial.

Da die Berechnungen die Möglichkeit einer mehrfachen Substitution der Chloratome von $N_3P_3Cl_6$ durch Carboranylgruppen bestätigen, wurde diese Hypothese experimentell überprüft (siehe **Schema 7.4.2**).

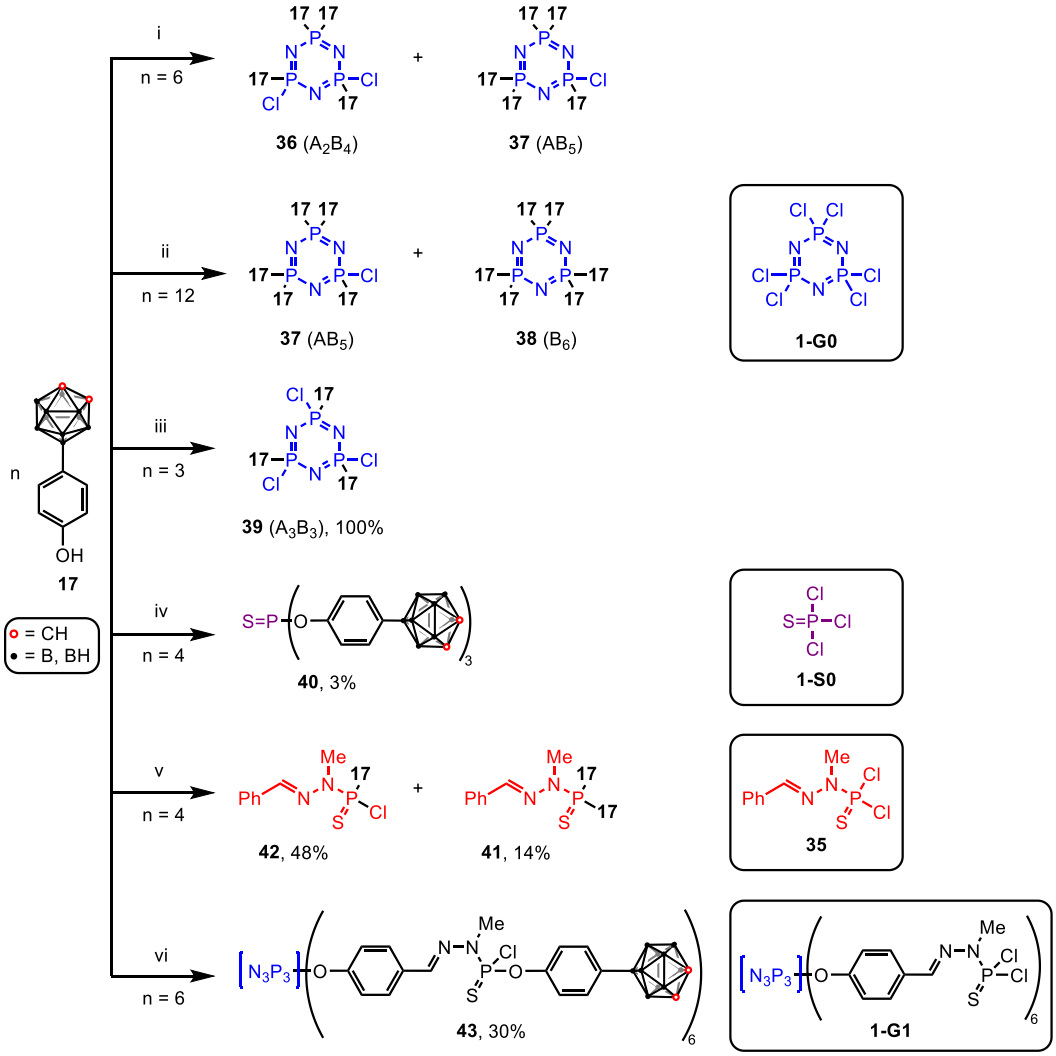


**Schema 7.4.2.** Reaktionen von mehreren Äquivalenten **17** mit $N_3P_3Cl_6$ (**1-G0**), $P(S)Cl_3$ (**1-S0**) und dem Modellmolekül **35**. Reaktionsbedingungen : (i) **1-G0**, $K_2CO_3$, Aceton, 40 °C für 120 h dann Raumtemperatur für 72 h ; (ii) **1-G0**, $Cs_2CO_3$, THF, Raumtemperatur 25 Tage ; (iii) **1-G0**, $K_2CO_3$, Aceton, Raumtemperatur, 72 h ; (iv) **1-S0**, $Cs_2CO_3$, THF, 40 °C, 96 h ; (v) **35**, DBU, THF, Raumtemperatur, 72 h ; (vi) **1-G1**, $Cs_2CO_3$, THF, Raumtemperatur für 72 h, dann 40 °C für 23 h. Alle gezeigten Strukturen wurden mittelsKernresonanzspektroskopie und Massenspektrometrie analysiert.

Die Reaktionen des Phenolcarborans (**17**) mit dem Modellmolekül **35**, verschiedenen phosphorhaltigen Verbindungen **1-G0** und **1-S0** sowie dem Dendrimer **1-G1** wurden getestet. Obwohl keine vollständige Substitution durch ein Carboranylphosphan erreicht wurde, konnten neue dendritische Verbindungen mit Carboranen synthetisiert werden. Insbesondere wurde die selektive Anbindung eines einzelnen Carborans an jedes $P(S)Cl_2$-Funktionsmolekül erfolgreich untersucht, was zur monofunktionalisierten dendritischen Verbindung a **43** führte (siehe **Fig. 7.4.1**).

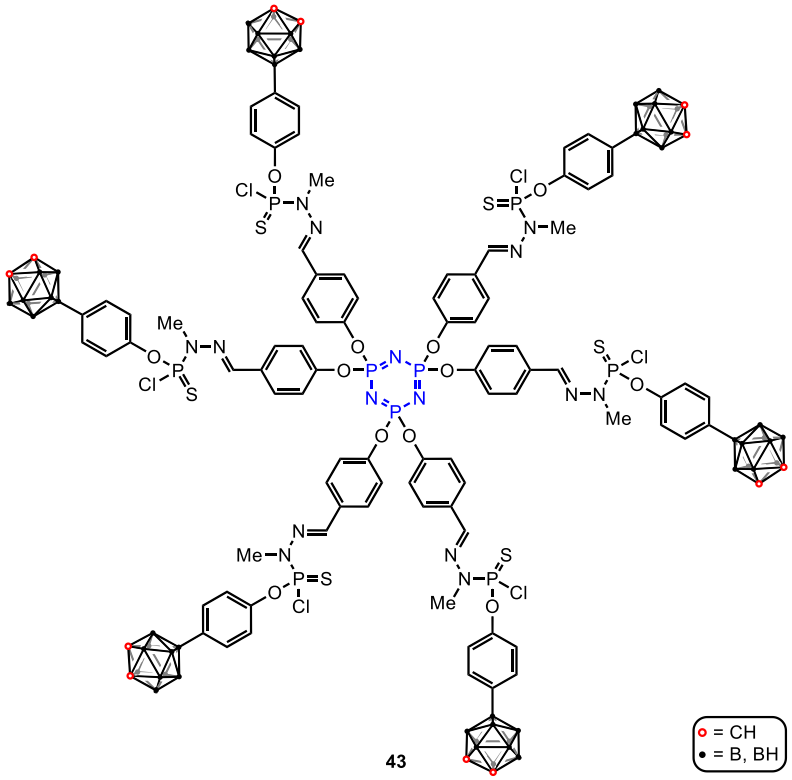


**Fig. 7.4.1**. Struktur des Dendrimers **43**.

Leider bleibt der Schritt der Auftrennung von Dendrimeren, die mit einer unterschiedlichen Anzahl von Carboranen substituiert sind, eine Herausforderung. Darüber hinaus sollte die selektive Substitution eines einzelnen Chloratoms an jeder P(S)$Cl_2$-Funktion durch ein Carboran für andere Generationen von Dendrimeren untersucht werden, da dies den Weg für die Herstellung zusätzlicher Funktionalitäten zur Ersetzung der verbleibenden Chloratome öffnen würde, beispielsweise Funktionen zur Löslichkeit der Dendrimere in Wasser für potenzielle Anwendungen im Bereich der Biologie.[23]

## 7.5 Zusammenfassung

Mehrere *ortho*-Carborane mit einer Phenoxy- oder Phenylaminogruppe in der B9-Position wurden unter Verwendung verschiedener Schutz- und Entschützungsstrategien hergestellt. Zusätzlich wurde im Rahmen dieses Dissertationsprojekts der synthetische Zugang zu neuen 1- oder 1,2-phosphanylierten Carboranen entwickelt. Die resultierenden Phosphane, wie Diisopropyl-, Diethyl-, Di-*tert*-butyl-, Diphenyl- oder Diethoxyphosphan, die ein modifizierbares *ortho*-Carboranmotiv tragen, könnten als interessante Liganden für zukünftige Anwendungen in der homogenen Katalyse oder im medizinischen Bereich dienen. Die Liganden haben durch die chelatiesierenden Carboranylphosphane einen Koordinationsmodus von 1:1 mit verschiedenen Übergangsmetallen gezeigt. Ein *in situ* erzeugter Katalysator aus einer Mischung von $Rh^{I}$- oder

$Ru^0$-Vorläufern und dem Carboranylphosphan **28** wurde zur Hydrierung und Hydroformylierung ungesättigter Olefine verwendet.

Unter Verwendung klassischer synthetischer Methoden wurden polyphosphorhydrazon-basierte Dendrimere aus einem Hexachlorocyclotriphosphazenkern oder Thiophosphorylchlorid hergestellt, und verschiedene Methoden zur Fixierung von B9-substituierten *ortho*-Carboranen in deren Peripherie experimentell und theoretisch (Dichtefunktionaltheorie) untersucht. Trotz der synthetischen Herausforderungen konnten mehrere Dendrimere mit Carboranen in der Peripherie erhalten werden, und die Ergebnisse sollten den Weg für Dendrimere ebnen, die auch Carboranylphospane enthalten, um deren katalytische Leistung zu untersuchen und neue Synthesewege zu erkunden. Weitere Studien zu Carboranylphosphanen mit verschiedenen Substituenten sowie weitere katalytische Anwendungen wären lohnenswert. Bisher wurden nur elektronenarme C–P-Carboranylphosphane in Betracht gezogen. Die Verwendung von elektronenreichen B–P-Carboranylphosphanen (ähnlich der Arbeiten der Gruppe von SPOKOYNY)[24], die die Carborane über ihre $C_{Carboran}$-Atome mit den Dendrimeren verbinden, könnte eine interessante Variante sein. Es ist offensichtlich, dass in diesem Forschungsbereich noch viel zu entdecken ist.

Dieses Dissertationsprojekt zielte darauf ab, ein neues Ligandensystem für anspruchsvolle katalytische Reaktionen zu entwickeln. Hierfür wurden zwei chemische Komponenten kombiniert: eine polyphosphorhydrazonische dendritische Struktur, die für ihre Anwendungen in der Katalyse bekannt ist, und Carboranylphosphanmotive, die bereits für ihre Komplexierungsfähigkeit und mögliche Anwendungen in der Katalyse untersucht wurden. Die Hauptphasen dieses Projekts können wie folgt zusammengefasst werden:

1. Herstellung von Dendrimeren: Verschiedene dendritische Verbindungen wurden aus $P(S)Cl_3$- oder $N_3P_3Cl_6$-Kernen hergestellt und erzeugten klassische Dendrimere mit guten Ausbeuten bis zu einer Generation von **1-G2** oder **2-S1**.

2. Synthese von substituierten Carboranen: Mehrere in der B9-Position substituierte Carborane wurden unter Verwendung verschiedener Schutz- und Entschützungsstrategien hergestellt und ergaben unterschiedliche Ausbeuten. Die Festkörperstrukturen dieser Verbindungen wurden durch Röntgenkristallstrukturanalyse bestimmt.

3. Koordinationschemie: Die neuen Carboranylphosphane, die zwei nahe beieinander liegende Phosphorgruppen tragen, zeigten eine interessante Komplexierungsfähigkeit mit verschiedenen Übergangsmetallen. Theoretische Berechnungen zeigten, dass die Bildung von Übergangsmetallkomplexen in den meisten Fällen thermodynamisch günstig sein sollte.

4. Vorläufige katalytische Tests wurden für die Hydrierung und Hydroformylierung organischer Verbindungen durchgeführt. Das Carboranylphosphin **28** zeigte eine vielversprechende Leistung bei der Hydrierung von Oct-1-en.

5. Fixierung von Carboranen an Dendrimeren: Verschiedene Dendrimere wurden als Träger für die Fixierung von Carboranen und Carboranylphosphanen mit einer Phenolfunktion in Betracht gezogen. Die Substitutionsreaktionen erfolgten über einen $S_N2$-Mechanismus. Die selektive Substitution eines einzelnen Chloratoms an den $P(S)Cl_2$-Funktionen durch Carborane wurde ebenfalls untersucht, was zu einem Dendrimer führte, bei dem die Hälfte seiner Chloratome noch für eine zweite Funktionalisierung zur Verfügung steht.

## 7.6 Quellenangaben


[1] A.-M. Caminade, R. Laurent, *Coord. Chem. Rev.* **2019**, *389*, 59–72.

[2] V. Maraval, R. Laurent, A.-M. Caminade, J.-P. Majoral, *Organometallics* **2000**, *19*, 4025–4029.

[3] M. Keller, A. Hameau, G. Spataro, S. Ladeira, A.-M. Caminade, J.-P. Majoral, A. Ouali, *Green Chem.* **2012**, *14*, 2807–2815.

[4] M. Keller, V. Collière, O. Reiser, A.-M. Caminade, J.-P. Majoral, A. Ouali, *Angew. Chem. Int. Ed.* **2013**, *52*, 3626–3629; *Angew. Chem*. **2013**, *125*, 3714–3717.

[5] P. Servin, R. Laurent, A. Romerosa, M. Peruzzini, J.-P. Majoral, A.-M. Caminade, *Organometallics* **2008**, *27*, 2066–2073.

[6] N. G. García-Peña, A.-M. Caminade, A. Ouali, R. Redón, C.-O. Turrin, *RSC Adv.* **2016**, *6*, 64557–64567.

[7] P. Servin, R. Laurent, L. Gonsalvi, M. Tristany, M. Peruzzini, J. P. Majoral, A.-M. Caminade, *Dalton Trans.* **2009**, 4432–4434.

[8] P. Neumann, H. Dib, A.-M. Caminade, E. Hey-Hawkins, *Angew. Chem. Int. Ed.* **2015**, *54*, 311–314; *Angew. Chem.* **2015**, *127*, 316-319.

[9] M. Petrucci-Samija, V. Guillemette, M. Dasgupta, A. K. Kakkar, *J. Am. Chem. Soc.* **1999**, *121*, 1968–1969.

[10] P. Servin, R. Laurent, H. Dib, L. Gonsalvi, M. Peruzzini, J. P. Majoral, A.-M. Caminade, *Tetrahedron Lett.* **2012**, *53*, 3876–3879.

[11] A. Ouali, R. Laurent, A.-M. Caminade, J. P. Majoral, M. Taillefer, *J. Am. Chem. Soc.* **2006**, *128*, 15990–15991.

[12] A. Gissibl, C. Padié, M. Hager, F. Jaroschik, R. Rasappan, E. Cuevas-Yañez, C. O. Turrin, A.-M. Caminade, J. P. Majorai, O. Reiser, *Org. Lett.* **2007**, *9*, 2895–2898.

[13] M. Keller, M. Ianchuk, S. Ladeira, M. Taillefer, A.-M. Caminade, J. P. Majoral, A. Ouali, *Eur. J. Org. Chem.* **2012**, *2012*, 1056–1062.

[14] I. B. Sivaev, M. Y. Stogniy, V. I. Bregadze, *Coord. Chem. Rev.* **2021**, *436*, 213795.

[15] E. V. Oleshkevich, E. G. Rys, V. V. Bashilov, P. V. Petrovskii, V. A. Ol'shevskaya, S. K. Moiseev, A. B. Ponomaryov, V. N. Kalinin, *Russ. J. Gen. Chem.* **2017**, *87*, 2589–2595.

[16] S. Bauer, E. Hey-Hawkins *dans Boron Science* (Ed. : N. S. Hosmane), CRC Press, **2011**, pp. 529–578.

[17] N. Launay, A.-M. Caminade, R. Lahana, J.-P. Majoral, *Angew. Chem. Int. Ed. Engl.* **1994**, *33*, 1589–1592.

[18] N. Launay, A.-M. Caminade, J. P. Majoral, *J. Organomet. Chem.* **1997**, *529*, 51–58.

[19] E. Cavero, M. Zablocka, A.-M. Caminade, J. P. Majoral, *Eur. J. Org. Chem.* **2010**, 2759–2767.

[20] F. A. Hart, D. W. Owen, *Inorg. Chim. Acta* **1985**, *103*, L1–L2.

[21] P. Coburger, G. Kahraman, A. Straube, E. Hey-Hawkins, *Dalton Trans.* **2019**, *48*, 9625–9630.

[22] R. P. Alexander, H. Schroeder, *Inorg. Chem.* **1963**, *2*, 1107–1110.

[23] A.-M. Caminade, M. Milewski, E. Hey-Hawkins, *Pharmaceutics* **2023**, *15*, 2117.

[24] A. M. Spokoyny, C. D. Lewis, G. Teverovskiy, S. L. Buchwald, *Organometallics* **2012**, *31*, 8478–8481.

# Chapter 8: Appendices

# 8 Appendices

## Scientific Curriculum Vitae

Max Milewski

Albert-Schweitzer_Straße 5, 04317 Leipzig

Phone: +49 151 17609766

Mail: max.milewski@lcc-toulouse.fr, milewskimax@gmail.com

**Education**

| | |
|---|---|
| Since Oct. 2020 | *PhD student*, CNRS - Laboratoire de Chimie de Coordination, Toulouse, European Union's Horizon 2020 research and innovation (CCIMC) program, title: "Carboranylphosphines meet dendrimers: Electron-deficient scaffolds for ligand design and application in catalysis" with Dr. Anne-Marie Caminade and Prof. Dr. h. c. Evamarie Hey-Hawkins<br>Member of Graduate School BuildMoNa |
| 10/2017 - 05/2020 | *Master of Science*, Leipzig University, studies of chemistry, Master thesis: Synthesis and Characterisation of Frustrated Lewis Pairs incorporating 9-*N*-Amino-1,7-dicarba-*closo*-dodecaboranes(12) with Prof. Dr. h. c. Evamarie Hey-Hawkins and Dr. Jan Schulz |
| 10/2014 - 09/2017 | *Bachelor of Science*, Leipzig University, studies of chemistry, Bachelor thesis (together with HZDR Dresden-Rossendorf): "Synthese und Entwicklung eines fluorierten Pyrimidin-grundkörpers für weiterführende Radiotracerentwicklungen" with Prof. Dr. Thorsten Berg, Prof. Dr. Peter Brust and Dr. Marcel Lindemann |
| 09/2007 - 06/2014 | *Secondary school*, Max-Steenbeck-Gymnasium, Cottbus, *German Abitur (Higher education entrance qualification)*, major courses: Chemistry, Physics, Mathematics, German, English |

**Scholarships/Grants**

| | |
|---|---|
| 22 - 24/03/2023 | Partial scholarship by Gesellschaft Deutscher Chemiker (GDCh) for PBSi 2023 (Conference) |
| 03 - 07/07/2022 | Partial scholarship by Gesellschaft Deutscher Chemiker (GDCh) for Euroboron Congress (Conference) |
| 04/2019 - 07/2019 | Erasmus+ European Union funds for research stay at Monash University, Melbourne (Australia) |

02/2018 - 08/2018 DAAD scholarship (German Academic Exchange Service) for Internationale Studien- und Ausbildungspartnerschaft (ISAP) with Monash University, Melbourne (Australia)

**Research Stays**

03/2023 - 05/2023 *Intern*, BASF SE Ludwigshafen, hydrofunctionalization reactions, group of Dr. Rocco Paciello

06/2022 - 07/2022 *Intern*, Universitat Autònoma de Barcelona, basic computational chemistry methods, group of Prof. Dr. Agustí Lledós

04/2019 - 07/2019 Monash University, Melbourne (Australia), Erasmus+ student Project: "Carbone – the slightly different carbon species: Synthesis and characterisation of carbon $Ag^{I}$ compounds" with Dr. Victoria Blair and Dr. Samantha Orr

02/2018 - 08/2018 Monash University, Melbourne (Australia), Exchange student and DAAD scholar, Projects: "Metalation attempts of (*S*)-*N*-(1-phenylethyl)prop-2-yn-1-amine" with Prof. Dr. Phil Andrews and Dr. Matt Flynn; Synthesis of modified indole-based ligands for the preparation of new Jacobsen catalysts (and their reactivity)" with Prof. Dr. David Lupton and Dr. Jared Fernando

**Conferences/Talks**

22-24/03/2023 Talk: PBSi 2023, Berlin, Germany, **From Carboranyl phosphines and Dendrimers - Investigation of Electron-deficient Scaffolds for Ligand Design**, co-authors: A.-M. Caminade, E. Hey-Hawkins, Agustí Lledós

20-21/03/2023 Talk: 15th Annual Conference of the Graduate School BuildMoNa, Leipzig, Germany, **Carboranylphosphines and Dendrimers: Experimental Investigation of Electron-deficient Scaffolds for Ligand Design**, co-authors: A.-M. Caminade, E. Hey-Hawkins

03-07/07/2022 Poster: Euroboron Congress 2022, Barcelona, Spain, **Carboranyl phosphines meet dendrimers - New scaffolds for ligand design**, co-authors: A.-M. Caminade, E. Hey-Hawkins, Agustí Lledós

29/03-01/04/2022 Talk: 2nd International Workshop - Cutting-Edge Homogeneous Catalysis, Leipzig, Germany, **Carboranylphosphines meet dendrimers: Electron-deficient scaffolds for ligand design and application in catalysis**, co-authors: A.-M. Caminade, E. Hey-Hawkins

| | |
|---|---|
| 14-15/03/2022 | Poster: 14th Annual Conference of the Graduate School BuildMoNa, Leipzig, Germany, **Anchoring of Carboranyl Phosphines to Dendrimers**, co-authors: A.-M. Caminade, E. Hey-Hawkins |
| 20-21/01/2022 | Poster: HC3A, Barcelona, Spain, **Carboranyl phosphines meet dendrimers - New scaffolds for ligand design**, co-authors: A.-M. Caminade, E. Hey-Hawkins |
| 04/05/2021 | Poster: **Cutting-Edge Homogeneous Catalysis CEHC-1**, online, **Carboranyl phosphines meet dendrimers - New scaffolds for ligand design**, co-authors: A.-M. Caminade, E. Hey-Hawkins |
| 29/03-01/04/2021 | Poster: GDCh JCF Spring symposium 2021, online, **Carboranylphosphines meet dendrimers - New scaffolds for ligand design**, co-authors: A.-M. Caminade, E. Hey-Hawkins |
| 08-09/03/2021 | Poster: 13th Annual Conference of the Graduate School BuildMoNa, online, **Carboranyl phosphines meet dendrimers - New scaffolds for ligand design**, co-authors: A.-M. Caminade, E. Hey-Hawkins |

**Publications**

Carboranylphosphines: B9-Substituted Derivatives With Enhanced Reactivity For The Anchoring To Dendrimers**,** M. Milewski, A.-M. Caminade, S. Mallet-Ladeira, A. Lledós, P. Lönnecke, E. Hey-Hawkins, to be submitted.

Dendritic Structures Functionalized with Boron Clusters, in Particular Carboranes, and Their Biological Properties, A.-M. Caminade, M. Milewski, E. Hey-Hawkins, *Pharmaceutics* **2023**, *15*, 2117. DOI: 10.3390/pharmaceutics15082117.

Pitfalls of a structure determination: The structure of closo -9-[4-(dibenzylamino)phenyl]-1,2-dicarbadodecaborane(12), M. Milewski, A.-M. Caminade, E. Hey-Hawkins, P. Lönnecke, *Acta Crystallogr. Sect. E Crystallogr. Commun.* **2022**, *78*, 1145–1150. DOI: 10.1107/S205698902201043X.